Impact of innate immunity of MDCK cells on virus replication in an influenza vaccine production process

Dissertation

zur Erlangung des akademischen Grades

Doktoringenieur

(Dr.-Ing.)

von: Dipl.-Ing. Björn Heynisch

geb. am: 27.09.1978 in Staaken

genehmigt durch die Fakultät für Verfahrens- und Systemtechnik

der Otto-von-Guericke-Universität Magdeburg

Promotionskommission: Prof. Dr.-Ing. Andreas Seidel-Morgenstern

Prof. Dr.-Ing. Udo Reichl

Prof. Dr. RJM (Rob) Moormann, PhD

PD Dr. Yvonne Genzel

eingereicht am: 22.11.2012

Promotionskolloquium am: 28.05.2013

Danksagung

Diese Dissertation entstand am Max-Planck-Institut für Dynamik komplexer technischer Systeme im Rahmen meiner Beschäftigung als wissenschaftlicher Mitarbeiter der Fakultät für Verfahrens- und Systemtechnik, Lehrstuhl Bioprozesstechnik, der Otto-von-Guericke-Universität Magdeburg. Für die erfolgreiche Vollendung dieses Werkes gebührt folgenden Personen mein großer Dank:

An erster Stelle danke ich Herrn Prof. Dr.-Ing. Udo Reichl für die Eröffnung der Möglichkeit, am Max-Planck-Institut als Doktorand in seiner Gruppe eine Promotion anfertigen zu dürfen. Das in mich gesetzte Vertrauen, die Bereitstellung eines ausgezeichneten Forschungsumfeldes, sowie ein stetiges offenes Ohr für sämtliche Belange habe ich über die Jahre tagtäglich immer sehr zu schätzen gewusst. An nächster Stelle gilt mein Dank Frau Dr. rer. nat. habil. Yvonne Genzel für die Schaffung der theoretischen Basis dieses Projekts und die initiale Betreuung sowie für den stets motivierenden Zuspruch. Herrn Dr. rer. nat. Timo Frensing gilt mein Dank für die fachliche und methodische Kompetenz, ohne die die Beantwortung wesentlicher Fragen dieses Projekts nicht möglich gewesen wäre. Herrn Prof. Dr. Rob Moormann, PhD, von der Universität Wageningen danke ich für die fachliche Begutachtung der von mir vorgelegten Arbeit sowie für die interessante Diskussion im Rahmen des Promotionskolloquiums. Herrn Prof. Dr.-Ing. Andreas Seidel-Morgenstern danke ich für die Übernahme des Vorsitzes des Promotionskolloquiums.

Am Institut für Experimentelle Innere Medizin der Otto-von-Guericke-Universität danke ich Herrn Prof. Dr. rer. nat. Michael Naumann, Frau Dr. rer. nat. Nadine Jurrmann, sowie Frau Dipl.-Ing. Melanie Fachet für die fachliche Unterstützung im Rahmen des Methodentransfers.

Für die exzellente methodische Unterstützung danke ich vielmals unserem technischen Personal, namentlich Claudia Best, Felicitas Hasewinkel, Susanne König, Ilona Behrendt und Nancy Wynserski, deren täglicher Beitrag als eine der tragenden Säulen der Aktivitäten der Forschungsgruppe anzusehen ist.

Susann Behling, Annegret Frauendienst und Thomas Mund danke ich für die jahrelange Unterstützung und Zusammenarbeit in organisatorischen Fragen sowie für die Verbreitung und Förderung guter Laune, die mit deutlich mehr Freude ans Werk gehen lässt.

Den vormals von mir im Rahmen ihrer Abschlussarbeiten betreuten Studenten Kristina Heinze, Bianca Kaps und Stefan Heldt danke ich für ihre Neugier und Unterstützung, ohne die das Projekt nicht so hätte gedeihen können, wie es der Fall gewesen ist.

Dem Kreis meiner doktorierenden und studentischen Weggefährten gebührt mein großer Dank, weil durch sie erst das menschliche Umfeld ins Leben gerufen wurde, in dem man sich in seiner Entwicklung als Doktorand erfolgreich entfalten kann. Dies gilt sowohl für kollegiale Zusammenarbeiten als auch für die Schaffung einer soliden, herzlichen, krisenfesten und vielerorts auch sehr witzigen freundschaftlichen Basis. Allen voran danke ich dabei Robert Janke, Marc Rüger und Alexander Rath, sowie Anja Serve, Linzhu Gou, Jana Rödig, Tim Rudolph, Arturo Padilla, Roberto Lemoine, Sabine Kluge, Susann Freund, Matthias Borowiak, Kay Schallert, Jonas Hohlweg, Michael Fricke, Julika Krohs, Maria Wetzel, Jadwiga Nowak, Anke Carius, Antje Lagoda, Susan Jahn, Israel Barrantes, Amit Katariya, Trupti Nahar, Diana Vester, Mareike Schulze und Claudius Seitz. Joachim Ritter danke ich nicht zuletzt wegen der Herstellung des ersten Kontakts.

Des Weiteren danke ich in Magdeburg sehr herzlich Julia Bütow und Anne Riewald.

Meinen langjährigen Mentorinnen Babette Regierer und Susanne Hollmann danke ich für viele inspirierende Gespräche und für die bei jeder sich bietenden Gelegenheit gezeigte herzliche Bereitschaft zur Unterstützung und Förderung.

Dem Bundesministerium für Bildung und Forschung danke ich für die großzügige Förderung des Projekts im Rahmen der FORSYS-Initiative, FKZ 0313922.

Mein größter und allerherzlichster Dank gilt jedoch meinen lieben Eltern, Ingrid und Richard, und meinem Bruder Lars, sowie meiner Oma Ruth, da mein Leben, wie ich es heute führen darf und immer habe führen dürfen, ohne ihre unermüdliche Liebe und Aufopferung kaum je hätte vorstellbar gewesen sein können.

Abstract

In spite of considerable progress in basic research regarding the investigation of virus-host cell interactions throughout the past decade, rather insignificant efforts have been undertaken to use at least part of the knowledge obtained for characterization of cell culture-based influenza vaccine production. Since producers are forced to manage to provide within limited time frames sufficient amounts of vaccine, fast, reliable and robust manufacturing processes are of fundamental importance. To cope with this annual challenge a detailed understanding of cellular events relevant for influenza A virus replication is needed. Particularly, it has for a long time remained unclear which role the induction of host cell innate immunity plays in influenza vaccine production and what impact this has on process yields.

During this study, the induction of several signaling cascades in MDCK cells relevant for influenza A virus replication (NF-κB, IRF-3, PI3K/Akt, Jak-Stat, Raf/MEK/ERK, PKR/eIF2-α) was analyzed using phospho-specific antibodies. For two variants of influenza virus A/Puerto Rico/8/34 (H1N1) that replicate to different final titers it could be illustrated that the aforementioned pathways are more strongly induced by the variant that performs less well during replication. These results were initially obtained in high multiplicity of infection experiments, yet could also be confirmed under bioprocess conditions and partially at a varying multiplicity of infection as well. Additional efforts were aimed at clarifying the actual significance of the monitored pathways, focusing on PKR/eIF2-α induction, for influenza virus replication by RNAi technology and by the use of small molecule inhibitors. Contrary to initial assumptions, the PKR-mediated phosphorylation of eIF2-α was not shown to constitute a limiting factor for influenza virus replication in MDCK cells. However, in the long run these efforts contribute to a better understanding of virus replication in cell culture-based vaccine production and might additionally facilitate the design and optimization of production cell lines.

Zusammenfassung

Trotz des großen Fortschritts, der im vergangenen Jahrzehnt bei der Aufklärung von Interaktionen zwischen Influenzaviren und ihren Wirtszellen erreicht werden konnte, sind bisher nur wenige experimentelle Ansätze verfolgt worden, um die gewonnen Erkenntnisse auf zellkulturbasierte Influenza Impfstoffproduktionsprozesse zu übertragen. Da die Hersteller von Influenza Impfstoffen gezwungen sind, innerhalb geringer Zeitspannen von nur wenigen Monaten Dauer eine genügende Menge an Impfstoff bereitzustellen, ist es von großer Notwendigkeit, über schnelle, verlässliche und wenig störanfällige Produktionsprozesse zu verfügen. Um dieser jährlich wiederkehrenden Herausforderung gerecht zu werden, ist ein detailliertes Verständnis der intrazellulären Vorgänge bei der Influenza Virusreplikation von großer Bedeutung. Dabei sind insbesondere den zellulären Prozessen, die mit der angeborenen Immunität der zur Impfstoffherstellung genutzten Epithelzellen in Verbindung stehen, in bisherigen Studien in diesem Kontext keine große Bedeutung beigemessen worden, sodass zu Beginn dieser Forschungsarbeit unklar war, ob diese einen limitierenden Faktor für die Produktionsprozessausbeuten darstellen könnten. Gegenstand dieser Studie war die Analyse der Influenzavirus vermittelten Aktivierung von Signaltransduktionskaskaden, die sich in anderen Untersuchungen als für die Virusreplikation bedeutsam herausgestellt hatten. Dies umfasste die Signaltransduktionskaskaden NF-κB, IRF-3, PI3K/Akt, Jak-Stat, Raf/MEK/ERK und PKR/eIF2-α, die in MDCK Zellen mittels phosphospezifischer Antikörper mit Hilfe von Immunoblots untersucht wurden. Dabei konnte für zwei Varianten des Influenza Virusstamms A/Puerto Rico/8/34 (H1N1), die während ihrer Replikation in MDCK Zellen unterschiedliche finale Virustiter erreichen, gezeigt werden, dass die zuvor genannten Signaltransduktionskaskaden in unterschiedlich hohem Maße induziert werden, wobei eine stärkere Induktion während der Infektion mit der weniger gut replizierenden Variante des Virusstamms beobachtet werden konnte. Anfänglich wurden diese Erkenntnisse durch Experimente gewonnen, in denen die MDCK Zellen mit einer *hohen multiplicity of infection* (MOI) infiziert worden sind. Später konnte dann gezeigt werden, dass sich diese Ergebnisse teilweise auch bei einer geringen MOI Infektion sowie unter Bedingungen reproduzieren ließen, die denen gleichen, die während des Impfstoffproduktionsprozesses im Bioreaktor vorherrschen. Zusätzlich dazu wurden Anstrengungen unternommen, um mit Hilfe der RNAi Technologie sowie mittels des Einsatzes eines *small molecule* Inhibitors zu klären, inwieweit sich die untersuchten Signalwege, und dabei insbesondere die Induktion

der PKR vermittelten Phosphorylierung von eIF2-α, tatsächlich auf die Replikation des Influenza Virus auswirken. Anders als dies ursprünglich erwarten worden war, konnte nicht gezeigt werden, dass die Aktivität der Kinase PKR einen limitierenden Faktor für die Replikation des Influenza Virus darstellt, gemessen an dem finalen erreichten Virustiter. Nichtsdestotrotz stellen die Ergebnisse, die erhalten werden konnten, einen wichtigen Beitrag für ein besseres Verständnis der Virusreplikationsvorgänge in einem zellkulturbasierten Impfstoffproduktionsprozess dar. Dies könnte in Zukunft dazu beitragen, die Generierung von optimierten Produktionszelllinien zu erleichtern.

Table of Contents

Abbreviations and Symbols

µL	Microliter
µM	Micromolar
2'-5' OAS/OAS	2’-5’-oligoadenylate synthetase 1
2-AP	2-aminopurine
A549	Adenocarcinomic human alveolar basal epithelial cells
AbD	AbD Serotec
ADAR1-L	Large isoform of double-stranded (ds) RNA-specific adenosine deaminase
AGE1.CR	Avian designer cell line
AIF	Apoptosis inducing factor
ANT	Adenine nucleotide translocator
AP-1	Activator protein 1
Apaf-1	Apoptotic protease activating factor 1
APS	Ammonium persulfate
ASA	Acetylsalicylic acid
ASK-1	Apoptosis signal-regulating kinase 1
ATCC	American Type Culture Collection
ATF-2	Activating transcription factor 2
ATP	Adenosine-5'-triphosphate
Bad	Bcl-2-associated death promoter
Bax	Bcl-2-associated X protein
BCA	Bicinchoninic acid
Bcl-2	B-cell lymphoma 2
Bcl-xL	B-cell lymphoma-extra large
beta-EtSH	Beta-mercaptoethanol
BPE	Bioprocess engineering
BSA	Bovine serum albumin
°C	Degrees Celsius
CARD	Caspase recruiting domain
CARDIF	Synonym for IPS-1/MAVS/VISA
CCD	Charge-coupled device (camera)
c-Jun	Protein that together with c-Fos forms AP-1
cm²	Square centimeter
cMx1, cMx2	Canine myxovirus-resistance protein 1, 2
CPSF4	Cleavage and polydenylation specificity factor 4
CREB-binding protein/ E1A binding protein (CBP/p300)	cAMP-response element-binding protein (CREB) binding protein (CBP)
c-Rel	Proto-oncogene encoded by the REL gene
CRM1/EXPO1	Exportin-1
cRNA	Complementary viral ribonucleic acid
CST	Cell Signaling Technology

CT	Cycle threshold value
DIP	Defective interfering particles
DMSO	Dimethyl sulfoxide
DNA	Deoxyribonucleic acid
Ds	Double-stranded
E	Amplification efficiency
E: Epitomics	Epitomics
EB66™	Vivalis cell line for biomanufacturing of vaccines and proteins
ECACC	European Collection of Animal Cell Cultures
EDTA	Ethylenediaminetetraacetic acid
eIF2	Eukaryotic initiation factor 2
eIF-2B	Eukarytic translation initiation factor 2B
EMA	European Medicines Agency
ER	Endoplasmic reticulum
ERK1/2	Extracellular signal-regulated kinase 1/2
ERK5	Extracellular signal-regulated kinase 5
FasL	Fas ligand
FCS	Fetal calf serum
FLI	Friedrich Loeffler Institute
G	Gram
G	Gravitational acceleration
GAPDH	Glyceraldehyde 3-phosphate dehydrogenase
GCN2	General control nonrepressed 2 (serine/threonine-protein kinase)
GDP	Guanosine 5'-diphosphate
GE	General Electric
GMEM	Glasgow minimum essential medium
GSK3-beta	Glycogen synthase kinase 3-beta
GTP	Guanosine 5'-triphosphate
GTPase-1	Guanosine 5'-triphosphatase-1
H	Hours
H_20ultrapure	ultrapure Milli-Q water
HA	Hemagglutinin
HA1, HA2	Hemagglutinin subunits of HA0
HAU	Hemagglutinin units
HBEC	Human bronchial epithelial cells
HCM	Human cilial muscle cells
HeLa	Henrietta Lacks immortal cell line
HGR	High growth reassortant
Hpi/hpt	Hours post infection/hours post transfection
HRI	Heme-regulated inhibitor kinase
HSP40	Heat shock protein 40
IAV	Influenza A virus
IFN	Interferon

IFNAR	Interferon-alpha/beta receptor
IgG	Immunoglobulin G
IKK	IκB kinase
IKK-1/IKK-α	IκB kinase-1/IκB kinase-alpha
IKK-2/IKK-β	IκB kinase-2/IκB kinase-beta
IPS-1	Interferon-beta promoter stimulator 1
IRF-3	Interferon regulatory factor 3
IRF-7	Interferfon regulatory factor 7
IRF-9	Interferon regulatory factor 7
ISG	Interferon-stimulated gene
ISGF-3	Interferon-stimulated gene factor 3
ISRE	Interferon-stimulated response element
IκBα	Nuclear factor kappa B inhibitor
Jak-1	Janus kinase 1
Jak-Stat	Janus kinase-signal transducer and activator of transcription pathway
JNK	c-Jun N-terminal kinases
kDa	Kilo Dalton
L	Liters
LAIV	Live-attenuated influenza vaccine
LPS	Lipopolysaccharide
M	Molar concentration
M1	Influenza A virus matrix protein 1
M2	Influenza A virus proton-selective ion channel protein
m7GpppXm	Monomethylated cap structure of viral mRNAs
mA	Milliampere
Malaysia	Influenza B/Malaysia/2506/2004
MAPK	Mitogen-activated protein kinases
MAVS	Mitochondrial antiviral-signaling protein
Mcl-1	Myeloid leukemia cell differentiation protein
MDCK	Madin-Darby canine kidney
MEK1/2	Mitogen-activated/extracellular signal-regulated kinase 1/2
MEK5	Mitogen-activated/extracellular signal-regulated kinase 5
Min	Minutes
MKK3/6	Mitogen-activated protein kinase kinase 3/6
MKK4/7	Mitogen-activated protein kinase kinase 4/7
mL	Milliliters
mM	Millimolar
Mm	Millimeter
MOI	Multiplicity of infection
MPI	Max Planck Institute
mRNA	messenger RNA
MVA	Modified vaccinia Ankara virus

Mx	Myxovirus resistance protein
MxA	Human myxovirus resistance protein A
MxB	Human myxovirus resistance protein B
NA	Neuraminidase
NEB	New England Biolabs®
NEMO/IKK-gamma	NF-kappa-B essential modulator/inhibitor of NF-kappa-B kinase subunit gamma
NEP/NS2	Nuclear export protein/non-structural protein 2
NF-κB	Nuclear factor kappa-light-chain-enhancer of activated B cells
Ng	Nanograms
NIBSC	National Institute for Biological Standards and Control
NS1	Non-structural protein 1
p100	NF-kappa-B subunit p100
p105	NF-kappa-B subunit p105
p38	Class of mitogen-activated protein kinases
p48	Synonymous for IRF-9
p50	Alias for p105 of NF-kappa-B
p56	Subunit of NF-kappa-B
P58IPK	Inhibitor of the IFN-induced dsRNA-activated protein kinase PKR
p65	NF-kappa-B family member, synonymous for RelA
p85β	PI3K regulatory subunit
PA	Polymerase acidic protein
PACT	Protein activator of PKR
PAMP	Pathogen-associated molecular patterns
PB1	Influenza virus polymerase subunit 1
PB1-F2	Influenza virus protein F2
PB2	Influenza virus polymerase subunit 2
PBS	Phosphate buffered saline
PER.C6	Human designer cell line
PERK	Eukaryotic translation initiation factor 2-alpha kinase 3
PI3K/Akt	Phosphatidylinositol 3-kinase/protein kinase B
PIAS	Protein inhibitor of activated STAT
PIP3	Phosphatidylinositol (3,4,5)-triphosphate
PKB	Protein kinase B
PKR/eIF2-α	Protein kinase R/eukaryotic translation initiation factor 2-alpha
PKR-FOR	Forward PKR PCR primer
PKR-REV	Reverse PKR PCR primer
PLB	Promega® passive lysis buffer
polyI:C	Polyinosinic:polycytidylic acid
PR8-NIBSC	Influenza A/Puerto Rico/8/34 (H1N1)-NIBSC
PR8-RKI	Influenza A/Puerto Rico/8/34 (H1N1)-RKI
PRR	Pattern recognition receptor
PTGS	Post translational gene silencing

PVDF	Polyvinylidene difluoride
qPCR/qRT-PCR	Quantitative real-time polymerase chain reaction
R^2	Correlation coefficient
Rac1	Ras-related C3 botulinum toxin substrate 1
Raf	Proto-oncogene serine/threonine-protein kinase
Raf/MEK/ERK	MAPK cascade
RANTES/ CCL5	Regulated upon activation, normal T-cell expressed, and secreted/ Chemokine ligand 5
RBC	Red blood cells
RelA	NF-kappa-B family member, synonymous for p65
RelB	NF-kappa-B family member
RIG-I	Retinoic acid-inducible gene 1
RIPA	Radioimmunoprecipitation assay buffer
RISC	Riboprotein silencing complex
RKI	Robert Koch Institute
RLU	Relative light unit
RNA	Ribonucleic acid
RNAi	RNA interference
RNase L	2-5A-dependent ribonuclease
RNP	Ribonucleoprotein
Rpm	Revolutions per minute
RQ	Relative quantity
RT	Reverse transcription/room temperature
RT-qPCR	Reverse transcription quantitative real-time polymerase chain reaction
S.D.	Standard deviation
Sc	Santa Cruz Biotechnology
SDS-PAGE	Sodium dodecyl sulfate polyacrylamide gel electrophoresis
Sec	Seconds
Ser473	Epitope amino acid serine 473
Ser51	Epitope amino acid serine 51
SH2	Src-homology 2 domain
shRNA	Short hairpin RNA
siRNA	Small interfering RNA
SMAC/ DIABLO	Second mitochondria-derived activator of caspases/ IAP-binding mitochondrial protein
SOCS	Suppressor of cytokine signaling
SOP	Standard operating procedure
Stat1/2	Signal transducer and activator of transcription 1/2
TANK	TRAF family member-associated NF-kappa-B activator
TBK-1	TANK-binding kinase 1/IκB kinase 1
TBS	Tris-buffered saline
TCID50	50% tissue culture infective dose
TEMED	Tetramethylethylenediamine

thaps	Thapsigargin
Thr308	Epitope amino acid threonine 308
TIR	Toll/IL-1R domain
TIR	Toll/interleukin-1 receptor
TLR-3,-7,-8	Toll-like receptor 3/7/8
TNF	Tumor necrosis factor
TRAF	TNF receptor-associated factor
TRAIL	TNF-related apoptosis-inducing ligand
TRIF	TIR-domain-containing adapter-inducing interferon-beta
TRIM25	Tripartite motif-containing protein 25
Tris	Tris(hydroxymethyl)methyl-amine
tris-Cl	Tris(hydroxymethyl)methyl-amine hydrochloride
TSE	Transmissible spongiform encephalopathy
TTBS	Tris-tween buffered saline
Tyk-2	tyrosine kinase 2
Uruguay	Influenza A/Uruguay/716/2007-like HGR
V	Volume
V	Volt
v/v	Volume per volume
VISA	Synonymous for MAVS
vRNA	Viral genomic RNA
vRNP	Viral ribonucleoprotein
w/	With
w/o	Without
w/v	Weight per volume
WHO	World Health Organization
Wisconsin	Influenza A/Wisconsin/87/2005-like HGR
WSN	Influenza A/WSN/33 (H1N1), WSN: Wilson Smith neurotoxic

1 Introduction

Influenza is a highly infectious disease of the upper respiratory tract that occurs in humans and in some animal species. Annually, the disease claims about 36,000 lives and is responsible for approximately 200,000 hospitalizations in the United States alone (Advisory Committee on Immunization et al. 2006). Pandemic influenza has afflicted humanity throughout the ages, which is indicated by historical descriptions of clinical symptoms, the extent and rapidity of disease spread, and the associated mortality, especially in the elderly (Hampson and Mackenzie 2006). Three major pandemics occurred in the 20th century, namely the Spanish influenza pandemic (1918-1919), claiming 50 million lives, and the Asian (1957) and Hong Kong (1968-1969) pandemics, resulting in the loss of 1-2 million lives each (Hampson and Mackenzie 2006). The best protection against seasonal influenza infection is offered by vaccination with a trivalent vaccine, containing surface antigens of two influenza A virus strains (H1N1, H3N2) and one influenza B virus strain. Traditionally, influenza vaccines have been produced in the allantoic cavity of embryonated chicken hens' eggs. Despite high yields of these egg-adapted viruses, this process is associated with a number of problems, which include limited flexibility regarding the expansion of manufacturing capacities, vulnerability of the embryonated-egg supply chain due to disease susceptibility of layer flocks, sterility problems in allantoic fluid processing, and poor growth of some viruses in eggs (Audsley and Tannock 2008). Hence, cell culture-based production processes have been thoroughly investigated and shown to be a viable alternative to egg-based production (Genzel and Reichl 2009; George et al. 2010; Mabrouk and Ellis 2002; Tree et al. 2001). The investigation of cell culture-based vaccine production processes aims at a better understanding of the numerous complex process-related aspects, which is a precondition for process optimization and enhancement.

Attempts for optimization of cell culture-based processes can be pursued from a number of main starting points, comprising the physical cultivation conditions provided by the utilized bioreactor system, optimization of cell culture growth media, characterization and optimization of the respective cell line, as well as a genetic reassortment of the viruses. The first three aspects have to be considered for any bioprocess that is established for the production of biopharmaceuticals, independent of whether the respective product is a monoclonal antibody, a recombinant complex glycoprotein, or a viral vaccine. In the bioprocess engineering (BPE) research group at MPI Magdeburg, all these three aspects are considered and investigated as part of the upstream processing subgroup.

To achieve higher virus yields, repeated fed-batch and perfusion modes are applied in order to raise cell densities and hence process productivity, constituting a process engineering approach for process enhancement (Bock et al. 2010). The cellular metabolism is described in detail during cell growth and virus replication using on- and offline analytical data, comprising cell culture medium metabolite concentration profiles of glucose, glutamine, lactate, ammonium, as well as of essential and non-essential amino acids (Genzel et al. 2004). Besides extracellular metabolite concentration profiles, intracellular metabolite concentrations as well as activities of key enzymes of central carbon metabolism can be measured (Janke et al. 2010; Ritter et al. 2010). Furthermore, the analysis of process-dependent N-glycosylation patterns of viral surface antigens is becoming increasingly important, as it has been shown that the antigenicity and hence vaccine efficacy is dependent on these structures (Abe et al. 2004; Saito et al. 2004). Hence, a method has been established to monitor glycosylation patterns of influenza virus surface antigens and determine their dependency upon process parameters and conditions such as the utilized production cell line (Roedig et al. 2011a; Schwarzer et al. 2009).

The complex issue of influenza virus-host cell interactions has been addressed by a number of studies in the BPE group. Schulze-Horsel et al. have developed a method for flow cytometric monitoring of influenza A virus infection in MDCK cells during vaccine production, which can be applied for the analysis of samples taken from bioreactors (Schulze-Horsel et al. 2008). Subsequently, the use of the method was further expanded, enabling the concomitant analysis of virus replication dynamics and virus-induced apoptosis of the host cell, with both phenomena additionally described by a mathematical model (Schulze-Horsel et al. 2009). Interestingly, Schulze-Horsel could show that different influenza A virus strains induced differences in infection dynamics and apoptosis induction in the infected host cells. Besides monitoring host cell apoptosis, global changes of virus infection on the host cellular proteome were analyzed (Vester et al. 2009). Here, a differential impact of several influenza A virus strains on the host cell proteome could be observed, including proteins whose expression is dependent upon autocrine or paracrine type I interferon (IFN) signaling (Vester et al. 2010). Since both the induction of apoptosis as well as type I IFN-induced protein expression are mediated by cellular signal transduction cascades, the motivation of this research project was to establish a suitable analytical assay to monitor the induction of host cellular signaling cascades by influenza virus infection. It was assumed that, if varying signaling pathway induction levels by the infection with different influenza virus strains were observed, this might reveal new strategies for cell line optimization or process design. Therefore, another aspect of this study was to clarify, if possible, whether the induction of the respective signaling cascades might be

relevant for influenza virus replication and hence process yields in vaccine production. Despite the compelling complexity of cellular signaling phenomena, previous studies have indicated that the assumption that interfering with signaling pathways of the host cell in order to enhance virus replication is justified and that there might thus indeed be room for cell line optimization (de Vries et al. 2008). In the context of the production of biotherapeutics such as monoclonal antibodies or recombinant proteins, cellular stress and the induction of apoptosis have been recognized as factors limiting cellular productivity (Arden and Betenbaugh 2004). Hence, cell engineering attempts have been undertaken to interfere with stress pathways and accordingly improve cell survival, for instance by expressing anti-apoptotic Bcl-2 protein family members (Jung et al. 2002; Mercille et al. 1999). Numerous studies have been performed to elucidate the impact of influenza virus infection on the induction of host cell signaling. The progress of these studies is summarized on a regular basis in a number of excellent review articles (Julkunen et al. 2001; Ludwig et al. 2006; Ludwig et al. 1999; Planz 2006; Takaoka and Yanai 2006). Accordingly, a number of cellular signaling cascades were selected for analysis, comprising the pathways NF-κB, IRF-3, Jak-Stat, Raf/MEK/ERK, PI3K/Akt, and the PKR-mediated phosphorylation of eIF2-α. The induction of host cell signaling cascades is mediated by pathogen-associated molecular pattern (PAMP) receptors (PRRs) upon recognition of conserved pathogenic molecular structures (Meylan et al. 2006). Viruses have evolved strategies to counteract the induction of antiviral signaling, usually by expressing non-structural proteins such as the influenza virus IFN-antagonistic NS1 protein (Fernandez-Sesma et al. 2006; Haller et al. 2006; Levy and Garcia-Sastre 2001; Wolff et al. 2008). In general, the aim of virological studies on the influenza virus-induced activation of host cell signaling pathways is the identification of novel targets for antiviral therapy (Ludwig et al. 2003). During this study, experiments were performed with the aim of identifying targets which, if interfered with, would possibly lead to an enhancement of virus replication. For the analysis of the influenza virus-mediated induction of host cellular signaling pathways, immunoblotting for the analysis of phosphorylation-dependent signaling events was established (Gilbert et al. 2002). Subsequently, studies on the induction of these pathways in MDCK cells by different influenza virus strains were performed (Heynisch et al. 2010). In the meantime, cumulative efforts have led to novel insights of the relevance of antiviral signaling in MDCK cells for influenza virus production, with the main focus on type I IFN signaling (Frensing et al. 2011; Seitz et al. 2010). Furthermore, RNAi technology and a small molecule inhibitor were applied to interfere with the activity of PKR and hence clarify to which degree the replication of influenza virus can be influenced by this interference. Overall,

the results obtained during this study facilitated the interpretation of studies conducted previously in which the impact of influenza virus infection on apoptosis induction and host cellular proteome were investigated (Schulze-Horsel et al. 2008; Vester et al. 2010). However, despite very rational reasons for their generation, the acquired data have also illustrated the difficulty of attempts aimed at a potential optimization of cell lines utilized during influenza vaccine production. Especially the revealed absence of antiviral potency of canine Mx proteins (Seitz et al.) displays that in cell lines selected for robust growth and outstanding virus productivity, a high degree of optimization based on mutation and adaption might already be in place, with no further room for improvement.

2 Background and Theory

2.1 Influenza virus

Annually recurring, influenza virus exerts its pathogenicity on a global scale, affecting millions of people at a staggering economic toll. In comparison, few other infections lead to such a high rate of suffering, medical consultations, hospital admission, absence from the workplace and hence, economic losses. The symptoms caused by this disease are diversified and range from barely noticeable through affection of the respiratory tract, heart, brain, liver, kidney, and muscles to fierce primary viral to secondary bacterial pneumonia. The progression of influenza is influenced by several factors, such as age, degree of pre-existing immunity, virus properties, smoking, comorbidities, immunosuppression, and pregnancy (Nicholson et al. 2003). Worldwide, approximately one in five children and roughly one in twenty adults develop symptomatic influenza A or B each year (Turner et al. 2003). Besides the annually recurring seasonal epidemics, global pandemics occur at irregular intervals of 10 to 40 years. Based on historical evidence, these pandemics have occurred since the 16th century, with Asia as their main point of origin. In the 20th century, three main pandemics have afflicted humanity. Presumably 50 million lives have been claimed by the so-called Spanish influenza pandemic of 1918-1919. Both the Asian (1957) and the Hong Kong (1968-1969) pandemics have resulted in the death of 1 to 2 million people (Hampson and Mackenzie 2006).

2.1.1 Classification and structure

Influenza viruses possess an encapsidated ssRNA genome of negative polarity and belong to the family of *orthomyxoviridae*. The three genera of influenza viruses A, B, and C are differentiated, which are distinguishable according to antigenic differences of the nucleoprotein (NP) and matrix (M) protein (Lamb and Krug 2001). While the RNA genome of influenza A and B is made up of 8 segments, influenza C virus has only 7 genomic RNA segments (Desselberger et al. 1980).

Influenza A viruses are known to infect several species, whereas infections with influenza B and C viruses are limited to humans. Influenza A virus is categorized into subtypes, based on antigenic differences of the viral membrane proteins hemagglutinin (HA) and neuraminidase (NA), of which 17

and 9 different subtypes have been characterized, respectively (Fouchier et al. 2005; Laver et al. 1984; Tong et al. 2012). However, only the subtypes H1N1, H2N2, H3N2, H5N1, H7N7, and H9N2 have so far been isolated from humans (Cheung and Poon 2007; Claas et al. 1998; Fouchier et al. 2004; Guan et al. 2003; Guan et al. 1999; Subbarao et al. 1998; Yuen et al. 1998).

Influenza virions are pleomorphic and can occur in shapes from long filaments to small spheres with a diameter of about 75 to 120 nm (Cheung and Poon 2007; Lamb and Krug 2001). Besides genetic determinants for virion shape, it has been found out that the respective host cell also has an influence on viral morphology (Elleman and Barclay 2004; Roberts and Compans 1998). The outer lipid bilayer of the virion is host cell membrane-derived and stems from the budding process (Kates et al. 1962). Both of the viral surface glycoproteins HA and NA as well as the matrix protein M2 are embedded in the lipid membrane.

HA is a homotrimer responsible for binding receptors on the cell surface that carry sialic acids. Furthermore, HA mediates the fusion of cellular and viral membrane and is therefore crucial for viral infectivity (Lamb and Krug 2001; Steinhauer 1999).

NA is a homotetrameric protein with a box-shaped globular head domain, a thin stalk, a transmembrane and a cytoplasmic domain (Hausmann et al. 1997; Varghese and Colman 1991). The receptor destroying activity of NA by cleaving the α-ketosidic linkage between a terminal sialic acid and an adjacent D-galactose or D-galactosamine residue is a precondition for the release of progeny viral particles (Colman 1999; Palese and Compans 1976; Palese et al. 1974).

The ion channel M2 exists as a disulphide-bonded tetramer and is responsible for the acidification of the interior of viral particles in the process of infecting the host cell (Holsinger and Lamb 1991; Pinto et al. 1992; Wang et al. 1994). It has been shown that this acidification is necessary for the release of the viral genome into the cytoplasm of the host cell (Bui et al. 1996; Martin and Helenius 1991).

The matrix protein M1 layer separates the outer lipid bilayer from the internal ribonucleoprotein complexes (vRNP) of the virus particle and has been shown to interact with both the vRNA as well as with the protein components of the vRNP during assembly and disassembly of influenza A viruses (Ruigrok et al. 2000; Ruigrok et al. 1989; Ye et al. 1999).

The internal vRNP complexes consist of the 8 RNA segments, each of which is, via its phosphate sugar backbone, bound to nucleoprotein (NP) and a polymerase complex made up of the three subunits PB2, PB1, and PA (Baudin et al. 1994; Lamb and Choppin 1983). It was shown that by forming a circular or supercoiled structure, both ends of the vRNA interact with each other (Hsu et al. 1987; Jennings et al.

1983). In addition to the vRNP complexes, nuclear export protein (NEP) or nonstructural protein 2 (NS2) is present in low amounts in the internal space of the virus encapsidated by M1 (Yasuda et al. 1993). The NEP is responsible for the nuclear export of vRNP complexes (O'Neill et al. 1998). An illustration of the influenza A virus is depicted in Figure 2.1-1.

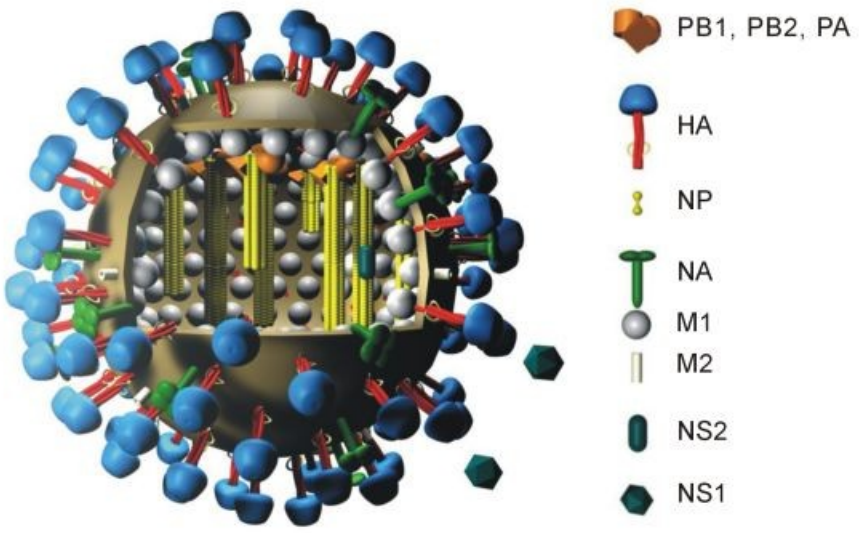

Figure 2.1-1: Structure of influenza A virus
Influenza virus particles are enclosed by a host cell-derived lipid bilayer, in which the glycoproteins HA and NA are embedded. The transmembrane ion channel M2 pervades the lipid bilayer and the structural protein M1 is localized directly underneath the membrane in the interior space. The interior virus core is constituted by single-stranded RNA of negative polarity, which is associated with NP and the three viral polymerases (PB1, PB2, PA), which together constitute the vRNP capsid complex. Picture from Wiki Commons (Eickmann 2005).

In addition to the aforementioned structural proteins of influenza A virus, the virus possesses two nonstructural proteins, namely PB1-F2 as well as the nonstructural protein 1 (NS1). PB1-F2 has been shown to possess a proapoptotic function mediated by the mitochondrial carrier protein adenine nucleotide translocator 1 (Chen et al. 2001).

The NS1 protein accumulates mainly in the nucleus of infected cells (Greenspan et al. 1988) and fulfills a multitude of diversified functions, which will be explained in more detail in chapter 2.2.

2.1.2 The lifecycle of influenza A virus

The replication of influenza A virus starts with the attachment of the influenza surface glycoprotein HA to either α2,3-linked sialic acid or to α2,6-linked sialic acid surface receptor molecules of the host cell, depending on the amino acid sequence in the binding pocket of HA (Connor et al. 1994; Vines et al. 1998). The attachment is followed by internalization of the virus particle, which predominantly occurs in a clathrin-dependent endocytosis (Matlin et al. 1981).

After internalization, the endosomal compartment is acidified by cellular proton pumps, which leads to irreversible conformational changes of the HA once a pH value between 5.0 and 6.0 is reached. These conformational changes lead to the extrusion of a hydrophobic domain of the HA protein that interacts with the endosomal membrane, referred to as 'fusion peptide'. This fusion peptide is a prerequisite for the fusion of viral and endosomal membranes (Skehel et al. 1995). It has been shown that if the endosomal pH value is raised by the effects of the antiviral drug amantadine, influenza virus replication is inhibited. Mutant viruses resistant to the drug have been shown to have a higher pH value of membrane fusion activity (Daniels et al. 1985). In addition to the conformational change of the HA protein induced during acidification of the endosome, a decrease of the pH value to about 5.0 leads to the activation of the viral M2 ion channels, which raises the proton concentration in the interior of the virus (Pinto et al. 1992). This acidification of the interior of the virus particle leads to conformational changes of the M1 protein, which provides for the dissociation of vRNPs, a process also called virus uncoating, and their subsequent nuclear import (Martin and Helenius 1991). All three viral RNA polymerase subunits PB1, PB2, and PA contain nuclear localization signals (Mukaigawa and Nayak 1991; Nath and Nayak 1990; Nieto et al. 1994). These nuclear localization signals are required for transport of vRNPs into the nucleus (Jones et al. 1986).

The nucleus of the infected host cell is the transcription and replication site for the genome of influenza virus (Herz et al. 1981; Jackson et al. 1982). The first step of transcription is the binding of the polymerase subunit PB2, which has endonucleolytic activity, to the 5' end of host cell mRNA, followed by its cleavage 10 to 15 nucleotides downstream from the monomethylated RNA cap structure (m^7GpppX^m) after mainly an A or a G residue (Plotch et al. 1981; Shi et al. 1995). PB2 binds the host mRNA cap structure and uses it to generate cap primers for the synthesis of viral mRNAs, a process that has come to be known as cap-snatching (Blaas et al. 1982; Plotch et al. 1979; Ulmanen et al. 1981). The

m^7GpppX^m cap structure of host cell mRNAs is the preferred primer of the viral polymerase complex for transcription (Bouloy et al. 1980).

A precondition for the initiation of viral transcription is the interaction of the conserved sequence structures of vRNA at the 5' and 3' ends (Fodor et al. 1994). While the generation of cap structures and initiation of transcription are functions of the polymerase subunit PB2, the polymerase subunit PB1 is responsible for RNA polymerization, which was indicated by the fact that the elongated RNA product, the vRNA template, and the substrate of the reaction could be photochemically cross-linked to this subunit (Asano and Ishihama 1997; Braam et al. 1983; Fodor et al. 1993). The termination of viral transcription occurs at a stretch of 5 to 7 uracil (U) residues 17 nucleotides from the 5' end of vRNA, which is then followed by polyadenylation of the viral mRNA transcript (Poon et al. 1998; Robertson et al. 1981). Both the mRNA cap structure as well as the poly (A)-tail have been shown to be required for the nuclear export of mRNA and its stabilization (Beelman et al. 1996; Carpousis et al. 1999; Eckner et al. 1991; Hamm and Mattaj 1990). The capped and polyadenylated viral mRNAs are transported from the nucleus to the cytoplasm where protein synthesis occurs.

During the replication of the viral genome, a copy of the genomic negative-stranded viral RNA is synthesized (cRNA), which then serves as a template for vRNA synthesis. As opposed to transcription, for which the PB2, PB1, and PA subunits of the viral polymerase complex are required, viral genome replication is dependent on the PB1 and PA subunits (Nakagawa et al. 1995). The 5'-triphosphate end of cRNA indicates that the synthesis of cRNA is primer-independent (Hay et al. 1982). Furthermore, the synthesized cRNAs have not been shown to be polyadenylated at their 3' ends. As the RNA-dependent influenza A virus RNA polymerase complex is responsible for both transcription and replication, a mechanism for switching between both processes would be deemed necessary. Yet, this mechanism is still not completely understood. However, it has been suggested that nascent cRNA as a replicative intermediate is degraded by host cell nucleases unless the molecule is stabilized by viral RNA polymerase and NP proteins that are newly synthesized. Hence, no switching from transcription to replication would be required (Vreede et al. 2004). As needed for the assembly of progeny viruses, vRNAs are synthesized accordingly in equimolar amounts (Shapiro et al. 1987; Smith and Hay 1982; Yasuda et al. 1993). The helical vRNP complexes are assembled in the nucleus of the host cell. Nuclear export of the vRNP complexes through the nuclear pores has been shown to be mediated by the M1 protein (Martin and Helenius 1991). Furthermore, experimental evidence suggests that the NS2 or NEP protein might also contribute to the process of nuclear export due to an interaction with the M1 protein

that might be regulatory or cooperative (Yasuda et al. 1993). It was later shown that the NEP protein interacts with the host cell CRM1/exportin-1 nuclear export protein, which further emphasized its significance in nuclear export of vRNPs (Boulo et al. 2007; Neumann et al. 2000).

The extent to which viral proteins are synthesized in the host cell is dependent on the amount of corresponding viral mRNA in the cell (Shapiro et al. 1987). Primary transcription occurs immediately after infection, at which stage all eight mRNAs are synthesized in equimolar amounts (Hay et al. 1977). The secondary stage of transcription is subdivided into early and late phase. During the early phase there is a preference for the synthesis of NS1 and NP vRNAs, which results in NS1 and NP being the predominant viral proteins synthesized in infected cells at this time. During the late stage of viral protein expression the NS1 protein is synthesized at a lower level and the structural proteins HA, NA, and M1 mRNAs are preferentially expressed. For protein maturation the three viral membrane proteins HA, NA, and M2 need to pass the secretory pathway of the trans-Golgi network. The post-translationally modified proteins NA and HA are transported to the cell surface in order to be integrated into the cellular membrane (Cheung and Poon 2007).

Budding is the process during which the newly synthesized virus particles leave the host cell, obtaining their lipid bilayer as chunks of the cellular membrane. Preconditions for this morphogenesis are that the three viral envelope glycoproteins HA, NA, and M2, the M1 protein, and the vRNPs are translocated to the assembly site at the apical plasma membrane of polarized epithelial cells (Schmitt and Lamb 2005). This translocation is facilitated either by lipid rafts, apical determinants, simple diffusion, or a combination of all these mechanisms. At the assembly site, virus particles are packaged in such a manner as to ensure that each virus particle obtains a full copy of each of the 8 viral genomic RNA segments. During the assembly process M1 fulfills a crucial function as it bridges the envelope glycoproteins with the vRNP complexes (Schmitt and Lamb 2005). The following outward membrane curvature of a bud is caused by several factors such as concentration of and interaction among viral components, increased viscosity and asymmetry of the lipid bilayer, as well as attracting and rejecting forces between viral and host cell components (Nayak et al. 2004).

Virus particles are released upon bud completion by the fusion of opposing membranes resulting in the detachment of the virus and release into the extracellular environment (Nayak et al. 2004). The membrane glycoprotein NA plays a crucial role in the detachment of virus particles from the cellular membrane, as it has been shown that if the enzyme activity of NA is blocked by inhibitors or deletions in the NA gene, virus particles are retained on the cellular surface (Barman et al. 2004; Palese and

Compans 1976; Palese et al. 1974). The function of NA is the removal of sialic acid from the cellular membrane glycolipids and glycoproteins, as sialic acid is the receptor for influenza virus. Thus, self-aggregation and reattachment of the influenza virus to the cell is prevented (Nayak et al. 2004). For a detailed overview of influenza A virus replication, see Figure 2.1-2.

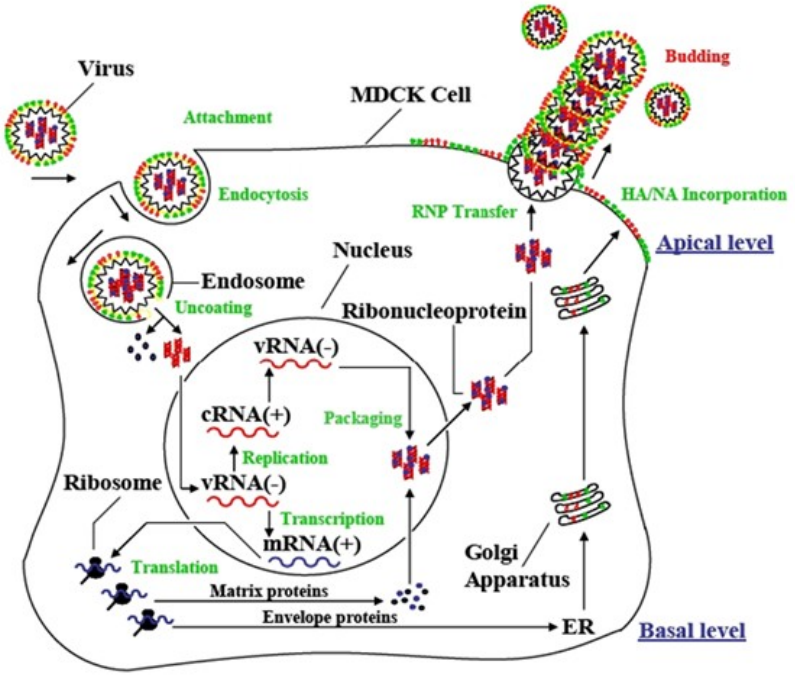

Figure 2.1-2: Influenza A virus replication.
The replication cycle of influenza virus is initiated with membrane attachment and fusion (1), uncoating (2), synthesis of cRNA (+) from vRNA (-), replication of vRNA (-), as well as transcription and translation of vmRNAs (+) in order to synthesize viral proteins (3-5). The cycle is completed by the post-translational modification of viral proteins (6), the assembly of structural components of the virus (7) and the release of progeny virus (8) (Sidorenko and Reichl 2004).

2.2 Interactions between influenza virus and host cell

The infection with influenza A virus has a vast impact on functions and processes of the host cell, which are in part either suppressed or actively exploited by the virus for the sake of its own replication. These altogether innumerable functions comprise the modification of cellular gene expression through the manipulation of signaling pathways and transcription factors, RNA processing, translation, posttranslational processing, the utilization of nuclear export mechanisms and of the cellular transport machinery, as well as apoptosis induction. Astoundingly, the virus has evolved the ability to suppress and even exploit processes originally triggered by the cell upon recognition of viral molecular patterns as part of distinct antiviral countermeasures.

A number of selected interactions will be explained in more detail in this chapter. However, by describing these few complex interactions one cannot even begin to fathom the real myriad of influenza virus-host cell interactions. As published in 2009 by Shapira et al., through the use of an experimental and computational approach host cell networks were uncovered that are contacted by viral proteins, and the cellular transcriptomal response to infection and functional roles of identified genes were revealed. Altogether, using gene expression profiling, 1,745 genes were discovered that play a role in influenza virus replication or in the corresponding host response to infection. Utilizing a yeast two-hybrid approach, it was discovered that there are 135 pairwise interactions between the ten major viral proteins (all but PB1-F2) and 87 proteins of the analyzed human bronchial epithelial cell line (HBEC). On average, each influenza virus protein interacts with 13.5 human proteins (Shapira et al. 2009).

An important interaction between virus and host cell that is vital to the replication of the virus is the aforementioned cap-snatching by the viral polymerase subunit PB2. These 5'-cap structures are taken from cellular polymerase II transcripts (Krug et al. 1979). Hence, the application of the cellular polymerase II inhibitor α-amanitin has been shown to inhibit virus replication (Rott and Scholtissek 1970). Another important interaction is the use of the host cellular transport machinery by the virus for transfer of its proteins with nuclear localization signals such as the viral polymerase subunits (Neumann et al. 1997; Wang et al. 1997; Weber et al. 1998).

The NS1 protein fulfills a diversity of functions in the infected cell from the regulation of viral and cellular mRNA processing and expression to the counteraction of antiviral defense. It binds to different RNA molecules, for instance polyadenylated cellular mRNA (Qiu and Krug 1994), vRNA (Hatada et al. 1992), and dsRNA (Hatada and Fukuda 1992).

NS1 negatively interferes with cellular RNA processing (Fortes et al. 1994; Lu et al. 1994), the nuclear export of cellular mRNAs (Qiu and Krug 1994), and cellular mRNA polyadenylation (Chen et al. 1999). It was later demonstrated that the interference with cellular mRNA processing by NS1 is mediated by the interaction with the cellular cleavage and polyadenylation specificity factor (CPSF4) (Nemeroff et al. 1998; Nemeroff et al. 1995). In turn, NS1 enhances the translation of mRNAs that carry the viral 5'-end sequences, which has been suggested to be mediated by the recruitment of the eukaryotic translation initiation factor 4GI (eIF4GI) specifically to the 5' untranslated region of the viral mRNA (Aragon et al. 2000; de la Luna et al. 1995; Enami et al. 1994). Furthermore, the activation of RIG-I (Guo et al. 2007; Mibayashi et al. 2007) as well as of PKR has been shown to be inhibited by NS1 (Lu et al. 1995). These active measures exerted by the NS1 protein to counteract the antiviral defense of the host cell will be described separately in section 2.2.4.

Influenza A viruses have to rely on the post-translational protein processing machinery of the host cell. The type I and II glycoproteins HA and NA pass the exocytotic cellular transport pathway via the rough endoplasmatic reticulum (rER), the Golgi complex, and the trans-Golgi network. In the rER, the N-glycosylation by oligosaccharyltransferases takes place. Furthermore, protein folding and intramolecular disulfide bond formation of the HA occur co- and post-translationally in the rER, which is catalyzed by disulfide isomerase (Braakman et al. 1991). Folding intermediates with incomplete disulfide bonds are bound by the chaperones calnexin and calreticulin. The rER is also the site where acetylation by acyltransferases takes place (Berger and Schmidt 1985). Once the rER is passed, further modifications occur in the Golgi complex, such as final oligosaccharide processing. Furthermore, protein phosphorylation by cellular kinases seems to be of importance, as the pronounced effect of kinase inhibitors on viral replication suggested (Ludwig et al. 1999).

2.2.1 Influenza virus infection and apoptosis induction

Apoptosis or programmed cell death is a biochemical program executed by the cell for cellular self-termination in response to a wide range of stimuli, which is mediated by intracellular apoptotic cascades (Kerr et al. 1972). Two modes of apoptosis induction have been described, namely the extrinsic and the intrinsic pathway involving either the procaspases 8 and 10, or procaspase 9, respectively. Caspases are a class of cysteine proteases known to orchestrate the intracellular biochemical events that lead to cell

death (Salvesen 1999), with the exception of the caspase-independent apoptotic pathway mediated by the apoptosis inducing factor (AIF).

Two groups of caspases are differentiated, namely the upstream initiator caspases and the downstream effector caspases, which comprise the caspases 2, 8, 9, and 10 or 3, 6, and 7, respectively (Thornberry 1998). Once activated, the purpose of upstream initiator caspases is to cleave the downstream procaspases and hence convert them into the active effector caspases, with caspase 3 being the main effector.

The extrinsic pathway of apoptosis induction is triggered by the stimulation of cell surface death receptors belonging to the family of tumor necrosis factor (TNF) receptors that detect extracellular apoptosis signals such as FasL, TNF-α, or TRAIL (Ashkenazi and Dixit 1999; Barber 2001; Wiley et al. 1995). This detection of external death signals induces the activation of the initiator caspases 8 and 10 that further implement the apoptotic program.

The intrinsic pathway is mediated by the release of mitochondrial membrane proteins such as cytochrome C, SMAC/DIABLO or AIF by mitochondrial membrane permeabilization (Brenner et al. 2000; Du et al. 2000; Li et al. 1997; Susin et al. 1999; Verhagen et al. 2000). The release of mitochondrial membrane proteins is regulated by the family of Bcl-2 proteins, whose members either promote (e.g. Bax, Bad) or inhibit (e.g. Bcl-2, Bcl-xL, Mcl-1) the onset of apoptosis in a tightly controlled process, which involves the adenine nucleotide translocator (ANT) (Brenner et al. 2000; Crompton 2000). Before the apoptotic program following the intrinsic mode is induced, caspase 9 exists in its inactive form as a procaspase, which is then activated upon cleavage by the apoptosome. The apoptosome is created by the association of cytochrome C released from the mitochondrial membrane with the apoptotic protease activating factor 1 (Apaf-1), ATP, and procaspase 9 (Li et al. 1997).

The targets of effector caspases include proteins vital for cellular integrity as well as some that prevent nuclear degradation and DNA fragmentation (Barber 2001). The morphological hallmarks of apoptosis such as membrane blebbing, chromosomal DNA fragmentation, chromatin condensation, and cell shrinkage are the eventual effects of caspase activation (Barber 2001; White 1996).

The infection with numerous viruses has been shown to lead to apoptosis induction in the host cell (Young et al. 1997). Takizawa et al. have shown that the infection with influenza A virus of cultures of MDCK and HeLa cells led to the induction of apoptosis (Takizawa et al. 1993). It has later been shown that apoptosis is induced in a wide range of host cells by the infection with numerous subtypes of all three influenza virus types A, B, and C (Hechtfischer et al. 1997; Hinshaw et al. 1994; Lin et al. 2002;

Mersich et al. 2004; Takizawa et al. 1999; Wurzer et al. 2003; Zhirnov et al. 1999). However, the degree to which apoptosis and cytotoxicity is induced in the cell by the infection with different types and subtypes of influenza virus varies (Hornickova 1997; Mersich et al. 2004; Mohsin et al. 2002; Price et al. 1997; Schulze-Horsel et al. 2009). The reasons for this varying impact on apoptosis induction in the host cell by different influenza virus strains, types, and subtypes remain incompletely understood. The wide range of potential molecular inducers of apoptosis testifies to the complexity of apoptosis inducing mechanisms. Evidence for an involvement of viral dsRNA in the induction of apoptosis in HeLa cells has been obtained (Takizawa et al. 1996). Furthermore, no fewer than 5 of the viral proteins (NS1, PB1-F2, NA, HA, and M) have been associated with the induction of apoptosis in the host cell (Coleman 2007; Morris et al. 2002; Ohyama et al. 2003; Schultz-Cherry et al. 2001; Schultz-Cherry and Hinshaw 1996). Interestingly, regarding the induction of apoptosis the viral protein NS1 has a bivalent character as it has also been shown to be antiapoptotic since recombinant influenza viruses missing the NS1 protein have been shown to be stronger apoptosis inducers than wild type viruses (Zhirnov et al. 2002). In addition to a direct involvement of viral molecules in the induction of apoptosis, it has been shown that the autocrine and paracrine action of IFN is also a strong mediator of apoptosis induction in epithelial cells (Balachandran et al. 2000; Kim et al. 2002; Ludwig et al. 2006). Many viruses modulate apoptosis either negatively or positively and have evolved a multitude of apoptosis modulating proteins (Galluzzi et al. 2008). Strong evidence supports the notion that during its replication influenza virus benefits from the induction of apoptosis, even though the original function of the apoptotic program initiated by the host cell is the limitation of viral infection. The overexpression of the antiapoptotic human protein Bcl-2 in MDKC cells resulted in impaired influenza A virus replication, which was furthermore correlated with a misglycosylation of the viral surface protein HA (Hinshaw et al. 1994; Olsen et al. 1996). Additionally, influenza virus propagation was strongly impaired in the presence of caspase inhibitors and in cells where caspase 3 was knocked down partially by the use of siRNA (Wurzer et al. 2003). Several cellular signaling pathways triggered by influenza virus infection have been associated with the induction of apoptosis, which will be explained in more detail in the next chapter.

2.2.2 Innate immunity induced by influenza virus

Cellular innate immunity constitutes the first barrier against pathogen intrusion and discriminates efficiently between self and non-self molecular structures despite the lack of adaptive mechanisms. This is achieved by a number of receptors that inherit their specificity through the genome and are expressed in all cells of a given cell type. These receptors recognize a large scope of microbial pathogens by the distinct molecular structures they carry and induce immediate responses. For an overview a number of excellent references is given in which the phenomenon of innate immunity is explained in further detail (Beutler 2004; Chaplin 2006; Magor and Magor 2001; Uthaisangsook et al. 2002).

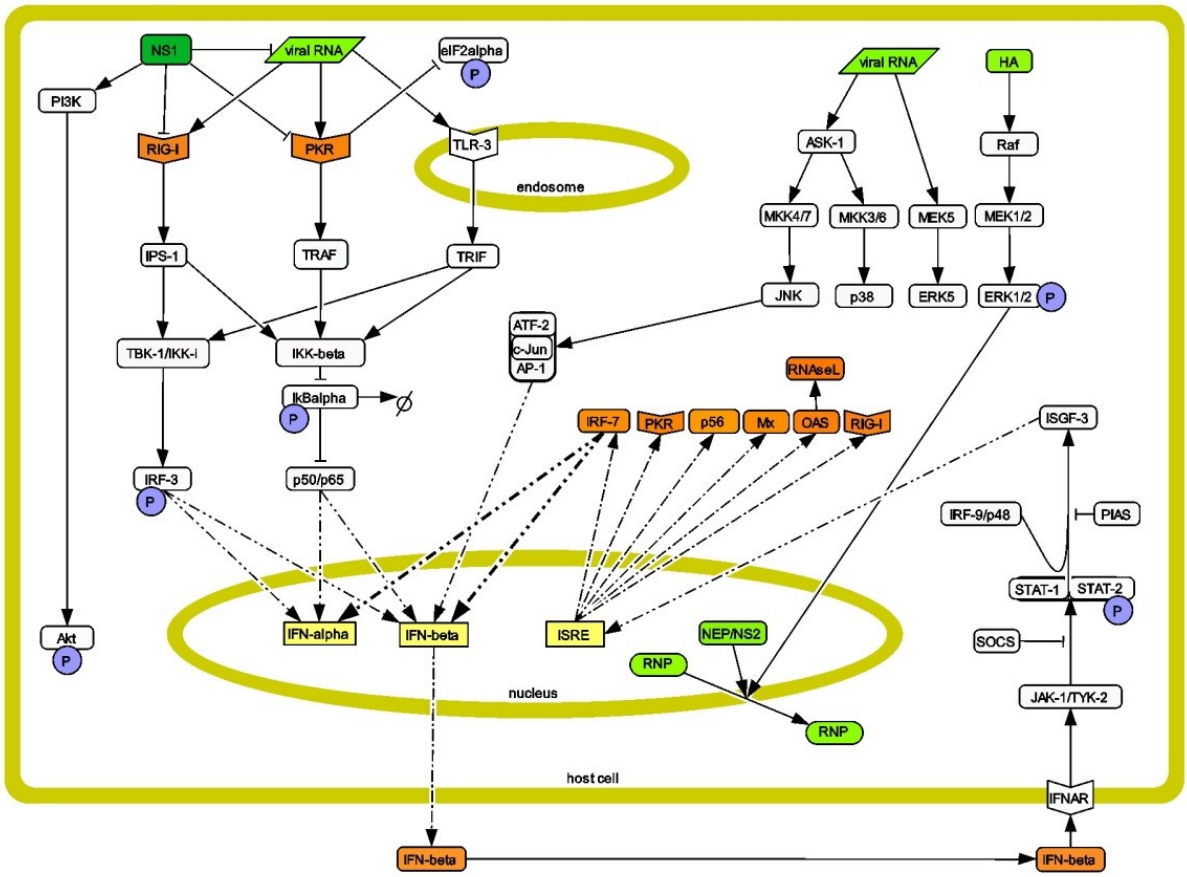

Figure 2.2-1: Cellular signaling pathways induced in epithelial cells by influenza A virus infection.
The depicted signaling pathways are relevant in cellular innate immunity. The scheme was created according to literature reviews (Ludwig 2007; Ludwig et al. 2006; Takaoka and Yanai 2006). Viral components are depicted in green, cellular genes in yellow, phosphorylation events chosen for analysis blue, whereas IFN and IFN-induced proteins are shown in orange (CellDesigner™ Ver.3.5, The Systems Biology Institute, Tokyo, Japan).

In the bioprocess for vaccine production that was investigated here only the single canine-derived epithelial cell line MDCK came to use. Therefore, the focus in this chapter is on basic mechanisms of innate immunity mediated by specific receptors and signaling pathways on a cellular and subcellular level. The first step in the induction of cellular innate immunity is the detection of pathogen-associated microbial patterns (PAMPs), denoting structural features of microbes, or viruses, by pattern recognition receptors (PRR) (Janeway 1989). The toll-like receptors (TLR) are an important family of PRRs, which act as sensors of the cellular innate immunity by detecting PAMPs such as, for instance, lipopolysaccharide (LPS), flagellin, or dsRNA. An overview of signaling pathways induced in epithelial cells upon influenza virus infection is given in Figure 2.2-1, which will be explained in more detail in the following chapter.

An important molecular structure of influenza viruses responsible for triggering innate immune reactions is dsRNA, which is a ligand for TLR3 (Alexopoulou et al. 2001). Another molecular structure associated with viral infection is ssRNA, which has been shown to be a ligand for TLR7 and TLR8 (Heil et al. 2004). Furthermore, dsRNA is sensed by the protein kinase R (PKR) and by the intracellular receptor retinoic acid inducible GTPase-I (RIG-I) and its homolog mda-5 (Kato et al. 2005; Lengyel 1987; Siren et al. 2006; Yoneyama et al. 2004). However, viral RNA is not the only molecular structure that leads to the activation of cellular receptors. The influenza A virus NS1 protein has been shown to activate Phosphatidylinositol 3-kinase (PI3K) by binding to its p85β subunit via a phosphorylated tyrosine residue (Ehrhardt et al. 2006; Hale et al. 2006). Additionally, other pathways have also been shown to be activated by viral proteins. The expression of the viral envelope protein HA has been found to correlate with the activation of ERK (Marjuki et al. 2006). Another aspect also makes the Raf/MEK/ERK signaling pathway exceptional, since neither did dsRNA lead to its activation nor could it be suppressed by the viral NS1 (Marjuki et al. 2006). In the following, the function and significance of signaling pathways that were analyzed in this study is explained.

2.2.3 Structure, mechanism and significance of signaling pathways

In this chapter, cellular signal transduction pathways relevant during influenza virus infection and replication are described in detail. An overview of these signaling cascades is illustrated in Figure 2.2-1. Due to their relevance for influenza virus replication, the induction of these signaling pathways was analyzed experimentally in the course of this project to compare the potency of different influenza virus strains and variants to induce or suppress the activation of these pathways. In epithelial cells, the most effective component of innate immunity is the IFN system, which mediates the activation of more than 300 genes, with a large fraction of them involved in the antiviral response (Content 2009; Katze et al. 2002; Randall and Goodbourn 2008; Samuel 2001a). The signaling pathways leading to the activation of the three transcription factors nuclear factor kappa-light-chain-enhancer of activated B cells (NF-κB), interferon regulatory factor 3 (IRF-3), and activating transcription factor (ATF-2), that, together with c-Jun, forms the activator protein 1 (AP-1), contribute to the expression and secretion of IFN-beta.

2.2.3.1 *Nuclear factor kappa-light-chain-enhancer of activated B cells (NF-κB)*

The expression of a vast number of cellular genes involved in the antiviral defense, cellular stress response, and immune system activation, such as cytokines, IFNs, immunoreceptors, and chemokines requires the activation of NF-κB (Genin et al. 2000; Pahl 1999). Multiple families of viruses, including influenza virus, induce the NF-κB signaling pathway upon infection of the host cell. In the course of this process, a number of functions have been ascribed to the pathway, which include the promotion of viral replication, the prevention of virus-induced apoptosis, as well as the mediation of the immune response to the invading pathogen (Hiscott et al. 2001). Besides the modes of activation by viral RNA described in more detail in chapter 2.2.3.5, NF-κB has also been shown to be induced by the expression of the influenza virus proteins HA, NP, and M1 (Flory et al. 2000).

The NF-κB family constitutes a group of dimeric transcription factors that belongs to the Rel family, which includes five members, namely NF-κB1 (p105/p50) and NF-κB2 (p100/p52) that, as homodimers, function as repressors since they are devoid of transcription activation domains, as well as the transcriptional activators RelA (p65), RelB, and c-Rel, with whom p50 as well as p52 form heterodimers, thereby also participating in target gene transactivation (Ludwig and Planz 2008). The

induction of NF-κB signaling takes place through the activation of the inhibitor of IκB-kinase (IKK) complex. This complex comprises the three members IKK1/IKK-alpha, IKK2/IKK-beta, and NEMO/IKK-gamma. The main kinase responsible for the phosphorylation of the inhibitor of NF-κB (IκBα) is IKK2/IKK-beta. The phosphorylation of IκBα subsequently leads to its degradation and to the release of the p65 and p50 transcription factors that migrate to the nucleus (Ludwig and Planz 2008).

As initially addressed, the NF-κB signaling pathway had been assumed to play a general role in the activation of the innate immunity defense of the host cell (Chu et al. 1999). However, later it was shown that the activity of NF-κB also displays characteristics beneficial for influenza virus replication. This is at least partially due to the NF-κB dependent expression of factors involved in apoptosis induction such as TRAIL or FasL (Wurzer et al. 2004). Wurzer et al. have furthermore shown that the siRNA mediated knockdown of caspase 3 leads to a pronounced impairment of influenza virus propagation (Wurzer et al. 2003). The reason for this impairment is seemingly given by a nuclear retention of vRNP complexes in the presence of caspase or NF-κB inhibitors (Mazur et al. 2007; Wurzer et al. 2003). As early as 1994, Hinshaw et al. showed that the cellular apoptotic machinery is induced by influenza viruses and that the overexpression of the antiapoptotic protein Bcl-2 leads to a retainment of vRNP complexes in the nucleus (Hinshaw et al. 1994).

A side effect of acetylsalicylic acid (ASA) is its function as an inhibitor that exerts a very efficient effect on IKK-beta, thereby preventing NF-κB activation (Yin et al. 1998). In turn, the activation of NF-κB by the expression of a constitutively active form of IKK-beta prior to infection led to an enhancement of influenza virus replication (Wurzer et al. 2004). This finding was confirmed in a second approach in which cells were infected with influenza virus that displayed different degrees of constitutive NF-κB activity (Nimmerjahn et al. 2004).

Besides the proapoptotic function of NF-κB that is exploited by the virus for its own replication, the upregulation of the suppressor of cytokine signaling 3 (SOCS3) in an NF-κB dependent manner by the accumulation of viral RNA is regarded as a second mechanism by which influenza virus might benefit from NF-κB activation. The family of SOCS proteins has been shown to block the activation of the Jak-Stat signaling pathway (Seki et al. 2003). Hence, antiviral gene expression responses conferred by type I IFN are limited by the action of SOCS3 (Pauli et al. 2008).

2.2.3.2 ***Interferon regulatory factors 3 and 7 (IRF-3, IRF-7)***

The IRFs are immunomodulatory proteins that are also involved in cell cycle control, apoptosis induction, and as tumor suppressors (Heylbroeck et al. 2000; Honda and Taniguchi 2006). To date, nine different IRFs have been identified in humans (Hiscott 2007). For the expression of the cytokine IFN-beta as well as of the chemokine RANTES, the activation of IRF-3 is preconditional (Barnes et al. 2002; Genin et al. 2000; Hiscott et al. 1999). The activation of IRF-3 upon viral infection by upstream kinases will be discussed in more detail in 2.2.3.5. In its inactive form, the constitutively expressed IRF-3 shuttles into and out of the nucleus, whereas its phosphorylation at the C-terminus induces a conformational change of IRF-3 that permits its homo- and heterodimerization as well as association with the co-activator CREB-binding protein/E1A binding protein (CBP/p300) resident in the nucleus (Lin and Hiscott 1999). This association of IRF-3 with CBP/p300 sequesters the transcription factor in the nucleus, leading to transcriptional activation of IFN-beta among other genes (Kumar et al. 2000).
Unlike IRF-3, IRF-7 is constitutively expressed only in B-cells and dendritic cells, whereas in other cell types, IRF-7 is virus- and IFN-inducible (Hiscott 2007). Similar to IRF-3, it is also a multifunctional protein that confers transcriptional activity, which is activated upon a C-terminal phosphorylation event (Lin et al. 2000; Sato et al. 1998). It has been demonstrated by Honda et al. that IRF-7 is substantial for the induction of the type I IFN response of the host, as the inhibition of IRF-7 led to reduced levels of IFN-beta mRNA (Honda and Taniguchi 2006). Most importantly, the activation of IRF-7 constitutes a positive feedback loop with regard to IFN-alpha/beta expression, as it regulates many IFN-alpha genes and has also been shown to interact with IRF-3 (Au et al. 2001; Marie et al. 1998; Sato et al. 1998).

2.2.3.3 ***Mitogen-activated protein (MAP) kinases***

MAP kinases are evolutionarily highly conserved signaling cascades that transform numerous extracellular signals, including virus infection, into diverse cellular responses ranging from proliferation and differentiation to activation of the immune response as well as cell death and apoptosis (Dong et al. 2002; Pearson et al. 2001; Planz 2006). Four different MAPK pathways are differentiated, namely the extracellular signal-regulated kinase (ERK1/2), the c-Jun N-terminal kinase (JNK), p38, and the Big MAP Kinase (BMK-1)/ERK5 signaling cascades (Pearson et al. 2001). All four pathways are activated

by a dual phosphorylation of threonin and tyrosin by upstream kinases called the MAP kinase kinases (MEK/MKK). Here, ERK1/ERK2, which are also referred to as p44/p42 MAPK, are activated by MEK1/MEK2, which in turn are activated by a dual phosphorylation through the serine and threonine specific kinase Raf. The Raf/MEK/ERK pathway is known as the classical mitogen-activated protein kinase pathway. The JNK pathway is activated by the upstream kinases MKK4/MKK7 and p38 is phosphorylated by MKK3/MKK6. Furthermore, ERK5, whose function is still not known as of yet, has been shown to be activated by MEK5 (Planz 2006). Both the activation of JNK as well as of p38 is mediated by the apoptosis signal-regulating kinase 1 (ASK-1), a kinase of the kinase of MAP kinases (MAPKKK) that activates MKK4 and MKK6 by a dual phosphorylation (Ichijo et al. 1997).

Although the exact biochemical mode of activation has not been revealed yet, it is known that the infection with influenza virus leads to an activation of all four MAPK signaling pathways through the accumulation of viral RNA (Kujime et al. 2000; Ludwig et al. 2001; Pleschka et al. 2001).

The functions of the MAP kinases are widespread. One of the more prominent functions is for example an involvement of JNK and p38 in the expression of the chemokine RANTES that is responsible for the recruitment of eosinophiles in inflammatory processes (Kujime et al. 2000). The activation of p38 after infection of macrophages with influenza virus was shown to be involved in the hyperinduction of cytokines such as TNF-alpha (Lee et al. 2005). Regarding the induction of type I IFNs, the activation of JNK regulates the activation of the transcription factors c-Jun and ATF-2, which are together in the protein complex AP-1 part of the enhanceosome that binds to the IFN-beta promoter (Karin et al. 1997). Accordingly, the finding that the inhibition of MKK7, JNK, or c-Jun with the help of dominant negative mutants led to a reduced transcription of IFN-beta and increased influenza virus replication rates in the respective cell line underlines the antiviral character of the MAPK JNK (Ludwig et al. 2001).

Due to this obvious distinctive antiviral characteristic of this member of the MAP kinase family, the results of the investigation of the role of the Raf/MEK/ERK signaling pathway in influenza virus replication were initially perhaps rather surprising. Marjuki et al. have shown that the Raf/MEK/ERK pathway is induced by the accumulation of the viral envelope protein HA at the cellular membrane and its corresponding association with lipid rafts (Marjuki et al. 2006). The finding that the disruption of the HA/lipid-raft association as well as the inhibition of the Raf/MEK/ERK pathway by dominant negative mutants or specific MEK inhibitors led to a retardation of the nuclear export of vRNP complexes and hence to a reduction of progeny virus titers showed that this pathway fulfills an important proviral function (Ludwig et al. 2004; Pleschka et al. 2001). This was furthermore accentuated by an experiment

in which the activation of the Raf/MEK/ERK pathway through active mutants of Raf or MEK led to increased virus titers (Olschlager et al. 2004). The block in nuclear vRNP complex transport could be ascribed to an impaired function of the viral NS2/NEP (Pleschka et al. 2001). In line with these previously described results, the inhibition of the Raf/MEK/ERK pathway could not be correlated with a reduction in the synthesis of viral RNA or protein (Pleschka et al. 2001). Hence, the active transport of viral RNP complexes is assumed to be an induced rather than a constitutive event, which is emphasized further by the fact that Raf/MEK/ERK is not just induced during the early, but also during the late phase of viral replication (Planz 2006).

2.2.3.4 ***Phosphatidylinositol-3-kinase (PI3K/Akt)***

Through lipid second messengers such as phosphatidylinositol-3, 4, 5-triphosphate (PIP3) generated from membrane phosphatidylinositol-4, 5-bisphosphate the enzyme family of PI3Ks regulates numerous cellular functions such as cell metabolism, proliferation, and survival (Ehrhardt and Ludwig 2009; Neri et al. 2002). The three main classes IA and IB, II, and III of this enzyme family are differentiated. The IA PI3Ks are heterodimeric enzymes that contain a regulatory (p85) and an enzymatic subunit (p110). Despite the main role of the kinase family to phosphorylate membrane phospholipids, an intrinsic protein-serine kinase activity could also be demonstrated (Dhand et al. 1994). The lipid second messenger molecules generated by PI3K interact with pleckstrin homology (PH) domain-containing proteins such as Akt/protein kinase B (PKB) or phosphoinositide-dependent kinase 1 (PDK-1) (Neri et al. 2002). Akt/PKB is one of the major effectors of PI3K, which requires a dual phosphorylation at Thr308 and Ser473 for its activation. PI3K does not directly phosphorylate Akt, but its post translational modification is strictly dependent on PI3K activity, whose activation state is often indirectly monitored by the Ser473 phosphorylation of Akt (Ehrhardt and Ludwig 2009).

Several functions of PI3K/Akt signaling have been described in the context of influenza virus infection. One of the downstream phosphorylation targets of PI3K is the small GTPase Rac1, which has been shown to regulate vesicular trafficking necessary for Ebola virus entry (Saeed et al. 2008). As Ehrhardt et al. have shown, PIP3 and PI3K are involved in the regulation of influenza virus uptake as well, since virus particles accumulated at the cell surface rather than fully infecting the cell when PI3K was inhibited. Furthermore, in this case the traffic to early endosomes during receptor mediated endocytosis

was impaired. Hence, the conclusion drawn from these results was that PIP3 and PI3K appear to control a step that precedes the endosomal transport and must therefore be involved in the initial virus uptake at the cellular membrane (Ehrhardt et al. 2006).

In addition to its function during virus entry, PI3K also exerts functions supporting virus replication at later stages of the infection cycle. Interestingly, during the late phase of virus replication, PI3K was shown to be only barely activated in cells infected with influenza A virus with a deletion of the NS1 protein (Ehrhardt et al. 2006). Accordingly, several studies have shown that the sole influenza A virus protein NS1 is required and sufficient for the activation of PI3K, as was suggested by the finding that the PI3K subunit p85 forms a complex with NS1 (Ehrhardt et al. 2007; Hale et al. 2006; Shin et al. 2007b; Zhirnov and Klenk 2007). The purpose of the interaction between NS1 and the p85 subunit of PI3K seems to be to postpone the onset of apoptosis in infected cells. This is due to the capability of PI3K/Akt to control the phosphorylation and therefore inhibition of pro-apoptotic factors such as caspase 3, caspase 9, and the glycogen synthase kinase 3 beta (GSK-3beta) (Ehrhardt et al. 2007; Shin et al. 2007a; Zhirnov and Klenk 2007). Despite these obvious proviral functions exterted by the PI3K/Akt signaling pathway, there are also antiviral functions of PI3K that have been described. Interestingly, the inhibition of PI3K as well as the blocking of its effector PIP3 have been shown to result in a misphosphorylation of IRF-3 and in an impaired transcriptional activation of the IFN-beta promoter (Ehrhardt et al. 2006). This had already been suggested by a previous study in which it was shown that PI3K is involved in the TLR-3 mediated activation of IRF-3 by dsRNA (Sarkar et al. 2004).

2.2.3.5 ***Type I interferons (IFNs), IFN-beta***

The IFN system is induced in the following manner. RIG-I and TLR3 recognize viral RNAs and trigger the activation of signaling cascades (Guillot et al. 2005; Kato et al. 2005; Kato et al. 2006b). The two tandem caspase recruitment domains (CARDs) of RIG-I recruit the downstream signaling protein IFN-beta promoter stimulator 1 (IPS-1), which has been independently identified by four different workgroups and hence carries the synonymous names mitochondrial antiviral signaling protein (MAVS), virus-induced signaling adaptor (VISA), and CARD adaptor inducing IFN-beta (CARDIF) (Kawai et al. 2005; Meylan et al. 2005; Seth et al. 2005; Xu et al. 2005; Yoneyama et al. 2004). Subsequently, IPS-1 activates tank binding kinase 1 (TBK-1) and IκB kinase beta (IKK-beta,

synonymous IKK2) (Meylan et al. 2005; Xu et al. 2005). TBK-1 and IKK-beta then directly activate the constitutively expressed IRF-3 and the inducible IRF-7 (Fitzgerald et al. 2003; Sharma et al. 2003). In addition to IRF-3 and IRF-7, RIG-I also mediates the activation of NF-κB via IPS-1 and IKK-beta (Kawai et al. 2005; Yoboua et al. 2010).

To this point, the signaling induced through TLR3 also contributes to the activation of the two kinases TBK-1 and IKK-beta. This takes place through the binding of the Toll/IL-1R (TIR) domain of TLR3 to the adaptor protein Toll/IL-1 receptor domain-containing adaptor-inducing IFN-beta (TRIF), which activates NF-κB and also TBK-1, leading to the activation of IRF-3, IRF-7, and NF-κB (Seth et al. 2006; Seth et al. 2005; Yamamoto et al. 2002). NF-κB and IRF-3, together with AP-1 form a multi-protein complex called enhanceosome that is assembled at and activates the IFN-beta promoter (Maniatis et al. 1998). As already described for NF-κB and IRF-3, the MAP kinases p38 and JNK are also activated by viral infection (Kujime et al. 2000). These MAP kinases then phosphorylate ATF-2/c-Jun, activating the third transcription factor AP-1 (Karin et al. 1997). The ensuing assembly of the enhanceosome leads to synthesis and secretion of IFN-beta.

2.2.3.6 Janus kinase (Jak) and Signal transducer and activator of transcription (Stat) pathway (Jak-Stat)

Together with IFN-alpha and IFN-omega, IFN-beta belongs to the type I IFNs and is an important antiviral cytokine expressed and secreted by virus infected epithelial cells. It acts in an autocrine as well as paracrine manner, binding to the transmembrane IFN-receptor composed of the two subunits IFN-alpha receptor 1 (IFNAR1) and 2 (IFNAR2) (Brierley and Fish 2002; Platanias 2005; Samuel 2001b). This coupling process of receptor and ligand rapidly activates the corresponding type I IFN specific Jak-Stat signaling pathway.

The Jak-Stat pathway is an evolutionarily highly conserved intracellular signaling cascade that is critical for developmental regulation, growth control, and homeostasis in multicellular organisms (Aaronson and Horvath 2002). The pathway is found in cells of a remarkably wide range of organisms, from very simple stages of development such as slime molds, worms, and flies to highly complex vertebrates (Darnell 1997).

In mammals, seven Stat genes are known (Stat1, Stat2, Stat3, Stat4, Stat5A, Stat5B, and Stat6). The inactive Stat transcription factors reside in the cytosol and, upon receptor activation, are recruited to its intracellular domain by the highly specific binding between the Stat Src-homology 2 (SH2) domain and receptor phosphotyrosine residues (Aaronson and Horvath 2002). The tyrosine kinase activity necessary for phosphorylation of tyrosine residues on the cytokine receptor signaling chains is provided by cytoplasmic proteins from the Janus kinase (Jak) family, which also catalyze their own phosphorylation (Aaronson and Horvath 2002; Leonard 2001). This creates docking sites for Stat proteins, which then also undergo activating phosphorylations of tyrosine residues, leading to Stat homo- and heterodimerization and subsequent rapid transportation of these dimers from the cytoplasm to the nucleus (Aaronson and Horvath 2002). In analogy to the Stat proteins, Jak proteins are also highly conserved evolutionarily, and four family members can be found in mammalian cells (Jak1, Jak2, Jak3, and Tyk2) (Aaronson and Horvath 2002).

Interestingly, the Jak proteins have their own inhibitors, the so called suppressor of cytokine signaling proteins (SOCS), which bind to and inactivate these kinases (Krebs and Hilton 2001). The SOCS proteins constitute a classic feedback inhibition loop since their expression is induced by the same cytokines that enhance STAT activation (Aaronson and Horvath 2002). Furthermore, Jak-Stat signaling can also be impaired by the protein inhibitors of activated Stats (PIAS), which bind to phosphorylated Stat dimers and prevent DNA recognition by the respective transcription factors (Shuai 2000). Jak-Stat signaling induced by type I IFNs is mediated by Stat1 and Stat2, while type II IFNs (IFN-gamma) use only Stat1 (Aaronson and Horvath 2002). Signaling via Stat3 and other Stat proteins takes place in a broad variety of cellular contexts (Aaronson and Horvath 2002). This, however, will not be further discussed as the focus here is on cellular signaling induced by viral infection. Type I IFN-induced Jak-Stat signaling is mechanistically distinct since besides Stat1 and Stat2, a third protein, namely IRF-9 or p48, is part of the trimeric transcription factor IFN-stimulated gene factor 3 (ISGF-3) that binds to the IFN stimulated response element (ISRE) present in the promoter region of IFN stimulated genes (ISGs) (Aaronson and Horvath 2002; Samuel 2001a).

2.2.3.7 ***IFN stimulated genes (ISGs) and their antiviral effects***

Several hundred genes have been shown to be induced by type I IFNs, leading to the establishment of an antiviral state by the host cell, affecting the replication of RNA as well as of DNA viruses (Der et al. 1998; Liu et al. 2012). In this section, some selected examples for IFN-induced antiviral proteins will be described in more detail in the following.

Among the antiviral ISGs, a prominent example is the family of myxovirus resistance (Mx) proteins, which have been described to interfere with virus replication (Zurcher et al. 1992a). Mx proteins are guanosine triphosphatases (GTPases) that belong to the dynamin family known to specifically sequester viral ribonucleoproteins to subcellular compartments (Garcia-Sastre and Biron 2006). In humans, two distinct Mx genes are known, designated MxA and MxB (Aebi et al. 1989). The modes of action that Mx proteins display against influenza viruses vary from species to species. The Mx1 protein of mice inhibits viral mRNA synthesis only in the nucleus of infected cells, whereas the human MxA protein was shown to be capable of inhibiting influenza virus replication in the cytoplasm as well as in the nucleus of the infected cell (Zurcher et al. 1992b).

The protein kinase RNA-activated (PKR) is a serine-threonine kinase that is able to sense dsRNA and phosphorylates downstream targets such as the eukaryotic translation initiation factor 2 alpha (eIF2-α), thereby inhibiting protein translation (Clemens et al. 1993; Meurs et al. 1993; Zilberstein et al. 1978). The activation and action of PKR will be further described in chapter 2.2.3.8.

The 2'-5' oligoadenylate synthetases (2'-5' OAS) are activated by dsRNA and their function is to generate 2'-5' oligoadenylates by oligomerizing ATP through an unusual phosphodiester linkage that subsequently activate ribonuclease L (RNase L). RNase L is able to degrade cellular as well as viral RNA (Diaz-Guerra et al. 1999; Zilberstein et al. 1978).

Adenosine deaminase is a cytoplasmic RNA editing enzyme upregulated by IFN. The large isoform adenosine deaminase acting on RNA (ADAR1-L) deaminates adenosines within double-stranded regions of RNA thereby generating inosines, which might mutate viral RNA (Randall and Goodbourn 2008). Hypermutation observed in the genomes of distinct RNA viruses could therefore be attributed to the action of this enzyme (Cattaneo 1994; Zahn et al. 2007).

Another example of potent antiviral proteins induced by IFNs is viperin, whose potency against influenza A virus infection was shown in cell culture systems (Wang et al. 2007). Although the precise

mechanism of action of viperin has not yet been revealed, it could be shown that its expression disrupts the formation of lipid rafts important in the budding process of some viruses (Wang et al. 2007).

2.2.3.8 ***Protein kinase RNA-activated (PKR)/eukaryotic translation initiation factor α (eIF2-α)***

PKR is a component of the eukaryotic initiation factor 2 α subunit protein kinase family (Hinnebusch 1994). The amino terminal part of the enzyme functions as a regulatory domain and the carboxy terminal as the protein kinase catalytic domain. Transcriptional and post-transcriptional processes regulate the activity of the enzyme (Clemens and Elia 1997). An important cellular regulator of PKR is the inhibitor $p58^{IPK}$, which regulates the autophosphorylation and activity of PKR (Gale et al. 1996; Polyak et al. 1996). Interestingly, the infection with influenza virus has been shown to lead to the induction of $p58^{IPK}$ expression (Lee et al. 1990). The stimulation with IFN leads to the transcriptional activation of PKR and the subsequent expression of high levels of mRNA. Double-stranded RNA released during influenza virus infection binds to PKR and thereby induces its autophosphorylation on several critical serine and threonine residues, rendering the kinase active (Taylor et al. 1996). The active kinase has several substrates that play a role in processes as diverse as growth factor and calcium-mediated signal transduction, regulation of transcription, and in the induction of apoptosis (Gale and Katze 1998). However, the most important substrate in the context of viral infection is eIF2-α, whose phosphorylation results in a block of the eIF-2B-mediated exchange of GDP for GTP, rendering eIF2 complexed with GDP and hence, inactive. This complexation and inactivation of eIF-2 leads to a limitation of functional eIF-2 and of the eIF-2-GTP-Met-tRNA ternary complex, that is necessary for the initiation of mRNA translation and hence, protein synthesis (Gale and Katze 1998). Apart from the role of PKR in inhibiting protein synthesis and accordingly cell growth arrest and inhibition of viral replication, the enzyme has also been implicated in the induction of the NF-κB pathway through the phosphorylation of IκB (Katze 1995; Kumar et al. 1994). In addition to NF-κB, PKR has also been implicated in contributing to the induction of IRF-3 through the mitochondrial IPS-1 signal transduction pathway (Zhang and Samuel 2008).

2.2.4 Functions of NS1 in antagonizing the antiviral defense and in apoptosis induction

The influenza A virus NS1 protein is generally assumed as the universal protein antagonist by which all strains of the influenza virus type A counteract the immune response of the host cell to some degree (Egorov et al. 1998; Garcia-Sastre et al. 1998). In addition to the aforementioned functions of NS1 in the processing of cellular and viral RNA, NS1 has the capability to modulate host cell apoptosis induction (Hale et al. 2008). The multifunctional protein has the ability to participate in protein-protein and protein-RNA interactions. The amino-terminal RNA binding domain comprises the amino acids 1 to 73 and binds to several RNA species in vitro regardless of their respective sequence (Chien et al. 2004; Hatada and Fukuda 1992; Qian et al. 1995). The carboxy-terminal domain mediates interactions with host cellular proteins and has a stabilizing effect on the RNA binding domain (Wang et al. 2002). Dimerization of NS1 is a prerequisite for binding dsRNA (Wang et al. 1999). With one to two nuclear localization sequences, the protein localizes mainly to the nucleus, although a considerable proportion was also shown to be in the cytoplasm of infected cells (Greenspan et al. 1988; Newby et al. 2007).

An important function of NS1 is the counteraction of the host cellular IFN response, mainly through the prevention of the dsRNA-mediated activation of the IRF-3, NF-κB, and c-Jun/ATF2 transcription factors (Ludwig et al. 2002; Talon et al. 2000; Wang et al. 2000). This pre-transcriptional block of the IFN response has been shown to be interceded by NS1 through the specific inhibition of TRIM25 mediated RIG-I CARD ubiquitination (Gack et al. 2009). A direct interaction of NS1 with RIG-I has still to be proven (Mibayashi et al. 2007; Pichlmair et al. 2006). Yet, the presence of viral single-stranded 5'-triphosphate RNA was shown to improve the stability of NS1-RIG-I complexes (Pichlmair et al. 2006). In addition to RIG-I, the activities of the IFN-induced proteins PKR and 2'-5' oligoadenylate synthetase (OAS) have been shown to be limited by NS1 (Min and Krug 2006; Min et al. 2007). The predominant function through which NS1 inhibits the antiviral function of OAS is to out-compete the interaction of this enzyme with dsRNA (Min and Krug 2006). The same strategy of competing for dsRNA binding was also suggested for PKR inhibition (Hatada et al. 1999; Lu et al. 1995). However, Li et al. have shown that an NS1 protein defective in RNA binding still could efficiently limit the activation of PKR in response to dsRNA or due to the action of the protein activator of PKR (PACT) (Li et al. 2006). According to domain-mapping it has been proposed that NS1 prevents a conformational change of PKR that is normally required for the release of its auto-inhibition by binding to a linker region of an amino acid sidechain (Li et al. 2006).

Regarding the induction of apoptosis in the host cell, NS1 has been shown to have both pro- as well as anti-apoptotic functions. Due to its aforementioned ability to limit the expression of IFN, NS1 clearly displays anti-apoptotic functions. As the catalytically active PKR was shown to be involved in apoptosis induction during influenza virus infection, the direct binding and inhibition of PKR by NS1 could lead to cell death suppression (Takizawa et al. 1996). Since the pro-apoptotic 2'-5' OAS/RNAseL was also shown to be inhibited by NS1, the anti-apoptotic effects of NS1 could additionally be mediated through this inhibitory mechanism (Min and Krug 2006). The finding that the infection with an influenza A virus with a genomic deletion of the NS1 protein (PR8 delNS1) led to the induction of higher levels of apoptosis in the host cell further underlined the anti-apoptotic function of NS1 (Zhirnov et al. 2002). Besides the limitation of apoptosis in the host cell through inhibitory mechanisms of NS1, the induction of apoptosis might also be counteracted by the NS1 mediated activation of anti-apoptotic pathways such as PI3K/Akt (Ehrhardt et al. 2007; Shin et al. 2007b; Zhirnov and Klenk 2007). However, despite the anti-apoptotic functions of NS1 described above, it has also been shown that NS1 fulfills pro-apoptotic functions. The sole expression of a cloned influenza A virus NS1 protein in human cell culture was shown to induce apoptosis in several studies (Lam et al. 2008; Schultz-Cherry et al. 2001; Stasakova et al. 2005). In contrast, van Wielink et al. showed that the recombinant expression of NS1 did not induce apoptosis in MDCK cells (van Wielink et al. 2011). These contradictory data may be due to variations in the experimental protocols, cell type specificities or variations between virus strains used. Alternatively, NS1 might contribute in a time-dependent manner both to an early suppression of apoptosis and to a late induction of this cellular process (Hale et al. 2008).

2.3 Influenza virus vaccines

The annual vaccination with a trivalent vaccine is the most effective method to prevent influenza virus infection and its complications in humans (Fiore et al. 2010). Human influenza vaccines first became commercially available in the United States in 1945 (Stanley 1945). In the generation of seed virus for vaccine production, the genetic reassortment of viral genomic segments has become routine practice, in which the genomic backbone of a high yield laboratory strain, e.g. influenza A/Puerto Rico/8/34, is combined with the genomic segments encoding for the viral glycoproteins HA and NA of the respective circulating strain (Kilbourne 1969; Kilbourne et al. 1971; Palese et al. 1997). HA and NA are the main

antigens responsible for the immune response. Additionally, the advancements in the field of reverse genetics have made possible the generation of influenza viruses exclusively from cloned plasmid DNA. Here, suitable cells are cotransfected with 8 or 12 plasmids that encode for influenza virus vRNA and mRNA (8 plasmid system), or vRNA and mRNA of the viral polymerases and NP to process the vRNA (12 plasmid system) (Subbarao and Katz 2004).

Both live-attenuated influenza vaccines (LAIV) and trivalent inactivated influenza vaccines (TIV) are available today. The LAIV and TIV both contain strains of influenza virus that are antigenically equivalent to the annually recommended strains and typically comprise one influenza A (H3N2) virus, one influenza A (H1N1) virus and one influenza B virus that are selected each year by the WHO based on global surveillance for influenza viruses and the emergence and spread of new strains (Fiore et al. 2010). LAIV are recommended for healthy, nonpregnant individuals aged 2 to 49 years, whereas TIV can be used for any person older than six months (Fiore et al. 2010).

Three types of TIV are available, namely whole virus vaccines, split virus vaccines, and subunit vaccines. Split virus vaccines are made by disrupting the virus using a detergent. In subunit vaccines, the envelope proteins HA and NA are further purified through the removal of other viral components (World Health 2005). In contrast to LAIV vaccines, TIV vaccines need an adjuvant to be effective. Mostly $Al(OH)_3$ are used, since they appear to be effective and safe. To spare antigen, more powerful oil based adjuvants have, however, also been used recently (H1N1 pandemic flu 2009-2010).

The technology of live attenuation by cold adaptation of influenza virus vaccine strains at a temperature range from 25° to 33°C has been applied for more than three decades (Wareing and Tannock 2001). LAIV are licensed in the Russian Federation and in the United States. In Russia, the current LAIV is based on cold-adapted H2N2 strain variants, reassorted with epidemic H1N1 and H3N2 strains additionally combined with a cold-adapted reassortant of influenza B virus. In the United States, the use of LAIV, which are based on genetic reassortment technologies, has been licensed since 2003. Here, the cold-adapted influenza vaccine comprises the viral envelope protein genes HA and NA of the three virus strains recommended by the WHO as well as genes from a cold-adapted master strain (World Health 2005). The LAIV are administered intranasally, whereas the TIV are injected intramuscularly (Tosh et al. 2010).

The majority of influenza vaccines that are used today is formulated with viral antigens produced in the allantoic fluid of 9- to 11-day-old embryonated chicken eggs, a technology that has been established for more than 60 years (Osterhaus et al. 2011). Despite its robustness and reliability, the chicken egg

process entails a number of drawbacks such as the lack of flexibility and a limitation of rapid up-scaling possibilities. Hence, novel vaccine production technologies are being explored and implemented, which comprise the application of continuous mammalian cell lines grown adherently or in suspension, the production of recombinant influenza virus glycoproteins HA and NA in plant or insect cells, or DNA vaccines, as well as in baculovirus systems (Mather et al. 1992; Osterhaus et al. 2011; Price et al. 1989).

2.3.1 The egg-based vaccine production process

Influenza virus produced in the allantoic cavities of embryonated chicken eggs is purified and concentrated. Unlike LAIV, which are exempt from this procedure, TIV are inactivated prior to formulation. As previously mentioned, despite the high yields obtainable during egg-based production and the additional safety measure provided by the cross-species cultivation of virus isolates, this process entails a number of drawbacks, which include the limited flexibility to expand the scale of the vaccine manufacturing process. Additionally, the supply chain of embryonated eggs is vulnerable to interruptions caused by disease in the chicken layer flocks. Furthermore, sterility problems might arise during the processing of infected allantoic fluids. Another problem posed during egg-based vaccine production is the poor growth that is encountered sometimes with certain influenza virus strain isolates. Additionally, it has to be considered that the growth of epidemic viruses in eggs oftentimes leads to the selection of virus variants that differ in their glycosylation patterns from the antigenically distinct original clinical isolates (Audsley and Tannock 2008). Further problems associated with egg-based influenza vaccines are caused by possible contaminants such as trace amounts of potentially reactogenic endotoxins, allergic reactions to egg proteins, formaldehyde and preservatives (Wright and Webster 2001). In summary, the drawbacks associated with the egg-based vaccine production process described here give a strong impetus for the use of stable mammalian cell lines for vaccine virus growth. By the use of cell culture-based processes, problems associated with egg-based production could largely be overcome if process yields were satisfactory and all connected safety issues could be successfully taken care of (Audsley and Tannock 2004).

2.3.2 The cell culture-based production process

The use of cell culture-based systems as an alternative to traditional egg-based influenza vaccine production has been thoroughly investigated for more than a decade now. As production cell lines lack specific host proteases necessary for the proteolytic cleavage of the HA glycoprotein to produce infectious virus, the addition of crystalline trypsin was shown to be a precondition for improving the virus yield of infected cell cultures (Klenk et al. 1975).

As of today, a number of different suitable cell lines for the production of influenza vaccines have been established successfully (Genzel and Reichl 2009). These comprise conventional adherently growing cell lines such as the aforementioned MDCK cell line (ATCC, e.g. CCL34; ECACC, e.g. 84121903), the African green monkey kidney epithelial (Vero) cell line (ATCC, e.g. CCL-81; ECACC, e.g. 88020401) that has been used to produce polio and rabies vaccines for more than two decades (Montagnon et al. 1981), or the proprietary Novartis 33016 MDCK suspension cell line (Novartis Vaccines). Furthermore, designer cell lines such as the immortalized human fetal retinoblast cell line PER.C6 developed by Crucell (Pau et al. 2001), the avian (duck retina) designer cell line AGE1.CR (Lohr et al. 2009), or the avian embryonic stem cell line EB66™ by Vivalis (Pearson 2007) have been established for influenza vaccine production.

Vero cells were shown to be a suitable host system for influenza A virus replication in 1995 (Govorkova et al. 1995; Govorkova et al. 1996). In 1998, Kistner et al. first described the development of a cell culture-based influenza vaccine production process using Vero cells, which are approved by the WHO (Kistner et al. 1998). Here, a multitude of influenza virus strains have been shown to grow to high titers in serum-free culture medium and fermenter production volume could be scaled up to 1,200 L. A Vero cell-derived whole influenza virus vaccine has been produced and marketed under the name Influject® by Baxter.

The origin of the MDCK cell line is the epithelium of a healthy cockerspaniel kidney from which it was isolated in 1958 (Gaush et al. 1966). Since the mid 1960s, the MDCK cell line has been used to perform plaque assay of influenza A and B virus and it is commonly used for the clinical isolation of influenza viruses (Gaush and Smith 1968; Meguro et al. 1979; Tobita 1975; Tobita et al. 1975). As an excellent model for kidney and epithelial development the cell line has been studied thoroughly (Simmons 1982). Since the mid 1990s, the production of influenza virus in MDCK cells has been investigated

experimentally and the resulting vaccines were found to be safe, well tolerated and sufficiently immunogenic (Halperin et al. 1998; Palache et al. 1997). This led to the development of an MDCK cell derived influenza vaccine (Influvac®TC) by Solvay Pharmaceuticals in 1999 (Brands et al. 1999). In 2005, a live cold adapted attenuated trivalent influenza vaccine produced in adherent MDCK cells grown on microcarriers at a 10 L scale under serum-free conditions was shown to be genetically stable and clinical trials were anticipated (Ghendon et al. 2005). Using an MDCK suspension cell line, the first cell culture-derived trivalent influenza vaccine (Optaflu®) developed by Novartis Vaccines was approved by the European Medicines Agency (EMA) in 2007 (Doroshenko and Halperin 2009).

2.3.2.1 ***Influenza virus production***

In the following, the three aspects of influenza virus production, namely cultivation vessels, growth medium, and virus infection and production are illustrated.

Cultivation vessels

Mammalian cells used for influenza virus production can be cultivated utilizing a diverse range of cell culture vessel formats of varying degrees of size and operational complexity. The smallest scale is the cultivation of cells in T-flasks, multiwell plates or petri dishes. Cell cultures grown in these vessels are referred to as static cultures, since these are grown under non-agitated conditions. Cultivation conditions such as temperature and atmospheric composition are solely controlled by an incubator. As there is no active mixing involved, the only driving force for mass transfer is diffusion. A larger scale of cell cultivation can be achieved by using stirrer flasks, which are also placed in an incubator for cell cultivation. To maintain sterility these vessels are sealed airtight, which limits gas exchange to the headspace volume. A magnetic stirrer adds an additional force to reduce concentration gradients in the cultivation medium and to enhance gas exchange of the liquid phase with the headspace volume. Microcarriers such as dextran beads are usually added to stirrer flasks or bioreactors to vastly expand the cultivation surface area (Genzel et al. 2004; Genzel et al. 2006). By the use of microcarriers the cultivation volume can be increased to a range of several cubic meters. The cultivation of mammalian cells at such large volumes is realized through the use of stainless steel stirred tank bioreactors or increasingly through disposable plastic vessels such as Wave bioreactors™, where mixing is realized

through shaking of the whole reactor. In these reactors cultivation conditions such as temperature, pH value, and dissolved O_2 are controlled.

If production scale is to exceed a volume of about 5 L, a cell culture expansion from static to dynamic cultivation vessels has to be implemented in a cascading manner. The use of roller bottles with a cultivation area of about 850 to 1750 cm² is an intermediate cultivation step on the way from static T-flasks to bioreactors. Roller bottles sealed airtight are constantly agitated in a rotational manner, whereas temperature is the only controlled parameter.

Growth medium

Regarding growth medium composition, the cultivation of mammalian cells is demanding since within the medium all the components need to be contained that are required for cell attachment and proliferation, as well as normal cell function. All these medium requirements are met by the addition of serum, which provides a complex mixture of hormones, growth factors, carrier proteins, nutrients, as well as attachment and spreading factors (Griffiths 1987). However, the use of serum poses a number of problems and resulting regulatory concerns that arise from lot to lot variability, ill-defined composition, cost, and potential introduction of contaminating agents such as fungi, bacteria, viruses, and agents of transmissible spongiform encephalopathies (TSE) (Merten 2002). To overcome these problems, the development of serum-free media, which still contain animal- or human-derived proteins including peptones, hydrolysates, and albumin fractions, and chemically defined, protein-free media is pursued (Keay 1978). This would hence minimize the risks from viruses or TSE, but obstacles are posed continually by the complicated development and the usual specific requirements for particular cell lines (Merten 2002).

Virus infection and production

Prior to infection, high concentrations of cells are aimed for that should usually be in the late exponential or early stationary growth phase. For infection, serum-containing cell growth medium has to be replaced by serum-free medium to prevent the inhibition of virus adsorption and the activity of trypsin necessary for cleavage and activation of HA (Genzel et al. 2004). After or during medium exchange, influenza virus and trypsin is added. To reduce the amount of seed virus consumed for infection and to dilute potentially defective interfering particles (DIP), low multiplicities of infection

(MOI) are typically used in influenza virus production. The MOI is the ratio of infectious virus particles to the number of to be infected live cells.

The first virion release is dependent on the adjusted MOI, and up to three waves of infection occur during a single cultivation. Usually the first release of virions occurs after 6 to 12 h until the infected cells die due to apoptosis or other environmental factors (Gaush and Smith 1968; Mohler et al. 2005; Schulze-Horsel et al. 2008). As determined in quantitative real-time PCR, each infected cell produces 1,000 to 10,000 virus particles, while only a small fraction of these virions was shown to be infectious based on $TCID_{50}$ or plaque assay analyses (Youil et al. 2004). As the end of the virus replication phase of the virus production process is approached, the viable cell number drops and the concentration of influenza virus particles in the supernatant reaches a maximum. Subsequently, the culture broth is harvested, clarified, inactivated, concentrated, and treated further in downstream processing to purify and concentrate whole virion particles (Kalbfuss et al. 2007; Nayak et al. 2005).

3 Materials and Methods

The following chapter provides a description of the cultivation of mammalian cell lines analyzed in this study as well as of the analytical methods that were applied in the course of this research project. The description of standard methods commonly used within the research group is complemented by standard operation procedure protocols in the Appendix (10), where detailed information is also given on utilized chemicals and analytical devices.

3.1 Mammalian cell culture

3.1.1 Media and solutions for mammalian cell culture

The cultivation of cells of mammalian origin necessitates the use of media of complex composition. For the cultivation of MDCK cells, Glasgow Minimum Essential Medium (GMEM) was used containing glucose, glutamine, essential amino acids such as arginine and histidine, vitamins, inorganic salts and phenol red as a pH indicator (Table 3-1). Fetal calf serum (FCS) is an important supplement to cell culture media due to the lack of artificial complex mixtures of growth factors and hormones essential for cell proliferation. In the following, the composition of media and solutions used in the course of this work for mammalian cell culture are described in detail.

Table 3-1: Medium composition for MDCK cell cultivation.

compound	cell growth medium	infection medium
GMEM powder	12.5 g/L	12.5 g/L
Glucose	5.5 g/L	5.5 g/L
$NaHCO_3$	4.0 g/L	4.0 g/L
Peptone	2.0 g/L	2.0 g/L
FCS	10% (v/v)	-
$H_2O_{ultrapure}$	ad 1 L	ad 1 L

After pH was adjusted to 6.8 with HCl, medium was sterile filtered (0.22 µm) and stored at 4 °C.

Besides MDCK cells, the human lung epithelial cell line A549 was used, which needed a different medium composition for cultivation (Table 3-2).

Table 3-2: Medium composition for A549 cell cultivation.

compound	cell growth medium	infection medium
Glutamine	2 mM	2 mM
FCS	10% (v/v)	-
Peptone	-	2 g/L
F12K medium	ad 1 L	ad 1 L

Medium was sterile filtered (0.22 µm) and stored at 4 °C.

For the subcultivation of cells, phosphate buffered saline (PBS) of a composition described in the following was needed (Table 3-3).

Table 3-3: PBS solution.

component	Concentration
NaCl	8.00 g/L
KCl	0.2 g/L
KH_2PO_4	0.2 g/L
NaH_2PO_4	1.15 g/L
$H_2O_{ultrapure}$	ad 1 L

The PBS solution was autoclaved and stored at room temperature (RT).

A trypsin/ethylenediaminetetraacetic acid (EDTA) solution was used for the subcultivation of cells. The composition of this solution is described in Table 3-4. For cell passaging, a 1x trypsin/EDTA solution was used, which was made by diluting the 10x trypsin/EDTA solution with PBS.

Table 3-4: Trypsin/EDTA solution (10x).

component	Concentration
trypsin (775 U/mg)	0.05 g/L
EDTA	0.02 g/L
PBS	ad 100 mL

After preparation, the solution was sterile filtered (0.22 µm) and stored at 4 °C.

3.1.2 Subcultivation and scale-up of mammalian cells

MDCK (ECACC 84121903) or A549 (ATTC CRL-185) cells taken from cryostocks were subcultivated up to 20 passages to avoid genetic alterations and senescence. Mammalian cells growing adherently attach to culture vessel surfaces via adhesion proteins. When passaging cells, these adhesion proteins are enzymatically cleaved by trypsin. The cell detachment process is additionally supported by the chelating agent EDTA, which binds to Ca^{2+} ions and hence prevents the joining of cadherins between cells. Prior to the addition of a 1x trypsin/EDTA solution, cells were washed twice with PBS to remove proteins included in FCS that inhibit the enzymatic activity of trypsin. After adding the 1x trypsin/EDTA solution, cells were incubated at 37 °C, 5% CO_2 for 20 min. Subsequently, the enzymatic reaction was stopped by adding an equal volume of prewarmed cell growth medium to halt the enzymatic activity of trypsin and prevent damage to the cells (Table 3-5).

Table 3-5: Amounts of PBS, trypsin, and cell growth medium used for MDCK cell cultivation.

cell culture vessel	PBS for washing (mL)	1x trypsin solution (mL) for cell detachment	cell growth medium (mL)
25 cm^2 T-flask	5-10	1	15
75 cm^2 T-flask	10-15	2-3	50
175 cm^2 T-flask	15-20	5-6	100
850 cm^2 roller bottle	40-50	10-15	250

After the transfer of a fraction of the cells to other cell culture vessels and addition of fresh, prewarmed cell growth medium, cultivation was continued at 37 °C, 5% CO_2.

3.1.3 Determination of cell concentration

For the determination of cell concentration prior to cell seeding, cell culture medium was aspirated and cells were washed twice with PBS and then incubated with 1x trypsin/EDTA, in an analogous manner as described under 3.1.2. The enzymatic activity of trypsin was halted by the addition of an equal volume of prewarmed cell growth medium. Cell density was then determined either manually by using a microscope and a Fuchs-Rosenthal counting chamber or in an automated fashion, using a ViCell XR counting device (Beckman-Coulter), (10.4.6).

3.1.4 Cryoconservation of mammalian cells

In order to prevent mammalian cell lines during long term storage from contamination and genetic instability cells were cryoconserved in the gas phase of liquid nitrogen. This was done in accordance with a group internal SOP (10.4.5). In brief, adherently grown cells were washed twice with PBS and subsequently trypsinized as described in 3.1.2. Cell suspension was then transferred to a 50 mL falcon tube, which was then filled up to 45 mL with FCS-containing or serum-free medium, depending on growth of the respective cell line in either one of both. 1 mL of the resulting cell suspension was then measured in the ViCell XR cell counter to determine cell concentration (3.1.3). The cell suspension was then centrifuged for 5 min at 500 x g, the cell pellet resuspended in FCS containing 10-15% (v/v) dimethylsulfoxide (DMSO), adjusting a concentration of 2-4 x 10^6 cells/cryovial at a volume of 1.6 mL. After a brief cooling to 4 °C, cryovials were stored at -20 °C for 2 h, followed by storage at -80 °C over night to prepare for final storage in the gas phase of liquid nitrogen. When subsequently thawing and resuspending cells in fresh, prewarmed cell growth medium, care had to be taken to act swiftly to remove the highly toxic DMSO as fast as possible.

3.1.5 Influenza virus infections

For infection, cells were grown to a density of 1-2 x 10^5 cells/cm^2, which corresponds to a confluency of 70-80%. Cell culture medium was aspirated and cells were washed twice with PBS prior to infection with one of the influenza virus strains listed in Table 3-6 at different multiplicities of infection (MOIs) based on viable cell concentration and infectious virus particle concentration determined as tissue-culture infectious dose 50 ($TCID_{50}$, 3.2.1.6). All virus strains used in infection experiments had previously been adapted to MDCK cells. Infection was performed with infection medium. Trypsin (Gibco) for infection was added at a concentration of 2 x 10^{-6} units/cell for cleavage and activation of viral hemagglutinin.

Table 3-6: Influenza viruses used for infection experiments.

Strain	Subtype	Source	Number
human A/Puerto Rico/8/34	H1N1	National Institute for Biological Standards and Control (NIBSC)	NIBSC code: 06/114
human A/Puerto Rico/8/34	H1N1	Robert Koch Institute (RKI)	
human A/Puerto Rico/8/34 ΔNS1	H1N1	Avir Green Hills Biotechnology	
human A/WSN/33	H1N1	Freiburg University Hospital, Virology Research Department	
human A/Uruguay/716/2007 (hgr*) (NYMC X-175c)	H3N2	NIBSC	NIBSC code: 07/360
human A/Wisconsin/67/2005 (hgr*) (NYMC X-161b)	H3N2	NIBSC	NIBSC code: 05/244
human B/Malaysia/2506/2004	-	NIBSC	NIBSC code: 07/132

** hgr: high growth reassortant*

The volume of seed virus was added according to the concentration of infectious virus particles and MOI (Equation 1). For mock infections, cells were treated in an identical manner, except that besides infection medium and trypsin, no seed virus was added.

Equation 1

$$V_{seedvirus} = \frac{N_{total}}{C_{IVPseedvirus}} \times MOI$$

$V_{seedvirus}$	volume of seed virus added	(mL)
N_{total}	total viable cell number	(cells)
$C_{IVPseedvirus}$	concentration of infectious virus particles	(viruses per mL)
MOI	multiplicity of infection	(viruses per cell)

3.1.6 Bioreactor cultivations

Cultivations of MDCK cells were done in a lab-scale 1.2 L Cellferm ProSpinner BS1600 (DasGip) stirred tank bioreactor operated in batch mode. Sterile-filtered oxygen was added through a dip pipe and controlled to 40% dissolved oxygen by pulsed aeration. Oxygen partial pressure was measured online by an oxygen probe. For mixing and dispersion, a pitched blade impeller was run at 50-60 rpm. Medium temperature was measured online by a probe and controlled to 37 °C. Heating was facilitated by an electric heating jacket attached to the glass reactor vessel. The pH value was measured online by pH

probes and controlled to pH 7.2-7.3, which was adjusted by the addition of 1 M NaOH. Sampling was done via a sterile sampling valve attached to a dip pipe. Cells were seeded at 2-3 x 10^5 cells/mL. Microcarriers (Cytodex, GE Healthcare, Nr. 17- 448-03) were added at 2 g/L, approximately 8000 microcarriers/mL, resulting in a cultivation surface area of 9 cm²/mL.

3.2 Analytical methods and molecular biology

3.2.1 Analytical methods

For a precise analysis of cellular signal transduction, virus infection, and replication processes, various analytical tools were applied. These comprised the determination of protein concentration in cell lysates, immunodetection of phosphorylated proteins as kinase-regulated mediators of signal transduction processes, the measurement of gene expression, as well as quantification of infectious and total virus particle content of a given sample. Furthermore, the viability of cell cultures was measured to determine the toxicity of a chemical compound used for kinase inhibition. Additionally, using a plaque assay, an attempt was made to purify viral variants assumed to exist in seed virus stocks.

3.2.1.1 ***BCA assay***

Total protein concentration of cell lysates was determined using the Pierce bicinchoninic acid (BCA) protein assay kit (Thermo Scientific) with BSA as a standard. The quantification of protein is based on the biuret reaction in which Cu^{2+} (cupric) ions are reduced to Cu^{+} (cuprous) ions. The chelation of cupric ions by peptides containing three or more amino acid residues in an alkaline environment containing sodium potassium tartrate yields a light blue chelate complex. In the second step of the reaction, two molecules of BCA react with one cuprous ion, which results in the formation of an intense water-soluble purple-colored reaction product. With increasing protein concentrations, this reaction product shows a linear absorbance at 562 nm.

3.2.1.2 ***Western blot***

3.2.1.2.1 Sample preparation

After medium samples were taken for subsequent analysis in the HA assay (3.2.1.5) and the remaining medium volume was aspirated, cells were washed twice with ice-cold PBS. Per 75 cm² T-flask, 1 mL RIPA cell lysis buffer was added. The RIPA cell lysis buffer was freshly prepared 1 h prior to sampling according to Table 3-7 and Table 3-8.

Table 3-7: Composition of RIPA stock buffer (pH 7.5).

component	amount	final concentration
tris base	3.03 g	33.5 mM
EDTA	5 mL of a 0.5 M solution	3.35 mM
NaCl	4.383 g	100.5 mM
K_2HPO_4	1.142 g	6.7 mM
Glycerol	50 mL	6.7%
triton X-100	5 mL	0.67%
SDS	0.25 g	0.0335% (w/v)
$H_2O_{ultrapure}$	ad 0.5 L	-

After preparation of RIPA stock buffer, the solution was stored at 4 °C for further usage.

Using the RIPA stock buffer solution (Table 3-7), the RIPA cell lysis buffer was prepared as described in Table 3-8.

Table 3-8: Composition of RIPA cell lysis buffer.

component	amount (for 10 mL)	final concentration
RIPA-stock buffer	6.7 mL	see above
$H_2O_{ultrapure}$	190 µL	-
Na_3VO_4	100 µL of a 100 mM stock solution	1 mM
Na_2MoO_4 x $2H_2O$	100 µL of a 100 mM stock solution	1 mM
NaF	200 µL of a 1 M stock solution	20 mM
PMSF	10 µL of a 200 mM stock solution	200 µM
$Na_4P_2O_7$	1 mL of a 100 mM stock solution	10 mM
glycerol-2-phosphate	1 mL of a 200 mM stock solution	20 mM
protease inhibitors (Roche)	400 µL of a 25 x stock solution	1x

In addition to RIPA cell lysis buffer, cells were removed manually from T-flasks using a cell scraper and lysates were transferred to reaction tubes on ice. For samples drawn from bioreactor cultivations of adherent cells growing on microcarriers (3.1.6), a volume of 7 mL culture medium was transferred to a 15 mL falcon tube. The sample was then washed twice with 5 mL ice-cold PBS and the supernatant was discarded. Then, 1 mL of ice-cold RIPA cell lysis buffer was added to the microcarrier sample and the suspension homogenized with a pipette. The lysate sample was vortexed at maximum intensity for 30 sec, filtrated through a 100 µM filter (Partec Celltrics, Nr. 04-0042-2318) to prevent clogging of the ViCell XR flow chamber (3.1.3) and then transferred to a fresh reaction tube. Lysates were subsequently homogenized on ice using 0.2 µm syringes (BBraun) by aspirating and ejecting five times. The following centrifugation step (12,000 x g, 10 min, 4 °C) in a precooled centrifuge yielded a soluble protein fraction. After centrifugation, supernatants were aliquoted in 100 µL aliquots and transferred to fresh reaction tubes for storage at -70 °C for subsequent analysis. Protein concentration was determined using the BCA assay kit (3.2.1.1).

Table 3-9: Reducing (4x) SDS sample buffer.

component	amount/volume	final concentration
tris-Cl (1 M, pH 6.8)	2 mL	250 mM
Glycerol	3.2 mL	40% (v/v)
SDS	0.64 g	8% (w/v)
bromophenol blue	0.32 g	0.01% (w/v)
β-mercaptoethanol	0.8 mL	10% (v/v)
$H_2O_{ultrapure}$	0.4 mL	-

After preparation, solution was stored in 500 µL aliquots at -20 °C.

For analysis in sodium dodecyl sulfate polyacrylamide gel electrophoresis (SDS-PAGE) and Western blot, an amount of about 15 to 50 µg of RIPA protein extract was diluted in SDS sample buffer (Table 3-9) and heated for 5 min at 95 °C.

3.2.1.2.2 Gel electrophoresis (SDS-PAGE) and Western blotting

The conduction of SDS-PAGE precedes the Western blotting technique. Due to its high resolution power, the discontinuous SDS-PAGE using Tris-HCl/Tris-glycine buffer systems as introduced by Laemmli has become a standard method of protein analysis (Laemmli 1970).

The Mini-Protean electrophoresis system (Bio-Rad) was used to conduct gel electrophoresis. Overall assay procedure is described in a workgroup internal SOP (10.4.10). At first, gels were prepared in a gel cassette assembly on the supplied casting stand. A gel thickness of 1 mm was chosen, which was adjusted by spacer plates included in the electrophoresis system. Short plates as well as spacer plates were thoroughly cleansed with detergent and subsequently 70% ethanol to provide for clean glass surfaces necessary for homogenous and even gel polymerization. Polyacrylamide gels were composed as described in Table 3-10.

Table 3-10: Composition of polyacrylamide gels.

components	separating gel, 7.5%	separating gel, 10%	stacking gel, 3%
$H_2O_{ultrapure}$	4.8 mL	3.97 mL	6.3 mL
acrylamide, 30% solution	2.5 mL	3.33 mL	1.0 mL
tris-Cl buffer, pH 8.8 or 6.8	2.5 mL	2.5 mL	2.5 mL
SDS, 10% (w/v) solution	0.1 mL	0.1 mL	0.1 mL
APS, 10% (w/v) solution	0.1 mL	0.1 mL	0.1 mL
TEMED, 10% (v/v) solution	0.1 mL	0.1 mL	0.1 mL

The preparation of individual buffers and solutions needed for the composition of polyacrylamide gels is described in Table 3-11.

Table 3-11: Buffers and solutions needed for preparation of SDS-PAGE gels.

components	stacking gel buffer, pH 6.8	separating gel buffer, pH 8.8	SDS	TEMED	APS	bromo-phenolblue
tris-Cl	0.5 M (12.14 g)	1.5 M (36.34 g)	-	-	-	-
SDS	-	-	10% (w/v)	-	-	-
TEMED	-	-	-	10% (v/v)	-	-
APS	-	-	-	-	10% (w/v)	-
bromophenolblue	-	-	-	-	-	0.05% (w/v)
$H_2O_{ultrapure}$	ad 0.2 L	ad 0.2 L	ad 50 mL	ad 1 mL	ad 5 mL	ad 100 mL

For this, all the liquid components were mixed in a conical flask using a magnetic stirrer. Polymerization was triggered by the addition of 100 µL 10% APS and 10 µL TEMED, which were hence added after all other components had been combined. Different concentrations of acrylamide were adjusted, ranging from 7.5% to 10% (Table 3-10), which were selected according to the size of the analyzed protein. After the separating gel mixture was pipetted between the short and spacer plates assembled as a gel cassette on the casting frame, the mixture was covered with a layer of isopropanol to provide for a smooth and even separating gel surface. After roughly 45 min, polymerization was complete and the layer of isopropanol rinsed off with $H_2O_{ultrapure}$. Then, the stacking gel was pipetted between the spacer and short plates and a gel comb was added. During the first minutes of stacking gel polymerization, small volumes of stacking gel mixture were added at times to prevent stacking gel pocket shrinking and bubble formation within the gel. After the stacking gel was polymerized, the gel cassette sandwich was inserted into the electrode assembly, which was then held together by the clamping frame. The electrode assembly, gel cassette sandwich, butter dam, and clamping frame together then formed the inner chamber, which was inserted into the mini tank and subsequently filled up with 1x electrophoresis buffer (Figure 3.2-1).

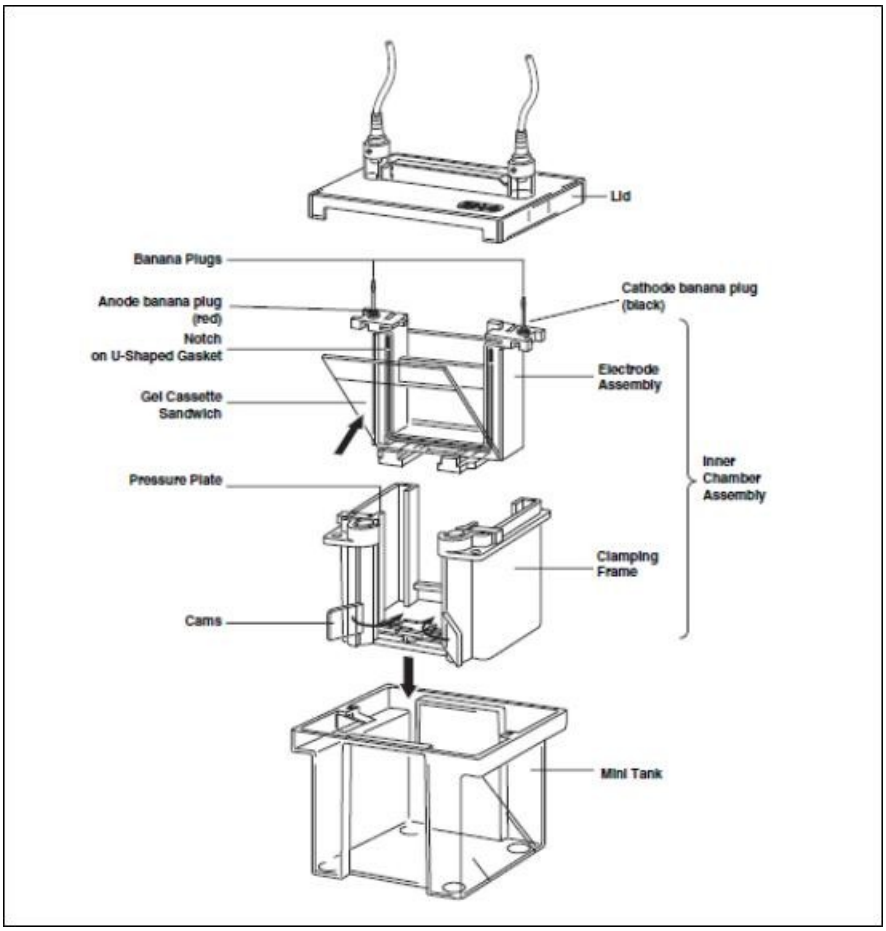

Figure 3.2-1: Assembly instruction of the Mini-Protean (Bio-Rad) SDS-PAGE system.
(http://www.plant.uoguelph.ca/research/homepages/raizada/Equipment/RaizadaWeb%20Equipment%20PDFs/9B.%20miniprotean3%20cell%20manual.pdf)

Once the mini tank was filled up, the gel combs were removed and gel pockets flushed with 1x electrophoresis buffer using a microliter syringe (Hamilton). Using the same syringe, the samples prepared according to (3.2.1.2.1) were injected into the gel pockets. Then, per gel a current of 15 mA was applied as long as the samples were focused in the stacking gel and once the interface to the separating gel was reached, the current was raised to 25 mA per gel. Once the SDS-PAGE was completed, the wet blot Western blotting procedure commenced. While the SDS-PAGE was run, polyvinylidene difluoride (PVDF) blotting membranes of a format of 6 x 9 cm were prepared. At first, membranes were equilibrated in methanol for 15 sec, followed by 2 min in $H_2O_{ultrapure}$. The last equilibration step was done in 1x transfer buffer for at least 5 min. A detailed description of the composition of buffers used for Western blotting is shown in Table 3-12.

Table 3-12: Additional buffers and solutions for SDS-PAGE and Western blotting (I).

components	electrophoresis buffer (10x)	transfer buffer (10x)	TBS (10x), pH 7.6	TTBS
SDS	1% (w/v)	-	-	-
Glycin	1.92 M	1.92 M	-	-
Tris	250 mM	250 mM	200 mM	-
NaCl	-	-	1.37 M	-
Tween 20	-	-	-	0.05% (v/v)
TBS (10x)	-	-	-	10% (v/v)
$H_2O_{ultrapure}$	ad 1 L	ad 1 L	ad 1 L	ad 1 L

After preparation all solutions and stock solutions were stored at 4 °C.

Besides the buffers listed in Table 3-12 that were needed in large amounts, a number of additional solutions, which were needed for assay procedure are listed in Table 3-13.

Table 3-13: Additional buffers and solutions for SDS-PAGE and Western blotting (II).

components	tris-Cl, pH 6.8	Ponceau S dye	stripping buffer, pH 7.6
SDS	-	-	2% (w/v)
β-EtSH	-	-	100 mM
tris-Cl	1 M (12.11 g)	-	-
Tris	-	-	62.5 mM
Ponceau S dye	-	0.05% (w/v)	-
acetic acid	-	10% (v/v)	-
$H_2O_{ultrapure}$	ad 100 mL	-	ad 1 L

APS solution was subsequently stored at -20 °C in 500 µL aliquots. Tris-Cl buffer was stored at 4 °C.
All other solutions were stored at RT.

As soon as the gel run was completed, the Mini-Protean electrophoresis system was dismounted and the SDS-PAGE gels were equilibrated in 1x transfer buffer, along with both the high grade blotting paper (Whatman) of a format of 7.5 x 9 cm and the supplied blotting fiber pads. Then the preparation of the gel sandwich commenced. First the gel holder cassette was placed in a tray with the black side down. Then one of the pre-wetted fiber pads was placed on the black side of the cassette. A sheet of blotting paper was put on top of the fiber pad, which was followed by the positioning of the equilibrated gel on top of this stack. The next step was to place the equilibrated PVDF membrane carefully on top of the gel at once, without repositioning it. Here, it was essential to roll out any air bubbles that might have formed between the gel and PVDF membrane with a glass tube or plastic falcon tube, as failing to do so would interrupt protein transfer. On top of the membrane another sheet of pre-wetted blotting paper was put,

followed by another pre-wetted fiber pad. This was followed by closing the cassette firmly, paying attention not to move the gel and filter paper sandwich. The white latch was closed and the cassette placed in the module.

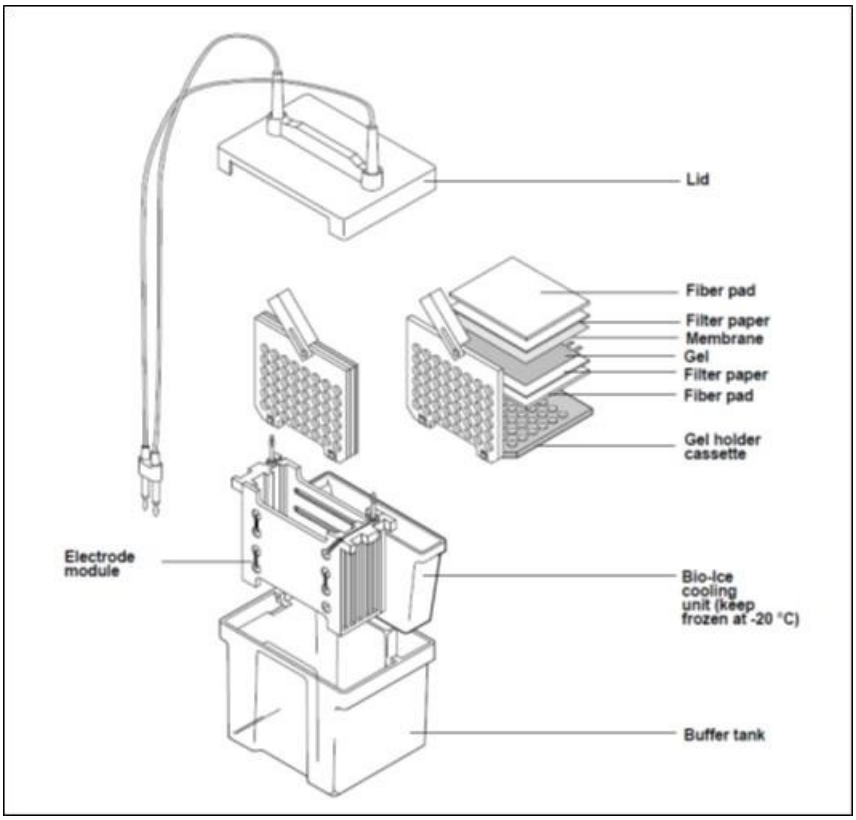

Figure 3.2-2: Instructions for assembly of the Mini Trans-Blot Cell (Bio-Rad).
(http://mcdonald.ucdavis.edu/uploads/1/8/5/3/1853874/minitransblotcell.pdf)

The whole procedure was repeated for another cassette. The cooling unit and the electrode module was inserted into the tank, which was then filled with 1x transfer buffer without SDS. Then a stir bar was put in the tank and the stirring speed set as fast as possible in order to prevent the formation of ion concentration or temperature gradients. Subsequently, the lid was put on, the voltage was set to 100 V, and the blot was run for 60 min. Upon completion of the run, the blotting system was disassembled and the membrane removed and put in a stainless steel tray for subsequent staining with Ponceau S dye. All components of the blotting system were cleaned with detergent and rinsed with deionized water.The Ponceau S dye was used to stain the PVDF membrane for 1 min in order to verify consistent protein transfer and to make visible individual lanes for Western blot optimization (3.2.1.3). Subsequently, the Ponceau S dye was rinsed off with deionized water prior to the addition of blocking reagent (TTBS

containing 5% (w/v) nonfat dry milk powder). The PVDF membranes were for 1 h at RT. Primary antibodies were diluted in TTBS containing either 1.5 to 5% (w/v) nonfat dry milk or 1.5 to 5% (w/v) BSA in experimentally optimized final dilutions (Table 4-1). Membranes were incubated with primary antibody dilutions over night at 4 °C. Prior to the addition of secondary antibodies membranes were washed three times for 5 min with TTBS. Secondary antibodies (peroxidase-conjugated donkey anti-rabbit or peroxidase-conjugated donkey anti-mouse, Jackson Immuno Research Laboratories) were added at experimentally determined optimal dilutions ranging from 1:5,000 to 1:30,000 in TTBS containing 5% (w/v) nonfat dry milk powder (Table 4-1). After incubation for 1 h, blots were again washed three times for 5 min with TTBS. Blots were developed with 1.5 mL of SuperSignal® West Dura Extended Duration Substrate (Thermo Scientific). Bands were detected with a chemoluminescence imager (Chemocam HR 16 3200, INTAS). After detection, Western blot membranes were stripped off of the bound primary antibody with stripping buffer (Table 3-13) in order to prepare membranes for re-probing with an antibody directed against a loading control (ERK2 or Stat2). For this, membranes were transferred to metal trays and heated in a water bath for 10 min at 50 °C with stripping buffer. Subsequently, PVDF membranes were washed four times with 1x TBS while agitated on an orbital shaker. After washing, PVDF membranes were treated for 60 min with blocking reagent (TTBS containing 5% (w/v) nonfat dry milk powder) and subsequently washed three times with TTBS for 5 min. The PVDF membrane was then re-probed with a primary antibody against ERK2 (anti-p44/42, sc-153, or Stat2, CST#4594) over night at 4 °C. After washing three times for 5 min, incubation with the respective secondary antibody for 60 min and another washing cycle (three times, 5 min) as described above, blots were developed and ERK2 or Stat2 bands detected. Subsequently, detected phosphoprotein band intensities were normalized to ERK2 or Stat2 levels as a loading control and quantified using the LabImage1D Software (INTAS). After normalization, maximum induction levels were arbitrarily set to 1 and induction levels compared for each time point. Statistical significance of the differences between respective induction levels caused by different influenza strains and variants was calculated using a paired sample t-test (*, $p<0.05$; **, $p<0.01$).

3.2.1.3 ***Generation of positive controls and Western blot optimization***

The first step in Western blot optimization was the generation of positive controls for the phospho-specific antibodies used in this study to detect the induction of signaling pathways of interest. Hence, as shown in Table 3-14, an inducing compound or agent was selected for each pathway, mainly according to information given in antibody data sheets supplied by manufacturers.

Table 3-14: Antibodies tested in MDCK cells for the analysis of signaling pathways.

Protein	Pathway	1st antibody	Stimulant / dose in MDCK cells	Exposure time	Detection successful (yes/no)
actin	-	sc-1616	-	-	Yes
NP	-	AbD MCA400	IAV, MOI=5	> 4 h	Yes
IRF-3	IFN-β	CST #4962	-	-	No
P-IRF-3	IFN-β	CST #4947	PR8-ΔNS1, MOI=5	t = 4 h	Yes
Stat2	Jak-Stat	CST #4594	-	-	Yes
P-Stat2	Jak-Stat	CST #4441	PR8-ΔNS1, MOI=0.5	t = 8 h	Yes
p44/42	MAPK	sc-153	-	-	Yes
P-p44/42	MAPK	CST #9101	TNF-α, 20 ng/mL	t = 10 min	Yes
p38α	MAPK	sc-535	-	-	No
P-p38	MAPK	sc-7973	TNF-α, 20 ng/mL	-	No
JNK	MAPK	CST #9252	-	-	No
P-JNK	MAPK	CST #4671	TNF-α, 20 ng/mL	-	No
IκBα	NF-κB	sc-371	-	-	Yes
P-IκBα	NF-κB	CST #9246	TNF-α, 20 ng/mL	t = 10 min	Yes
p65	NF-κB	sc-8008	-	-	Yes
P-p65	NF-κB	CST #3031	TNF-α, 20 ng/mL	t = 10 min	Yes
P-Akt	PI3K/Akt	CST #2965	IAV, MOI=5	> 8 h	Yes
PI3K	PI3K/Akt	CST #4292	-	-	No
P-PI3K	PI3K/Akt	CST #4228	IAV, MOI=5	-	No
eIF2-α	PKR/eIF2-α	CST #9722	-	-	Yes
P-eIF2-α	PKR/eIF2-α	CST #9721	thapsigargin, 300 nM	t = 30 min	Yes
PKR	PKR/eIF2-α	E #1508-1	-	-	No
P-PKR	PKR/eIF2-α	E #1120-1	IAV, MOI=5	-	No

E: Epitomics, Inc.; sc: Santa Cruz Biotechnology, Inc.; CST: Cell Signaling Technology, NEB, Inc.; AbD: AbD Serotech; IAV: influenza A virus; ΔNS1: IAV PR8-ΔNS1

Optimum concentrations of these compounds or agents for the treatment of MDCK cells had to be experimentally determined, as well as exposure times. To do so, MDCK or A549 cells were grown to near confluency for 24 h and washed twice with PBS. Then, serum-free cell growth medium was added containing the respective compound or agent at different concentrations or MOIs, with final optimum conditions given in Table 3-14. Samples were collected with RIPA cell lysis buffer according to 3.2.1.2

and subjected to SDS-PAGE and Western blot analysis (3.2.1.2.2). Once suitable positive controls had been generated, the optimization of antibody usage commenced. This comprised finding the optimal concentration and combination of concentrations of primary and secondary antibodies as well as blocking reagents and conditions (Table 4-1).

As a preparation for the optimization procedure, MDCK cells were seeded in T-flasks at a concentration of 5.0 x 10^4 cells/cm². After 24 h of cell growth, cells were stimulated with compounds or agents listed in Table 3-14. Samples were collected with RIPA cell lysis buffer according to 3.2.1.2 and subjected to SDS-PAGE, in which identical protein amounts of the same sample were loaded to each gel pocket. After the Western blotting procedure, to test combinations of different primary and secondary antibody concentrations, the PVDF membrane was stained with Ponceau S dye and then cut into strips corresponding with gel lane width. Different concentrations of primary and secondary antibodies were then applied to each membrane strip, respectively. Prior to blot exposure, Western blot strips were reassembled and then measured for strongest band intensity concomitant with the highest possible reduction of background noise. As a blocking reagent, different concentrations of BSA as well as powdered milk in TTBS with varying concentrations of Tween 20 were tested. Once Western blotting conditions and procedure were optimized for the phospho-specific antibodies, infection experiments could be performed.

3.2.1.4 ***Reverse transcription (RT) and quantitative real-time PCR (qPCR)***

Transfected MDCK cells were seeded in 6-well tissue culture plates at 1.5 x 10^6 cells/well. Except for the direct addition of 350 µL buffer RA1 to washed cells and subsequent immediate sample collection, total RNA isolation from infected cells and DNAse digestion of genomic DNA was done using the NucleoSpin RNA II Kit, protocol #5.1 (Macherey-Nagel) according to instructions of the manufacturer. Per sample, 1 µg isolated RNA were transcribed to cDNA in a total reaction volume of 10 µL using 0.5 µL RevertAid™ H-Minus Reverse Transcriptase (Fermentas), 2 µL reaction buffer, 0.25 µL RiboLock™ RNAse-inhibitor (Fermentas), 1 µL dNTPs (10 mM), 0.5 µL Oligo (dT)-primer (0.5 ng/µL, Invitrogen), and 0.75 µL of DEPC-treated water in a T3000 thermocycler (Biometra). Reverse transcription reaction conditions were chosen as recommended by Fermentas (65 °C, 5 min; 4 °C, 5 min;

42 °C, 1 h; 70 °C, 10 min; 4 °C). The resulting RT reaction product was then diluted at a rate of 1:5 by the addition of 40 µL DEPC-treated water. The quantitative real-time PCR (qPCR) was set up by combining 2 µL diluted RT reaction product and a volume of 0.24 µL of PCR primers (0.1 µg/µL, Table 3-15) with 6 µL Rotor-Gene SYBR Green PCR Mix and 3.76 µL DEPC-treated water by a QIAgility benchtop pipetting automat (Qiagen) using the QIAgility software (version 4.1.4.2).

Table 3-15: qRT-PCR primers.

PKR_FOR	TGCTGGGCTGGGGAAGATTACA
PKR_REV	TCCAGAGCCAAAGGTTTGTCTTGTT
IκBα_FOR	CATGAAGGACGAGGAGTACGAGCAG
IκBα_REV	TGGCGGACCACTTCCATGGT
GAPDH_FOR	AACATCATCCCTGCTTCCAC
GAPDH_REV	GACCACCTGGTCCTCAGTGT

The qPCR was performed on a Rotor-Gene Q thermocycler (Qiagen). Reaction set up and thermal cycling parameters were taken from the technical data sheet of the mastermix (95 °C, 5 min; 40x (95 °C, 3 sec; 60 °C, 25 sec); 95 °C, 1 min; temperature ramping from 50 °C to 95 °C). Gene expression of PKR and IκBα was calculated by the $2^{-\Delta\Delta ct}$ method. The differences in expression levels of gene of interest minus endogenous control under untreated conditions ($\Delta CT_{untreated}$) are subtracted from the corresponding difference under stimulated conditions ($\Delta CT_{stimulated}$). The negative value of this subtraction (-ΔΔCT) is then used as the exponent of 2.

Equation 2 $$2^{-\Delta\Delta CT} = 2^{-(\Delta CT\ stimulated - \Delta CT\ untreated)}$$

GAPDH-RNA was used for data normalization and untransfected or uninfected cells as calibrator sample.

3.2.1.5 Virus titer determination in hemagglutination assay

Influenza virus titers were determined by hemagglutination (HA). Assay procedure was done as described in SOP (10.4.8). To conduct this assay, medium samples were taken and filled into sterile tubes, which were then centrifuged at 4 °C for 5 min at 300 x g. The supernatant was then transferred to

a fresh tube and stored at -80 °C for analysis at a later time point. This indirect quantification assay is based on the property of the viral membrane protein HA to bind to N-acetylmuramic acid (sialic acid) modifications of mammalian membrane glycoproteins, thereby agglutinating erythrocytes, forming a lattice structure that prevents the sedimentation of these red blood cells (RBC) in a round-bottomed 96-well microtiter plate. In this assay, virus titers are determined regardless of their infectivity. The virus titer is defined as the highest dilution factor of a dilution series in which hemagglutination still occurs. At this degree of dilution, there is an equal concentration of virus particles and of erythrocytes in the well. As soon as the concentration of erythrocytes (2 x 10^7 cells/mL) exceeds that of the virus particles, no lattice structure is formed and the erythrocytes sediment, leading to their accumulation at the deepest point of each round-bottomed well, which becomes macroscopically visible as a red dot. Virus titers are expressed as HA units per test volume (log HA units/100 µL).

Equation 3

$$C_{VP} = C_{RBC} \, x \, 10^{HA}$$

C_{VP}	total concentration of virus particles	(virus particles/100 µL)
C_{RBC}	concentration of red blood cells	(cells/ mL)
HA	total virus titer	(log HA units/100 µL)

The chosen method is based on an automatic photometric evaluation of a $1:2^{0.5}$ dilution series with a mean confidence interval (95%) of the HA-activity of +15% and -13% (Kalbfuss et al. 2008).

3.2.1.6 ***Immunotitration of infectious virus particles***

The concentration of infectious virus particles was determined in an immunotitration assay and expressed as tissue culture infectious dose 50 ($TCID_{50}$). Assay procedure was conducted according to a workgroup internal SOP (10.4.9). In brief, confluent MDCK cells were harvested by trypsinization and cell concentration was adjusted to 4-5 x 10^5 cells/mL including 1% (v/v) gentamicin prior to seeding in 96-well microtiter plates at 100 µL per well. Microtiter plates were then incubated for 1 to 2 days at

37 °C, 5% CO_2. A ten-fold serial dilution of the virus suspension was prepared in virus medium containing 1% (v/v) gentamicin. Eight replicate wells of a microtiter plate with MDCK cells were infected with 100 µL of each dilution of the virus suspension, respectively. After infection, microtiter plates were incubated for 24 h at 37 °C, 5% CO_2. Then, virus medium containing 0.04% (v/v) trypsin and 1% (v/v) gentamicin was added and cells were subsequently incubated for another 24 h at 37 °C, 5% CO_2. For the following antibody incubation step, antiserum containing polyclonal antibodies had to be prepared by absorbing antibodies binding to cellular components on a confluent layer of cells grown for 1 to 2 days. Cells were washed three times with 100 µL PBS and fixated for 30 min at 0 °C with 100 µL ice-cold 80% (v/v) acetone per well. After cells were washed three times with 100 µL PBS per well, 50 µL of a 1:100 or 1:200 dilution in PBS of the respective purified polyclonal primary antibody (nanoTools, Germany or NIBSC, UK) were added per well and incubated for 60 min at 37 °C. Cells were again washed three times with 100 µL PBS prior to the addition of 50 µL per well of a 1:500 dilution in PBS of the secondary antibody coupled to the fluorescent dye Alexa Fluor 488 (Invitrogen). After incubation for another 60 min at 37 °C, cells were washed three times with 100 µL PBS before the final addition of 100 µL PBS per well. Microtiter plates were then evaluated with a fluorescence microscope and the $TCID_{50}$ calculated according to a method by Spearman-Kaerber (Mahy and Kangro 1996a). The limit of detection of this assay was 3.2 x 10² infectious virus particles/mL with a standard error of ±0.3 log $TCID_{50}$.

3.2.1.7 ***Plaque assay***

At first, MDCK cells were seeded into 6-well tissue culture plates at 1 x 10^6 cells/well with 2 mL cell growth medium per well. 24 h after cell seeding, a ten-fold dilution series of PR8-NIBSC seed virus ($TCID_{50}$ = 5.43 x 10^6 V/mL) in infection medium was prepared. Then, MDCK cells were washed twice with PBS and subsequently infected by adding 800 µL of the 10^{-3}, 10^{-4}, and 10^{-5} dilutions of the PR8-NIBSC seed virus stock. After infection, 6-well tissue culture plates were incubated for 1 h at 37 °C and 5% CO_2. Medium was aspirated and cells were covered with 2 mL of fresh infection medium, containing 0.1% (v/v) trypsin, 1% (v/v) gentamicin, and 1% (w/v) soft agar (melting point 30 °C, Applichem A3477) tempered in a drying oven (Heraeus UT6), followed by an incubation period of 48 to

72 h at 37 °C and 5% CO_2. At 48 hpi, macroscopically visible plaques were picked with 100 µL pipette tips and transferred to T25 tissue culture flasks containing confluent MDCK cells with 5 mL infection medium, respectively, containing 1% (v/v) gentamicin. After 72 h, medium samples were taken and analyzed with both the HA assay (3.2.1.5) as well as the $TCID_{50}$ assay (3.2.1.6).

3.2.1.8 ***CellTiter-Glo viability assay***

To study the impact of PKR activity on influenza virus replication in MDCK cells, the chemical inhibitor 2-aminopurine (2-AP) was used. At first, to determine the toxicity of the compound, the CellTiter-Glo® luminescent cell viability assay (Promega) was conducted. In brief, the ATP that is released after cell lysis generates a luminescent signal that is directly proportional to the number of metabolically active, viable cells. The luminescence signal is generated by a thermostable luciferase that catalyzes the following reaction:

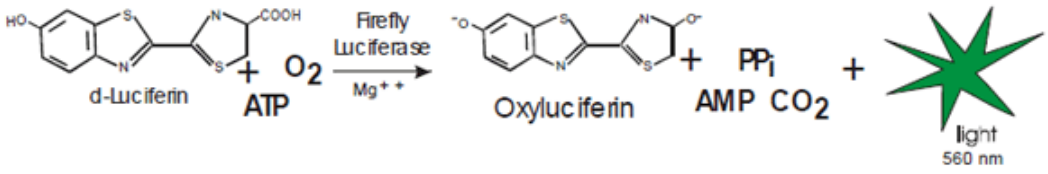

Figure 3.2-3: Bioluminescent reaction catalyzed by firefly luciferase
*(*http://www.biotek.com/resources/articles/luciferase-measurements-plate-reader.html*)*.

For use in cell culture experiments, a 150 mM stock solution of 2-AP (2-aminopurine nitrate salt, 198.1 g/Mol, Sigma A2380) was prepared. 100 µL of an MDCK cell suspension with a concentration of 1 x 10^5 cells/mL were seeded into each well of a 96-well plate. After 24 h of cell growth at 37 °C, 5% CO_2, 2-AP was added to the medium at final concentrations of 0, 5, 20, 40, and 80 mM. On the next day, CellTiter-Glo buffer and CellTiter-Glo substrate were prepared according to instructions of the manufacturer (Promega, Part# TB288). The 96-well plate was removed from the incubator and equilibrated for 30 min at RT before cell culture medium was decanted. Then, 50 µL of serum-free GMEM was added to each well prior to the addition of 50 µL of CellTiter-Glo reagent. Then, in order to induce cell lysis, 96-well plates were incubated at RT on an orbital shaker for 2 min, followed by

another incubation step for 10 min at RT. Subsequently, from each well 90 µL of the cell lysate were transferred to an opaque-walled 96-well plate. After a brief centrifugation at 2000 rpm, luminescence was recorded for 0.5 s/well in the LB960 luminometer (Berthold).

3.2.1.9 ***Luciferase reporter assay***

Two days prior to transfection, MDCK cells were seeded into T-flasks, assuring that at time of transfection, cells were growing at an exponential rate. After trypsinization, the amount of cells needed for transfection (3 x 10^5 cells/well) was pelletized by centrifugation for 5 min at 300 x g. Cells were transfected using 2.5 µL/well of Lipofectamine 2000 (Invitrogen) with the following plasmids: 200 ng/well pGL4.10+TK (firefly-luciferase under the control of a weak constitutive herpes virus thymidine kinase promoter), 200 ng/well pGL4 (renilla-luciferase), and 200 ng/well pMax (plasmid encoding green fluorescent protein) as a transfection control. At first, cells were aliquoted in serum-free GMEM. Then, for each transfection, 200 ng plasmid-DNA were included in 10 µL serum-free GMEM. Additionally, for each transfection, 2.5 µL Lipofectamine 2000 were included in 50 µL serum-free GMEM. Plasmid-DNA and Lipofectamine 2000 preparations were then mixed and incubated for 20 min at 37 °C to allow for complex formation. Subsequently, for each well 60 µL of plasmid-DNA complex solution was added to 3 x 10^5 cells in 440 µL GMEM. Following brief mixing, 500 µL per well of the MDCK cell plasmid-DNA mixture were then seeded in 24-well plates and incubated at 37 °C over night. 24 h post transfection (hpt) cells were infected with A/Puerto Rico/8/34 variants in the presence of trypsin (2 x 10^{-6} units/cell) at an MOI of 5 to ensure synchronous infection. At 12 and 16 hpi, cells were washed twice with PBS and subsequently 100 µL/well of passive lysis buffer (PLB, Promega) were added and 24-well plates were incubated for 15 min at RT on an orbital shaker. Lysates were then scraped off with pipette tips, transferred to 1.5 mL reaction tubes and stored at -20 °C. Luciferase activity measurement was prepared and conducted according to the technical manual 040, VI.C standard protocol (Promega) using the Tech Centro luminometer LB 960 (Berthold) and the Centro Symbol software.

3.2.2 Cell manipulation techniques

Interpreting the results gained in the analysis of cellular signal transduction and virus replication, several strategies were subsequently employed to manipulate cellular processes. These tools comprised the use of the chemical kinase inhibitor 2-AP and the transfection of cells with a structural mimic of viral RNA or with siRNA by electroporation in order to stimulate innate immunity or to temporarily silence gene expression.

3.2.2.1 ***Polyinosinic:polycytidylic acid (polyI:C) transfection***

PolyI:C is considered a synthetic analog of double-stranded viral RNA and was used to stimulate the IFN response in MDCK cells and accordingly to generate positive controls for phospho-Stat2 Western blots. At first, MDCK cells were seeded into T75 tissue culture flasks at a cell density of about 3.0 x 10^4 cells/cm². After a confluency of about 80% was reached, cells were trypsinized and cell suspensions from the different T-flasks pooled. Then, cells were centrifuged at RT for 10 min at 300 x g. Cell pellets were washed twice with PBS and resuspended in buffer "R" (Neon™ Transfection System, Invitrogen) to adjust a final cell concentration of 0.5 to 1.5 x 10^7 cells/mL. For each transfection reaction, a cell suspension volume of 100 µL was needed. 4 µL of polyI:C (5 µg/µL) were added to 100 µL of cell suspension. Electroporation was done with the electroporating device of the Neon™ Transfection System kit by Invitrogen (1700V, 20 ms, 1 pulse). After electroporation, cells were seeded in 60 mm petri dishes with 5 mL of fresh, prewarmed cell growth medium added previously. Petri dishes were incubated at 37 °C, 5% CO_2. Subsequently, samples were taken at indicated time points according to the Western blot sample preparation protocol using RIPA cell lysis buffer (3.2.1.2.1).

3.2.2.2 ***RNAi knockdown experiments***

MDCK cells were seeded in T-flasks at a cell density of 2.5 x 10^4 cells/cm², assuring that at time of transfection with siRNA (Table 3-16) cells were growing at an exponential rate.

Table 3-16: Sequences of siRNA. Two pairs of siRNA molecules were used for each gene (Eurogentec).

Gene	siRNA sequence (5'→3')
PKR #1	GCA-GAU-UUC-UUC-ACA-AGA-A55
	UUC-UUG-UGA-AGA-AAU-CUG-C55
PKR #2	GGC-GGU-UAG-UUC-UUU-AUC-A55
	UGA-UAA-AGA-ACU-AAC-CGC-C55
IκBα #1	CCG-AGA-CUU-UCG-AGG-AAA-U55
	AUU-UCC-UCG-AAA-GUC-UCG-G55
IκBα #2	GCU-GAU-GUC-AAC-AGA-GUU-A55
	UAA-CUC-UGU-UGA-CAU-CAG-C55

Prior to transfection, cells were trypsinized and cell concentration determined according to 3.1.3 using a ViCell XR counting device (Beckman-Coulter). Then, cells were centrifuged at RT for 10 min at 300 x g. Cell pellets were washed twice with PBS and resuspended in buffer "R" (Neon™ Transfection System, Invitrogen) to adjust a final cell concentration of 2 x 10^7 cells/mL. For each transfection reaction, a cell suspension volume of 100 µL was needed. The concentration of siRNA during the electroporation procedure in volumes of 100 µL was adjusted so that a final concentration of 100 nM in the medium volume of each well of the 6-well plates was reached. Electroporation was done with the electroporating device of the Neon™ transfection system kit (Invitrogen) by setting off 1 pulse at 1700 V for 20 ms. After electroporation, cells were seeded in 6-well plates containing 2 mL per well of cell growth medium prewarmed to 37 °C. 48 h post transfection, cells were either lysed and corresponding RNA samples were collected or cells were infected with influenza A/Puerto Rico/8/34 virus at an MOI of 0.025 to study the effects of gene knockdown on virus replication. Hence, at 16, 20, 24, 48 hpi or 96 hpt, samples were taken and total RNA isolated according to 3.2.1.4.

4 Results

4.1 Generation of positive controls

The aim of this project was to analyze the influenza virus-induced activation of antiviral signaling cascades in MDCK cells used as a substrate for virus replication in a bioprocess for vaccine production. The method of choice for monitoring the induction of signaling cascades was Western blot due to the applicability of several phospho-specific antibodies and the ready availability of the method. However, during the initial set up of the method, an obstacle was posed by the limited availability of canine specific antibodies. Therefore, commercially distributed antibodies with cross-species specificities had to be tested for their applicability in the analysis of MDCK cells. Accordingly, the first step was to generate positive controls with the human bronchial epithelial cell line A549 or, if feasible, directly with MDCK cells. These positive controls could then be used in further Western blot optimization with MDCK cell-derived samples. Hence, cells were treated with a number of different stimulants for indicated periods of time (Table 3-14).

In the experiment described in the following, A549 cells grown to near confluency in T-flasks were stimulated with 20 ng/mL recombinant human TNF-α (Calbiochem) included in serum-free A549 cultivation medium to activate the NF-κB signaling pathway.

As shown in Figure 4.1-1, the stimulation with TNF-α led to a peak induction level of IκBα phosphorylation after 45 min. At 15 min post stimulation no phosphorylation of IκBα could yet be measured. Within 30 and 60 min after stimulation with TNF-α, a strong phosphorylation of IκBα could be observed.

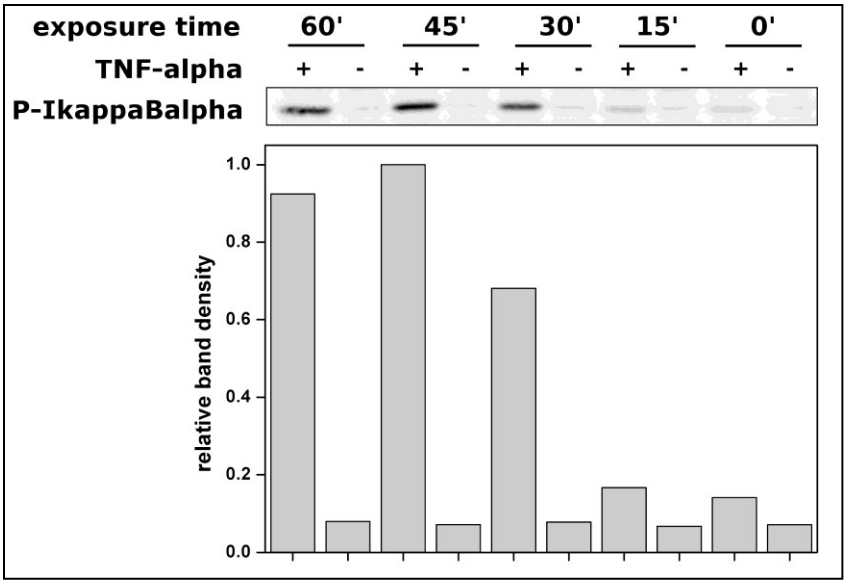

Figure 4.1-1: Induction of the NF-κB signaling pathway in A549 cells after stimulation with TNF-α.
In order to generate positive controls for the analysis of signaling pathways in Western blot, A549 cells were cultivated in T-flasks and stimulated with recombinant human TNF-α (Calbiochem). Samples were taken according to the RIPA cell lysis protocol at 15, 30, 45, and 60 min post stimulation for subsequent analysis in Western blot with an antibody against phospho-IκBα (CST, #9246), followed by densitometric analysis of the PVDF membranes. Band intensity of phospho-IκBα was normalized to ERK2 expression levels, with maximum induction levels set to 1.

In Figure 4.1-2, the Western blot analysis of the induction of the Jak-Stat (A) and the NF-κB (B) signaling pathways in MDCK cells through treatment with different agents is shown. The phosphorylation of Stat2 in MDCK cells could not be induced by cytokine treatment due to a lack of commercially available canine-specific IFN-beta. Therefore, alternative ways had to be found to induce the signaling pathway in order to generate samples for Western blot optimization.

Hence, MDCK cells were transfected with a structural mimic of viral dsRNA, polyI:C. At 5 h post transfection, the phosphorylation of Stat2 could be clearly detected (Figure 4.1-2-A) with a phospho-specific primary antibody (Table 4-1) and a secondary antibody derived from donkey against rabbit IgG (Jackson ImmunoResearch, #711-036-152). Despite the fact that cross-species reactivity for this human Stat2 specific antibody was stated only for rabbit and bovine Stat2 by the manufacturer, the antibody proved as applicable for canine samples as well. A previous in-silico comparison of amino acid epitope sequences had already indicated this possibility (10.3). The samples gained in the transfection with polyI:C then served as positive control in the analysis of Jak-Stat activation in MDCK cells infected with influenza A/Puerto Rico/8/34 (Table 3-6) carrying a deletion of the genome segment encoding for the NS1 protein (PR8-ΔNS1). MDCK cells were grown to near confluency in cell culture dishes with a

diameter of 60 mm for three days. Subsequently, MDCK cells were infected with PR8-ΔNS1 at an MOI of 0.5 for up to 8 h as described in chapter 3.1.5.

At 8 hpi, the virus-induced phosphorylation of Stat2 in MDCK cells could clearly be observed. As densitometric analysis showed, the phosphorylation of Stat2 induced by the infection with PR8-ΔNS1 was about two-fold stronger than the signal detected in polyI:C transfected MDCK cells samples.

In Figure 4.1-2-B, the Western blot analysis of IκBα phosphorylation of MDCK cell samples treated with TNF-α is shown. MDCK cells were grown to near confluency in T-flasks and stimulated with 20 ng/mL recombinant human TNF-α. As shown in Figure 4.1-2-B, it was possible to induce the NF-κB signaling pathway in MDCK cells with recombinant human TNF-α and to detect its induction with a phospho-specific primary antibody (1:100 in TTBS with 5% (w/v) milk, Table 4-1) and a peroxidase-conjugated anti-mouse IgG derived from donkey (1:10,000 in TTBS with 5% (w/v) milk). As for the detection of phospho-Stat2, the samples obtained by the stimulation of MDCK cells with recombinant human TNF-α were subsequently used for further Western blot optimization.

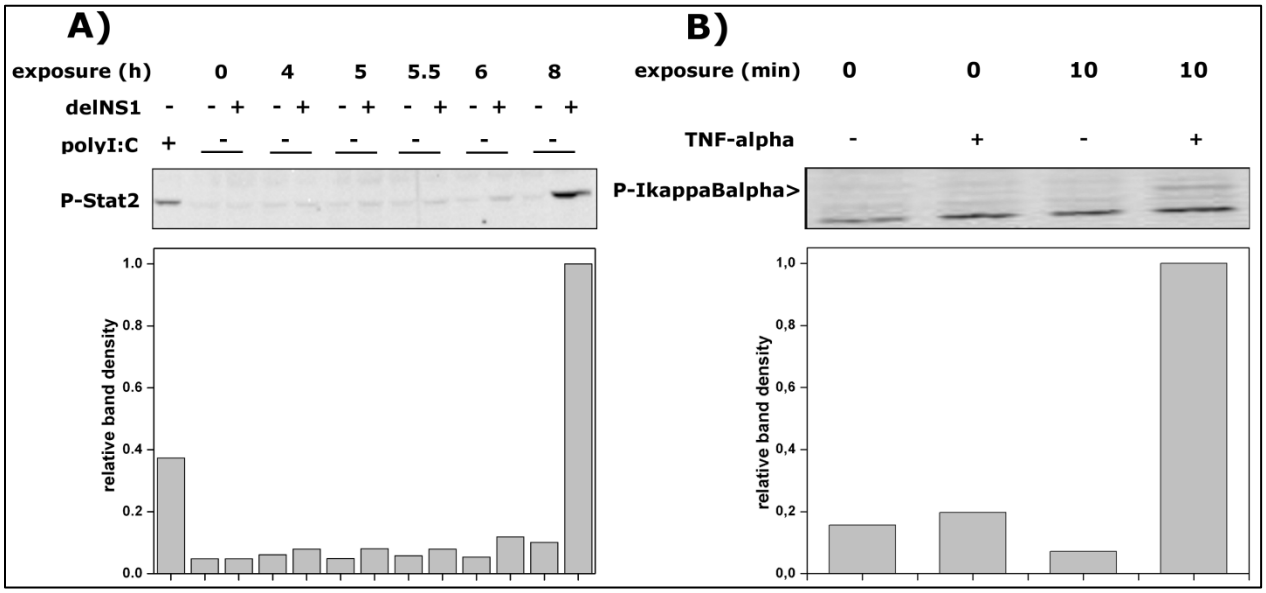

Figure 4.1-2: Induction of the Jak-Stat and the NF-κB signaling pathways in MDCK cells to generate positive controls.

MDCK cells were grown in T-flasks and either (A) infected with influenza A/PR/8/34-delNS1 or transfected with polyI:C for 5 h or (B) stimulated with TNF-α (Calbiochem). Samples were taken after indicated exposure times according to the RIPA cell lysis protocol and analyzed in Western blot with antibodies against (A) phospho-Stat2 (CST, #4441) or (B) phospho-IκBα (CST, #9246), followed by densitometric analysis of the PVDF membranes. Band intensities of phospho-IκBα and phospho-Stat2 were normalized to ERK2 expression levels, with maximum induction levels set to 1. These samples then served as positive control for further Western blot optimization.

In addition to the generation of positive controls described here for the detection of phospho-Stat2 and phospho-IκBα, similar procedures were chosen for all other phospho-specific antibodies used in this study. However, positive controls could not be obtained for each phosphoprotein of interest since obstacles regarding a lack of specificity/sensitivity could not be overcome in all cases. A complete summary of the antibodies tested for applicability in the analysis of MDCK cells is shown in Table 3-14.

4.2 **Western blot optimization**

Western blot optimization was done using the positive controls obtained as previously described in chapter 4.1. The aim of Western blot optimization was to achieve a combination of the strongest possible specific Western blot band intensity, elimination or at least strong reduction of background and as little consumption as possible of primary and secondary antibodies, i.e. the highest possible antibody dilutions. Furthermore, concentrations of primary and secondary antibodies had to be optimized because the specifications by the manufacturer for antibody use differed in most cases from the optimal concentrations determined experimentally for the analysis of MDCK cells. In addition to antibody dilutions, the concentrations of BSA or skimmed milk powder as well as Tween 20 contained in TTBS were modified and optimized. As a result, the detection of specific bands could be enhanced while unspecific background signals were repressed.

Hence, as shown in Figure 4.2-1, equal amounts (15 µg) of identical protein samples obtained during the generation of positive controls were separated in SDS-PAGE and analyzed in Western blot (3.2.1.2.2).

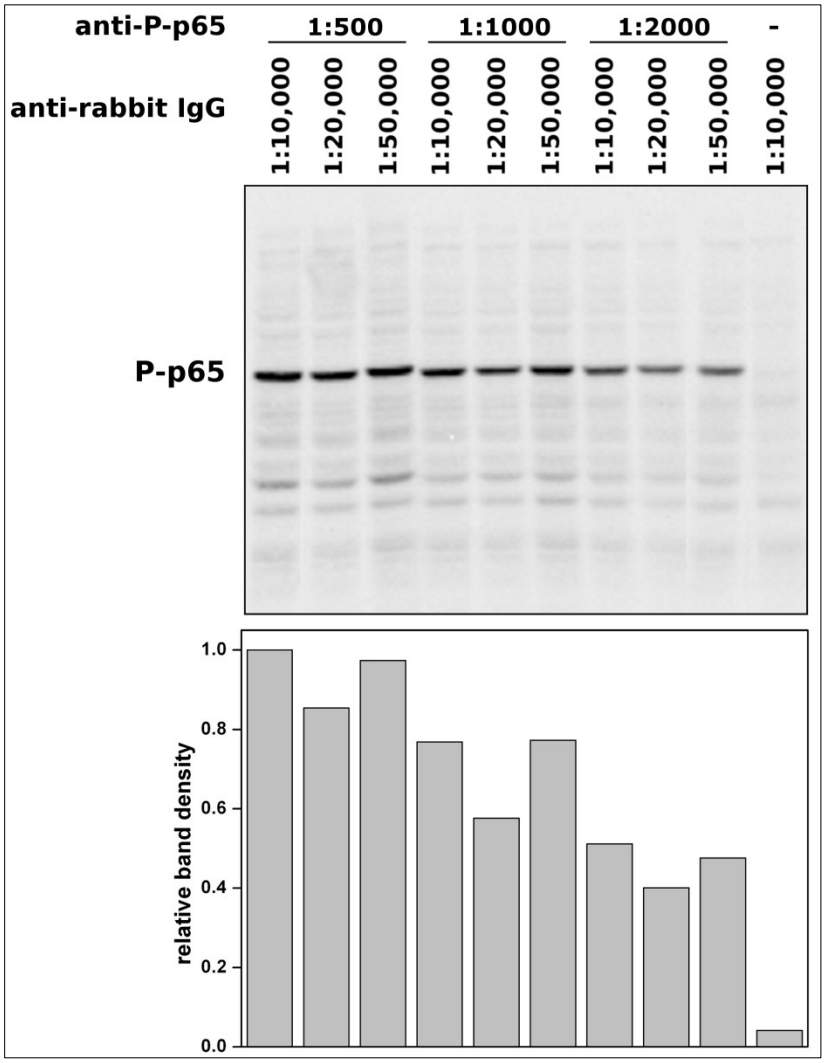

Figure 4.2-1: Western blot optimization by adjusting primary and secondary antibody concentrations.
Equal amounts (15 µg) of identical protein samples of positive controls generated previously by the treatment of MDCK cells with TNF-α (Calbiochem) were separated in an SDS-PAGE gel and subsequently analyzed in Western blot. After protein transfer, membranes were cut in strips corresponding with lane width and different concentrations of primary and secondary antibodies were applied to each lane strip. Membranes were reassembled prior to signal detection. Band intensity of phospho-p65 was normalized to p65 expression levels, with maximum induction levels set to 1.

After electrotransfer of proteins from SDS-PAGE gel to blot membrane, the membrane was cut in strips corresponding with gel lane width. Subsequently, different concentrations of primary and secondary antibodies were applied to each strip, respectively. Following the incubation with the tested antibody dilutions, the strips were reassembled for chemoluminescence band detection.

In the example shown in Figure 4.2-1, the primary antibody (anti-phospho-p65, CST #3031) was diluted in TTBS with 1.5% (w/v) BSA at dilutions of 1:500; 1:1,000 and 1:2,000. In addition to these three

primary antibody concentrations, three different concentrations (1:10,000; 1:20,000; 1:50,000) of the secondary antibody were tested (donkey anti-rabbit IgG in TTBS with 1.5% (w/v) BSA). It could be observed that signal intensity was reduced by about 50% if primary antibody concentration was decreased four-fold from 1:500 to 1:2,000. Surprisingly, signal intensity was lowest at a dilution of the secondary antibody of 1:20,000 in combination with all tested primary antibody concentrations and equally high for dilutions of both 1:10,000 and 1:50,000. In order to reduce the economic cost caused in the long run by antibody consumption, it was decided to apply a dilution of the primary antibody of 1:1,000 instead of 1:500. Therefore, for all future analyses of phospho-p65 in MDCK cell samples, a 1:1,000 dilution of the primary antibody was combined with a 1:50,000 dilution of the secondary antibody. According to the scheme illustrated in Figure 4.2-1 for the optimization of phospho-p65 detection, conditions for use of all antibodies were optimized if the detected specific band could not be differentiated clearly from background or if the specific signal was altogether not clearly visible. A summary of the experimentally optimized concentrations of respective combinations of primary and secondary antibodies is presented in Table 4-1.

Table 4-1: Final dilutions of primary and secondary antibodies for use in Western blotting.

protein	1st antibody	concentration/matrix	2nd antibody	concentration/matrix
actin	sc-1616	1:1000; TTBS/5% milk	donkey anti-goat IgG	1:10,000; TTBS/5% milk
NP	AbD MCA400	1:1000; TTBS/5% milk	donkey anti-mouse IgG	1:10,000; TTBS/5% milk
P-IRF-3	CST #4947	1:500; TTBS/5% BSA	donkey anti-rabbit IgG	1:10,000; TTBS/5% milk
Stat2	CST #4594	1:500; TTBS/5% BSA	donkey anti-rabbit IgG	1:5000; TTBS/5% milk
P-Stat2	CST #4441	1:500; TTBS/5% BSA	donkey anti-rabbit IgG	1:5000; TTBS/5% milk
p44/42	sc-153	1:10,000; TTBS/5% milk	donkey anti-rabbit IgG	1:30,000; TTBS/5% milk
P-p44/42	CST #9101	1:10,000; TTBS/5% BSA	donkey anti-rabbit IgG	1:30,000; TTBS/5% milk
IκBα	sc-371	1:1000; TTBS/5% milk	donkey anti-rabbit IgG	1:10,000; TTBS/5% milk
P-IκBα	CST #9246	1:100; TTBS/5% milk	donkey anti-mouse IgG	1:10,000; TTBS/5% milk
P-p65	CST#3031	1:1000; TTBS/1.5% BSA	donkey anti-rabbit IgG	1:50,000; TTBS/1.5%BSA
P-Akt	CST #2965	1:500; TTBS/5% BSA	donkey anti-rabbit IgG	1:10,000; TTBS/5% milk
eIF2-α	CST #9722	1:5000; TTBS/5% BSA	donkey anti-rabbit IgG	1:100,000; TTBS/5% milk
P-eIF2-α	CST #9721	1:250; TTBS/5% BSA	donkey anti-rabbit IgG	1:4000; TTBS/5% milk

For the analysis of samples obtained in follow-up infection experiments, the experimentally determined conditions for respective pairs of primary and secondary antibodies were applied accordingly.

4.3 Comparison of several influenza virus strains and variants with regard to replication and concomitant induction of antiviral signaling pathways

Manufacturers of influenza vaccines have only little time to adapt the cell culture-based production process to the respective virus strains and provide sufficient amounts of vaccine. Each year by early spring, the WHO announces a combination of two influenza A virus and one influenza B virus strains with the highest presumed risk to human health during the course of the anticipated flu season. Hence, only a rather short time frame of approximately six months remains for manufacturers to establish the process and realize a sufficient vaccine supply line.

The following experiment was aimed at answering the question of whether a correlation exists between the induction of antiviral signaling in the host cell during influenza virus replication and the final virus titers reached by each individual influenza virus strain or variant. This was meant to assess whether antiviral signaling in the host cell might state a limiting factor to influenza virus replication in the vaccine production process. Therefore, a number of influenza A virus strains and a single influenza B virus strain were chosen for analysis (Table 3-6).

MDCK cells were grown to near confluency, washed twice with PBS and were subsequently infected by adding infection medium containing trypsin and one of the influenza virus strains or variants at a defined MOI, respectively. Medium samples were taken at 12, 24, and 96 hpi for analysis in the HA assay. At 8 and 12 hpi, samples were taken according to the RIPA cell lysis protocol for analysis in Western blot. After protein concentration of the lysates had been determined, an equal amount of protein of each sample was added to an SDS-PAGE gel for protein sample separation. In the following, Western blotting was conducted and membranes were probed with primary antibodies against the influenza A virus NP, and host cell phospho-eIF2-α, or phospho-Stat2 under previously optimized conditions (Table 4-1). After Western blot band detection and quantification, PVDF membranes were stripped and reprobed with a primary antibody against ERK2. NP and phosphoprotein bands were normalized to ERK2 expression levels.

The HA titers reached by each respective virus strain or variant during the replication in MDCK cells at 0, 12, 24, and 96 hpi are shown in Figure 4.3-1-A.

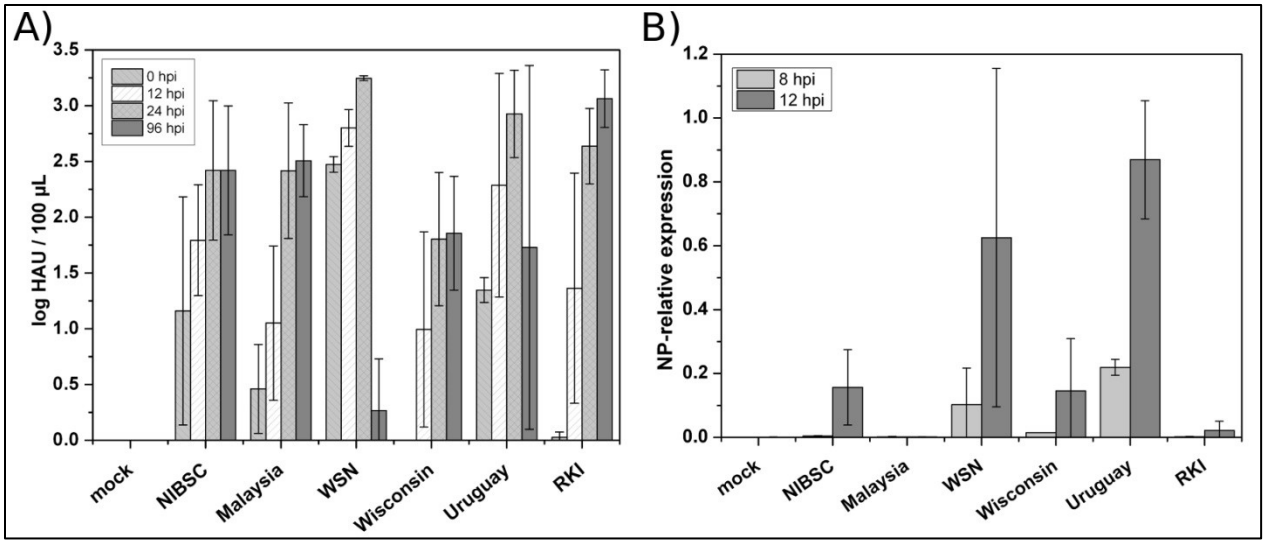

Figure 4.3-1: Infection of MDCK cells with different influenza virus strains and variants.
MDCK cells grown in T-flasks were infected with different influenza strains and variants at an MOI of 5 or 1 (B/Malaysia/2506/2004). The course of infection was monitored at indicated time points by measuring HA titers in cell culture medium samples (A) using the HA assay or (B) in Western blot analysis of samples obtained by RIPA lysis of infected cells using an antibody against influenza A virus NP (AbD, MCA400). The expression of influenza B/Malaysia/2506/2004 NP could not be detected with the utilized primary antibody due to lack of specificity. Values represent the mean ± S.D. of three independent infection experiments. NP band intensity was normalized to ERK2 expression levels. Abbreviations of influenza viruses: NIBSC: A/Puerto Rico/8/34 (NIBSC); Malaysia: B/Malaysia/2506/2004; WSN: A/WSN/33; Wisconsin: A/Wisconsin/67/2005-like HGR; Uruguay: A/Uruguay/716/200-like HGR; RKI: A/Puerto Rico/8/34 (RKI).

It is noteworthy that in the infection experiment done at an MOI of 5, the initial HA titers determined at 0 hpi differ significantly between the various strains, which is attributed to different ratios of infectious over non-infectious virus particles in the seed virus. For instance, at 0 hpi, an average HA titer of 1.2 log HAU/100 µL or even 2.5 log HAU/100 µL was determined for the infection with PR8-NIBSC or A/WSN/33, respectively. The high standard deviation of the HA titer measured for the PR8-NIBSC infection at time point 0 hpi indicates the existence of different ratios of infectious over non-infectious virus particles in the seed virus batches used during the three infection experiments, since with a standard deviation of about 1.0 log HAU/100 µL, an error can almost be excluded. Hence, during the evaluation of the results with regard to the induction of signaling pathways, special care has to be taken. To the contrary, initial HA titers of nearly 0 log HAU/100 µL or 0.5 log HAU/100 µL for infections with PR8-RKI or B/Malaysia/2506/2004, respectively, point to a low ratio of infectious over non-infectious virus particles. Striking differences were also observed in the final HA titers reached. While at 96 hpi PR8-RKI had grown to 3.1 log HAU/100 µL, the A/Wisconsin/67/2005-like high growth reassortant (HGR) had only reached 1.9 log HAU/100 µL. The maximum HA titers reached by each respective strain where as follows: 2.4 log HAU/100 µL at 96 hpi by PR8-NIBSC;

2.5 log HAU/100 µL at 96 hpi by B/Malaysia/2506/2004; 3.3 log HAU/100 µL at 24 hpi by A/WSN/33; 1.9 log HAU/100 µL at 96 hpi by the A/Wisconsin/67/2005-like HGR; 2.9 log HAU/100 µL at 24 hpi by the A/Uruguay/716/2007-like HGR; and 3.1 log HAU/100 µL at 96 hpi by PR8-RKI. For two different influenza virus strains, A/WSN/33 and the A/Uruguay/716/2007–like HGR, a sharp decrease in HA titers was observed between 24 and 96 hpi, which is difficult to explain. The HA titers measured at 24 hpi dropped from 3.3 log HAU/100 µL and 2.9 log HAU/100 µL to 0.3 log HAU/100 µL and 1.7 log HAU/100 µL, respectively. Besides the HA assay, the progression of virus replication was also monitored in Western blot with an antibody specific for influenza A virus NP (Figure 4.3-1-B).

Due to its specificity for influenza A virus NP, using this antibody the replication of influenza B/Malaysia/2506/2004 could not be monitored. Because of the detachment of adherently growing cells from the surface of the cultivation vessel triggered by virus infection, no RIPA cell lysis samples were taken beyond 12 hpi. Thus, the expression of NP mirrors the progression of virus replication only at an initial stage. Since the aim of these infection experiments was to compare the induction of signaling pathways, a comparable progression of virus replication would be desirable. It has been previously described that actual virus replication is a precondition for the induction of signaling pathways with a predominantly antiviral character (Rehwinkel et al. 2010).

As shown in Figure 4.3-1-B, the progression of virus replication at 8 and 12 hpi varied from strain to strain. As indicated by NP expression levels, the replication of the A/Uruguay/716/2007-like HGR progressed the most until 12 hpi, followed by A/WSN/33. Only a fraction of these expression levels of NP was reached in MDCK cells infected with PR8-NIBSC, the A/Wisconsin/67/2005-like HGR, and PR8-RKI.

In Figure 4.3-2, the comparison of the analyzed influenza virus strains and variants regarding their impact on the induction of eIF2-α (A) and Stat2 (B) phosphorylation is shown. The phosphorylation of eIF2-α by PKR has been described as a crucial event of the antiviral defense of the host cell. As an important translation initiation factor of eukaryotic cells, its inactivation by PKR leads to a shut-down of cellular protein synthesis, thereby impairing virus replication. Additionally, as an indicator for the activation of the Jak-Stat signaling cascade, the phosphorylation of Stat2 was analyzed.

Comparing different influenza strains and variants, the most striking observation made was that only the infection with PR8-NIBSC as well as with the A/Wisconsin/67/2005-like HGR led to a strong, statistically significant phosphorylation at 12 hpi, which was considerably above the base level reached in mock infected cells with an about 2.5-fold higher induction level. The infection with all other

influenza virus strains and variants at 12 hpi led to average eIF2-α phosphorylation levels only about 20 to 50% above the level reached in mock infected cells. At 8 hpi for all tested influenza strains and variants, including PR8-NIBSC and the A/Wisconsin/67/2005-like HGR, the average eIF2-α phosphorylation level reached differed only slightly and not statistically significant from that reached at 0 hpi in mock infected cells.

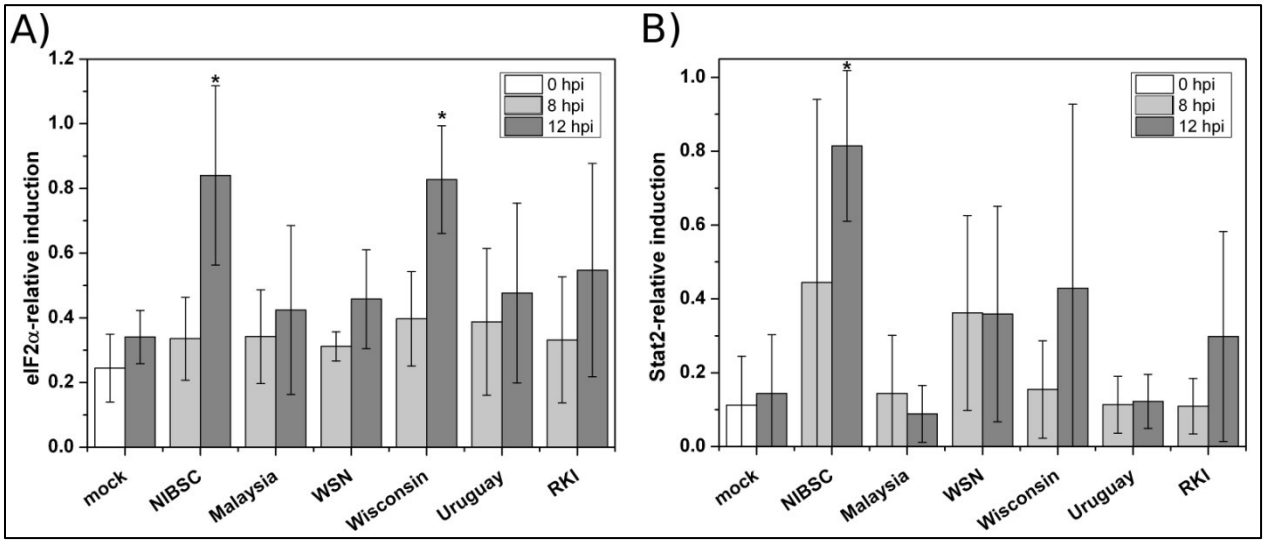

Figure 4.3-2: Western blot analysis of eIF2-α phosphorylation and Jak-Stat activation in MDCK cells induced by infection with different influenza virus strains and variants.
MDCK cells grown in T-flasks were infected with different influenza virus strains and variants at an MOI of 5 or 1 (B/Malaysia/2506/2004). Samples were taken at indicated time points according to the RIPA cell lysis protocol and the (A) induction of eIF2-α phosphorylation and (B) Jak-Stat activation were analyzed in Western blot using phospho-specific antibodies (anti-phospho-eIF2-α, CST, #9721; anti-phospho-Stat2, CST, #4441). Values represent the mean ± S.D. of three independent infection experiments (* p<0.05). Band intensity of phospho-eIF2-α and phospho-Stat2 was normalized to ERK2 expression levels, with maximum induction levels set to 1. Abbreviations of influenza viruses: NIBSC: A/Puerto Rico/8/34 (NIBSC); Malaysia: B/Malaysia/2506/2004; WSN: A/WSN/33; Wisconsin: A/Wisconsin/67/2005-like HGR; Uruguay: A/Uruguay/716/2007-like HGR; RKI: A/Puerto Rico/8/34 (RKI).

Followed by the expression and secretion of IFN-beta, the Jak-Stat pathway is induced in an autocrine and paracrine manner, which mediates the expression of up to 300 IFN-regulated genes. As displayed in Figure 4.3-2-B, the infection with PR8-NIBSC led to the strongest average phosphorylation level of Stat2 as compared to the infections with all other influenza strains and variants. At 8 hpi, the average level of Stat2 phosphorylation was about 4-fold higher as compared to mock infected samples at 0 hpi. At 12 hpi, the average level of Stat2 phosphorylation increased to a roughly 8-fold higher average level as compared to mock infected cells. Visibly no induction of the pathway could be observed in B/Malaysia/2506/2004 and the A/Uruguay/716/2007-like HGR infected cells. The average Stat2

phosphorylation level in A/WSN/33 infected cells was about 3.5-fold higher at 8 and 12 hpi as compared to mock infected cells at 0 or 12 hpi, respectively. In with PR8-RKI or the A/Wisconsin/67/2005-like HGR infected cells at 12 hpi, the average phosphorylation level of Stat2 increased between 3 to 4-fold as compared to mock infected cells, respectively. To the contrary, at 8 hpi with the latter of the two influenza strains, the average phosphorylation level of Stat2 was indifferent as compared to mock infected cells.

In summary, an infection of MDCK cells with either one of the two influenza A virus strains PR8-NIBSC and the A/Wisconsin/67/2005-like HGR led to the strongest observable average phosphorylation levels of eIF2-α as well as Stat2 in this experimental setting. At the same time, the HA titers measured in medium supernatants of cells infected with either one of the two strains as well as the corresponding NP expression levels were the lowest of all compared influenza virus strains and variants. Yet, this experiment was only suited to draw first careful conclusions in assessing whether a correlation exists between the induction of antiviral signaling and virus replication efficiency. Especially the obvious differences in initial replication velocity, that hint at considerably different replication rates from strain to strain, illustrate the difficulties that can arise in the attempt to undertake a one to one comparison of several virus strains with regard to the induction of signaling cascades. A synchronous infection is a precondition for a precise comparison of the induction of antiviral signaling, as virus replication should in this case progress at similar rates in all compared MDCK cell populations infected with either one of the analyzed influenza virus strains and variants.

Additionally, the high standard deviations observed for nearly all replicate samples analyzed in Western blotting point to high batch to batch variations of the analyzed influenza virus strains. Furthermore, the high standard deviations emphasize the limited resolution power of the analytical tool that yields only semiquantitative results with regard to the minute differences between the analyzed virus strains and variants in the induction of antiviral signaling pathways. Based upon these observations, a more detailed investigation of two selected influenza A virus variants followed.

4.4 Comparison of two variants of influenza A/Puerto Rico/8/34 virus with regard to replication and concomitant induction of antiviral signaling

As it was described in the previous chapter (4.3), the infection of MDCK cells with two of the six analyzed influenza virus strains, A/Puerto Rico/8/34 (NIBSC) and the A/Wisconsin/67/2005-like HGR led to the strongest average phosphorylation levels of eIF2-α and Stat2 as compared to mock infected cells. Due to high standard deviations measured between replicate samples and only two analyzed time points, a more detailed investigation was deemed necessary in order to obtain more precise insights into the dynamics of complex host cell signaling phenomena in the context of the analyzed bioprocess for influenza vaccine production.

In this regard, the focus was on a comparison of two variants of the influenza virus strain A/Puerto Rico/8/34, PR8-NIBSC and PR8-RKI, as both variants showed considerably different impacts on the induction of host cell signaling pathways in the previously described experimental setting (4.3). In addition, regardless of their alleged uniformity, both variants had previously been observed to differ concerning their replication behavior, final virus titer reached and apoptosis induction in infected MDCK cells (Schulze-Horsel et al. 2009).

The chosen approach described in the following combined a number of different experiments and experimental settings. At first, MDCK cells grown to near confluency in T-flasks were infected with either one of the two A/Puerto Rico/8/34 variants in order to analyze the induction of antiviral signaling in detail. Medium samples were taken at indicated time points and analyzed in the HA assay (Figure 4.4-1).

Infection experiments were done under three different conditions, which were as follows:

(A) T-flask cultivations of MDCK cells, which were infected at a high MOI of 5,

(B) Cultivation of MDCK cells in a 1.5 L stirred tank bioreactor operated in batch mode; infection was done at a low MOI of 0.025,

(C) T-flask cultivations of MDCK cells, which were infected at a low MOI of 0.025

The experimental setting (A) whose results are shown in Figure 4.3-2-A to Figure 4.4-7-A was chosen to ensure simultaneous infection of all cells and hence maximum immediate induction of cellular signaling

pathways. The experimental set-up (B) was selected in accordance with standard vaccine production process conditions. Finally (C), the experiments whose results are illustrated in Figure 4.4-2-C to Figure 4.4-7-C were conducted to investigate how cellular signaling is induced in MDCK cells grown in a static cultivation system that are infected at a low MOI as frequently chosen in stirred tank bioreactor based vaccine production processes. Furthermore, infecting cells grown in a static environment at a low MOI of 0.025 was also meant to elucidate how soon after infection cellular signaling pathways are induced if only a fraction of the cell population is infected.

In addition to three signaling pathways functional in the IFN system (NF-κB, IRF-3; Jak-Stat), the induction by both influenza A/Puerto Rico/8/34 variants of the Raf/MEK/ERK and the PI3K/Akt signaling cascades, as well as of the PKR-mediated phosphorylation of eIF2-α were analyzed comprehensively.

4.4.1 Comparison of PR8-NIBSC vs. PR8-RKI: Virus titers determined in the HA assay

This experiment was conducted by infecting two populations of MDCK cells grown to near confluency in T-flasks at an MOI of 5 with either PR8-NIBSC or PR8-RKI concomitantly with medium exchange after washing cells twice with PBS. At time points indicated in Figure 4.4-1, medium samples were taken for subsequent analysis in the HA assay (3.2.1.5). From 0 to 12 hpi there was no noticeable increase in the number of detached cells in the supernatant of cultures infected with PR8-NIBSC or PR8-RKI, respectively. For both infected MDCK cell populations, titers increased visibly between 8 and 10 hpi. However, initially the HA titer increased earlier in the PR8-NIBSC infected population as compared to the PR8-RKI infected cells. At 12 hpi, HA titers were roughly similar at about 2.1 log HAU/100 µL before they started to show a difference (0.35 log HAU/100 µL at 24 hpi).

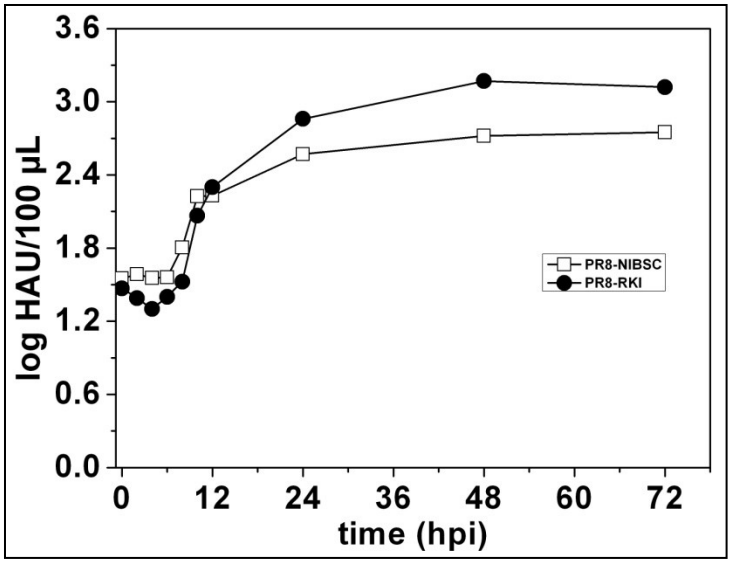

Figure 4.4-1: Hemagglutinin titers after infection of MDCK cells with two variants of A/Puerto Rico/8/34 (H1N1). ***MDCK cells grown in T-flasks were infected at an MOI of 5 with PR8-NIBSC (□) or PR8-RKI (●). Medium samples were taken at indicated time points (hpi) and analyzed in the HA assay. Shown are data of one representative experiment (read-out: log HA units/100 µL ±0.08 standard deviation of validated assay). Abbreviations of influenza viruses: PR8-NIBSC: A/Puerto Rico/8/34 (NIBSC); PR8-RKI: A/PR/8/34 (RKI).***

Final HA titers were 2.8 log HAU/100 µL for PR8-NIBSC and 3.1 log HAU/100 µL for PR8-RKI, respectively.

4.4.2 Comparison of PR8-NIBSC vs. PR8-RKI: Induction of the IFN system in MDCK cells

As demonstrated previously in the HA assay, both analyzed variants of influenza A/Puerto Rico/8/34, PR8-NIBSC and PR8-RKI grew to different final HA titers. The experiments described in this chapter were conducted in order to find out whether there is a difference in the induction of the IFN system between cell populations infected with either one of the two influenza A/Puerto Rico/8/34 variants. The IFN system is a key player of innate immunity in epithelial cells. The activation of NF-κB and IRF-3, constituting two main transcription factors of the IFN promoter, is a decisive event in the induction of the IFN system. As an indicator for the activation of NF-κB and IRF-3, the phosphorylation of IκBα at serine 32/36 and of IRF-3 at serine 396 was detected. A secondary event is the activation of the Jak-Stat pathway that signals downstream from the IFN receptor, mediating autocrine and paracrine signals. Since the activation of Stat2 is specific for type I IFNs, its phosphorylation at tyrosine 690 was detected

as an indicator for the activated pathway. The induction of these three signaling pathways functional in the IFN system by both variants of influenza A/Puerto Rico/8/34 was analyzed.

For MDCK cells grown in T-flasks that were infected at a high MOI of 5 (Figure 4.4-2-A), IRF-3 pathway induction was monitored from 0 to 12 hpi, with samples taken every 2 h. A more frequent sampling was not feasible due to a time consuming sample taking procedure. Additionally, the availability of only 14 sample pockets on each SDS-PAGE gel posed a limitation of the analytical method, so that only seven time points could be compared for both infected populations. Western blot results showed that a steady increase in the level of phosphorylated IRF-3 in the PR8-NIBSC infected population could be observed from 0 to 12 hpi. The strongest band intensity was observed at 12 hpi, which was confirmed by densitometric analysis. In contrast, PR8-RKI infected cells showed no detectable induction of IRF-3 above the background level observed at 0 hpi in both infected populations. The final level of phosphorylated IRF-3 was about three-fold higher in PR8-NIBSC infected cells than in the PR8-RKI infected population.

In the 1.5 L stirred tank bioreactor cultivations, the induction of IRF-3 was measured from 0 to 24 hpi (Figure 4.4-2-B) because of the expected delayed induction of the signaling pathway attributable to the initial low MOI. Samples were taken only every 4 h to widen the time frame of the analysis in face of a limited capacity of the analytical method as previously mentioned. The phosphorylation level of IRF-3 increased from 0 to 16 hpi in the PR8-NIBSC infected population. The strongest induction of IRF-3 with an about 9-fold higher induction level as compared to the initial level at 0 hpi was measured at 16 hpi, marking the turning point from which on phosphorylation levels of IRF-3 declined to an eventual level of about 75% of the maximum level at 24 hpi. As opposed to PR8-NIBSC, the infection of MDCK cells with PR8-RKI in a stirred tank bioreactor did not lead to a measureable induction of the IRF-3 signaling pathway.

In MDCK cells grown in T-flasks that were infected at the same MOI as chosen in the bioreactor cultivations (Figure 4.4-2-C), no induction of IRF-3 could be measured prior to 16 hpi with neither of both PR8 variants. From 16 to 29 hpi in the PR8-NIBSC infected population the phosphorylation level of IRF-3 increased sharply. From 29 to 33 hpi, a slight drop in the level of IRF-3 phosphorylation was observed.

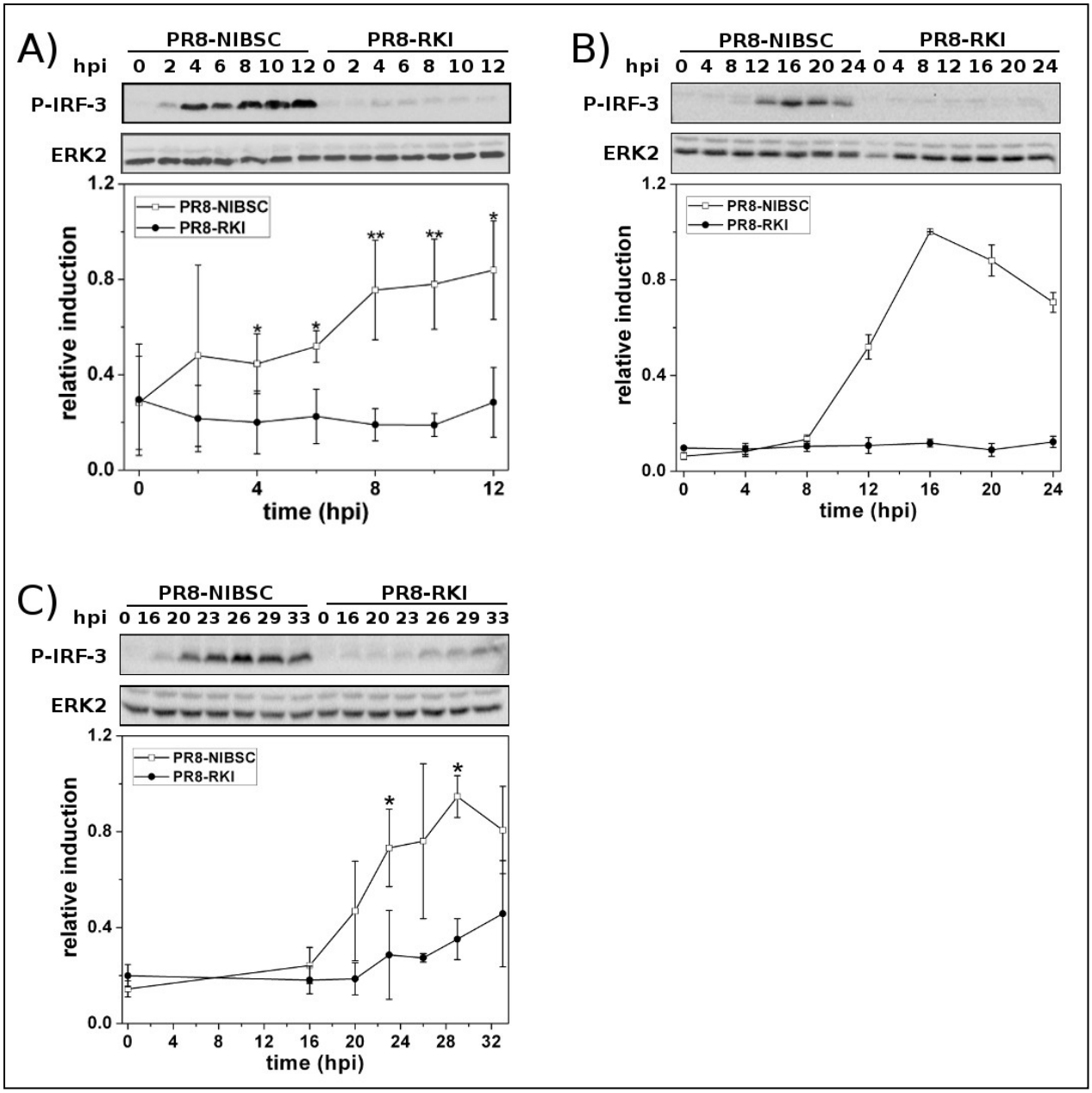

Figure 4.4-2: Western blot analysis of IRF-3 pathway induction in MDCK cells infected with two variants of A/Puerto Rico/8/34 (H1N1).

Analysis of phosphorylated IRF-3 in MDCK cells grown (A) in T-flasks infected at an MOI of 5 from 0 to 12 hpi; (B) in a 1.5 L stirred tank bioreactor infected at an MOI of 0.025 from 0 to 24 hpi; (C) in T-flasks infected at an MOI of 0.025 from 0 to 33 hpi. Phosphorylation of IRF-3 was normalized to ERK2 expression levels, with maximum induction levels set to 1. Each data point shown represents the mean ±S.D. (*p<0.05; **p<0.01), and the average experimental value is calculated from (A) four, (C) three, or (B) one independent experiment. In (B), data from two bioreactor cultivations are shown, one infected with PR8-NIBSC and the other infected with PR8-RKI. Data points shown in (B) represent technical duplicates of samples analyzed in Western blot. For each experimental setup, one representative Western blot is shown. Abbreviations of influenza viruses: PR8-NIBSC: A/Puerto Rico/8/34 H1N1 (NIBSC); PR8-RKI: A/PR/8/34 H1N1 (RKI).

As opposed to weak or non-detectable induction levels of IRF-3 under both previously described infection conditions (Figure 4.4-2-A, -B) a slight induction of IRF-3 was measured in MDCK cells grown in T-flasks that were infected at a low MOI of 0.025 with PR8-RKI. From 20 to 33 hpi, a moderate increase in IRF-3 phosphorylation in PR8-RKI infected cells was observed, with the maximum level reached at 33 hpi, which amounted to an about 2.5-fold weaker induction level as compared to PR8-NIBSC infected cells at 33 hpi in the same experimental setup. Overall, the infection with PR8-NIBSC led to a roughly 3-fold higher peak phosphorylation level of IRF-3 than measured for the infection with PR8-RKI.

Data similar to those resulting from the analysis of IRF-3 induction were obtained monitoring the activation of NF-κB as indicated by the phosphorylation of IκBα. It could be shown that the level of phosphorylated IκBα increased over the whole time interval monitored in cells infected with PR8-NIBSC at an MOI of 5 (Figure 4.4-3-A). The strongest band intensity was observed at 12 hpi, which was confirmed by densitometric analysis. In the last sample taken at 12 hpi, a 3-fold higher level of phosphorylated IκBα was measured in cells infected with PR8-NIBSC as compared to PR8-RKI infected cells, where no significant induction of IRF-3 phosphorylation was observed throughout the whole monitored time course.

In MDCK cells grown in a stirred tank bioreactor that were infected at an MOI of 0.025 with PR8-NIBSC (Figure 4.4-3-B) there was a pronounced increase in the phosphorylation level of IκBα from 8 to 20 hpi, when the maximum induction was reached. From 20 to 24 hpi, the phosphorylation level decreased by about 25%. Again, similar to the data previously described for the induction of IRF-3, there was no induction of NF-κB measureable in MDCK cells grown in a stirred tank bioreactor infected with PR8-RKI.

The activation profile of NF-κB in MDCK cells grown in T-flasks that were infected at an MOI of 0.025 (Figure 4.4-3-C) was also similar to that measured for the induction of IRF-3. Prior to 16 hpi, no phosphorylation of IκBα could be measured in MDCK cells, neither for those infected with PR8-NIBSC nor PR8-RKI. From 16 to 33 hpi, a steady increase in both infected populations could be observed. The maximum level of IκBα phosphorylation was measured at 33 hpi, with a 1.5-fold stronger induction caused by the infection with PR8-NIBSC as compared to PR8-RKI.

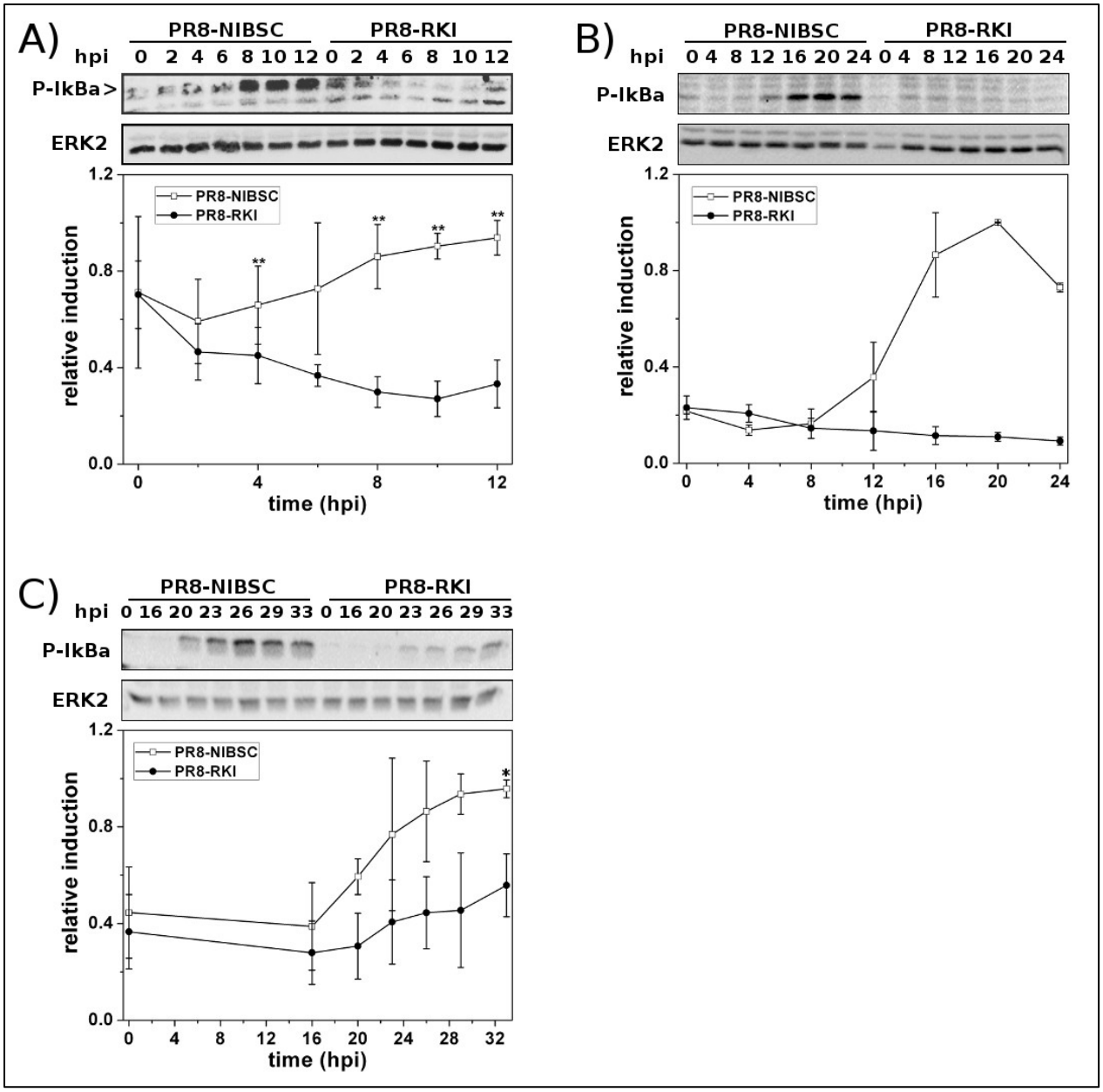

Figure 4.4-3: Western blot analysis of NF-κB pathway induction in MDCK cells infected with two variants of A/Puerto Rico/8/34 (H1N1).

Analysis of phosphorylated IκBα in MDCK cells grown (A) in T-flasks infected at an MOI of 5 from 0 to 12 hpi; (B) in a 1.5 L stirred tank bioreactor infected at an MOI of 0.025 from 0 to 24 hpi; (C) in T-flasks infected at an MOI of 0.025 from 0 to 33 hpi. Phosphorylation of IκBα was normalized to ERK2 expression levels, with maximum induction levels set to 1. Each data point shown represents the mean ±S.D. (*p<0.05; **p<0.01), and the average experimental value is calculated from (A) four, (C) three, or (B) one independent experiment. In (B), data from two bioreactor cultivations are shown, one infected with PR8-NIBSC and the other infected with PR8-RKI. Data points shown in (B) represent technical duplicates of samples analyzed in Western blot. For each experimental setup, one representative Western blot is shown. Abbreviations of influenza viruses: PR8-NIBSC: A/Puerto Rico/8/34 (NIBSC); PR8-RKI: A/PR/8/34 (RKI).

The induction of the two signaling pathways NF-κB and IRF-3 precedes the activation of the Jak-Stat signaling pathway, which is indicated by the phosphorylation of Stat2.

In MDCK cells infected at a high MOI, the level of Stat2 phosphorylation in PR8-NIBSC infected cells increased sharply from 0 to 8 hpi, at which time point the maximum induction level was reached (Figure 4.4-4-A). From 8 to 24 hpi, the level of Stat2 phosphorylation decreased to about the initial level measured at 0 hpi. Throughout the infection experiment, only a very slight induction of the Jak-Stat signaling pathway was measured in cells infected with PR8-RKI. At 8 hpi, the phosphorylation level in PR8-NIBSC infected cells was about 4.5-fold stronger than in PR8-RKI infected cells.

In a stirred tank bioreactor (Figure 4.4-4-B), the level of Stat2 phosphorylation in PR8-NIBSC infected cells increased sharply from 4 to 12 hpi, which was followed by a decline of similar steepness until 24 hpi, when the phosphorylation level was back to about the initial level. In PR8-RKI infected cells, by contrast, only a very slight induction of Stat2 phosphorylation could be measured between 12 and 24 hpi. The maximum induction of the Jak-Stat signaling pathway caused by the PR8-NIBSC infection was 7-fold stronger than the peak value in PR8-RKI infected cells.

In T-flask cultures of MDCK cells infected at a low MOI of 0.025 (Figure 4.4-4-C), a slight increase in the level of Stat2 phosphorylation from 0 to 16 hpi was observed. At 16 hpi, the phospho-Stat2 band intensity in PR8-NIBSC infected cells was nearly 2-fold stronger compared to the PR8-RKI infected population. A steep increase of Stat2 phosphorylation in PR8-NIBSC infected cells occurred between 16 and 20 hpi, followed by a steady decline until 33 hpi to about 40% of the maximum level. The maximum phosphorylation level at 20 hpi in PR8-NIBSC infected cells was about 4-fold stronger than in PR8-RKI infected cells.

Overall, under all three analyzed cultivation and infection conditions, the infection with PR8-NIBSC was observed to lead to a much stronger phosphorylation level of Stat2 than that which was caused by PR8-RKI.

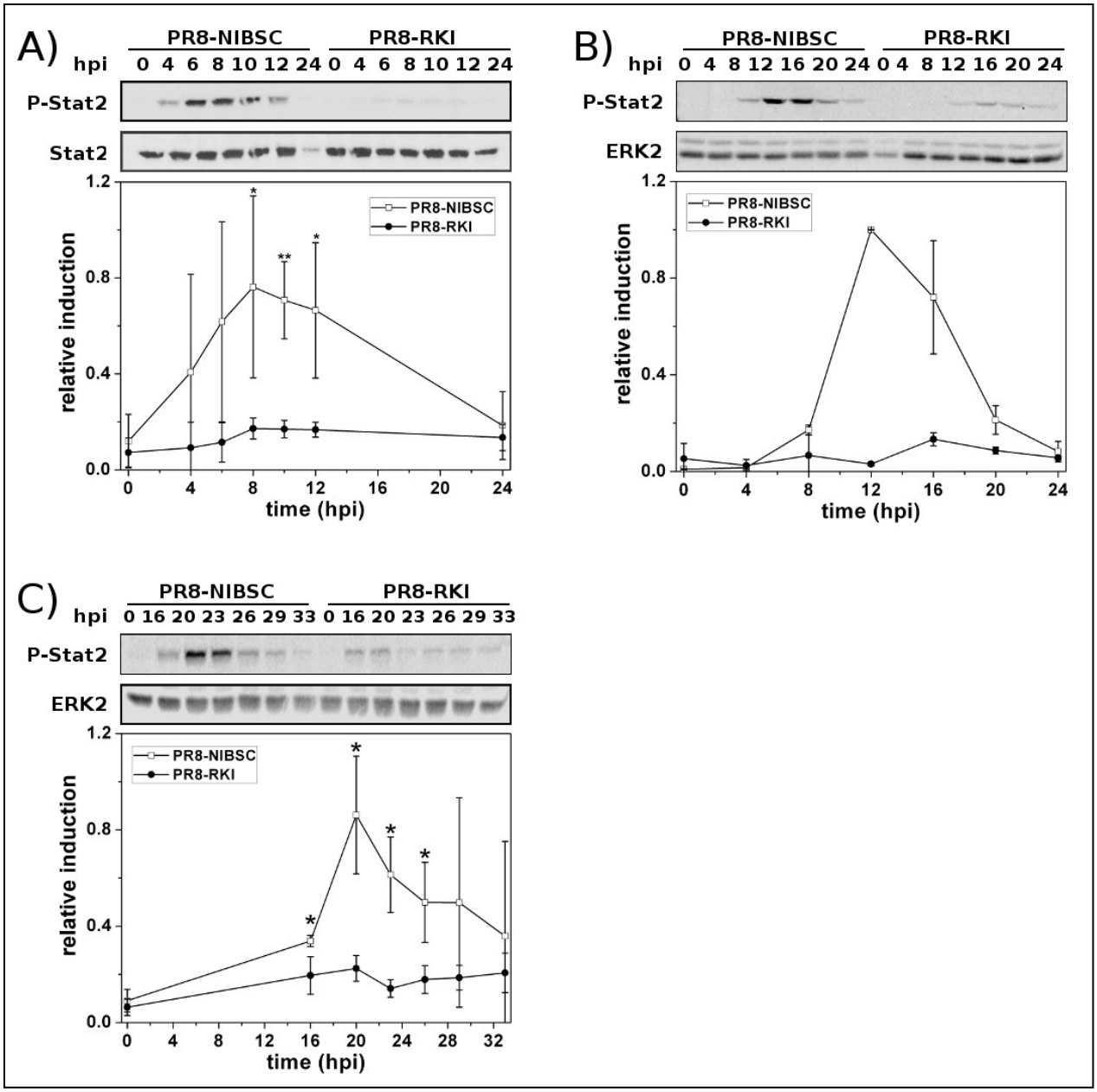

Figure 4.4-4: Western blot analysis of Jak-Stat pathway induction in MDCK cells infected with two variants of A/Puerto Rico/8/34 (H1N1).

Analysis of phosphorylated Stat2 in MDCK cells grown (A) in T-flasks infected at an MOI of 5 from 0 to 12 hpi; (B) in a 1.5 L stirred tank bioreactor infected at an MOI of 0.025 from 0 to 24 hpi; (C) in T-flasks infected at an MOI of 0.025 from 0 to 33 hpi. Phosphorylation of Stat2 was normalized to (A) Stat2 or (B, C) ERK2 expression levels, with maximum induction levels set to 1. Each data point shown represents the mean ±S.D. (*p<0.05; **p<0.01), and the average experimental value is calculated from (A) four, (C) three, or (B) one independent experiment. In (B), data from two bioreactor cultivations are shown, one infected with PR8-NIBSC and the other infected with PR8-RKI. Data points shown in (B) represent technical duplicates of samples analyzed in Western blot. For each experimental setup, one representative Western blot is shown. Abbreviations of influenza viruses: PR8-NIBSC: A/Puerto Rico/8/34 (NIBSC); PR8-RKI: A/PR/8/34 (RKI).

4.4.3 Differential activation of the Raf/MEK/ERK signaling pathway

The Raf/MEK/ERK signaling pathway was monitored because it has been described to play a crucial role in nuclear export of vRNPs and therefore in virus replication, as well as in cell differentiation and proliferation (Ludwig et al. 2004). The induction of ERK2 in MDCK cells infected with both PR8 variants at a high MOI of 5 is illustrated in Figure 4.4-5-A. Comparing cells infected with PR8-NIBSC and PR8-RKI, a differential activation of the MAPK pathway was observed. Immediately after infection, the strongest activation of the pathway took place in both populations, which could, besides virus infection, at least partially also be attributable to the removal of growth medium containing FCS. The induction of the pathway by PR8-RKI showed only about 60% of the phospho-ERK2 level measured in PR8-NIBSC infected cells. For PR8-NIBSC infected cells, a two-peak behavior was observed. After the maximum induction immediately after infection the level of phospho-ERK2 decreased continuously until a minimum value was reached at 6 hpi. From 6 to 12 hpi levels of phospho-ERK2 increased once more. A very different ERK2 induction profile was observed in cells infected with PR8-RKI, as the strongest induction took place shortly after infection and no second increase in the phosphorylation level occured. Here, the level of phospho-ERK2 measured in PR8-RKI infected cells 12 hpi was approximately 4-fold lower than the level in PR8-NIBSC infected cells. In MDCK cells cultivated in a stirred tank bioreactor that were infected at an MOI of 0.025 (Figure 4.4-5-B), a two-peak behavior of ERK2 pathway induction was again observed for PR8-NIBSC infected cells, with the strongest phosphorylation levels measured shortly after infection and at 20 hpi. From 20 to 24 hpi in PR8-NIBSC infected cells the level of ERK2 phosphorylation decreased slightly to about 80% of the maximum level. The phosphorylation of ERK2 measured in PR8-RKI infected cells did not exceed background level. At the time point of maximum pathway induction caused by the infection with PR8-NIBSC, the ERK2 phosphorylation level was about 5-fold higher than in PR8-RKI infected cells. In MDCK cells grown in T-flasks that were infected at an MOI of 0.025 (Figure 4.4-5-C), the induction profile of ERK2 in the PR8-NIBSC infected population strongly resembled the one measured in cells infected at a high MOI of 5 except for a retardation of about 12 hours. However, as opposed to Figure 4.4-5-A, no significant difference occurred between the ERK2 phosphorylation levels in the two populations infected with either one of the two PR8 variants. Instead, for both populations infected with either PR8-NIBSC or PR8-RKI, the strongest and in this case similarly strong induction was measured right after infection, followed by a decline in the level of phosphorylation until base level was reached at 16 hpi.

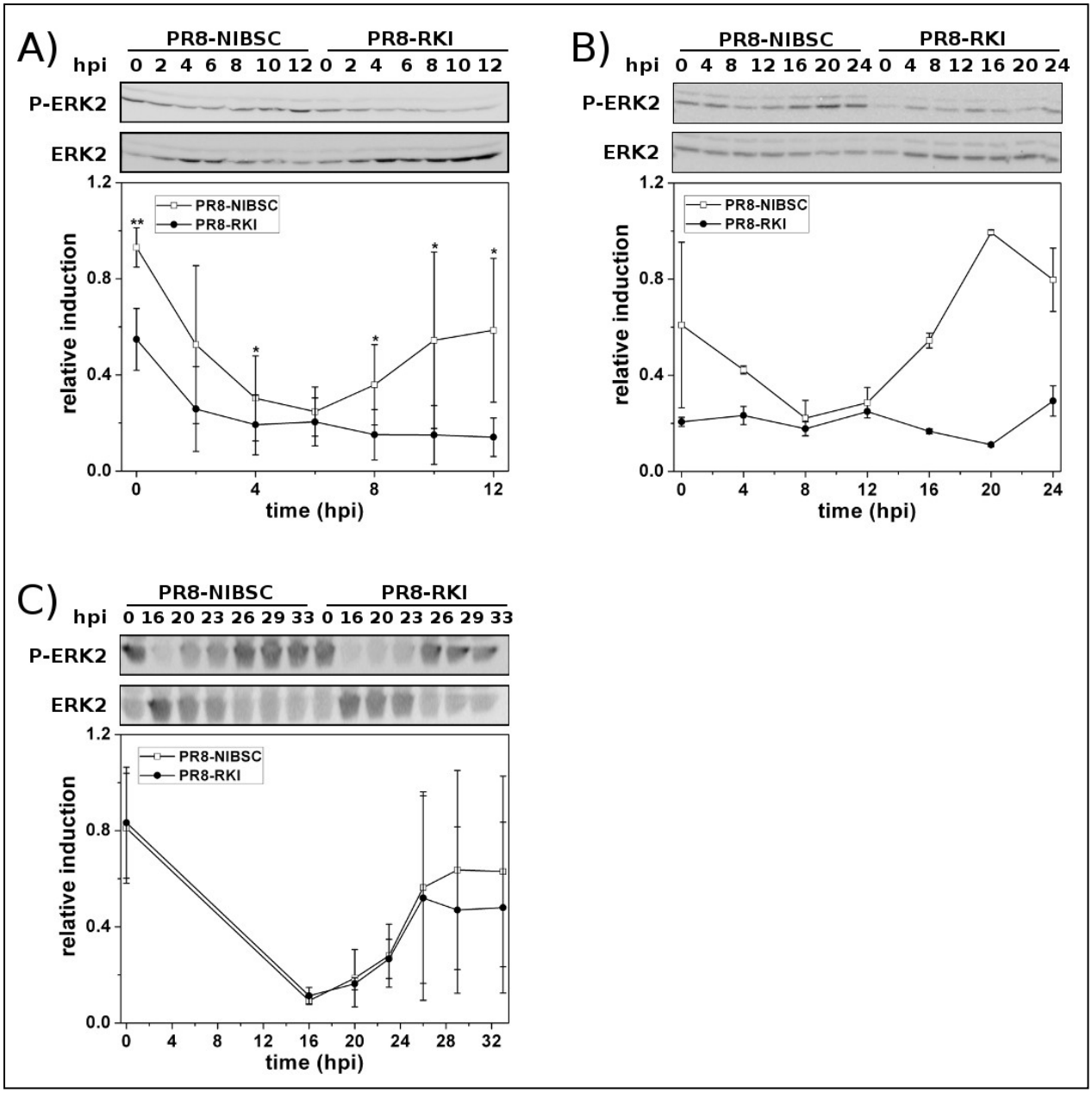

Figure 4.4-5: Western blot analysis of ERK2 pathway induction in MDCK cells infected with two variants of A/Puerto Rico/8/34 (H1N1).

Analysis of phosphorylated ERK2 in MDCK cells grown (A) in T-flasks infected at an MOI of 5 from 0 to 12 hpi; (B) in a 1.5 L stirred tank bioreactor infected at an MOI of 0.025 from 0 to 24 hpi; (C) in T-flasks infected at an MOI of 0.025 from 0 to 33 hpi. Phosphorylation of ERK2 was normalized to ERK2 expression levels, with maximum induction levels set to 1. Each data point shown represents the mean ±S.D. (*p<0.05; **p<0.01), and the average experimental value is calculated from (A) four, (C) three, or (B) one independent experiment. In (B), data from two bioreactor cultivations are shown, one infected with PR8-NIBSC and the other infected with PR8-RKI. Data points shown in (B) represent technical duplicates of samples analyzed in Western blot. For each experimental setup, one representative Western blot is shown. Abbreviations of influenza viruses: PR8-NIBSC: A/Puerto Rico/8/34 H1N1 (NIBSC); PR8-RKI: A/PR/8/34 H1N1 (RKI).

From that time point and on, the phosphorylation of ERK2 increased sharply in both infected populations until 26 hpi. The final average level of ERK2 phosphorylation measured at 33 hpi in PR8-NIBSC infected cells was slightly higher than that measured in PR8-RKI infected cells, yet not significantly.

4.4.4 Differential activation of the PI3K/Akt signaling pathway

The activating phosphorylation of Akt through phosphatidyl-inositol-3-kinase (PI3K) has been described as an important anti-apoptotic event. However, this pathway also contributes to the activation of IRF-3 and hence to IFN-beta induction.

The activation of the pathway in MDCK cells infected with either PR8-NIBSC or PR8-RKI at a high MOI of 5 is illustrated in Figure 4.4-6-A. Shortly after infection, the highest phosphorylation level of Akt was visible, which is most likely attributable to the removal of growth medium containing FCS, and hence was of comparable intensity for both infected populations. From 0 to 2 hpi, the level of phosphorylated Akt decreased. For PR8-RKI infected cells, there was almost no further increase of phospho-Akt levels. In contrast, the level of phospho-Akt in PR8-NIBSC infected cells increased again and was about 2-fold higher compared to the PR8-RKI infected population. However, due to the high standard deviations of individual measurements (three independent experiments) there were no significant statistical differences between the populations infected with PR8-NIBSC and PR8-RKI.

In the stirred tank bioreactor, the infection with PR8-NIBSC was observed to lead to a sharp increase in the phosphorylation level of Akt from 0 to 20 hpi, with the maximum induction reached between 16 and 20 hpi (Figure 4.4-6-B). This was then followed by an abrupt reduction in the level of Akt phosphorylation to a 3-fold lower level. The phosphorylation of Akt in the PR8-RKI infected population was on a much lower level throughout the entire monitored cultivation time. At 16 hpi, the phosphorylation level in the PR8-RKI infected population peaked. However, comparing maximum phosphorylation levels of Akt, in PR8-NIBSC infected MDCK cells this level was nearly 2-fold higher than in PR8-RKI infected cells.

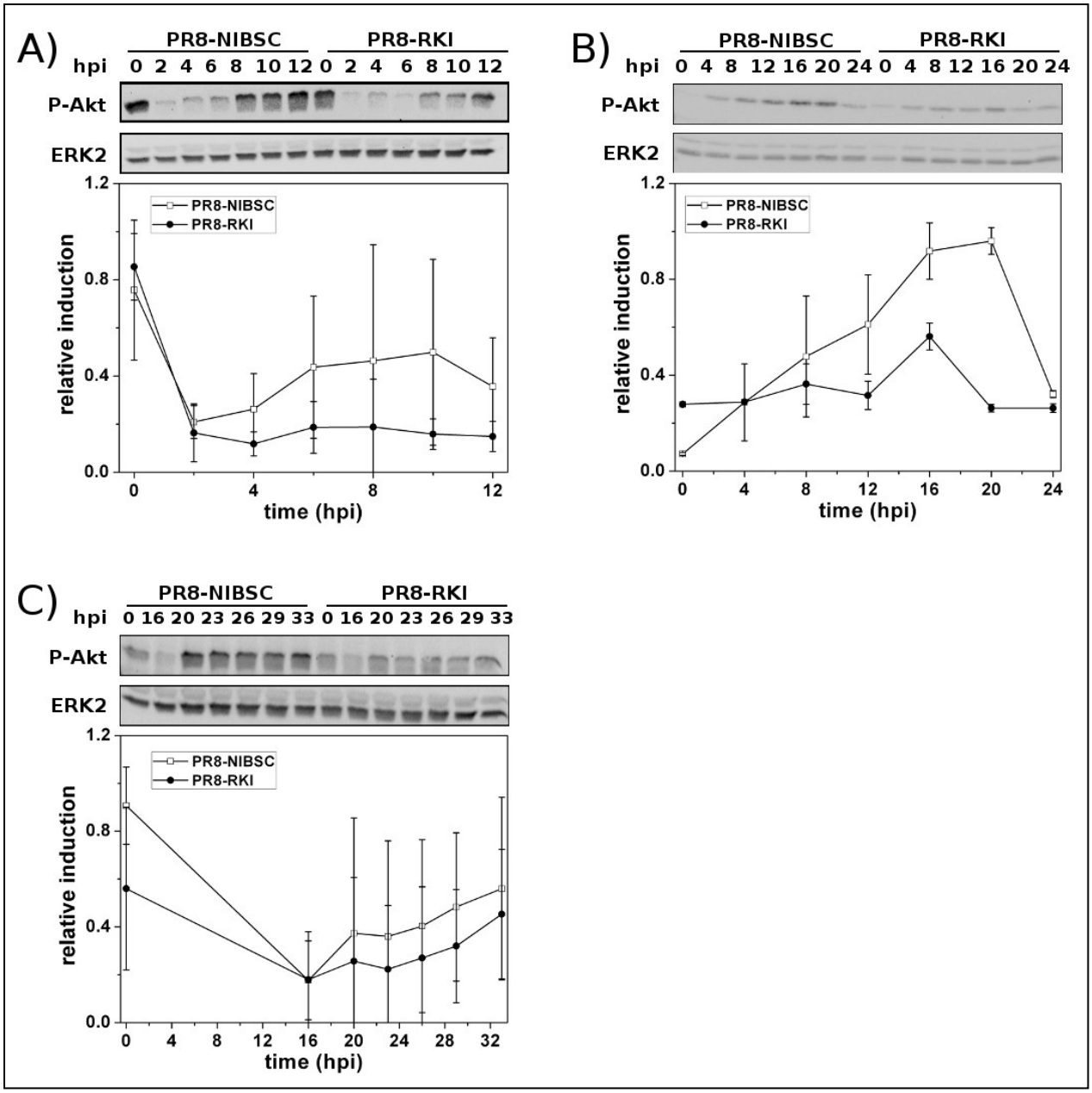

Figure 4.4-6: Western blot analysis of PI3K/Akt pathway induction in MDCK cells infected with two variants of A/Puerto Rico/8/34 (H1N1).

Analysis of phosphorylated Akt in MDCK cells grown (A) in T-flasks infected at an MOI of 5 from 0 to 12 hpi; (B) in a 1.5 L stirred tank bioreactor infected at an MOI of 0.025 from 0 to 24 hpi; (C) in T-flasks infected at an MOI of 0.025 from 0 to 33 hpi. Phosphorylation of Akt was normalized to ERK2 expression levels, with maximum induction levels set to 1. Each data point shown represents the mean ±S.D. (*p<0.05; **p<0.01), and the average experimental value is calculated from (A) four, (C) three, or (B) one independent experiment. In (B), data from two bioreactor cultivations are shown, one infected with PR8-NIBSC and the other infected with PR8-RKI. Data points shown in (B) represent technical duplicates of samples analyzed in Western blot. For each experimental setup, one representative Western blot is shown. Abbreviations of influenza viruses: PR8-NIBSC: A/Puerto Rico/8/34 (NIBSC); PR8-RKI: A/PR/8/34 (RKI).

In MDCK cells grown in T-flasks infected at a low MOI of 0.025, maximum levels of Akt phosphorylation were measured right after both populations were infected (Figure 4.4-6-C), which again was most likely due to the serum contained in the growth medium prior to infection. Phosphorylation levels decreased until 16 hpi, followed by a moderate increase in Akt phosphorylation in both monitored populations until 33 hpi. The final phosphorylation level measured at 33 hpi was only about 60% of the level measured at 0 hpi for PR8-NIBSC or PR8-RKI, respectively. Yet, the average phosphorylation level of Akt was slightly higher in the PR8-NIBSC infected population as compared to PR8-RKI infected cells at the final time point analyzed. However, as already observed in the high MOI infection experiments, because of the considerable standard deviations between replicate samples, there were no significant statistical differences between the populations infected with either PR8-NIBSC or PR8-RKI.

4.4.5 Analysis of the PKR-induced phosphorylation of eIF2-α

The phosphorylation of eIF2-α by PKR has been described as a crucial event of the antiviral defense of the host cell. As an important translation initiation factor of eukaryotic cells, its phosphorylation by PKR leads to a shut-down of cellular protein synthesis, thereby impairing virus replication.

A sharp increase in the level of phospho-eIF2-α from 6 to 12 hpi was measured in MDCK cells infected with PR8-NIBSC at a high MOI of 5 (Figure 4.4-7-A). The strongest signal intensity was reached at 12 hpi, which was about 3-fold higher as compared to that in PR8-RKI infected cells. In the PR8-RKI infected cell population, there was no significant increase of the eIF2-α phosphorylation level throughout the entire monitored time course.

In the stirred tank bioreactor cultivation, an initial slight induction of eIF2-α phosphorylation right after infection could be detected in the PR8-NIBSC infected population (Figure 4.4-7-B). The phosphorylation level of eIF2-α decreased until 8 hpi and remained low until 12 hpi. At 12 hpi the level of eIF2-α phosphorylation increased sharply until the maximum induction level was reached at 24 hpi. In PR8-RKI infected cells, the phosphorylation of eIF2-α increased slightly from 4 hpi until 20 hpi, at which time point the peak induction was reached. Yet, the maximum induction level caused by the infection with PR8-NIBSC at 24 hpi was about 2-fold higher than that measured at the peak induction level in PR8-RKI infected cells.

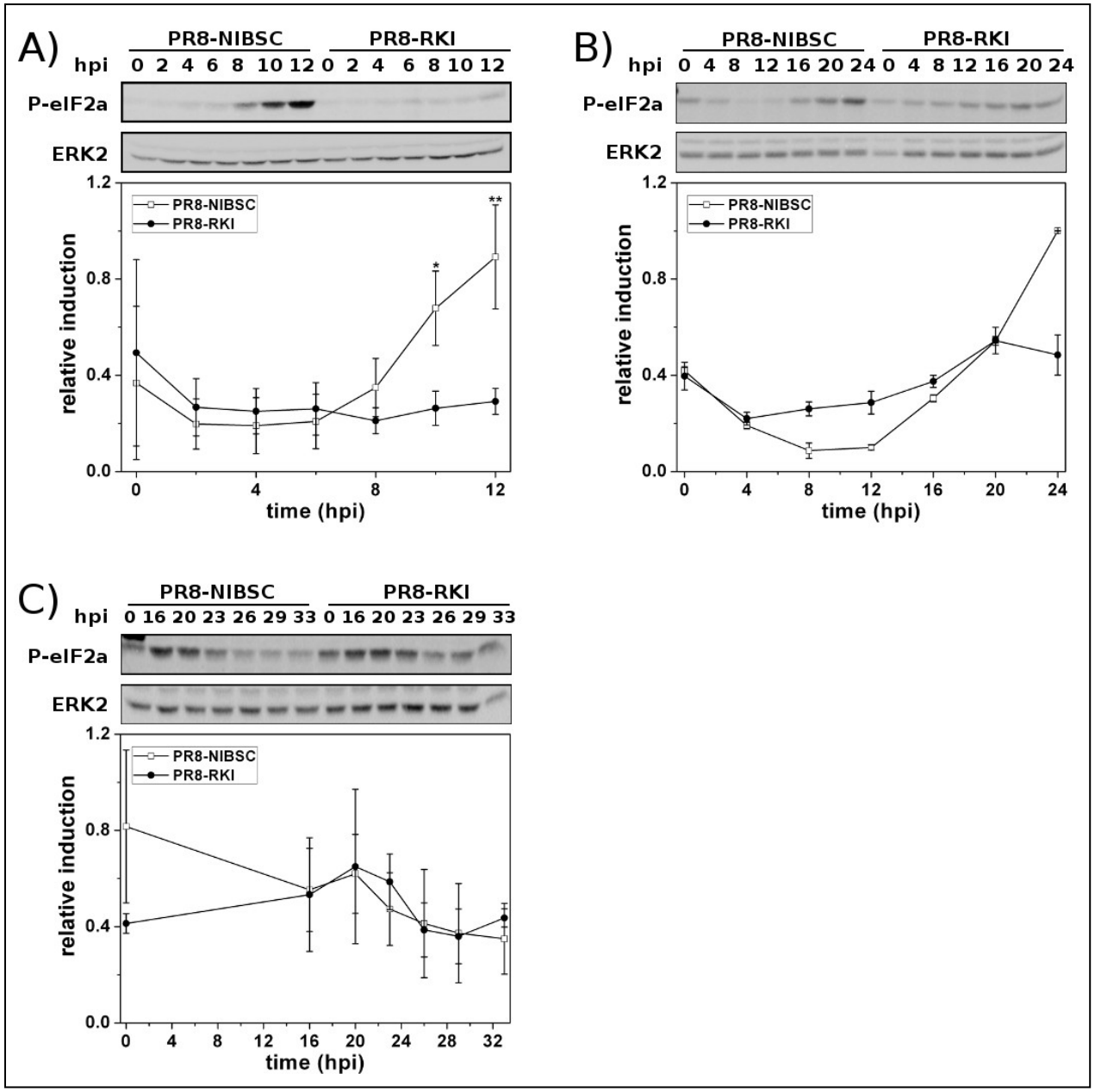

Figure 4.4-7: Western blot analysis of PKR/eIF2-α pathway induction in MDCK cells infected with two variants of A/Puerto Rico/8/34 (H1N1).

Analysis of phosphorylated eIF2-α in MDCK cells grown (A) in T-flasks infected at an MOI of 5 from 0 to 12 hpi; (B) in a 1.5 L stirred tank bioreactor infected at an MOI of 0.025 from 0 to 24 hpi; (C) in T-flasks infected at an MOI of 0.025 from 0 to 33 hpi. Phosphorylation of eIF2-α was normalized to ERK2 expression levels, with maximum induction levels set to 1. Each data point shown represents the mean ±S.D. (*p<0.05; **p<0.01), and the average experimental value is calculated from (A) four, (C) three, or (B) one independent experiment. In (B), data from two bioreactor cultivations are shown, one infected with PR8-NIBSC and the other infected with PR8-RKI. Data points shown in (B) represent technical duplicates of samples analyzed in Western blot. For each experimental setup, one representative Western blot is shown. Abbreviations of influenza viruses: PR8-NIBSC: A/Puerto Rico/8/34 (NIBSC); PR8-RKI: A/PR/8/34 (RKI).

In MDCK cells grown in T-flasks infected at a low MOI of 0.025 with either PR8-NIBSC or PR8-RKI an increase in the level of phosphorylated eIF2-α, starting at 16 hpi, could be observed in both populations (Figure 4.4-7-C). The phosphorylation of eIF2-α was most pronounced between 16 to 23 hpi. However, under these experimental conditions there was no distinguishable difference in the phosphorylation levels of eIF2-α induced by the infection with either PR8-NIBSC or PR8-RKI between 16 and 33 hpi. This sets the data measured for eIF2-α phosphorylation at these respective infection conditions apart from those measured under different experimental settings as illustrated in Figure 4.4-7-A, -B.

In summary, the results illustrated and described in chapter 4.4 show that the two variants of influenza A/Puerto Rico/8/34, PR8-NIBSC and PR8-RKI not only differ in their replication, yield, and in the induction of host cell apoptosis as previously shown, but also in the induction of all investigated signaling pathways of the host cell (IRF-3, NF-κB, Jak-Stat, Raf/MEK/ERK, PI3K/Akt, PKR/eIF2-α). With the exceptions of the pathways Raf/MEK/ERK (Figure 4.4-5-C), PI3K/Akt (Figure 4.4-6-C), and PKR/eIF2-α (Figure 4.4-7-C), the infection with PR8-NIBSC led to a significantly stronger induction of the analyzed signaling pathways under all investigated cultivation and infection conditions. At this point, the assumption was justified that the differential induction of host cell signaling pathways of mainly antiviral character might, if not fully causative, be at least contributive to the poor replication of PR8-NIBSC as compared to PR8-RKI. Additional experiments were now needed to clarify whether the induction of antiviral signaling in MDCK cells did indeed have an impact on the replication performance of a given influenza virus strain. The use of luciferase reporter assays, the repression of signaling pathways with chemical agents as well as the application of RNAi technology to reduce kinase activity were regarded as suitable tools to analyze the respective significance of each analyzed pathway in more detail.

4.5 Luciferase reporter assay to compare total protein synthesis in MDCK cells infected with PR8-NIBSC, PR8-RKI, or PR8-ΔNS1

The PKR-mediated phosphorylation of eIF2-α has been described as an important event of the antiviral host cell defense triggered by influenza A virus infection. As shown in previous studies, phosphorylation and consequent inactivation of eIF2-α is followed by a complete host cell shut-off due to impairment of protein synthesis. Since it was shown that the infection with PR8-NIBSC led to a higher level of eIF2-α phosphorylation than triggered by PR8-RKI (Figure 4.4-7), the aim of this experiment was to compare both influenza A virus variants with regard to their impact on total protein synthesis in the host cell.

Hence, using the reagent Lipofectamine 2000 (Invitrogen), MDCK cells were transfected with either one of the plasmids pGL4.10+TK (firefly-luciferase under the control of a weak constitutive herpes virus thymidine kinase promoter), and pMax (plasmid encoding green fluorescent protein as transfection control). After the incubation at 37 °C for 24 h, the transfected MDCK cells were either mock infected or infected with either one of the three influenza A/Puerto Rico/8/34 variants (PR8-NIBSC, PR8-RKI, or PR8-ΔNS1). At 12 or 16 hpi, samples were taken with passive lysis buffer (PLB, Promega) for subsequent measurement of luciferase activity (3.2.1.9).

As the infection with PR8-NIBSC led to a much more pronounced phosphorylation of eIF2-α, it was expected that this would be reflected in a lower level of total protein synthesized in MDCK cells infected with this variant as opposed to those infected with PR8-RKI. If this assumption had indeed applied, a reduction of luciferase activity in the PR8-NIBSC infected population as compared to PR8-RKI infected cells would have been observed. Besides a mock infected control, cells were also infected with PR8-ΔNS1, a PR8 variant known to strongly induce the IFN response of the host cell.

As shown in Figure 4.5-1, the average luciferase activity levels at 12 hpi were nearly identical in PR8-ΔNS1 as compared to mock infected cells. In PR8-RKI and PR8-NIBSC infected cells, the average level of luciferase activity at 12 hpi was slightly yet insignificantly higher than in mock infected cells, respectively. At 16 hpi, the average relative luciferase activity level in PR8-ΔNS1 infected cells was only about 60% of that measured in mock infected cells. In PR8-RKI and PR8-NIBSC infected cells at 16 hpi, the average relative luciferase activity level was slightly above or equal to the level measured in mock infected cells, respectively. Hence, neither at 12 nor at 16 hpi significant differences in the average relative luciferase activity levels could be observed between PR8-RKI and PR8-NIBSC infected cells. With the exception of a reduction of the average relative luciferase activity at 16 hpi in PR8-ΔNS1

infected cells, infection with influenza A virus led to a slight increase in luciferase activity in all analyzed samples, which was, however, not statistically significant.

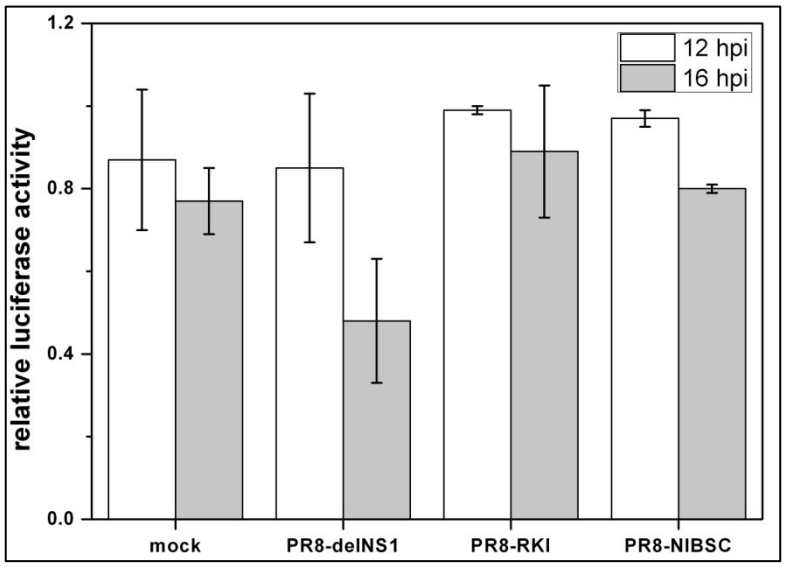

Figure 4.5-1: Luciferase reporter assay to measure the impact of influenza A virus infection on total protein synthesis in MDCK cells.
MDCK cells were transfected with a firefly luciferase reporter plasmid under the control of a weak constitutive herpes virus thymidine kinase promoter. At 48 hpt, cells were infected at an MOI of 5 for 12 or 16 h with the A/Puerto Rico/8/34 H1N1 variants PR8-ΔNS1, PR8-RKI, or PR8-NIBSC, and then lysed. Firefly luciferase activity was measured in two independent biological experiments and normalized to total cellular protein content. Relative luciferase activity is expressed as mean ±S.D. Abbreviations of influenza viruses: PR8-NIBSC: A/Puerto Rico/8/34 (NIBSC); PR8-RKI: A/Puerto Rico/8/34 (RKI), PR8-ΔNS1: A/Puerto Rico/8/34 ΔNS1.

Overall, the results obtained were in disagreement with the initial expectations, since it could not be shown that in MDCK cells infected with PR8-NIBSC, the variant that has previously been observed to induce a stronger phosphorylation of eIF2-α, the total amount of protein synthesized differed from that synthesized in cells infected with PR8-RKI. However, the influenza virus-induced, PKR-mediated phosphorylation of eIF2-α was investigated further since by the experimental approach pursued here, it could not be clarified whether experimentally interfering with PKR activity has a direct impact on virus replication.

4.6 Inhibiting PKR activity via 2-AP treatment to achieve a reduction of eIF2-α phosphorylation

In order to identify suitable strategies to enhance influenza virus replication in MDCK cells, the chemical inhibition of the PKR-mediated eIF2-α phosphorylation was attempted. MDCK cells were seeded into T25 tissue culture flasks at 2.5 x 10^4 cells/cm². After 72 h, cell culture medium was aspirated and cells were washed twice with PBS. Then, infection medium containing 5 mM 2-AP was added to the cells. As a control, infection medium containing no 2-AP was added. After incubating for 2 h at 37 °C, 5% CO_2, the pharmacological agent thapsigargin was added at a final concentration of 300 nM to induce eIF2-α phosphorylation. To the control, no thapsigargin was added. 30 min after the addition of thapsigargin, cells were harvested according to the RIPA lysis protocol (3.2.1.2.1) and samples were subsequently analyzed for eIF2-α phosphorylation in Western blot (3.2.1.2.2).

As shown in Figure 4.6-1, the addition of thapsigargin at a final concentration of 300 nM led to an about 2-fold higher level of eIF2-α phosphorylation as compared to the untreated control.

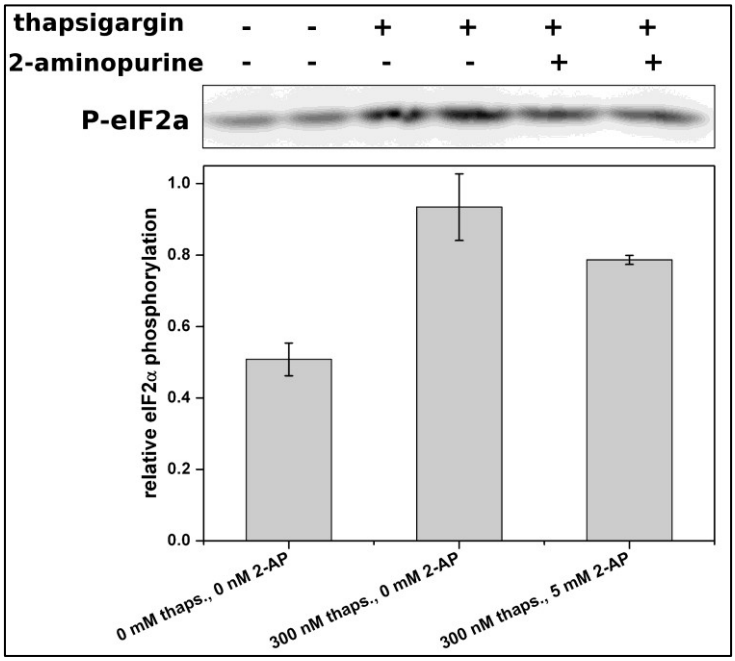

Figure 4.6-1: Reduction of the eIF2-α phosphorylation level by treatment of MDCK cells with the PKR inhibitor 2-AP.

MDCK cells were grown in T25-flasks and treated with or without 5 mM 2-AP. 2 h after the addition of 2-AP to the medium, cells were stimulated with or without 300 nM thapsigargin. After a 30 min exposure, cells were lysed according to the RIPA lysis protocol and eIF2-α phosphorylation was analyzed in Western blot. Results are shown as mean ±S.D. of two technical replicates.

The addition of 2-AP 2 h prior to the addition of thapsigargin reduced the average level of eIF2-α phosphorylation slightly from a 2-fold to an about 1.5-fold higher level as compared to the level measured in the untreated control sample. Therefore, the efficacy of 2-AP in reducing the phosphorylation of eIF2-α could be shown. However, since the reduction was only slight, the conditions for the application of this inhibitor had to be optimized further.

Therefore, the next step was to determine the toxicity of rising concentrations of 2-AP imposed on MDCK cells. As illustrated in Figure 4.6-2, the addition of 5 or 20 mM 2-AP to the growth medium led to a slight reduction of MDCK cell viability as compared to untreated cells. A further increase of the concentration of 2-AP to 40 or 80 mM led to a steep drop of cell viability to about 5% of the level measured in untreated controls. Therefore, in experiments conducted in the following, the maximum concentration of the PKR inhibitor 2-AP applied was set not to exceed 20 mM.

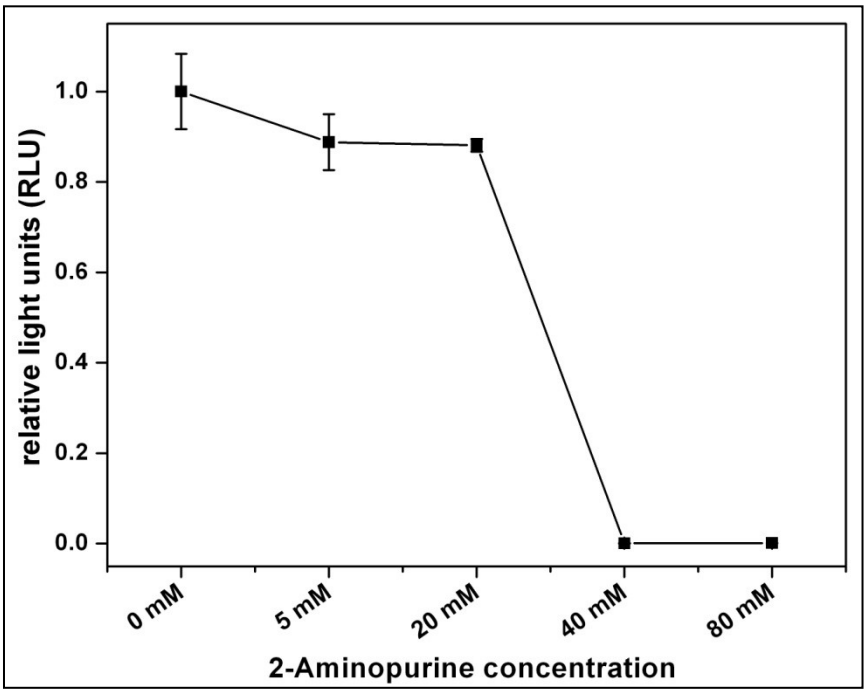

Figure 4.6-2: Determination of the impact of 2-AP on MDCK cell viability.
Final concentrations of 0, 5, 20, 40, or 80 mM 2-AP were added to the growth medium of adherent MDCK cells. 24 h after 2-AP addition, cells were lysed and cell viability was determined in the CellTiterGlo® viability assay. Results are expressed as mean ±S.D. of three technical replicates.

In a subsequent experiment, the impact of 2-AP on the induction of host cell signaling and virus replication was analyzed in Western blot. Therefore, MDCK cells were either infected or mock infected with PR8-NIBSC at an MOI of 5 and concomitantly treated with or without 5 or 20 mM 2-AP, which

was added to the infection medium. Samples were taken according to the RIPA cell lysis protocol (3.2.1.2.1) for follow-up analysis in Western blot (3.2.1.2.2). Additionally, medium samples were taken at 24 hpi for analysis in the HA assay (3.2.1.5).

After electrotransfer of protein samples the PVDF blot membranes were probed with either one of the primary antibodies against phospho-eIF2-α, influenza virus NP, and against the IFN-induced Mx protein. The antibody against phospho-eIF2-α was applied to see whether the application of the PKR inhibitor 2-AP would indeed lead to a reduction in the phosphorylation level of eIF2-α in infected cells. Hence, it was expected that by applying 2-AP, the level of eIF2-α phosphorylation would decrease in infected cells and that no effect would be observable in mock infected cells. The antibody against NP was applied as an indicator for the progression of virus replication. Rising levels of NP expression would have been expected by applying 2-AP. In addition, the antibody against Mx was applied in order to monitor the induction of the IFN-induced antiviral state in the host cell, as PKR is known to also contribute to the induction of the IFN system, meaning that Mx expression would have had to go down.

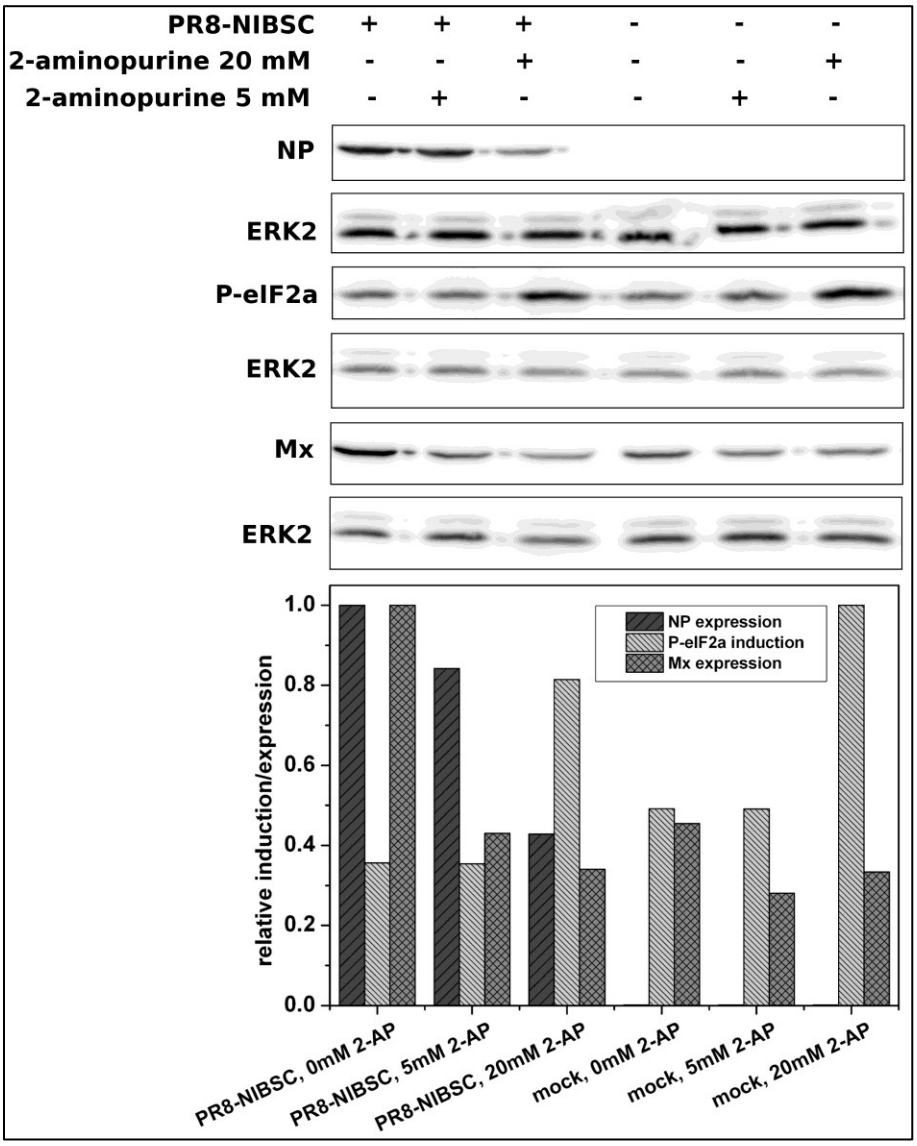

Figure 4.6-3: The impact of 2-AP on the PR8-NIBSC induced phosphorylation of eIF2-α and IRF-3, as well as on the expression of Mx and NP.
MDCK cells were mock infected or infected with PR8-NIBSC at an MOI of 5 in the presence of 0, 5, or 20 mM 2-AP. Cells were lysed at 12 hpi according to the RIPA lysis protocol and samples were subsequently analyzed in Western blot. After densitometric evaluation, phosphoprotein bands were normalized to ERK2 expression levels.

Subsequent to the application of the respective primary antibody, membranes were probed with a corresponding secondary antibody (Table 4-1) prior to Western blot band detection. After PVDF membrane stripping, membranes were reprobed with a primary antibody against ERK2. Phosphoprotein band intensity was normalized to ERK2 expression levels. As displayed in Figure 4.6-3, the expression

of influenza virus NP in PR8-NIBSC infected cells decreased to 80 or 50% with a concomitant increase of 2-AP concentrations from 5 to 20 mM, respectively.

Furthermore it was observed that the level of eIF2-α phosphorylation in MDCK cells remained constant while the concentration of 2-AP in the cell growth medium increased from 0 to 5 mM in both the infected as well as the mock infected cell population. When the concentration of 2-AP was raised further from 5 to 20 mM, the level of eIF2-α phosphorylation increased approximately by a factor of 2 in both populations regardless of influenza virus infection.

Regarding the IFN mediated expression of Mx in MDCK cells infected with PR8-NIBSC it was observed that the expression level decreased sharply to about 40% in the presence of 2-AP as compared to the control not exposed to this PKR inhibitor.

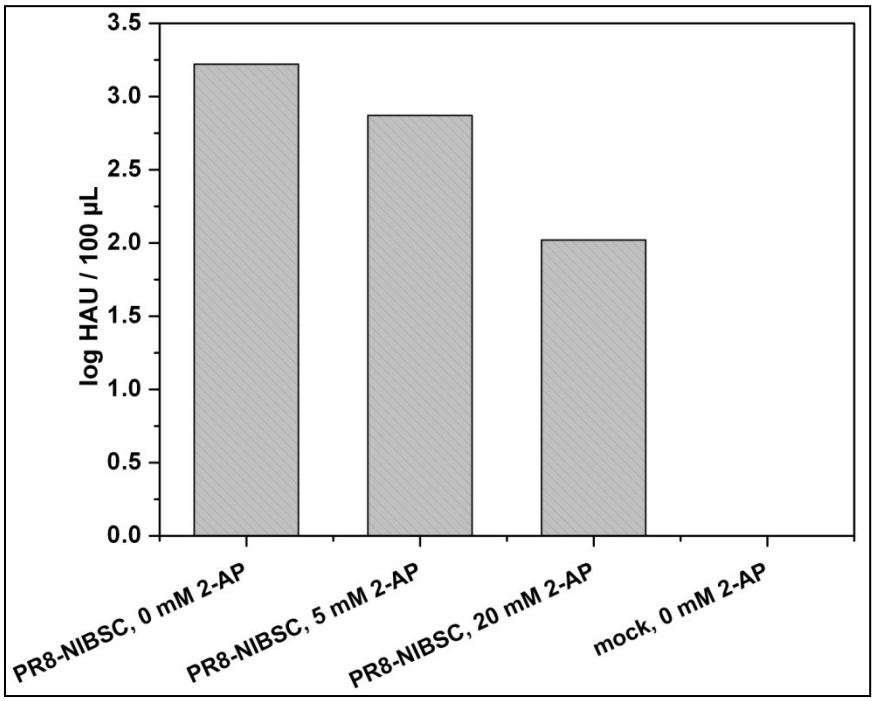

Figure 4.6-4: The impact of 2-AP on the replication of PR8-NIBSC.
MDCK cells were infected or mock infected with PR8-NIBSC at an MOI of 5 in the absence or presence of 2-AP (0, 5, 20, or 40 mM). At 24 hpi, medium samples were taken and virus titers determined in HA assay (log HA units/100 µL ±0.08 standard deviation of validated assay).

The HA titers measured in the HA assay are in accordance with the results obtained in Western blot analysis. As shown in Figure 4.6-4, the influenza A virus titer measured in the growth medium at 24 hpi was highest in the absence of 2-AP with 3.2 log HAU/100 µL. In the presence of 5 mM 2-AP, the virus

titer decreased to 2.9 log HAU/100 µL and was eventually even lower in the presence of 20 mM 2-AP with 2.0 log HAU/100 µL.

Concluding this experiment it was striking to note that the initial expectation was not fully met. Adding the PKR inhibitor 2-AP did neither lead to an increase in the level of NP expression nor to a reduction of eIF2-α phosphorylation. Instead, the exact opposite was observed, namely a reduced expression of NP and an increased phosphorylation level of eIF2-α. The only result that was in agreement with the initial expectation was the observation that the expression of the IFN-induced Mx protein was indeed reduced. As not just the reduced expression of NP but also the measured drop of the HA titer clearly showed, the initial aim of the experiment to enhance influenza virus replication by adding a small molecule inhibitor of PKR such as 2-AP could not be fulfilled. Hence, further strategies had to be tested in order to circumvent eIF2-α phosphorylation and to enhance influenza virus replication in MDCK cells. In the following chapter, the application of RNAi technology in an attempt to establish a knockdown of PKR expression and enhance virus replication accordingly is described.

4.7 Interference with NF-κB and PKR/eIF2-α signaling by the use of RNAi technology

In an attempt to elucidate the question of whether influenza virus replication could be enhanced by interfering with signaling pathways of MDCK cells, in addition to the use of the small molecule inhibitor 2-AP (4.6), RNAi technology was applied. The aim was to enhance influenza virus replication by activating the NF-κB signaling pathway through a knockdown of IκBα gene expression and by preventing the phosphorylation of eIF2-α realized by the siRNA mediated knockdown of PKR.

Thus, MDCK cells growing at an exponential rate were electroporated according to the Neon™ transfection kit (Invitrogen) with siRNA molecules (Table 3-16) against either PKR, or IκBα, or against luciferase as a control (Eurogentec) as described in chapter 3.2.2.2. Samples were taken according to either the RIPA cell lysis protocol (3.2.1.2.1) for Western blot analysis of knockdown efficiency or using the RNA extraction protocol (3.2.1.4) for sample analysis in qRT-PCR. Additionally, since the aim was to study the impact of a gene knockdown on virus replication, MDCK cells previously transfected with siRNA were subsequently infected with influenza virus 48 hpt according to chapter 3.1.5.

To analyze the effect of gene knockdown on virus replication, RNA was extracted and the expression of the influenza virus RNA genome segment 7 quantified in qRT-PCR (3.2.1.4). Both the expression of PKR as well as of the influenza A virus RNA genome segment 7 were normalized to GAPDH expression levels. Furthermore, virus titers in medium samples were measured in the HA assay (3.2.1.5). As determined in Western blot (Figure 4.7-1), the efficiency of IκBα knockdown was higher at 48 hpt as compared to the value measured at 24 hours. At 24 hpt, the protein expression level of IκBα was reduced by roughly 25% as compared to the control sample. At 48 h, the expression level of IκBα was reduced to about 50% relative to the control.

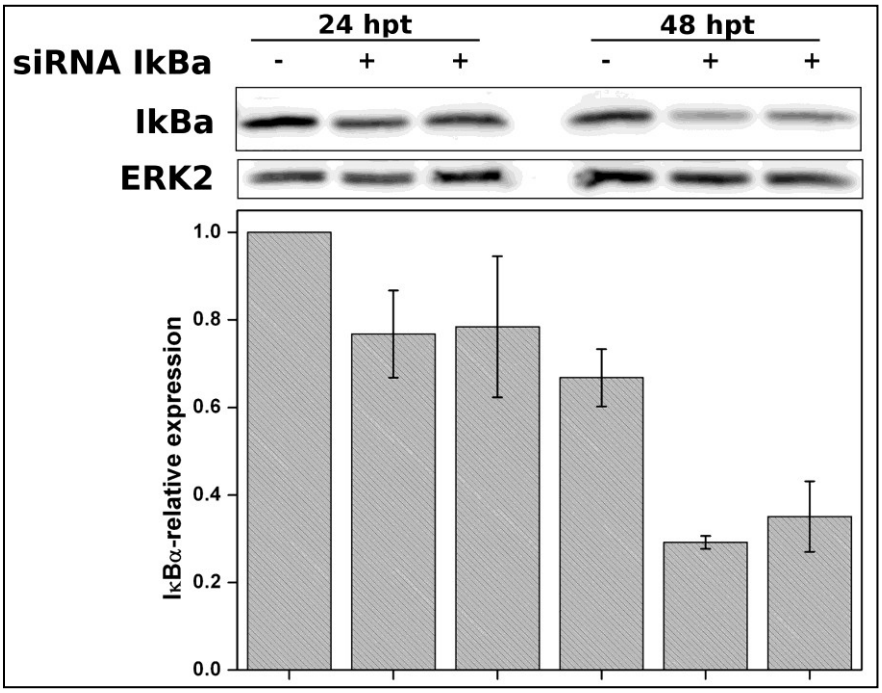

Figure 4.7-1: Evaluation of IκBα knockdown efficiency in Western blot.
MDCK cells were transfected with 100 nM siRNA against canine IκBα and lysed according to the RIPA lysis protocol at 24 or 48 hpt. Lysates were then analyzed in Western blot. Expression of IκBα was normalized to ERK2 expression levels. Values represent the mean ±S.D. of two technical replicates.

Due to the unavailability of a canine specific antibody against PKR applicable for the analysis of MDCK cells, siRNA mediated knockdown efficiency of PKR could only be determined in qRT-PCR. As shown in Figure 4.7-2, the expression of PKR could be drastically reduced. At 16, 20, 24, and 48 hpt, the expression level of PKR was decreased by about 80 to 90%.

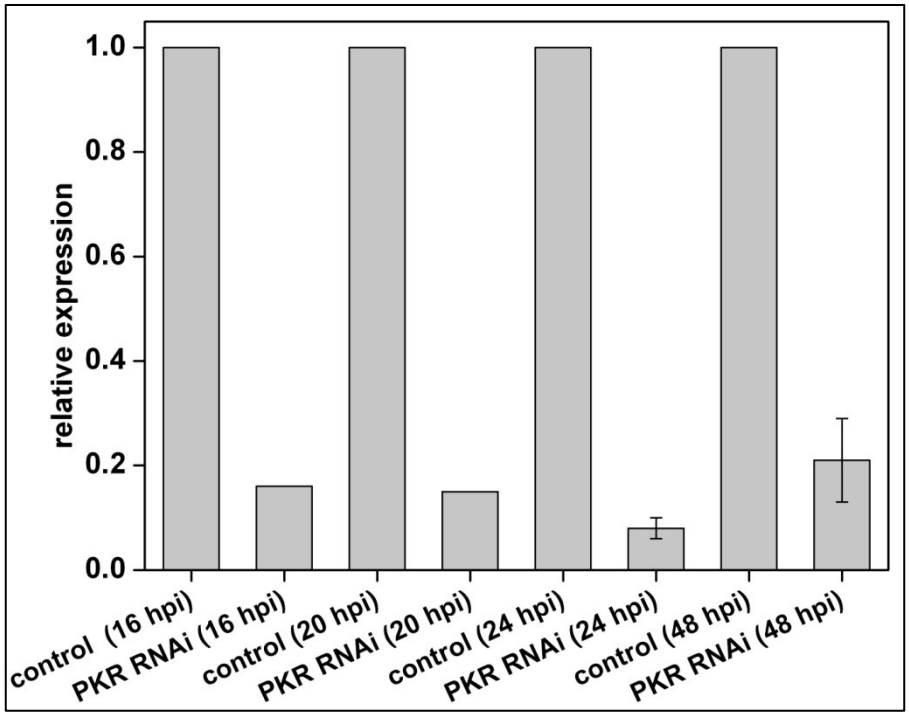

Figure 4.7-2: Measurement of PKR knockdown efficiency in qRT-PCR.
MDCK cells were transfected with 100 nM siRNA against canine PKR or with 100 nM siRNA against luciferase as a control. At 16, 20, 24, and 48 hpt, cells were lysed and RNA was extracted for subsequent analysis in qRT-PCR. Gene expression of PKR was normalized to GAPDH expression levels. Values represent the mean ±S.D. of four independent knockdown experiments (except for samples taken at 16 and 20 hpi as these sampling time points were included in only one of the four knockdown experiments).

After an effective knockdown of PKR as well as IκBα had thus been established (Figure 4.7-1 and Figure 4.7-2), the impact of the silencing of both genes on virus replication had to be clarified by measuring the expression of the influenza A virus RNA genome segment 7 in infected cells. Hence, after MDCK cells had been transfected for 48 h with the respective siRNAs, cells were infected with influenza A virus at a low MOI. It was expected that by knocking down the expression of PKR as well as by inducing NF-κB signaling by a knockdown of IκBα, the replication of influenza A virus could be enhanced.

To the contrary, as illustrated in Figure 4.7-3, at 24 hpi the average expression of the influenza A virus RNA genome segment 7 was reduced to about 60% in MDCK cells in which IκBα had been knocked down as compared to the control samples. At 48 hpi the average expression level of influenza A virus RNA genome segment 7 was still reduced at a similar magnitude as compared to the control. The NF-κB signaling pathway is known to possess proviral as well as antiviral characteristics with regard to influenza virus replication. A discussion of the observation illustrated in Figure 4.7-3 will follow in detail. Yet, it can already be stated that by knocking down IκBα, either the proviral characteristics of the

pathway were impaired, or the antiviral characteristics were amplified. Both possible outcomes had not been expected.

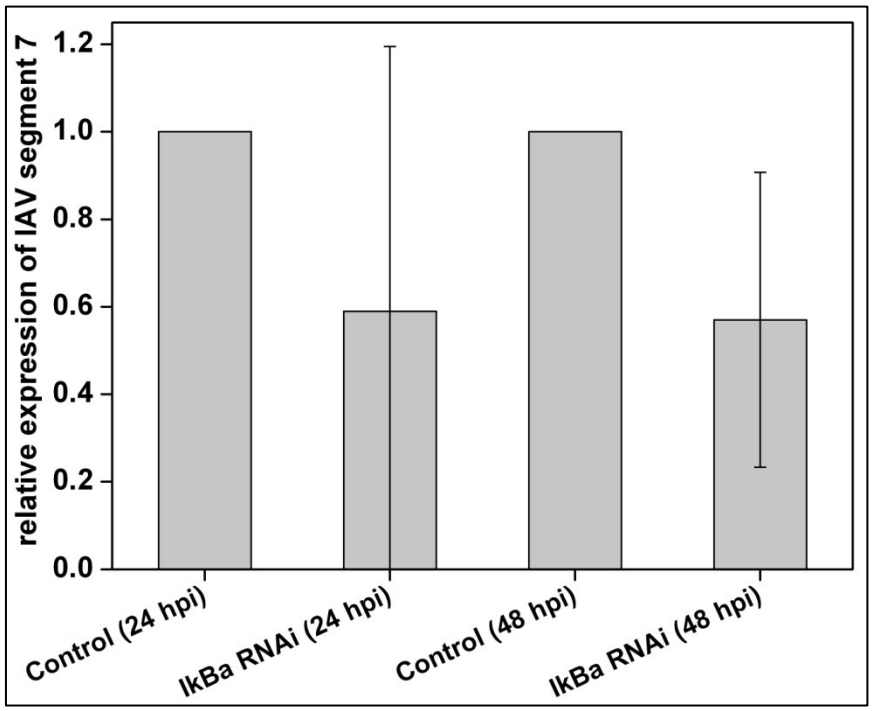

Figure 4.7-3: Impact of siRNA mediated gene silencing of IκBα on the expression of influenza A virus genome segment 7.
MDCK cells were transfected with 100 nM siRNA against either IκBα or luciferase as a control and were subsequently infected at 4 hpt with PR8-NIBSC at an MOI of 0.025. At 24 and 48 hpi, cells were lysed and RNA was extracted for subsequent analysis in qRT-PCR. Gene expression of influenza A virus genome segment 7 was normalized to GAPDH expression levels. Values represent the mean ±S.D. of two independent knockdown experiments.

As shown in Figure 4.7-4, the knockdown of PKR had a quite different effect on the replication of influenza A virus than the knockdown of IκBα did, and the experimental result was more in agreement with the initial expectation.

At all analyzed time points with the exception of 24 hpi, an elevated average expression level of RNA genome segment 7 could be measured in influenza A virus infected MDCK cells in which the expression of PKR had previously been reduced down to 10 to 20% (Figure 4.7-2). At 16 hpi, the expression level of RNA genome segment 7 was about 70% higher as compared to the control. At 20 hpi, the average expression level of RNA genome segment 7 was elevated by roughly 40% as compared to the control. The analysis of the sample taken at 24 hpi yielded a result that was contrary to the observations made at all other time points (16, 20, 48 hpi). Here, the average expression level of RNA genome segment 7 was reduced to about 70% as compared to the control. At 48 hpi, the average expression level of RNA

genome segment 7 in infected MDCK cells with a confirmed PKR knockdown was raised by almost 50% as compared to control samples.

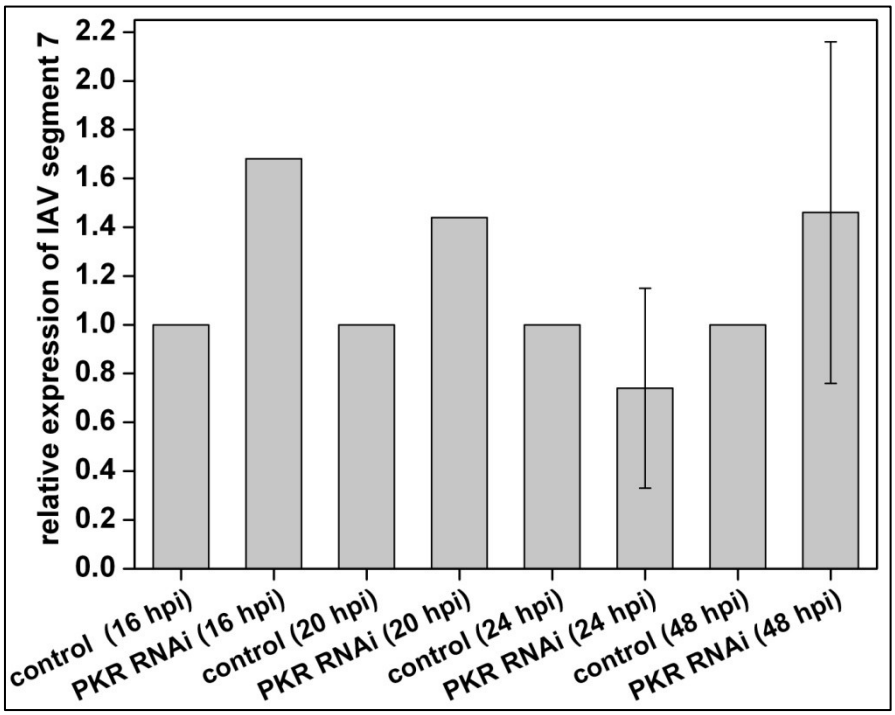

Figure 4.7-4: Impact of siRNA mediated gene silencing of PKR on the expression of influenza A virus RNA genome segment 7.
MDCK cells were transfected with 100 nM siRNA against PKR or luciferase as a control and were subsequently infected at 48 hpt with PR8-NIBSC at an MOI of 0.025. At 16, 20, 24 and 48 hpi, cells were lysed and RNA was extracted for subsequent analysis in qRT-PCR. Gene expression of influenza A virus genome segment 7 was normalized to GAPDH expression levels. Values represent the mean ±S.D. of four independent knockdown experiments (except for samples taken at 16, 20 hpi as these sampling time points were included in only one of the four knock down experiments).

Overall, except for the analysis of the samples taken at 24 hpi and despite the high standard deviations measured between replicate samples taken at either 24 or 48 hpi, first evidence was provided that the knockdown of PKR 48 h prior to virus infection may have had a positive impact on influenza A virus replication. This clear tendency is reflected in the enhanced expression of the influenza A virus RNA genome segment 7 that was measured in cells with a valid knockdown of PKR. In addition to the measurement of the expression of influenza A virus RNA genome segment 7, the impact of the siRNA mediated PKR knockdown on virus replication was also monitored in the HA assay (Figure 4.7-5).

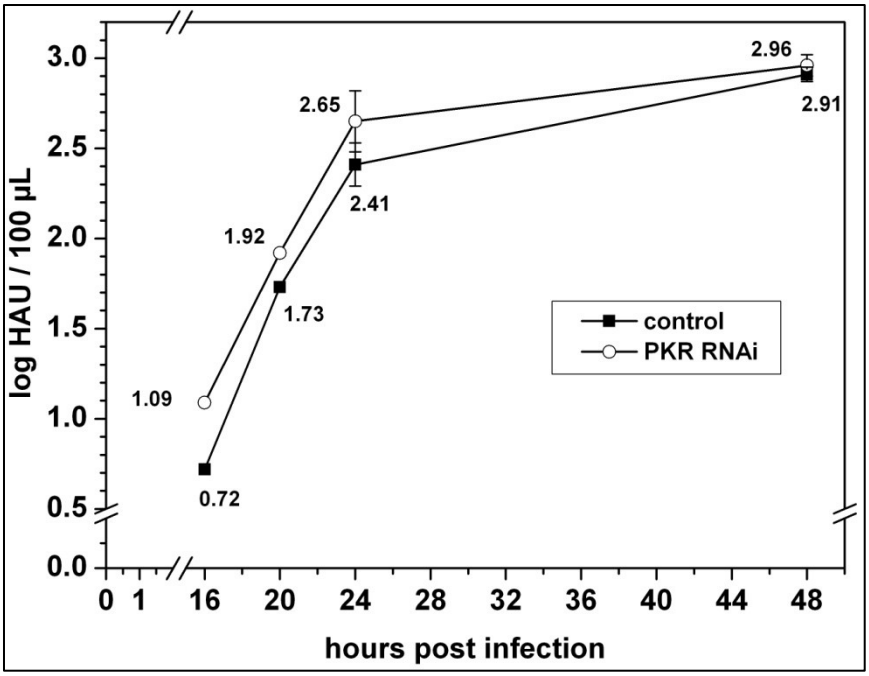

Figure 4.7-5: Impact of siRNA mediated gene silencing of PKR on the replication of PR8-NIBSC.
MDCK cells were transfected with 100 nM siRNA against PKR or luciferase as a control and were subsequently infected at 48 hpt with PR8-NIBSC at an MOI of 0.025. At 16, 20, 24 and 48 hpi, medium samples were taken and virus titers determined in a hemagglutination assay (log HA units/100 µL ±0.08 standard deviation of validated assay). Values represent the mean ±S.D. of three independent knockdown experiments (except for samples taken at 16 and 20 hpi as these sampling time points were included in only one of the three knockdown experiments).

Here, medium samples were taken at 16, 20, 24, and 48 hpi and the replication in MDCK cells with a confirmed PKR knockdown was compared to that in control cells that had been transfected with siRNA against luciferase. At 16 hpi, the virus titer measured in the PKR knockdown sample was about 0.4 log HAU/100 µL higher as compared to the control. At 20 hpi, the value measured in the PKR knockdown sample was 0.2 log HAU/100 µL higher in comparison with the control sample. At 24 hpi, the difference was 0.25 log HAU/100 µL, with the higher value measured in PKR knockdown samples. At 48 hpi, the difference between PKR knockdown compared to control samples had diminished considerably to almost 0, with a maximum value of about 3.0 log HAU/100 µL measured in the PKR knockdown sample.

In summary, the attempt to considerably reduce the expression of IκBα as well as PKR in MDCK cells by the application of RNAi technology was successful. The analysis of the impact of the knockdown of both genes on influenza A virus replication could also be accomplished. However, the obtained results were not entirely in agreement with the initial expectations. Knocking down the expression of IκBα did not prove to be beneficial for influenza A virus replication, as the expression of the RNA genome

segment 7 was reduced considerably. Nevertheless, the RNAi mediated knockdown of PKR did prove to be a positive stimulus for influenza A virus replication at an early stage. This was reflected by the enhanced expression of the RNA genome segment 7 as well as by raised HA titers measured at the early time points post infection (16, 20, 24 hpi). Unfortunately, the final virus titers measured at 48 hpi in the HA assay did not show a difference between PKR knockdown and control samples. For a successful outcome of this experimental approach with regard to vaccine production process improvement, final virus titers would have had to be raised in PKR or IκBα knockdown samples.

4.8 Analysis of the influence of trypsin used to facilitate virus replication in the bioprocess on the induction of signaling pathways

Trypsin is added to cell culture medium during the influenza vaccine production process to facilitate virus replication through the cleavage of HA into its active subunits. As the expression and secretion of IFN-beta is triggered by influenza virus infection the function of this cytokine might be impaired by the extracellular protease activity exerted by trypsin in the cell growth medium. Hence, the induction of antiviral signaling in influenza virus infected MDCK cells was monitored with regard to the effect of trypsin in the growth medium.

Therefore, MDCK cells subconfluently grown in T-flasks were infected with PR8-NIBSC at a low MOI according to chapter 3.1.5 in the presence or absence of trypsin. Samples were taken at indicated time points (Figure 4.8-1) according to the RIPA cell lysis protocol (3.2.1.2.1) for subsequent analysis of IRF-3 and Jak-Stat pathway induction in Western blot (3.2.1.2.2). Due to the observed delay in the induction of both signaling pathways in the absence of trypsin, sampling time points were in this case retarded by 4 hours. Considering the potential outcome of this experiment, several factors had to be taken into account. On the one hand, trypsin added to the growth medium has a beneficial impact for influenza virus replication, as the HA protein is cleaved into its active subunits. A resulting accelerated virus replication would also induce signaling pathways in the infected cells at a higher velocity. On the other hand, the antiviral cytokine IFN that is secreted by virus infected cells might be degraded to an unknown extent in the serum-free infection medium due to the proteolytic activity of trypsin, leading to a reduction of signaling intensity. Consequently, it was unclear which of these two effects would be observable in the analysis of the induction of signaling pathways in this context.

As shown in Figure 4.8-1-A, the induction of IRF-3 was analyzed from 16 to 44 hpi. In the presence of trypsin, the levels of IRF-3 phosphorylation increased sooner than in cells which were infected in the absence of trypsin. At 28 hpi in the cells infected in the presence of trypsin, the maximum average phosphorylation level was reached with an about 5-fold higher induction as compared to the initial level measured at 16 hpi. From 28 to 40 hpi there was no further increase in the phosphorylation level of IRF-3 measured. Moreover, the eventual average level of IRF-3 phosphorylation in these cells at 40 hpi was only about 75% of the maximum level. To the contrary, in MDCK cells infected with PR8-NIBSC in the absence of trypsin, the peak phosphorylation level was reached with an 8-hour delay at 36 hpi. As compared to the peak phosphorylation level of IRF-3 in cells infected in the presence of trypsin, in the absence of trypsin the peak phosphorylation level was approximately 25% higher. From 36 to 44 hpi, the IRF-3 phosphorylation level decreased slightly.

Similar results were obtained for the IFN mediated activation of the Jak-Stat signaling pathway (Figure 4.8-1-B). In MDCK cells infected with PR8-NIBSC in the presence of trypsin, the average level of Stat2 phosphorylation increased about 10-fold from 16 to 28 hpi, when the peak phosphorylation level of Stat2 was reached. From 28 until 40 hpi this maximum induction was followed by a steep decline leading to an average Stat2 phosphorylation level slightly above the initial value measured at 16 hpi.

In the absence of trypsin, the peak Stat2 phosphorylation level was reached again with an 8-hour delay at 36 hpi, which corresponds with peak IRF-3 induction levels (Figure 4.8-1-A). At 36 hpi in this population, a slightly higher average phosphorylation level of Stat2 was reached in the absence of trypsin as compared to the MDCK cells infected with PR8-NIBSC in the presence of trypsin. From 36 to 44 hpi in the absence of trypsin, the average level of Stat2 phosphorylation decreased to about the same level measured for the maximum induction of Jak-Stat in the presence of trypsin.

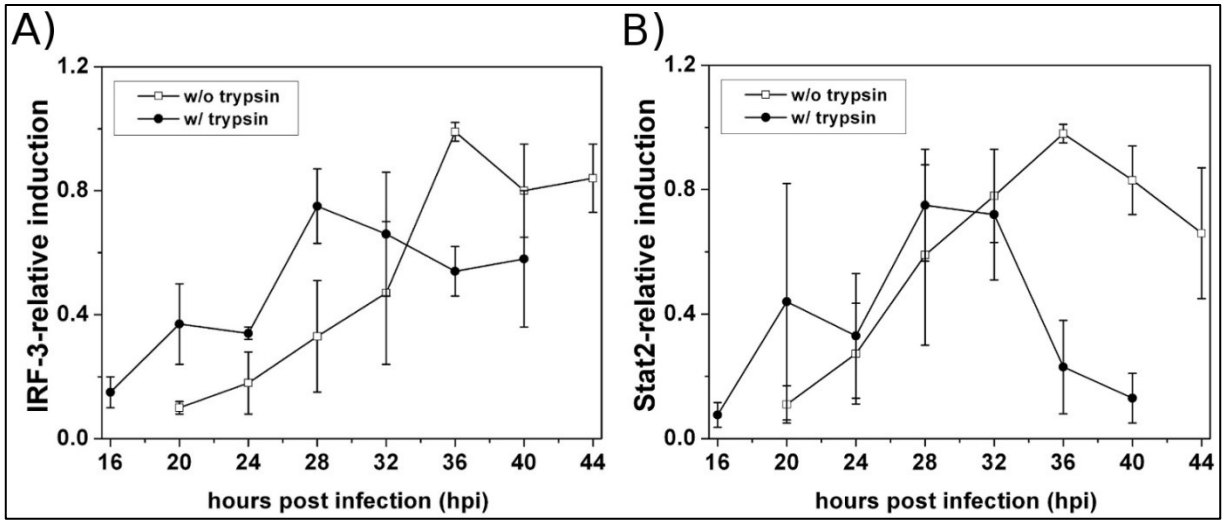

Figure 4.8-1: Western blot analysis of the impact of trypsin on IRF-3 and Jak-Stat pathway induction in MDCK cells infected with influenza A virus.

MDCK cells were grown in T-flasks and infected before full confluency was reached with PR8-NIBSC at an MOI of 0.025 in the presence or absence of 2 x 10^{-6} units/cell trypsin. Samples were taken at indicated time points from 16 to 44 hpi according to the RIPA lysis protocol and analyzed in Western blot to investigate the impact of trypsin on the induction of (A) the IRF-3 and (B) the Jak-Stat signaling cascade in infected cells. Phosphorylation of IRF-3 and Stat 2 was normalized to ERK2 expression levels and was expressed as relative induction with the highest induction level set to 1. Each data point shown represents the mean ±S.D. of two independent experiments.

Concluding this experiment, it was shown that in the presence of trypsin in the growth medium, there was an earlier response by the MDCK cells infected with PR8-NIBSC at a low MOI. This earlier response was observed for both the the intracellular signaling cascade IRF-3 and the IFN-mediated induction of the Jak-Stat signaling pathway, despite the proteolytic activity of trypsin. To the contrary, in MDCK cells infected in the absence of trypsin, the peak induction of signaling cascades was delayed considerably.

However, the peak induction levels of IRF-3 as well as Jak-Stat in these cells were slightly higher than in cells infected in the presence of trypsin. This might be attributable to the missing extracellular proteolytic activity exerted by trypsin, leading to stronger pathway induction. Overall, the described observations were shown to be in agreement with the initial expectations regarding the outcome of this experiment.

4.9 Characterization of PR8-NIBSC variant plaque isolates

Within the bioprocess engineering group it has been observed over a longer period of time that the final HA titers of the PR8-NIBSC variant have steadily risen from 2.2 log HAU/100 µL (Schulze-Horsel et al. 2009) to 2.8 log HAU/100 µL (Heynisch et al. 2010; Schulze-Horsel et al. 2009), and even further to nearly 3.2 log HAU/100 µL (Figure 4.6-4). Furthermore, the results of a deep sequencing project in collaboration with Dr. Hoeper at the Friedrich Loeffler Institute (FLI), Greifswald have shown that the PR8-NIBSC seed virus is composed of numerous subpopulations. The assumption hence was whether the increase in the final HA titers that was observed might be attributable to the long term selection of a specific variant of PR8-NIBSC with a deviating geno- and phenotype that displays a more rapid and robust replication leading to the domination of this variant in the seed virus stock. To further elucidate whether this assumption was plausible, a plaque assay was performed in which MDCK cells were infected with 10^{-3}, 10^{-4}, and 10^{-5} dilutions of PR8-NIBSC seed virus stock as described in chapter 3.2.1.7. After a 48 hour incubation of the infected MDCK cells, plaques were picked for the infection of fresh cells with these isolates. At 72 hpi, samples were taken and HA titers measured (Figure 4.9-1). The 14 plaques that were successfully isolated grew to final virus titers from 2.4 to 3.0 log HAU/100 µL after three days, with an average value of 2.66 log HAU/100 µL and a standard deviation of 0.17.

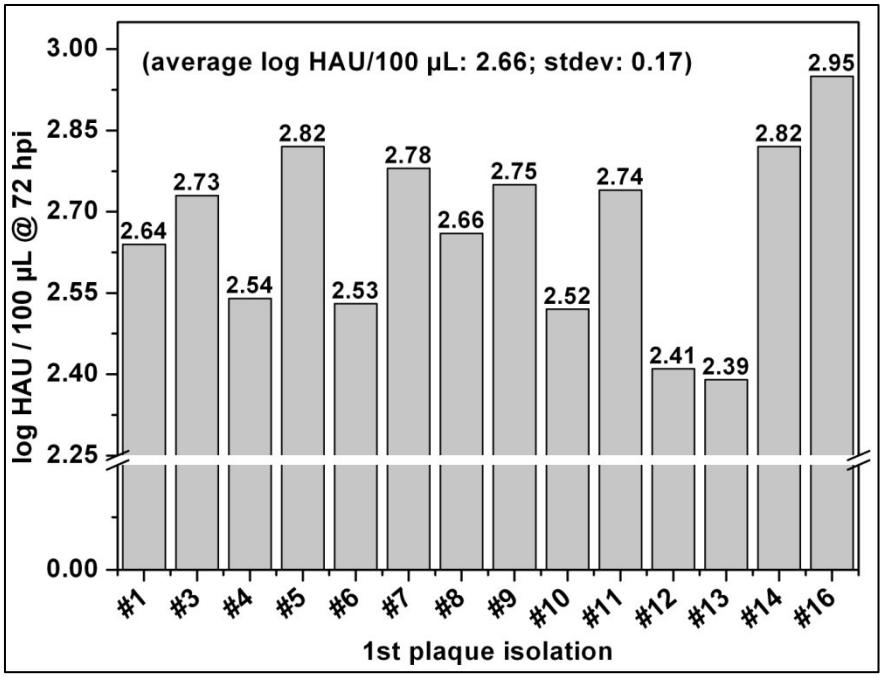

Figure 4.9-1: Plaque assay using MDCK cells to isolate and purify PR8-NIBSC variants in seed virus stocks.
MDCK cells were grown in 6-well tissue culture plates for 24 h and infected with the 10^{-3}, 10^{-4}, and 10^{-5} dilutions of a 10-fold serial dilution of PR8-NIBSC seed virus. After infection, the cell layer was covered with fresh prewarmed growth medium containing 1% (w/v) soft agar. After an incubation period of 48 h, visible plaques were picked and each plaque was transferred to a fresh tissue culture flask with a confluent layer of MDCK cells. At 72 hpi, medium samples were taken and analyzed in the HA assay (read-out: log HA units/100 µL ±0.08 standard deviation of validated assay).

Besides the medium samples taken for analysis in the HA assay, additionally a $TCID_{50}$ assay was performed to determine the concentration of infectious virus particles in the isolated variant samples (Figure 10.2-1). After the $TCID_{50}$ for each plaque isolate had been determined, MDCK cells were infected with a defined MOI of 0.025. After 72 h, medium samples were taken and subsequently analyzed in the HA assay according to chapter 3.2.1.5. The data obtained in the infection experiments with these 14 plaque isolates are displayed in Figure 4.9-2. The lowest virus titer measured at 72 hpi for the isolates 12 and 13 was 2.6 log HAU/100 µL, and the highest titer was 3.0 log HAU/100 µL for isolate 16. The average value of all analyzed plaque isolate samples was 2.7 log HAU/100 µL with a standard deviation of 0.13. Remarkably, comparing the HA titers measured directly after plaque isolation with those measured after propagation of the isolates in T-flasks for one passage were all in a similar range, and, except for isolate 9, differed by less than 0.2 log HAU/100 µL.

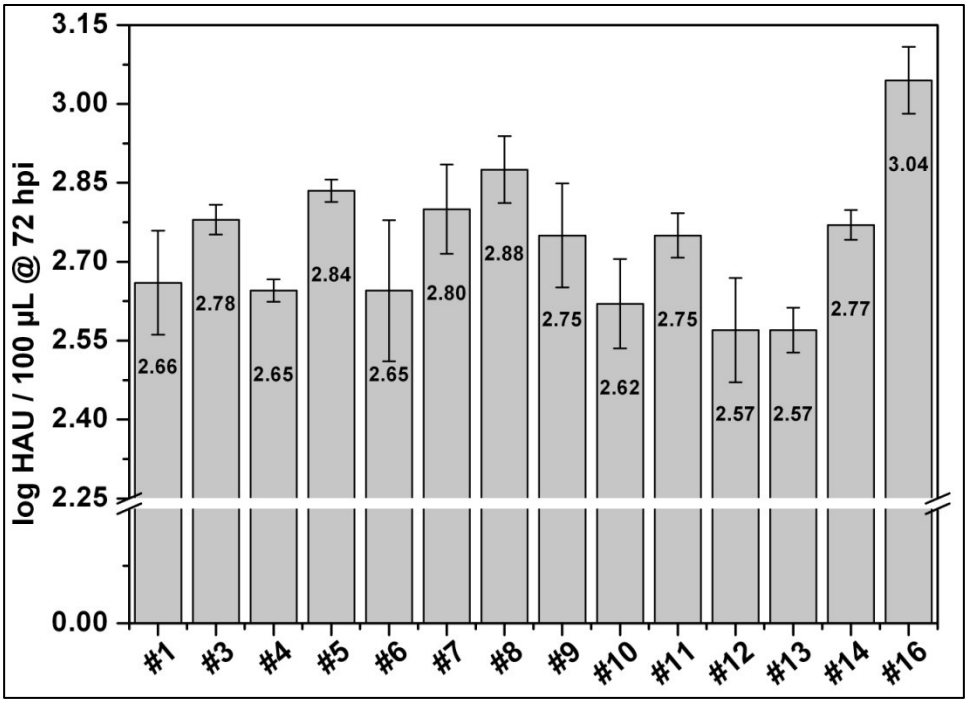

Figure 4.9-2: Virus titers measured in infection experiments with PR8-NIBSC variant isolates.
After propagation in T-flasks for one passage, plaque isolates were harvested and the concentration of infectious virus particles determined in the TCID50 assay. Subsequently, MDCK cells were infected with one plaque isolate per T-flask at an MOI of 0.025. Samples were taken at 72 hpi and analyzed in the HA assay (read-out: log HA units/100 µL ±0.08 standard deviation of validated assay). Each data point shown represents the mean ±S.D. of two independent experiments.

Subsequently, infection experiments were conducted to assess whether the plaque isolates 13 and 16 that replicated to either the lowest or highest virus titers measured exhibit a differential impact on the induction of IFN signaling in the host cell. As illustrated in Figure 4.9-3, the induction of the IRF-3 and the Jak-Stat signaling pathway was analyzed in Western blot according to chapter 3.2.1.2 after infection of MDCK cells at an MOI of 1 with both isolated variants. Shortly after infection at 0 hpi, a relative induction of IRF-3 of roughly 0.5 or 0.6 by both analyzed variants could be detected. At 4 hpi, the phosphorylation level of IRF-3 caused by the infection with both variants had not changed. Compared to 0 and 4 hpi, at 8 hpi the phosphorylation level of IRF-3 increased roughly 1.3 to 1.5-fold in cells infected with plaque isolates 16 or 13, respectively.

At 12 hpi, the maximum IRF-3 phosphorylation levels of this experimental setting were reached in both populations infected with either one of the two plaque isolates. At that time point, relative to the induction measured at 4 hpi, the phosphorylation level of IRF-3 had increased approximately either 1.5 or 2-fold through the infection with both plaque isolates, respectively.

The initial relative induction values at time point 0 hpi of the Jak-Stat signaling cascade had risen only slightly in both infected populations by 4 hpi. Compared to the initial level, the phosphorylation level of Stat2 was roughly 2-fold higher in cells infected with plaque isolate 13 at 8 hpi. The level of Stat2 phosphorylation remained at about the same level in isolate 16 infected cell samples as compared to the value measured at 4 hpi. As it had already been observed in the analysis of the induction of IRF-3 signaling, maximum phosphorylation levels of Stat2 in this experimental setting were measured at 12 hpi in both infected populations. Compared to the initial level measured at 0 hpi, the phosphorylation level of Stat2 in plaque isolate 13 infected cells had risen roughly 5-fold. The phosphorylation level of Stat2 in plaque isolate 16 infected cells was about 3-fold higher as compared to the initial level measured at 0 hpi. However, despite the difference of final virus titers of approximately 0.5 log HAU/100 µL measured between both plaque isolates (Figure 4.9-2), only a slight, insignificant difference in the maximum phosphorylation levels of IRF-3 or Stat2 measured at 12 hpi in cell samples of infection experiments with either one of the two plaque isolates could be observed.

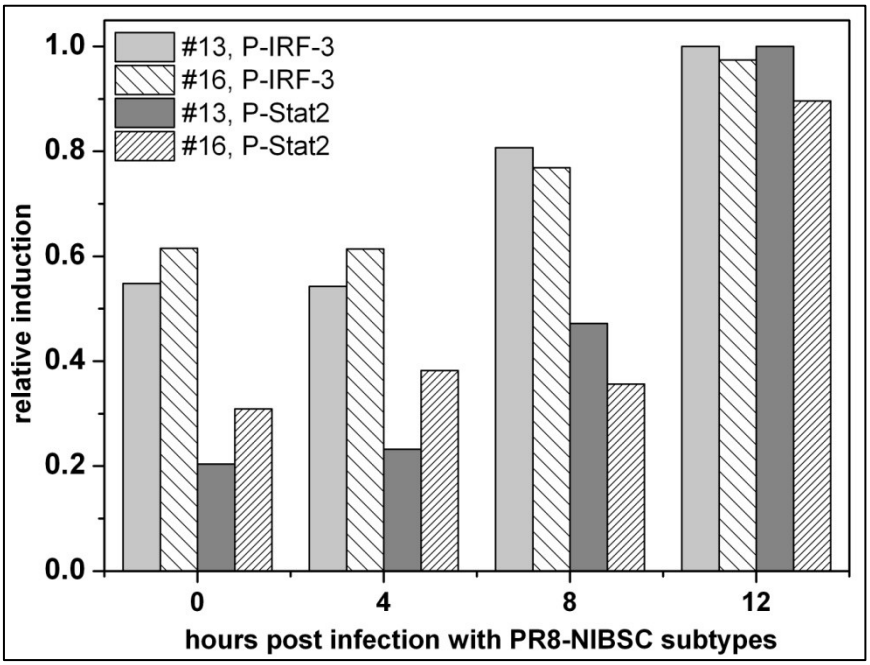

Figure 4.9-3: Western blot analysis of IRF-3 and Jak-Stat pathway induction in MDCK cells infected with two variants (subtypes) of PR8-NIBSC.
MDCK cells subconfluently grown in T-flasks were infected with two plaque isolates of PR8-NIBSC (#13, #16) at an MOI of 1. The induction of IRF-3 and Stat2 phosphorylation at indicated time points was measured in Western blot. Phosphorylation levels of IRF-3 and Stat2 were normalized to ERK2 expression levels, with maximum induction levels set to 1. Samples were taken according to the RIPA lysis protocol. Data shown are derived from one representative experiment.

Therefore, the conclusion was drawn that the induction of the signaling cascades IRF-3 and Jak-Stat2 could not be held responsible for the difference in the final HA titers determined in the comparison of the plaque isolates 13 and 16, which were seen as putative variants of PR8-NIBSC.

5 Discussion

In the focus of this study was the analysis of intracellular signaling cascades in MDCK cells that are of relevance in innate immunity and influenza virus replication, including the pathways IRF-3, NF-κB, Jak-Stat, PI3K/Akt, PKR/eIF2-α, and Raf/MEK/ERK. After Western blotting as the analytical method of choice had been successfully established, several influenza virus strains were screened regarding their potential to induce the above mentioned signaling pathways. The most striking result was the differential induction of all analyzed signaling pathways by two variants of influenza A/Puerto Rico/8/34 (H1N1) virus, termed PR8-NIBSC and PR8-RKI. These two variants have been investigated before with regard to their impact on the host cell proteome and apoptosis induction (Schulze-Horsel et al. 2009; Vester 2009). Noticeably, the infection with the variant PR8-NIBSC shown to trigger host cell apoptosis sooner than PR8-RKI and to have a more profound impact on alterations of the host cellular proteome was shown here to also induce a stronger degree of intracellular signaling than PR8-RKI. These initial descriptive screening experiments were subsequently complemented by a more investigative approach, using a chemical inhibitor of PKR as well as RNAi technology. It could be shown that by using the chemical inhibitor 2-AP, PKR activity could be suppressed slightly. Furthermore, the use of RNAi technology resulted in suppression of IκBα and PKR gene expression. However, neither did influenza virus benefit from these gene knockdowns nor from chemical inhibition of PKR with regard to final virus titers reached in the course of its replication in MDCK cells. In the following, the results obtained throughout this study are discussed in detail and in a logical order. At first, aspects connected to the establishment of the main analytical method are discussed, with the generation of positive controls as the introducing theme.

5.1 Generation of positive controls

The generation of positive controls is a precondition for Western blot optimization, which posed the first obstacle that had to be overcome before the analysis of influenza virus-induced signaling pathways could be initiated. For the pathways IRF-3, NF-κB, Jak-Stat, PI3K/Akt, PKR/eIF2-α, and Raf/MEK/ERK, positive controls could be obtained and hence Western blotting procedure was

successfully optimized, which allowed for subsequent analysis of pathway induction in influenza virus infected MDCK cells. The pathways that had to be excluded from analysis were the MAP kinases p38 and JNK due to failed attempts to generate positive controls in MDCK cells. This illustrates a drawback of the analytical method, which relies on the availability of species-specific antibodies. None of the tested antibodies except anti-phospho-IκBα were clearly stated by the manufacturer to possess canine specificity. However, if the sequence of the respective epitope was identical or at least similar to that of the species to which the antibody was most specific, attempts to detect signaling proteins in MDCK cell samples were promising (some examples shown in 10.3).

Three different strategies were applied for the generation of positive controls, which always aimed for the strongest possible pathway induction. These comprised (1) the stimulation of cells with extracellular agents, such as cytokines, e.g. TNF-α, or with small molecules such as thapsigargin. Another approach used was (2) the stimulation of cells with polyI:C, a structural mimic of viral RNA used to trigger cellular innate immunity. Another strategy was (3) the infection of cells with influenza virus at a high MOI or with an influenza virus variant carrying a deletion of the NS1 protein, an important viral antagonist of cellular antiviral mechanisms.

Due to a number of reasons, positive control generation might fail, wich includes the manner of cell stimulation, lacking antibody specificity, or Western blotting procedure.

Attempting to use cytokines to stimulate cells, care has to be taken that these bind specifically to the corresponding receptor of the respective species. *In silico* resources (http://blast.ncbi.nlm.nih.gov/) have to be used prior to experimental planning to check for sequence similarity in case of unavailability of species-specific cytokines. Another important aspect is to assure that cells are exposed to sufficient concentrations of stimuli for a sufficient duration of time, long enough to fully induce the respective pathway of interest. It is also important to choose a suitable method for the delivery of stimuli. Regarding cytokine stimulation, it is sufficient to add appropriate concentrations to the culture medium. Stimulants such as polyI:C, however, need to be transfected, which requires choosing a suitable tranfection method, which varies from cell line to cell line. Some cell lines can be transfected easily with lipid-based transfection reagents, while others have to be electroporated for sufficient delivery of the respective agent to the interior of the cell.

Regarding the selection of antibodies, the limited availability of canine specific antibodies posed an obstacle. However, although commercially available antibodies were generally stated to be non-specific for canine proteins, initial *in silico* analyses were done to assess whether epitope sequences were

identical or at least similar to those found in the organism to which the respective antibody possessed the highest specificity. Antibodies were obtained only if this initial precondition was met. Albeit confirmed identical or similar epitope sequences and cross-species specificity, some antibodies could still fail to detect the target protein because epitope damage can occur during cell lysis, yielding the protein of interest in cell lysates undetectable. This applies especially to phosphoproteins, whose phosphorylated epitopes are easily damaged by phosphatases or due to insufficient cooling during cell lysis.

However, even if cell stimulation and antibody selection are carefully done, the Western blotting procedure itself can cause positive control generation to fail. This might be due to too low protein concentrations applied to SDS gels, and it could also be ascribed to only weak hydrophobic interaction between protein of interest and blotting membrane.

Nevertheless, despite these obstacles in establishing Western blotting procedure, positive controls for the pathways IRF-3, NF-κB, Jak-Stat, PI3K/Akt, PKR/eIF2-α, and Raf/MEK/ERK could eventually be generated for subsequent optimization.

5.2 **Western blot optimization**

The application of the antibodies needed to reliably detect the induction of the pathways IRF-3, NF-κB, Jak-Stat, PI3K/Akt, PKR/eIF2-α, and Raf/MEK/ERK was optimized for the analysis of influenza virus-induced signaling processes in MDCK cells. The overall aim here was to systematically analyze the induction of several signaling pathways in MDCK cells triggered by influenza virus infection in parallel. Hence, at the beginning of this study, no sources of information were accessible with respect to how antibodies had to be used for successful analysis of canine signaling proteins in MDCK cell samples. Additionally, most antibodies could not be used and diluted according to instructions of the manufacturer referring to cell samples derived from organisms to which respective antibodies react most specifically. The aim of the optimization of the Western blotting procedure is to achieve the strongest possible specific Western blot band intensity and concomitant elimination or at least strong reduction of background. Furthermore, for economic reasons, performing Western blot it is desirable to always consume only little amounts of antibody. Several undesirable conditions can be observed in Western blots that require optimization, such as weak signals, a quick fading of the signal, failure to observe neither specific signal nor background, the occurrence of non-specific bands, diffuse bands, and blotchy

or speckled background. The specific activity and specificity of each antibody for its antigen requires an optimal combination of antibody and antigen and therefore appropriate primary and secondary antibody as well as antigen concentrations and blocking conditions (Alegria-Schaffer et al. 2009). Establishing Western blotting procedure, all these parameters needed optimization. This could be accomplished for the respective signaling pathways, providing the analytical foundation for a systematic analysis of influenza virus-induced signaling processes in MDCK cells.

5.3 Comparison of several influenza virus strains and variants with regard to replication and concomitant induction of antiviral signaling pathways

Measuring the induction of signaling cascades in MDCK cells by several influenza virus strains and variants was aimed at broadening knowledge and understanding of virus-host cell interactions in a bioprocess for vaccine production. The signaling pathways introduced in chapter 2.2.3 play important roles in cellular innate immunity, apoptosis induction, and hence, virus replication. The analysis of signaling pathways was meant to complement data generated in previous studies whose aim it was to investigate virus-host cell interactions with regard to the impact of virus infection on the proteome of the host cell and on apoptosis induction (Schulze-Horsel et al. 2009; Vester et al. 2010). Furthermore, it was unclear whether the induction of these signaling pathways might be one possible reason for poor replicative behavior observed for some influenza virus strains.

At first, a number of influenza virus strains, namely influenza A/Puerto Rico/8/34 (NIBSC), B/Malaysia/2506/2004, A/WSN/33, A/Wisconsin/67/2005-like HGR, A/Uruguay/716/2007-like HGR, and A/Puerto Rico/8/34 (RKI) were screened regarding their potential to induce signaling cascades in MDCK cells. The influenza viruses A/Puerto Rico/8/34 (NIBSC), A/Puerto Rico/8/34 (RKI), A/Wisconsin/67/2005-like HGR were chosen because they have been subject of detailed analyses in the BPE group regarding replicative behavior, apoptosis induction, and host cell proteome alterations (Schulze-Horsel et al. 2009; Vester et al. 2010). Furthermore, the influenza virus A/Uruguay/716/2007-like HGR was chosen in addition to influenza A/Wisconsin/67/2005-like HGR virus as another example of an A/Puerto Rico/8/34 based HGR that is also characterized comprehensively in the BPE group regarding its potential to induce host cell apoptosis (Isken et al. 2012). As an example of an influenza B virus strain, influenza B/Malaysia/2506/2004 was included in

the analysis. The influenza A/WSN/33 virus was analyzed as an example of a strain known to induce the IFN system rather weakly, while at the same time being comparably unsusceptible to the antiviral actions of IFN (Seitz et al. 2012).

Prior to the analysis of signaling pathway induction, the replicative behavior of the viruses was analyzed by HA assay and through measuring the level of NP expression in infected cells at 8 and 12 hpi. The HA titers that were reached by A/Puerto Rico/8/34 (NIBSC), A/Puerto Rico/8/34 (RKI), and A/WSN/33 correspond with data previously obtained in the research group (Schulze-Horsel et al. 2009; Seitz et al. 2010). Regarding the replication of the influenza A/Wisconsin/67/2005-like HGR, the HA titer did not exceed 2.0 log HAU/100 µL, as opposed to the results obtained by Schulze-Horsel and during other previous analyses in the BPE research group. However, for the A/Wisconsin/67/2005-like HGR a strong MOI dependency has been observed. While infections at a low MOI lead to HA titers of approximately 3.0 log HAU/100 µL, infecting cells at a high MOI has been observed to lead to reduced HA titers below 2.5 log HAU/100 µL (Isken et al. 2012). The HA titers measured for influenza B/Malaysia/2506/2004 and A/Uruguay/716/2005-like HGR were in agreement with previous results obtained in the research group (BPE group, unpublished data). For influenza A/WSN/33 a steep drop in the measured HA titer was observed from 24 to 96 hpi, which can only be attributed to a time-dependent deterioration of the generally very stable HA protein, which is highly unlikely, since neither had it previously been observed elsewhere, nor was this observed for any of the other influenza viruses analyzed here. Furthermore, although it is known that hemagglutination by influenza virus can be effectively inhibited by artificially synthesized polymers possessing active ester groups (Mammen et al. 1995), due to their physical absence these reagents could not have contaminated the respective sample during the analytical procedure. Hence, the observation made here cannot be explained satisfactorily. The highest titers as measured in the HA assay were reached by A/Puerto Rico/8/34 (RKI), A/Uruguay/716/2005-like HGR, and A/WSN/33.

Assessing the progression of virus replication by monitoring the expression of NP in Western blot cannot be done over an extended period of time as it is possible to do in the HA assay, since only cells attached to the cultivation vessel surface are included in the analysis. Nevertheless, the data obtained in Western blot qualitatively correspond with the HA assay data with regard to the state of the progression of the infection at 12 hpi. The HA titers of medium samples of infections with A/Puerto Rico/8/34 (NIBSC), A/Uruguay/716/2005-like HGR, and A/WSN/33 taken at 12 hpi were higher than those of infections with the other three analyzed viruses. Accordingly, NP expression rates are most pronounced

in cells infected with A/Puerto Rico/8/34 (NIBSC), A/Uruguay/716/2005-like HGR, and A/WSN/33 at 12 hpi. However, the NP expression levels at 12 hpi do not allow predictions regarding the final outcome of virus replication. For example, at 12 hpi almost no NP expression was detectable in A/Puerto Rico/8/34 (RKI) infected cells, although this virus reached an HA titer of more than 3.0 log HAU/100µL at 96 hpi, which was at that time point higher than those reached by all the other analyzed viruses. The most important observation regarding NP expression levels is that virus replication does not proceed at an equal pace for all six compared viruses, but rather is most pronounced in cells infected with influenza virus A/Puerto Rico/8/34 (NIBSC), A/Uruguay/716/2005-like HGR, and A/WSN/33. Interpreting the induction of signaling pathways by influenza virus infection, this has to be kept in mind, as it has been shown that actual virus replication is a prerequisite for signaling pathway induction in mammalian cells (Rehwinkel et al. 2010). Subsequently, the hypothesis to be tested was whether virus strains that do not replicate to high titers induce antiviral signaling cascades to a stronger degree than those that replicate better. Comparing the induction of antiviral signaling cascades through the different influenza viruses was an approach meant to provide an explanation for their differing replication behavior, reflected in HA titers and NP expression levels. Providing such an explanation was complicated by the lacking availability of the genomic sequences of the analyzed influenza A/Puerto Rico/8/34 virus variants PR8-NIBSC and PR8-RKI at the beginning of this study.

The cumbersome and time-consuming method of Western blotting limited sample throughput considerably, despite its still being the analytival method of choice. Since this study started out with the aim of analyzing a broad panel of influenza viruses with regard to their potential to induce all the signaling cascades described in chapter 2.2.3, during initial analyses the number of analyzed time points was limited to 8 and 12 hpi. These time points were deemed suitable for analysis since it was shown that during infection with A/Puerto Rico/8/34 (NIBSC) and A/Puerto Rico/8/34 (RKI), virus release started at 10.5 hpi and 14 hpi, respectively, even for infections at a low MOI of 0.025 (Schulze-Horsel et al. 2009). The displayed results of the induction of Jak-Stat and PKR/eIF2-α are exemplary for all other analyzed pathways. Only the infection with influenza virus A/Puerto Rico/8/34 (NIBSC) and the influenza virus A/Wisconsin/67/2005-like HGR led to a phosphorylation of eIF2-α considerably above the level of the mock infected control, whereas for all other analyzed viruses, no significant difference in the phosphorylation level could be observed. Analyzing the induction of Jak-Stat signaling, only the infection with A/Puerto Rico/8/34 (NIBSC) led to a comparably high average phosphorylation level. Hence, a first experimental result could be obtained, which seemed to indicate that there might be a

correlation between the induction of antiviral signaling pathways and rather poor replication behavior. However, due to high standard deviations, differences as compared to the mock infected control were blurred for any other analyzed influenza virus.

Once the results of the first attempt to systematically measure the induction of antiviral signaling pathways for a broad panel of influenza viruses at once were obtained, the limitations of the semi-quantitative, experimentally fault-prone method of Western blotting became obvious. The high standard deviations of the experimental data and the insufficient resolving power led to the conclusion that, by further relying on the analytical method, it would only be feasible to compare two different influenza viruses and as many time points as possible at once. This was further justified by the insight that the induction of signaling pathways by influenza virus is a dynamic process that does not necessarily proceed at equal velocity during every infection experiment, which might also be one reason for the high standard deviations of the results. Additionally, as previously mentioned, no systematic approach to measure the dynamics of the induction of several antiviral signaling pathways by influenza virus infection at once throughout a time-course of up to 12 to 24 hpi had previously been attempted and could hence not be referred to.

5.4 Comparison of two variants of influenza A/Puerto Rico/8/34 virus with regard to replication and concomitant induction of antiviral signaling

The first attempt at screening a multitude of influenza viruses regarding their potential to induce signaling pathways in MDCK cells at only two time points after infection was deemed unsuitable due to the low resolving power of the semi-quantitative analytical method and high standard deviations. Hence it was concluded that a wider time course had to be analyzed, while comparing only two influenza viruses. For this more detailed analysis, two variants of influenza A/Puerto Rico/8/34 were compared, namely PR8-NIBSC and PR8-RKI, that, despite initially assumed uniformity (same strain, only different supplier), subsequently had been shown to differ in their replicative behavior (Schulze-Horsel et al. 2009; Vester et al. 2009).

The differences in maximum HA titers measured in samples taken from T-flask cultures infected at a high MOI of 5 with both variants were similar to those obtained in previous bioreactor cultivations (Schulze-Horsel et al. 2009). In particular, virus yields for PR8-NIBSC were lower than for PR8-RKI. In

a previous study conducted in the BPE research group the analysis of cellular NP content using flow cytometry showed that PR8-NIBSC replication starts sooner than in the PR8-RKI infected population (Schulze-Horsel et al. 2009). This results in a faster release of new virions from PR8-NIBSC-infected cells, which can slightly be seen in the HA assay data shown in Figure 4.4-1. At these early time points until 12 hpi there is no difference in the viable cell concentration between both virus infections. However, the PR8-NIBSC variant induces apoptosis more rapidly and in a larger fraction of infected cells leading to a faster decrease in viable cell concentration at later time points. This can partially explain different virus yields, but cannot completely explain the differences found in the replication behavior of these two variants. As Schulze-Horsel et al. have demonstrated by mathematical models, the specific apoptosis death rate caused by the infection with PR8-NIBSC only accounts for a small decrease in final virus titer of 0.2 log HAU/100 µL as compared to the PR8-RKI infection (Schulze-Horsel et al. 2009).

Additional infection experiments were also conducted at a lower MOI of 0.025 in T-flask and bioreactor cultivations. Here, in general, similar observations were made regarding the activation of signaling cascades as during high MOI infections. Deviations that were observed regarding the induction of signaling cascades between the different analyzed cultivation conditions will be commented on for each respective pathway or set of pathways.

Analyzed signaling cascades participating in the induction of the IFN system (IRF-3, NF-κB) and in IFN signal transmission (Stat2) were activated significantly stronger by PR8-NIBSC compared to PR8-RKI in cells infected at a high MOI in a static cultivation system. The induction of the respective signaling pathways in T-flask and bioreactor cultivations of MDCK cells infected at a low MOI was delayed by roughly 12 h or 4 h, respectively, which is ascribed to the non-synchronous infection at a low MOI. Nevertheless, significant differences between the observed activation profiles for PR8-NIBSC and PR8-RKI infections remained. The results obtained for low MOI infections under static cultivation conditions support the notion that active virus replication is a precondition for the induction of signaling pathways (Rehwinkel et al. 2010).

In general, although the underlying mechanisms remain to be elucidated, the experimental data obtained support interpretation of previous findings. Vester et al. have shown that many proteins involved in signal transduction, stress response and apoptosis (i.e. UV excision repair protein RAD23, protein kinase C inhibitor protein-1, myxovirus resistance protein 1) are induced significantly stronger by PR8-NIBSC (Vester 2009). These results can be attributed to the differential induction of IFN-beta and

NF-κB signaling described in this study. The cellular antiviral state established by induction of the IFN system comprises more than 300 genes (de Veer et al. 2001). Furthermore, NF-κB alone, whose activation is crucial for induction of the IFN system, accounts for the regulation of more than 150 genes, many of which are involved in inflammation and apoptosis (Pahl 1999).

Generally, PR8 strains of influenza A virus have been proven to be weak inducers of IFN (Hayman et al. 2006; Kochs et al. 2007). This is in line with the IFN-beta induction through infection with PR8-RKI shown in this study. The stronger induction of signaling pathways by PR8-NIBSC might be due to a less potent IFN antagonizing NS1 protein. Sequence analysis has shown that the NS1 protein of PR8-RKI carries glutamic acid at positions 55 and 101. On the other hand, PR8-NIBSC has been shown to possess lysine at position 55 and aspartic acid at position 101 (Seitz et al. 2010). It has been reported that PR8 strains with glutamic acid at position 55 of NS1, and hence also our PR8-RKI variant, induce lower levels of IFN signaling (Murakami et al. 2008). However, other research groups have shown that active suppression of the innate immune response through antagonist proteins is not the only factor increasing pathogenicity of virus strains. The sheer velocity of virus replication caused by increased polymerase activity may be an important virulence factor to overcome cellular defense mechanisms (Grimm et al. 2007). For example, Murakami et al. have shown that a single amino acid difference at position 360 of PB2 along with a minor contribution from the NS1 protein can lead to a more than 1000-fold enhancement of viral growth of a PR8 strain in MDCK cells (Murakami et al. 2008).

Besides constituting the front line of innate immunity, reports show that another effect of IFN-beta secretion is the increased sensitivity of cells towards apoptosis inducers (Balachandran et al. 2000; Ludwig et al. 2006). The experimental results of Schulze-Horsel et al. suggest that the late onset of apoptosis in cells infected by PR8-RKI leads to high virus yields, whereas an early apoptosis induction by PR8-NIBSC reduces yields (Schulze-Horsel et al. 2009). The observed differential induction of signaling cascades such as Jak-Stat and NF-κB that are involved in apoptosis induction clearly supports hypotheses raised by Schulze-Horsel et al.

The Raf/MEK/ERK pathway is neither involved in apoptosis induction, nor could it be shown that it contributes to the induction of the IFN system. However, its importance for influenza virus replication is clear, as Ludwig et al. have shown that nuclear export of vRNPs in influenza A and B virus infection is crucially dependent upon an active Raf/MEK/ERK pathway (Ludwig et al. 2004; Pleschka et al. 2001). Again, results are contradictory since the pathway is more strongly induced by PR8-NIBSC. The better, more efficient replication of PR8-RKI can hence not be correlated with a stronger induction of

Raf/MEK/ERK signaling. Regarding the comparison of cultivation conditions, it is noteworthy that in addition to the time-delay observed between the high and low MOI infections, statistically significant differences between PR8-NIBSC and PR8-RKI infections vanished comparing static and dynamic cultivation conditions at low MOI infections (T-flask vs. bioreactor). This further emphasizes the initially assumed necessity to synchronously infect cells in experiments aimed at analyzing the induction of signaling pathways. Results also showed that, except for the time delay, pathway induction profiles are very similar in T-flask infection experiments at a high MOI compared to bioreactor cultivations with infections done at a low MOI.

Because of its role in apoptosis induction, analysis of the activation of the PI3K/Akt pathway was another focus of this study. Since infection with PR8-RKI leads to a weaker induction of apoptosis (Kato et al. 2006a; Schulze-Horsel et al. 2009), it was assumed that Akt would be phosphorylated stronger in this population compared to PR8-NIBSC infected cells. This assumption is based on studies showing that activation of PI3K/Akt initiates an anti-apoptotic program in cells (Downward 2004) by inactivating pro-apoptotic factors (Zhirnov and Klenk 2007). Interestingly, in both populations infected with either PR8-NIBSC or PR8-RKI, a very early strong phosphorylation of Akt was detected. However, the reason for this early induction of Akt in both populations is presumably not due to virus infection. Jackson et al. have shown that serum contained in the culture medium induces the PI3K/Akt pathway (Jackson et al. 2009). Therefore, the removal of serum-containing culture medium after the cell growth phase and the use of serum-free medium during infection are likely to be responsible for the initial sharp decline in Akt phosphorylation.

During the time course of infection between 6-12 hpi it was shown that Akt was phosphorylated more strongly in the PR8-NIBSC infected population, as compared to only a slight induction by PR8-RKI. Except for a time-delay, this stronger, yet not statistically significant phosphorylation of Akt in PR8-NIBSC infected MDCK cells compared to those infected with PR8-RKI could not only be observed in a static cultivation system with cells infected at a high MOI, but also at a low MOI in static as well as dynamic cultivation systems. Regarding the initial assumption on apoptosis induction, these results are contradictory. However, a recent study has shown that the activation of the PI3K/Akt pathway alone is insufficient to prevent influenza A virus-induced apoptosis in host cells (Jackson et al. 2009). Furthermore, PI3K/Akt has additionally been described to be involved in IRF-3 activation and hence induction of the IFN system (Ji and Liu 2008; Sarkar et al. 2004).

Another focus of attention was the PKR-mediated inhibition of eIF2-α caused by influenza virus infection. It is, again, noteworthy that under dynamic cultivation conditions with infections done at a low MOI, the stronger induction of eIF2-α phosphorylation in PR8-NIBSC infected cells persisted, despite a time-delay and lacking statistical significance of the data. The static cultivation system with infections done at a low MOI was not deemed suitable for a comparison of both virus variants as no differences in eIF2-α phosphorylation levels could be observed. This once more emphasizes the need for a simultaneous infection of cells or a high dispersion of virus particles after the first wave of infection through sufficient stirring. The phosphorylation of eIF2-α is a known antiviral mechanism by inhibiting translation of the host cell. The NS1 protein of influenza A has been shown to counteract this antiviral mechanism (Bergmann et al. 2000), by limiting activation of PKR (Kochs et al. 2007; Lu et al. 1995). The strong phosphorylation of eIF2-α observed in the PR8-NIBSC infected population may have a significant impact on the replication of this PR8 variant through inhibiting the translation of viral mRNAs. Therefore, the highly increased phosphorylation of eIF2-α might be one factor to explain the lower replication of PR8-NIBSC.

In summary, all analyzed signal transduction pathways are induced differentially by both PR8 variants differing in replication dynamics and virus yields. Since the variant displaying poor replication was shown to be a stronger inducer of signal transduction pathways, the question concluding from these data was whether the analyzed signaling pathways negatively interfere with influenza virus replication in MDCK cells. Therefore, in addition to the analysis of influenza virus-induced signal transduction, a loss of function and gain of function study was performed in the BPE research group with influenza A as well as influenza B virus. This approach focused on the role of the IFN system during influenza virus replication in MDCK cells. Surprisingly, it was shown that neither the transient expression of NS1 nor the artificial induction of the IFN system prior to infection by stimulating MDCK cells with conditioned medium containing canine-derived IFN had an impact on final virus yields. This result is in stark contrast to previous studies describing pronounced sensitivity of PR8 strains to IFN in other cell lines (Hayman et al. 2006; Seo et al. 2002). This missing inhibitory potency of the IFN system was suggested to be caused by the absence of an inhibitory effect of the canine Mx1 and Mx2 (cMx1, cMx2) proteins on viral polymerase activity concluded from a minireplicon assay (Frensing et al. 2011; Seitz et al.). Accordingly, since the action of IFN seemed to be only of minor importance for influenza virus replication in MDCK cells, subsequent studies were focused on PKR, whose activation leads to the phosphorylation of eIF2-α, which constitutes an important antiviral mechanism of the host cell.

5.5 Luciferase reporter assay to compare total protein synthesis in MDCK cells infected with PR8-NIBSC, PR8-RKI, or PR8-ΔNS1

The observation that the infection of MDCK cells with PR8-NIBSC caused a stronger phosphorylation of eIF2-α than the infection with PR8-RKI led to more detailed investigations. At first the question was whether a strong phosphorylation of eIF2-α actually reduces the amount of total protein synthesized by the infected MDCK cell. The phosphorylation of eIF2-α on serine 51 has been shown to cause a dramatic inhibition of protein synthesis in the cell, including the translation of viral mRNA (Garcia et al. 2006; Hershey 1991). Here, however, this was neither observed in PR8-NIBSC nor in PR8-RKI infected cells, since the level of total cellular protein synthesized as reflected by the measured luciferase activity did not differ significantly in both cases from the mock infected control sample. The stronger phosphorylation of eIF2-α observed in PR8-NIBSC infected cells clearly should have resulted in reduced luciferase activity levels as compared to PR8-RKI infected cells. As early as in 1981 Leroux et al. have shown that already a modest concentration of phosphorylated eIF2-α suffices to inhibit the initiation of protein synthesis in reticulocytes (Leroux and London 1982). In line with initial expectations, the infection with influenza A virus carrying a deletion of the NS1 protein has led to a considerable reduction of the luciferase activity level at 16 hpi. This is in accordance with previous findings that mutant influenza A viruses with a defective NS1 protein cannot block the activation of PKR in infected cells (Hatada et al. 1999). Generally, the NS1 protein of influenza virus has been shown to efficiently counteract the activation of PKR (Bergmann et al. 2000). Opposed to the reduction of luciferase activity at 16 hpi is the finding that the luciferase activity in PR8-delNS1 infected cells at 12 hpi is unaltered compared to mock infected cells. This is contradictory to previous results for PR8-NIBSC infections showing that in MDCK cells infected at a high MOI already 8 to 10 hpi a considerable increase in eIF2-α phosphorylation could be observed as described in chapter 4.4.5.

Concluding this experiment, a reduction of luciferase activity should have been observable for both PR8-delNS1 as well as PR8-NIBSC infected cells in comparison to the mock infected control. The observation that PR8-RKI infection did not lead to reduced luciferase activity levels is in line with the previous finding that no eIF2-α phosphorylation could be detected in MDCK cells infected with this PR8 variant. Since the most unexpected finding was that the infection with PR8-NIBSC did not lead to a reduction in luciferase activity despite its previously observed capability to strongly induce eIF2-α phosphorylation, further investigations to clarify the function of PKR in MDCK cells were necessary.

5.6 Inhibiting PKR activity via 2-AP treatment to achieve a reduction of eIF2-α phosphorylation and a concomitant enhancement of virus replication

As described in the previous chapter, no direct inhibitory effect of PR8-NIBSC infection on total protein synthesis reflected in reduced luciferase reporter activity levels could be observed. Therefore, the aim of this experiment was to find out whether the direct inhibition of PKR activity and subsequent reduction of eIF2-α phosphorylation levels would lead to an enhancement of influenza virus replication. In order to achieve this, a chemical inhibitor of PKR activity was selected. Autophosphorylation of PKR and subsequent phosphorylation of eIF2-α were shown to be inhibited by the application of 10 mM 2-AP in vitro. Further studies indicated that 2-AP is a competitive inhibitor of the kinase with respect to ATP (Hu and Conway 1993). The phosphorylation of eIF2-α was induced by treatment with thapsigargin, which has been shown to activate the pancreatic endoplasmic reticulum protein kinase through destabilization of Ca^{2+} stores in the endoplasmic reticulum (Treiman et al. 1998). PKR has been implicated in mediating the phosphorylation of eIF2-α occurring in response to the perturbation of ER Ca^{2+} homeostasis (Prostko et al. 1995). Despite the application of the PKR inhibitor 2-AP, considerable phosphorylation levels of eIF2-α were observed in thapsigargin stimulated cell samples. This can be explained by the fact that eIF2-α can be phosphorylated by several different stress-regulated kinases, namely HRI, GCN2, or PERK (Harding et al. 2000; Wek et al. 2006). Hence, the observed slight reduction in eIF2-α phosphorylation in 2-AP treated samples was regarded as sufficient proof for the applicability of 2-AP as PKR inhibitor in subsequent experiments. Hu et al. have demonstrated that 2-AP sufficiently inhibits PKR at concentrations of 10 mM (Hu and Conway 1993). The compound was subsequently titrated to determine applicable concentrations in a viability assay, in which a sharp drop in cellular viability was observed for concentrations of 2-AP exceeding 20 mM. Subsequently, an infection experiment was conducted in which 2-AP was concomitantly applied to suppress PKR activity and hence find out whether virus replication benefits from this suppression. To the contrary, results did not meet the initial expectations, as neither could eIF2-α phosphorylation levels be reduced by 2-AP application nor NP expression levels be raised by the action of 2-AP. Opposedly, NP expression levels in infected cells were reduced and eIF2-α phosphorylation levels increased. Interestingly, by the application of 2-AP in infected cells, the expression levels of the IFN-induced Mx protein were reduced considerably, which could be attributed to the role of PKR in the induction of the IFN system (Bonnet et al. 2000). The increased levels of eIF2-α could be ascribed to generally elevated stress levels occurring

during influenza virus infection. Furthermore, the action of 2-AP itself might induce considerable stress levels, as also in the mock infected samples, eIF2-α phosphorylation levels were elevated. Surprisingly, Mx expression was also found in mock infected cells, which cannot be further explained at this point. Additionally, as opposed to the initial expectation, HA titers were not raised in infected samples due to 2-AP treatment but were rather reduced, which is in agreement with the observations made regarding NP expression levels.

5.7 Interference with PKR/eIF2-α and NF-κB signaling by the use of RNAi technology

Knockdown of PKR

Since the attempt of inhibiting the PKR-mediated phosphorylation of eIF2-α by the chemical inhibitor 2-AP and the presumed according enhancement of influenza virus replication did not turn out successfully (discussed in chapter 5.6), an siRNA based approach was chosen to inhibit the action of PKR specifically without having to consider possible side-effects of the inhibitor.

PKR was deemed a suitable gene knockdown target in the attempt to enhance virus replication since its cellular function is of a clearly antiviral character (see chapter 2.2.3.8). This is further emphasized by the fact that besides the influenza virus NS1 protein, a number of other virus families have evolved PKR antagonizing proteins, including retroviruses, herpesviruses, vaccinia viruses, and flaviviruses (Brand et al. 1997; Hatada et al. 1999; Leib et al. 2000; Romano et al. 1998; Taylor et al. 1999). In addition to the expression of the NS1 protein whose function is described in more detail in chapter 2.2.4, influenza virus inhibits the activation of PKR also by exploiting the function of Hsp40 that interacts with influenza virus NP. The expression of NP in influenza virus infected cells coincides with the dissociation of the cellular inhibitor of PKR, $P58^{IPK}$ from Hsp40, which subsequently leads to a reduction of PKR activity (Sharma et al. 2011). Hence, influenza virus replication was meant to be further enhanced in MDCK cells by complementing inherent PKR antagonizing functions of influenza virus through a PKR gene knockdown.

An shRNA mediated knockdown of PKR has been demonstrated in B16-F10 mice melanoma cells (Delgado Andre and De Lucca 2007). However, despite the extensively studied role of PKR in influenza virus replication, data of a successful knockdown of PKR in MDCK cells have not been published yet.

Due to the lack of a commercially available antibody against canine PKR, the siRNA mediated gene knockdown efficiency was measured on the transcript level in qRT-PCR rather than Western blot.

During the replication of influenza virus in MDCK cells in which PKR had been knocked down, slightly elevated expression levels of influenza virus genome segment 7 were measured. As the PKR-mediated phosphorylation of eIF2-α targets the translation of RNAs, another function of PKR must be responsible for this observation. The altered expression of genome segment 7 might be due to the contribution of PKR to the induction of NF-κB and hence the expression of type I IFNs (Garcia et al. 2006). Another possible explanation could be the contribution of PKR to the activation of the apoptosis signal-regulating kinase 1 (ASK1) that mediates the induction of the stress-activated MAPK family members JNK and p38 that contribute to the induction of apoptosis (Takizawa et al. 2002). Furthermore, it was shown that PKR seems to up-regulate the expression of the apoptotic receptor Fas, which is induced by viral infection (Takizawa et al. 1995; Wada et al. 1995). Accordingly, the overexpression of wild-type PKR was shown to induce apoptosis in HeLa cells (Kibler et al. 1997; Lee and Esteban 1994). In turn, it was documented that the deletion of the PKR gene in mouse embryonic fibroblasts leads to their ability to resist apoptosis in response to dsRNA, TNF-α, or LPS (Goh et al. 2000). The knockdown of PKR therefore might have enhanced virus replication as reflected in the expression of genome segment 7 at an early stage of infection by suppressing the induction of premature apoptosis. The monitored time frame from 16 to 48 hpi corresponds with the one observed by Schulze-Horsel, who found that the proportion of infected apoptotic cells in bioreactor cultivations of MDCK cells infected with PR8-NIBSC was highest between 18.5 to 30.5 hpi (Schulze-Horsel et al. 2009).

In addition to the slightly enhanced expression of genome segment 7, a slight increase could also be observed in the HA titers measured during the early phase of virus replication monitored from 16 to 24 hpi. This clearly indicates that during this phase of replication, the virus must have benefited mildly from the PKR knockdown. Here, this could either be ascribed to a reduced activation of the NF-κB signaling pathway or to a suppression of eIF2-α phosphorylation leading to an enhanced mRNA translation by the cell. It is a widely accepted notion that influenza virus has evolved mechanisms to avoid the activation of cellular PKR and hence the total block of protein synthesis by the induction of the cellular inhibitor $p58^{IPK}$ and by the expression of NS1 (Hatada et al. 1992; Katze and Krug 1990; Katze et al. 1988). However, this notion has been challenged by Zurcher et al., who demonstrated in single-cycle infections in normal versus PKR defective cells that the host cell shut-down is independent of the action of PKR (Zurcher et al. 2000). Furthermore, it has been shown that in influenza virus-

infected cells, viral mRNAs are translated preferentially over cellular ones, which might be attributable to alterations in the translation apparatus of the cell and the activity of the NS1 protein (de la Luna et al. 1995; Enami et al. 1994; Feigenblum and Schneider 1993). Zurcher et al. therefore concluded that the inhibition of cellular mRNA translation would induce their destabilization, possibly resulting in their selective degradation (Zurcher et al. 2000). Nevertheless, in this study a mildly enhanced influenza virus replication was observed during the early phase in MDCK cells with a siRNA induced knockdown of PKR. However, at the final analyzed time point the slight differences in HA titers measured during the early phase could no longer be observed, which corresponds with previous observations in which the IFN response was suppressed (Seitz et al.). The mildy enhancing effect of the PKR knockdown is therefore more likely attributable to the contributive function of PKR in the induction of type I IFNs as Seitz et al. had observed previously in a like manner. Failure to raise final HA titers might be due to the rather ineffective inhibitory action of the type I IFN system in MDCK cells regarding influenza virus replication, partly due to a lack of inhibitory potential of the canine Mx proteins described before (Frensing et al. 2011; Seitz et al.). Additionally, the failure to detect differences in final HA titers in PKR knockdown versus control MDCK cells indicates that the PKR-mediated phosphorylation of eIF2-α on Ser51 might not lead to a complete translational shut-off. In these cells an alteration in the translational apparatus might have occurred allowing for the circumvention of the otherwise inhibitory effect of phosphorylated eIF2-α. This is furthermore supported by the observation that despite a strong phosphorylation of eIF2-α in PR8-NIBSC infected MDCK cells, the virus still was able to replicate to final HA titers above 2.5 log HAU/100 µL, which could not have occurred in cells with a complete translational shut-off. In summary, despite the observed efficient siRNA mediated PKR knockdown in MDCK cells and a mildly enhanced virus replication during the early phase of virus replication, this artificial interference with the host cell did not prove to be successful with regard to a raise in the final virus titers measured. Therefore, interfering with PKR in MDCK cells did not occur as a suitable strategy for production cell line improvement.

Knockdown of IκBα

Eventually, siRNA mediated knockdown experiments were performed in an attempt to enhance influenza virus replication in MDCK cells. Two targets were selected for these knockdown experiments: IκBα and PKR. IκBα was chosen as a target because the knockdown was meant to induce the transient activation of NF-κB. A siRNA induced knockdown of IκBα has previously been demonstrated in human

ciliary muscle (HCM) cells to stimulate the NF-κB mediated expression of metalloproteinase-2 (Lan et al. 2009). The authors observed a significant translocation of NF-κB p65 from the cytoplasm to the nucleus after 24 to 72 hours. Therefore, in this human HCM cell line, the principle of activating NF-κB by knocking down IκBα was proven to work. However, a knockdown of IκBα in MDCK cells has not been shown by any other group as yet. Despite its contribution to the induction of type I IFN signaling, the activation of the NF-κB signaling pathway has been shown to be a cellular event that influenza virus also benefits from during replication. This has been suggested to be due to the contribution of NF-κB to the expression of pro-apoptotic factors such as TRAIL or FasL (Wurzer et al. 2004). Furthermore, it was shown that the replication of influenza virus is enhanced by the expression of a constitutively active form of IKK-β, an upstream activating kinase of NF-κB, transfected prior to infection (Wurzer et al. 2004). In turn, inhibiting NF-κB signaling has been shown to impair influenza virus replication, reducing final virus titers (Mazur et al. 2007). Additionally, despite the contribution of NF-κB signaling to the induction of type I IFNs, the pathway has also been implicated in mediating the inhibition of type I IFN signaling in the manner of negative feedback by upregulating SOCS-3, a function that has been suggested to be exploited by influenza virus (Pauli et al. 2008). Although the cellular level of IκBα could be reduced considerably by siRNA, this knockdown failed to enhance influenza virus replication in MDCK cells, as reflected in the reduced RNA expression level of the influenza virus genome segment 7. Since the NF-κB signaling pathway has been described to possess proviral as well as antiviral characteristics, the observed failure of the IκBα knockdown to enhance virus replication could have two different causes. It could either be that by the partial knockdown of IκBα, proviral functions of the NF-κB signaling pathway were impaired, or that antiviral characteristics of the pathway were amplified.
For this latter assumption to be true one would have to assume that knocking down IκBα had the effect of transiently activating NF-κB signaling strongly, whereby exerting a predominantly antiviral role. A possible positive indicator for the validity of this assumption would be an increase in the level of IFN expression, known as a clear antiviral cellular function to which NF-κB contributes. This could possibly explain the reduction in influenza virus genome segment 7 RNA levels, as it is known that the IFN-induced Mx protein interferes with virus replication. However, it has already been shown that even if suppressed during the initial phase of replication, type I IFN signaling seems to be only of minor importance for influenza virus replication in MDCK cells with regard to final virus titers (Seitz et al.).
An inhibiton of the proviral functions of NF-κB could have also occurred by the knockdown of IκBα. Although the knockdown of IκBα was shown to be about 50% effective at the timepoint chosen for

infection 48 h after transfection, a strong suppression of NF-κB activity might have followed shortly thereafter as it has been shown that NF-κB activity is under the influence of negative feedback regulation through the NF-κB-dependent induction of IκBα gene transcription (Sun et al. 1993). Additionally, it has been pointed out that the rebound of IκBα shows a surprisingly fast kinetic in cytokine stimulated cells (Place et al. 2001). Place et al. concluded that besides IκBα gene transcription, other mechanisms might take action to allow for this fast replenishment of IκBα, such as its protection from degradation. Hence, by knocking down IκBα in MDCK cells in order to enhance influenza virus replication, due to the resulting increase in NF-κB activity achieved, the extent to which negative feedback occurred might have increased as well. The consequent reduction in NF-κB activity might have caused a diminished influenza virus replication as reflected in the expression of influenza virus genome segment 7. However, at this point it has to be noted that the proviral functions of NF-κB signaling are mainly ascribed to events related to apoptosis induction and hence virus particle release from the infected cell. A supportive function of NF-κB signaling during transcription and replication of viral RNA has so far not been described. Yet, the finding that the influenza virus genome segment 7 is expressed at a lower rate in infected cells with a valid IκBα knockdown might suggest the existence of such a virus supportive function of NF-κB signaling. At this point, one can only speculate whether knocking down IκBα had the effect of suppressing virus-supportive cellular functions or enhancing antiviral effects of NF-κB signaling in the cell. Nevertheless, despite the reduction of influenza virus genome segment 7 transcript levels, no effect could be observed regarding final HA titers.

5.8 Analysis of the influence of trypsin used to facilitate virus replication in the bioprocess on the induction of signaling pathways

During the influenza vaccine production process, trypsin is included in the cultivation medium to facilitate multi-cycle replication by cleavage and activation of the viral HA0 protein into its active subunits HA1 and HA2 (Klenk et al. 1975). Since the aim of this study was the analysis of antiviral signaling pathway induction in MDCK cells, the effect of the extracellular protease activity of trypsin had to be considered with regard to autocrine and paracrine signaling mediated by cytokines such as IFN, which has been shown to be sensitive to trypsin-mediated proteolytic degradation (Isaacs and Burke 1959). Therefore, MDCK cells were infected with influenza virus in the presence or absence of

trypsin and subsequently, the induction of two signaling pathways that are important mediators of the antiviral host cell response, namely IRF-3 and Jak-Stat, was analyzed. Results showed that in the presence of trypsin the induction of antiviral signaling pathways in the host cell occurred earlier than under conditions where trypsin was omitted. Here, the earlier induction of IRF-3 indicated faster virus spread, as this pathway is activated by intracellular PRRs as opposed to the autocrine and paracrine signaling leading to Jak-Stat activation. However, despite the delayed peak induction levels of IRF-3 and Jak-Stat, in the absence of trypsin these peak induction levels were slightly more elevated than in cells infected in the presence of the protease (results summarized in chapter 4.8), indicating the existence of a function of trypsin that counteracts the activation of type I IFN signaling.

In agreement with the results described in chapter 4.8, Seitz et al. could also show by qRT-PCR that the transcript levels of both IFN-β as well as Mx1 are more strongly upregulated in the absence of trypsin (Seitz et al. 2012). Furthermore it was demonstrated that a considerably higher proportion of apoptotic cells was detected in trypsin-free infections at later stages of infection, which correlated with higher IFN signaling activity. This is in agreement with previous findings in which the induction of apoptosis could be correlated with IFN signaling activity (Balachandran et al. 2000). Altogether, in trypsin-free infections, in addition to increased levels of IFN signaling, faster apoptosis induction, delayed virus propagation, and reduced virus yields could be demonstrated by our group. These results have a number of implications for the influenza vaccine production process. Although in the bioprocess trypsin has routinely been added to cleave and activate the HA protein and hence promote virus replication, the question had previously not been addressed whether and to what degree virus replication is also enhanced by the proteolytic degradation of IFN mediated by trypsin. Therefore, we have substituted and analyzed these two functions of trypsin independently in trypsin-free infections in order to better characterize their individual contribution to virus replication.

In the absence of trypsin, the growth of the highly IFN sensitive PR8-delNS1 characterized by Egorov et al. and García-Sastre et al. was severely impaired (Egorov et al. 1998; Garcia-Sastre et al. 1998). Results from our group showed that the transfection with viral IFN antagonists could partially rescue the growth of PR8-delNS1, yet not to the extent that was reached under trypsin-containing infection conditions. The inhibition of antiviral signaling could therefore only partially be ascribed to the direct proteolytic degradation of IFN by trypsin. We assumed that the fast virus replication mediated by trypsin might lead to the circumvention of cellular defense mechanisms. This is in agreement with the finding by Schulze-Horsel et al. that slow virus spread in combination with faster induction of apoptosis corresponds with a

reduction of final virus titers (Schulze-Horsel et al. 2009). Previously it was shown that the time frame in which cells can establish an effective antiviral state is limited in face of high virus replication velocity (Ueda et al. 2008).

Concluding, results from our group proved that the impact of the antiviral state mediated by type I IFN signaling in MDCK cells was limited by the effect of trypsin, both by promoting fast replication dynamics and by proteolytic degradation of IFN. As we have argued, the data gained suggest that attempts to reduce process duration in vaccine production, including strain adaptation for fast replication and optimization of infection conditions such as trypsin concentrations contribute in preventing a negative impact of host cell defense on virus yields (Seitz et al. 2012). Despite the obvious benefits of trypsin usage in the bioprocess, its use in vaccine production has been controversially discussed, since torque teno viruses (TTV) were recently detected in trypsin preparations of porcine origin (Kekarainen et al. 2009). This example illustrates why animal-derived products are generally considered a safety risk in the production of biopharmaceuticals (Audsley and Tannock 2008; Merten 2000). Nevertheless, results from our group have illustrated a startingly simple beneficial characteristic of trypsin usage in influenza vaccine production, preventing a negative impact of type I IFN signaling through promoting fast virus replication dynamics and proteolytic IFN degradation (Seitz et al. 2012).

5.9 Characterization of PR8-NIBSC variant plaque isolates

The in-depth pyrosequencing analysis of the influenza A/Puerto Rico/8/34 (PR8-NIBSC) virus has revealed that respective virus seeds were not uniform but rather comprised several strain variants with slight genomic sequence differences (Roedig et al. 2011b). Previously, it has already been known that instead of a homogenous composition, RNA virus populations can oftentimes be made up of complex distributions of mutant or recombinant genomes, constituting a population structure referred to as quasispecies (Domingo et al. 1998). As early as in 1978 it was described that an RNA phage genome cannot be viewed as a unique defined structure, but is more likely defined as a weighted average of different individual sequences (Domingo et al. 1978). As described in a review article by Biebricher et al., a quasispecies comprises a number of mutants that compete with each other under selective pressure, leading to the eventual formation of a steady state in which each mutant type is represented according to its fitness and its formation by mutation (Biebricher and Eigen 2006). In a given influenza virus

population, new variants constantly arise due to the ability of the virus to reassort in a mechanism called genetic shift, or due to high error rates of the viral polymerase (Scholtissek 1995; Steinhauer and Holland 1987). Roedig et al. have shown that virus seeds of the PR8-NIBSC variant of influenza A/Puerto Rico/8/34 comprised eight variants with regard to genome segment 4 encoding for the HA protein alone (Roedig et al. 2011b). Interestingly, after several passages of growth in a different cell line (Vero), the composition of the PR8-NIBSC variant had changed, bringing about new amino acid substitutions and altogether a shifted ratio of the different variants, reflecting adaptive mechanisms with regard to the altered cultivation environment (Roedig et al. 2011b). The assumption was therefore made that the altered PR8-NIBSC HA titers observed over a longer period of time might be attributable to a shifting ratio of the PR8-NIBSC virus seed variant composition, resulting in a selection and increasing dominance of a variant with better adapted replication capabilities. The results of the plaque assay mediated isolation of PR8-NIBSC variants seemingly confirmed the existence of variants with differing levels of replication fitness within this virus seed, as reflected in differing final HA titers. As for the previous comparison of the PR8-NIBSC with the PR8-RKI variant (Heynisch et al. 2010), the question arose if the infection of MDCK cells with isolated variants found within the PR8-NIBSC seed virus might also lead to different induction levels of antiviral signaling cascades. Since the conducted experiments could not further substantiate this assumption, differences in replication behavior of the different PR8-NIBSC variant isolates as reflected in the measured HA titer differences could not be attributed to a differential induction of antiviral signaling cascades. Hence, this furthermore underlines our estimation, that for influenza virus replication in MDCK cells, the function of antiviral signaling cascades belonging to the cellular type I IFN system seem to be of only minor importance (Frensing et al. 2011; Seitz et al. 2010). Nevertheless, the rather stable HA titers that were observed here for most plaque isolates during the short history of passaging indicate that unique variants were isolated that could most likely also be unique with regard to their genomic composition. Furthermore, these data provide further evidence for an inhomogeneous composition of seed virus stocks, which seem to consist of multiple subpopulations, referred to as quasispecies. The question remaining to be answered is what underlying molecular characteristics of the respective virus variants are causative for their observed differences in final HA titers. Due to the complexity of processes during influenza virus replication and innumerable interactions of influenza viruses with their host cells (Karlas et al. 2010; Shapira et al. 2009), answers given at this point can only be speculative and the topic clearly needs further in-depth investigation. In order to pursue this, the next experimental step would have to be a genomic sequence

analysis and comparison of the different plaque isolates. At least some of the genomic differences a sequence analysis would possibly reveal between the plaque isolates could assumably be responsible for the differences in HA titers. It has been shown in several studies that only minute alterations of the genomic sequence of influenza virus can give rise to significant changes in viral growth and resistance to host cellular IFN-mediated antiviral defense (Murakami et al. 2008), antiviral pharmaceutical agents (van der Vries et al. 2012), or host-specific transmissibility (Herfst et al. 2012). However, experience with influenza virus has shown that nucleotide sequence-based attempts to predict virus phenotype and virus replication fitness are imperfect (Lipsitch et al. 2012). Therefore, this implies that for every single genomic sequence mutation found in the comparison between plaque isolates, a reverse genetics approach would have to be pursued to clarify the respective effect on virus replication fitness. This is further complicated by the necessity to additionally perform reverse genetics studies in which the effect of several combinations of mutations are analyzed regarding replication behavior, as additive effects might exist.

6 Conclusion and Outlook

In this study, the induction of the signaling cascades NF-κB, IRF-3, Jak-Stat, PI3K/Akt, PKR/eIF2-α, and Raf/MEK/ERK in MDCK cells by influenza virus infection in the context of a cell culture-based influenza vaccine production process was analyzed.

Since previously there has not been a systematic, vaccine production process-oriented analysis of influenza virus-induced signaling cascades in MDCK cells that could have been referred to, at first Western blotting as the analytical method of choice was established. Despite the obstacles posed initially by a lack of commercially available canine-specific antibodies, positive controls for the induction of the aforementioned signaling pathways of interest could be generated for subsequent Western blot optimization. Eventually, after the Western blotting procedure had been established and optimized successfully, the analysis of the induction of signaling pathways by influenza virus infection of MDCK cells commenced. The motivation for these analyses was to find out whether a general correlation exists between a strong induction of the indicated signaling pathways of a predominantly antiviral character and a poor replication of the respective influenza A or B virus strains with regard to final HA titers in the vaccine production process. During these analyses it became obvious that only slight differences in the induction of the signaling pathways exist between most of the different influenza virus strains, and that these differences could not be revealed entirely due to limitations of the analytical method. These limitations were constituted by a lack of sensitivity of the immunodetection of phosphoprotein epitopes, and by the relatively large standard deviations of data resulting from the semi-quantitative method of Western blotting, which is prone to subjective error. Another aspect that cannot be underestimated, especially when comparing the induction profiles of signaling cascades induced by different influenza virus strains over a time course of several hours, is the frequently occurring batch to batch variations in virus replication dynamics for respective influenza virus strains. Thus, real differences between influenza virus strains regarding the induction of host cell signaling pathways might not be easily identifiable, especially when focusing only on a few time points throughout virus replication.

Nevertheless, two influenza virus candidates were chosen for a more detailed investigation, representing two variants of influenza A/Puerto Rico/8/34 (H1N1), namely PR8-NIBSC and PR8-RKI. These two variants have previously been analyzed in closer detail within the BPE group. Both variants have been shown to replicate differently, with PR8-NIBSC causing a stronger degree of apoptosis at an earlier time point in infected MDCK cells as compared to PR8-RKI (Schulze-Horsel et al. 2009). Furthermore, both

variants have been reported to have a differential impact on the host cellular proteome during infection, with PR8-NIBSC inducing more profound changes (Vester 2009). Regarding the vaccine production process the most important observation was that both strains also differ in the final HA titers that are reached during replication. Therefore, the question was asked whether both PR8 variants also display a differential impact on the induction of the aforementioned signaling pathways in MDCK cells during infection. As initially assumed, it could indeed be shown that the impact of both variants on the induction of signaling pathways differs, with PR8-NIBSC leading to a stronger induction of all analyzed pathways than PR8-RKI (Heynisch et al. 2010). These differences occurred in most cases under different infection conditions (MOI) as well as in different cultivation systems (T-flasks, stirred tank bioreactors).

Despite this interesting finding, studies that were conducted in the meantime in the bioprocess engineering group showed that in a loss of function/gain of function experimental approach, type I IFN signaling in MDCK cells can be regarded as being only of minor importance for the replication of influenza A and B virus strains oftentimes used in influenza virus vaccine production (Frensing et al. 2011; Seitz et al. 2010). These findings came largely as a surprise, as previous studies convincingly illustrated that by negatively interfering with type I IFN signaling virus replication could be affected positively. For instance, in a study conducted by de Vries et al. it could be shown that virus replication can be enhanced by expression of viral IFN antagonists (de Vries et al. 2008). It has already been shown by Young et al. that human diploid cells can simply be engineered to express the V protein of simian virus 5 to become insensitive to IFN and hence allow a number of viruses with deletions in their IFN antagonizing proteins to grow to higher titers (Young et al. 2003).

Furthermore, it was illustrated that trypsin that is added to the culture medium during the virus replication phase to facilitate HA cleavage and hence virus spread indirectly also serves to counteract the action of type I IFN mediated cellular antiviral defense by i) cleaving and hence inactivating the extracellular cytokine IFN, leading to a reduced level of activation of the Jak-Stat pathway, and by ii) enabling fast virus spread, thereby outrunning the establishment of the antiviral state by the host cell that takes time to build up (Seitz et al. 2012).

Subsequently, the influenza virus infection-induced PKR-mediated phosphorylation of eIF2-α was investigated more closely, as this is an important antiviral defense measure of the infected cell. A specific targeting of PKR was attempted by the use of a chemical inhibitor of the kinase, 2-AP. Surprisingly, in cells infected with influenza A virus that were concomitantly treated with 2-AP, neither

could the expression level of the viral protein NP be raised by the treatment with the PKR inhibitor, nor could the phosphorylation level of eIF2-α be reduced. In addition, the HA titers that were reached after 24 h of influenza virus replication were also reduced. Nevertheless, it was shown that the protein level of Mx in influenza virus infected cells was reduced in the presence of 2-AP, which might be due to the contribution of PKR to the induction of type I IFN signaling described previously. The negative impact of 2-AP on virus replication could be attributed to higher cellular stress levels induced by treatment with the compound. This assumption was reflected in the increased phosphorylation level of eIF2-α even in cells that had not been infected with influenza virus. Overall, no beneficial effect of the 2-AP treatment for influenza virus replication could be observed.

Therefore, a more specific tool was chosen and established for a more detailed characterization of the relevance of PKR during influenza virus infection. The transfection by electroporation of siRNA targeting cellular PKR expression efficiently reduced PKR transcript levels to about 10% as compared to control values, which classified as a valid knockdown. This PKR knockdown in MDCK cells did seem to have a positive effect on influenza virus replication, as reflected by slightly enhanced expression levels of the influenza genome segment 7 in infected MDCK cells and also by increased HA titers during 16 to 24 hpi, i.e. the early stage of replication. However, despite this seemingly mild enhancement of influenza virus replication, the PKR knockdown did not have an influence on the main indicator for a positive or negative interference with virus replication, which is the final HA titer measured at 48 hpi. Therefore, it was concluded that in MDCK cells, despite its widely accepted antiviral function, PKR does not seem to profoundly affect influenza virus replication.

Since the knockdown of PKR expressed by MDKC cells could be efficiently accomplished, another target of siRNA mediated interference with cellular gene expression was selected, namely IκBα. Although the knockdown of IκBα could also be achieved, no beneficial influence on influenza virus replication could be observed. To the contrary, average influenza virus genome segment 7 expression levels were reduced, and no impact on HA titers could be measured throughout the entire monitored time course of virus replication. Since the knockdown of IκBα did not lead to enhanced virus replication, one could transfect MDCK cells with a plasmid encoding for a constitutively active upstream kinase of IκBα and hence activate NF-κB, which could enhance influenza virus replication as previously shown by Mazur et al. (Mazur et al. 2007).

Another issue that was addressed in this study was the putative composition of influenza virus seed by manifold variants that has been described elsewhere (Roedig et al. 2011b). The assumption here was that

the alterations of final HA titers reached in different influenza virus production processes throughout longer periods of time could be caused by shifting ratios of virus variant composition of virus seed, selecting variants with more favorable replication characteristics. Hence, a plaque assay was conducted and a number of variants with differing replication characteristics, as reflected in final HA titers, were successfully isolated. Subsequently, infection experiments were done with either the plaque isolate reaching highest final HA titers or the isolate replicating most poorly. Then, the impact of both variants on the induction of the signaling pathways IRF-3 and Jak-Stat were analyzed. However, despite the initial assumption that, again, the more poorly replicating variant might induce both pathways to a stronger degree could not be confirmed. This result is, overall, in line with the general observation gained throughout this study that the induction of signaling pathways with a predominantly antiviral function does not seem to be of high relevance for influenza virus replication in MDCK cells.

Overall, the results obtained throughout this study are of high value when considering attempts for cell line optimization in the context of influenza vaccine production. Neither can findings and observations that have been made for one specific cell line easily be transferred to another cell line, nor should the complexity of cellular signaling processes be underestimated. Hence, current attempts for a more systematic approach to the investigation of complex cellular networks are very desirable and have led to the establishment of the novel research field of systems biology. This discipline aims at combining the availability of sophisticated ‘state of the art’ high throughput technologies such as genome-wide RNAi screenings with a more feasible analysis of the resulting large datasets through the application of computational methodology originating in the engineering sciences. Here, regarding the mathematical modeling of biochemical pathways, chemical and physical principles, preceding knowledge of regulatory pathways and experimental data are connected by physicochemical modeling of signal transduction, as reviewed by Aldridge et al. (Aldridge et al. 2006). Systems biology approaches are also used increasingly in characterizing the host response to viral infection (Tan et al. 2007). For instance, MATLAB-based toolboxes such as the CellNetAnalyzer for structural and functional analysis of cellular networks or PROMOT for modular systems biology modeling approaches are very needful inventions for aiding current and future attempts in cell line optimization (Klamt et al. 2007; Mirschel et al. 2009). However, attempting to describe only a single pathway such as Jak-Stat with the help of complex systems biology approaches has been shown to necessitate the application of considerable resources, involving *in silico* as well as knockdown/deletion and perturbation experimental efforts (Soebiyanto et

al. 2007). Due to this enormous complexity, attempts are undertaken to describe signaling pathways by reduced, hierarchically structured models (Conzelmann et al. 2006). The availability of large siRNA libraries allowing the knockdown of all proteins known to be encoded by the human genome can be used to identify host cell proteins required for the replication of several viruses (Hirsch 2010). By the application of this technology, numerous host cell factors could be identified recently that are crucial for influenza virus replication (Karlas et al. 2010). In addition to genome-wide RNAi screens, high-throughput yeast two-hybrid analysis and genome-wide expression analysis have been applied to identify interactions of viral proteins with host proteins and pathways (Shapira et al. 2009). In turn, since these studies are predominantly conducted to discover new therapeutic intervention strategies, the results gained in these high-throughput experiments could also be applied in cell line optimization, as some host cell factors have been identified that can enhance virus replication if being interfered with (Frensing, Karlas, personal communication). In mammalian cell based production of protein therapeutics, genome-scale technologies comprising genomics, transcriptomics and proteomics are being applied more and more frequently to identify factors that contribute to optimal producer cell lines (Griffin et al. 2007). Recently, avian designer cell lines growing in serum-free medium have been created for the application in influenza virus and MVA production, which underlines the significance and desirability of systems biology approaches and synthetic biology also for vaccine production purposes (Lohr et al. 2009).

7 List of figures

List of figures

8 List of tables

9 References

WHO, 2005. Influenza vaccines. Wkly Epidemiol Rec 80(33):279-87.

Aaronson DS, Horvath CM. 2002. A road map for those who don't know JAK-STAT. Science 296(5573):1653-5.

Abe Y, Takashita E, Sugawara K, Matsuzaki Y, Muraki Y, Hongo S. 2004. Effect of the addition of oligosaccharides on the biological activities and antigenicity of influenza A/H3N2 virus hemagglutinin. J Virol 78(18):9605-11.

Advisory Committee on Immunization P, Smith NM, Bresee JS, Shay DK, Uyeki TM, Cox NJ, Strikas RA. 2006. Prevention and Control of Influenza: recommendations of the Advisory Committee on Immunization Practices (ACIP). MMWR Recomm Rep 55(RR-10):1-42.

Aebi M, Fah J, Hurt N, Samuel CE, Thomis D, Bazzigher L, Pavlovic J, Haller O, Staeheli P. 1989. cDNA structures and regulation of two interferon-induced human Mx proteins. Mol Cell Biol 9(11):5062-72.

Aldridge BB, Burke JM, Lauffenburger DA, Sorger PK. 2006. Physicochemical modelling of cell signalling pathways. Nat Cell Biol 8(11):1195-203.

Alegria-Schaffer A, Lodge A, Vattem K. 2009. Performing and optimizing Western blots with an emphasis on chemiluminescent detection. Methods Enzymol 463:573-99.

Alexopoulou L, Holt AC, Medzhitov R, Flavell RA. 2001. Recognition of double-stranded RNA and activation of NF-kappaB by Toll-like receptor 3. Nature 413(6857):732-8.

Aragon T, de la Luna S, Novoa I, Carrasco L, Ortin J, Nieto A. 2000. Eukaryotic translation initiation factor 4GI is a cellular target for NS1 protein, a translational activator of influenza virus. Mol Cell Biol 20(17):6259-68.

Arden N, Betenbaugh MJ. 2004. Life and death in mammalian cell culture: strategies for apoptosis inhibition. Trends Biotechnol 22(4):174-80.

Asano Y, Ishihama A. 1997. Identification of two nucleotide-binding domains on the PB1 subunit of influenza virus RNA polymerase. J Biochem 122(3):627-34.

Ashkenazi A, Dixit VM. 1999. Apoptosis control by death and decoy receptors. Curr Opin Cell Biol 11(2):255-60.

Au WC, Yeow WS, Pitha PM. 2001. Analysis of functional domains of interferon regulatory factor 7 and its association with IRF-3. Virology 280(2):273-82.

Audsley JM, Tannock GA. 2004. The role of cell culture vaccines in the control of the next influenza pandemic. Expert Opin Biol Ther 4(5):709-17.

Audsley JM, Tannock GA. 2008. Cell-based influenza vaccines: progress to date. Drugs 68(11):1483-91.

Balachandran S, Roberts PC, Kipperman T, Bhalla KN, Compans RW, Archer DR, Barber GN. 2000. Alpha/beta interferons potentiate virus-induced apoptosis through activation of the FADD/Caspase-8 death signaling pathway. J Virol 74(3):1513-23.

Barber GN. 2001. Host defense, viruses and apoptosis. Cell Death Differ 8(2):113-26.

Barman S, Adhikary L, Chakrabarti AK, Bernas C, Kawaoka Y, Nayak DP. 2004. Role of transmembrane domain and cytoplasmic tail amino acid sequences of influenza a virus neuraminidase in raft association and virus budding. J Virol 78(10):5258-69.

Barnes B, Lubyova B, Pitha PM. 2002. On the role of IRF in host defense. J Interferon Cytokine Res 22(1):59-71.

Baudin F, Bach C, Cusack S, Ruigrok RW. 1994. Structure of influenza virus RNP. I. Influenza virus nucleoprotein melts secondary structure in panhandle RNA and exposes the bases to the solvent. EMBO J 13(13):3158-65.

Beelman CA, Stevens A, Caponigro G, LaGrandeur TE, Hatfield L, Fortner DM, Parker R. 1996. An essential component of the decapping enzyme required for normal rates of mRNA turnover. Nature 382(6592):642-6.

Berger M, Schmidt MF. 1985. Protein fatty acyltransferase is located in the rough endoplasmic reticulum. FEBS Lett 187(2):289-94.

Bergmann M, Garcia-Sastre A, Carnero E, Pehamberger H, Wolff K, Palese P, Muster T. 2000. Influenza virus NS1 protein counteracts PKR-mediated inhibition of replication. J Virol 74(13):6203-6.

Beutler B. 2004. Innate immunity: an overview. Mol Immunol 40(12):845-59.

Biebricher CK, Eigen M. 2006. What is a quasispecies? Curr Top Microbiol Immunol 299:1-31.

Blaas D, Patzelt E, Kuechler E. 1982. Identification of the cap binding protein of influenza virus. Nucleic Acids Res 10(15):4803-12.

Bock A, Schulze-Horsel J, Schwarzer J, Rapp E, Genzel Y, Reichl U, Reichl U. 2010. High-density microcarrier cell cultures for influenza virus production. Biotechnol Prog.

Bonnet MC, Weil R, Dam E, Hovanessian AG, Meurs EF. 2000. PKR stimulates NF-kappaB irrespective of its kinase function by interacting with the IkappaB kinase complex. Mol Cell Biol 20(13):4532-42.

Boulo S, Akarsu H, Ruigrok RW, Baudin F. 2007. Nuclear traffic of influenza virus proteins and ribonucleoprotein complexes. Virus Res 124(1-2):12-21.

Bouloy M, Plotch SJ, Krug RM. 1980. Both the 7-methyl and the 2'-O-methyl groups in the cap of mRNA strongly influence its ability to act as primer for influenza virus RNA transcription. Proc Natl Acad Sci U S A 77(7):3952-6.

Braakman I, Hoover-Litty H, Wagner KR, Helenius A. 1991. Folding of influenza hemagglutinin in the endoplasmic reticulum. J Cell Biol 114(3):401-11.

Braam J, Ulmanen I, Krug RM. 1983. Molecular model of a eucaryotic transcription complex: functions and movements of influenza P proteins during capped RNA-primed transcription. Cell 34(2):609-18.

Brand SR, Kobayashi R, Mathews MB. 1997. The Tat protein of human immunodeficiency virus type 1 is a substrate and inhibitor of the interferon-induced, virally activated protein kinase, PKR. J Biol Chem 272(13):8388-95.

Brands R, Visser J, Medema J, Palache AM, van Scharrenburg GJ. 1999. Influvac: a safe Madin Darby Canine Kidney (MDCK) cell culture-based influenza vaccine. Dev Biol Stand 98:93-100; discussion 111.

Brenner C, Cadiou H, Vieira HL, Zamzami N, Marzo I, Xie Z, Leber B, Andrews D, Duclohier H, Reed JC and others. 2000. Bcl-2 and Bax regulate the channel activity of the mitochondrial adenine nucleotide translocator. Oncogene 19(3):329-36.

Brierley MM, Fish EN. 2002. Review: IFN-alpha/beta receptor interactions to biologic outcomes: understanding the circuitry. J Interferon Cytokine Res 22(8):835-45.

Bui M, Whittaker G, Helenius A. 1996. Effect of M1 protein and low pH on nuclear transport of influenza virus ribonucleoproteins. J Virol 70(12):8391-401.

Carpousis AJ, Vanzo NF, Raynal LC. 1999. mRNA degradation. A tale of poly(A) and multiprotein machines. Trends Genet 15(1):24-8.

Cattaneo R. 1994. Biased (A-->I) hypermutation of animal RNA virus genomes. Curr Opin Genet Dev 4(6):895-900.

Chaplin DD. 2006. 1. Overview of the human immune response. J Allergy Clin Immunol 117(2 Suppl Mini-Primer):S430-5.

Chen W, Calvo PA, Malide D, Gibbs J, Schubert U, Bacik I, Basta S, O'Neill R, Schickli J, Palese P and others. 2001. A novel influenza A virus mitochondrial protein that induces cell death. Nat Med 7(12):1306-12.

Chen Z, Li Y, Krug RM. 1999. Influenza A virus NS1 protein targets poly(A)-binding protein II of the cellular 3'-end processing machinery. EMBO J 18(8):2273-83.

Cheung TK, Poon LL. 2007. Biology of influenza a virus. Ann N Y Acad Sci 1102:1-25.

Chien CY, Xu Y, Xiao R, Aramini JM, Sahasrabudhe PV, Krug RM, Montelione GT. 2004. Biophysical characterization of the complex between double-stranded RNA and the N-terminal domain of the NS1 protein from influenza A virus: evidence for a novel RNA-binding mode. Biochemistry 43(7):1950-62.

Chu WM, Ostertag D, Li ZW, Chang L, Chen Y, Hu Y, Williams B, Perrault J, Karin M. 1999. JNK2 and IKKbeta are required for activating the innate response to viral infection. Immunity 11(6):721-31.

Claas EC, Osterhaus AD, van Beek R, De Jong JC, Rimmelzwaan GF, Senne DA, Krauss S, Shortridge KF, Webster RG. 1998. Human influenza A H5N1 virus related to a highly pathogenic avian influenza virus. Lancet 351(9101):472-7.

Clemens MJ, Elia A. 1997. The double-stranded RNA-dependent protein kinase PKR: structure and function. J Interferon Cytokine Res 17(9):503-24.

Clemens MJ, Hershey JW, Hovanessian AC, Jacobs BC, Katze MG, Kaufman RJ, Lengyel P, Samuel CE, Sen GC, Williams BR. 1993. PKR: proposed nomenclature for the RNA-dependent protein kinase induced by interferon. J Interferon Res 13(3):241.

Coleman JR. 2007. The PB1-F2 protein of Influenza A virus: increasing pathogenicity by disrupting alveolar macrophages. Virol J 4:9.

Colman PM. 1999. A novel approach to antiviral therapy for influenza. J Antimicrob Chemother 44 Suppl B:17-22.

Connor RJ, Kawaoka Y, Webster RG, Paulson JC. 1994. Receptor specificity in human, avian, and equine H2 and H3 influenza virus isolates. Virology 205(1):17-23.

Content J. 2009. Mechanisms of induction and action of interferons. Verh K Acad Geneeskd Belg 71(1-2):51-71.

Conzelmann H, Saez-Rodriguez J, Sauter T, Kholodenko BN, Gilles ED. 2006. A domain-oriented approach to the reduction of combinatorial complexity in signal transduction networks. BMC Bioinformatics 7:34.

Crompton M. 2000. Mitochondrial intermembrane junctional complexes and their role in cell death. J Physiol 529 Pt 1:11-21.

Daniels RS, Downie JC, Hay AJ, Knossow M, Skehel JJ, Wang ML, Wiley DC. 1985. Fusion mutants of the influenza virus hemagglutinin glycoprotein. Cell 40(2):431-9.

Darnell JE, Jr. 1997. Phosphotyrosine signaling and the single cell:metazoan boundary. Proc Natl Acad Sci U S A 94(22):11767-9.

de la Luna S, Fortes P, Beloso A, Ortin J. 1995. Influenza virus NS1 protein enhances the rate of translation initiation of viral mRNAs. J Virol 69(4):2427-33.

de Veer MJ, Holko M, Frevel M, Walker E, Der S, Paranjape JM, Silverman RH, Williams BR. 2001. Functional classification of interferon-stimulated genes identified using microarrays. J Leukoc Biol 69(6):912-20.

de Vries W, Haasnoot J, van der Velden J, van Montfort T, Zorgdrager F, Paxton W, Cornelissen M, van Kuppeveld F, de Haan P, Berkhout B. 2008. Increased virus replication in mammalian cells by blocking intracellular innate defense responses. Gene Ther 15(7):545-52.

Delgado Andre N, De Lucca FL. 2007. Knockdown of PKR expression by RNAi reduces pulmonary metastatic potential of B16-F10 melanoma cells in mice: possible role of NF-kappaB. Cancer Lett 258(1):118-25.

Der SD, Zhou A, Williams BR, Silverman RH. 1998. Identification of genes differentially regulated by interferon alpha, beta, or gamma using oligonucleotide arrays. Proc Natl Acad Sci U S A 95(26):15623-8.

Desselberger U, Racaniello VR, Zazra JJ, Palese P. 1980. The 3' and 5'-terminal sequences of influenza A, B and C virus RNA segments are highly conserved and show partial inverted complementarity. Gene 8(3):315-28.

Dhand R, Hiles I, Panayotou G, Roche S, Fry MJ, Gout I, Totty NF, Truong O, Vicendo P, Yonezawa K and others. 1994. PI 3-kinase is a dual specificity enzyme: autoregulation by an intrinsic protein-serine kinase activity. EMBO J 13(3):522-33.

Diaz-Guerra M, Rivas C, Esteban M. 1999. Full activation of RNaseL in animal cells requires binding of 2-5A within ankyrin repeats 6 to 9 of this interferon-inducible enzyme. J Interferon Cytokine Res 19(2):113-9.

Domingo E, Baranowski E, Ruiz-Jarabo CM, Martin-Hernandez AM, Saiz JC, Escarmis C. 1998. Quasispecies structure and persistence of RNA viruses. Emerg Infect Dis 4(4):521-7.

Domingo E, Sabo D, Taniguchi T, Weissmann C. 1978. Nucleotide sequence heterogeneity of an RNA phage population. Cell 13(4):735-44.

Dong C, Davis RJ, Flavell RA. 2002. MAP kinases in the immune response. Annu Rev Immunol 20:55-72.

Doroshenko A, Halperin SA. 2009. Trivalent MDCK cell culture-derived influenza vaccine Optaflu (Novartis Vaccines). Expert Rev Vaccines 8(6):679-88.

Downward J. 2004. PI 3-kinase, Akt and cell survival. Semin Cell Dev Biol 15(2):177-82.

Du C, Fang M, Li Y, Li L, Wang X. 2000. Smac, a mitochondrial protein that promotes cytochrome c-dependent caspase activation by eliminating IAP inhibition. Cell 102(1):33-42.

Eckner R, Ellmeier W, Birnstiel ML. 1991. Mature mRNA 3' end formation stimulates RNA export from the nucleus. EMBO J 10(11):3513-22.

Egorov A, Brandt S, Sereinig S, Romanova J, Ferko B, Katinger D, Grassauer A, Alexandrova G, Katinger H, Muster T. 1998. Transfectant influenza A viruses with long deletions in the NS1 protein grow efficiently in Vero cells. J Virol 72(8):6437-41.

Ehrhardt C, Ludwig S. 2009. A new player in a deadly game: influenza viruses and the PI3K/Akt signalling pathway. Cell Microbiol 11(6):863-71.

Ehrhardt C, Marjuki H, Wolff T, Nurnberg B, Planz O, Pleschka S, Ludwig S. 2006. Bivalent role of the phosphatidylinositol-3-kinase (PI3K) during influenza virus infection and host cell defence. Cell Microbiol 8(8):1336-48.

Ehrhardt C, Wolff T, Pleschka S, Planz O, Beermann W, Bode JG, Schmolke M, Ludwig S. 2007. Influenza A virus NS1 protein activates the PI3K/Akt pathway to mediate antiapoptotic signaling responses. J Virol 81(7):3058-67.

Eickmann M. 2005. Image: Flu_und_legende_color_c.jpg. Wikimedia Commons in Wikipedia, http://upload.wikimedia.org/wikipedia/commons/0/02/Flu_und_legende_color_c.jpg (accessed 19 October 2012).

Elleman CJ, Barclay WS. 2004. The M1 matrix protein controls the filamentous phenotype of influenza A virus. Virology 321(1):144-53.

Enami K, Sato TA, Nakada S, Enami M. 1994. Influenza virus NS1 protein stimulates translation of the M1 protein. J Virol 68(3):1432-7.

Feigenblum D, Schneider RJ. 1993. Modification of eukaryotic initiation factor 4F during infection by influenza virus. J Virol 67(6):3027-35.

Fernandez-Sesma A, Marukian S, Ebersole BJ, Kaminski D, Park MS, Yuen T, Sealfon SC, Garcia-Sastre A, Moran TM. 2006. Influenza virus evades innate and adaptive immunity via the NS1 protein. J Virol 80(13):6295-304.

Fiore AE, Uyeki TM, Broder K, Finelli L, Euler GL, Singleton JA, Iskander JK, Wortley PM, Shay DK, Bresee JS and others. 2010. Prevention and control of influenza with vaccines: recommendations of the Advisory Committee on Immunization Practices (ACIP), 2010. MMWR Recomm Rep 59(RR-8):1-62.

Fitzgerald KA, McWhirter SM, Faia KL, Rowe DC, Latz E, Golenbock DT, Coyle AJ, Liao SM, Maniatis T. 2003. IKKepsilon and TBK1 are essential components of the IRF3 signaling pathway. Nat Immunol 4(5):491-6.

Flory E, Kunz M, Scheller C, Jassoy C, Stauber R, Rapp UR, Ludwig S. 2000. Influenza virus-induced NF-kappaB-dependent gene expression is mediated by overexpression of viral proteins and involves oxidative radicals and activation of IkappaB kinase. J Biol Chem 275(12):8307-14.

Fodor E, Pritlove DC, Brownlee GG. 1994. The influenza virus panhandle is involved in the initiation of transcription. J Virol 68(6):4092-6.

Fodor E, Seong BL, Brownlee GG. 1993. Photochemical cross-linking of influenza A polymerase to its virion RNA promoter defines a polymerase binding site at residues 9 to 12 of the promoter. J Gen Virol 74 (Pt 7):1327-33.

Fortes P, Beloso A, Ortin J. 1994. Influenza virus NS1 protein inhibits pre-mRNA splicing and blocks mRNA nucleocytoplasmic transport. EMBO J 13(3):704-12.

Fouchier RA, Munster V, Wallensten A, Bestebroer TM, Herfst S, Smith D, Rimmelzwaan GF, Olsen B, Osterhaus AD. 2005. Characterization of a novel influenza A virus hemagglutinin subtype (H16) obtained from black-headed gulls. J Virol 79(5):2814-22.

Fouchier RA, Schneeberger PM, Rozendaal FW, Broekman JM, Kemink SA, Munster V, Kuiken T, Rimmelzwaan GF, Schutten M, Van Doornum GJ and others. 2004. Avian influenza A virus (H7N7) associated with human conjunctivitis and a fatal case of acute respiratory distress syndrome. Proc Natl Acad Sci U S A 101(5):1356-61.

Frensing T, Seitz C, Heynisch B, Patzina C, Kochs G, Reichl U. 2011. Efficient influenza B virus propagation due to deficient interferon-induced antiviral activity in MDCK cells. Vaccine 29(41):7125-9.

Gack MU, Albrecht RA, Urano T, Inn KS, Huang IC, Carnero E, Farzan M, Inoue S, Jung JU, Garcia-Sastre A. 2009. Influenza A virus NS1 targets the ubiquitin ligase TRIM25 to evade recognition by the host viral RNA sensor RIG-I. Cell Host Microbe 5(5):439-49.

Gale M, Jr., Katze MG. 1998. Molecular mechanisms of interferon resistance mediated by viral-directed inhibition of PKR, the interferon-induced protein kinase. Pharmacol Ther 78(1):29-46.

Gale M, Jr., Tan SL, Wambach M, Katze MG. 1996. Interaction of the interferon-induced PKR protein kinase with inhibitory proteins P58IPK and vaccinia virus K3L is mediated by unique domains: implications for kinase regulation. Mol Cell Biol 16(8):4172-81.

Galluzzi L, Brenner C, Morselli E, Touat Z, Kroemer G. 2008. Viral control of mitochondrial apoptosis. PLoS Pathog 4(5):e1000018.

Garcia-Sastre A, Biron CA. 2006. Type 1 interferons and the virus-host relationship: a lesson in detente. Science 312(5775):879-82.

Garcia-Sastre A, Egorov A, Matassov D, Brandt S, Levy DE, Durbin JE, Palese P, Muster T. 1998. Influenza A virus lacking the NS1 gene replicates in interferon-deficient systems. Virology 252(2):324-30.

Garcia MA, Gil J, Ventoso I, Guerra S, Domingo E, Rivas C, Esteban M. 2006. Impact of protein kinase PKR in cell biology: from antiviral to antiproliferative action. Microbiol Mol Biol Rev 70(4):1032-60.

Gaush CR, Hard WL, Smith TF. 1966. Characterization of an established line of canine kidney cells (MDCK). Proc Soc Exp Biol Med 122(3):931-5.

Gaush CR, Smith TF. 1968. Replication and plaque assay of influenza virus in an established line of canine kidney cells. Appl Microbiol 16(4):588-94.

Genin P, Algarte M, Roof P, Lin R, Hiscott J. 2000. Regulation of RANTES chemokine gene expression requires cooperativity between NF-kappa B and IFN-regulatory factor transcription factors. J Immunol 164(10):5352-61.

Genzel Y, Behrendt I, Konig S, Sann H, Reichl U. 2004. Metabolism of MDCK cells during cell growth and influenza virus production in large-scale microcarrier culture. Vaccine 22(17-18):2202-8.

Genzel Y, Fischer M, Reichl U. 2006. Serum-free influenza virus production avoiding washing steps and medium exchange in large-scale microcarrier culture. Vaccine 24(16):3261-72.

Genzel Y, Reichl U. 2009. Continuous cell lines as a production system for influenza vaccines. Expert Rev Vaccines 8(12):1681-92.

George M, Farooq M, Dang T, Cortes B, Liu J, Maranga L. 2010. Production of cell culture (MDCK) derived live attenuated influenza vaccine (LAIV) in a fully disposable platform process. Biotechnol Bioeng 106(6):906-17.

Ghendon YZ, Markushin SG, Akopova, II, Koptiaeva IB, Nechaeva EA, Mazurkova LA, Radaeva IF, Kolokoltseva TD. 2005. Development of cell culture (MDCK) live cold-adapted (CA) attenuated influenza vaccine. Vaccine 23(38):4678-84.

Gilbert C, Rollet-Labelle E, Caon AC, Naccache PH. 2002. Immunoblotting and sequential lysis protocols for the analysis of tyrosine phosphorylation-dependent signaling. J Immunol Methods 271(1-2):185-201.

Goh KC, deVeer MJ, Williams BR. 2000. The protein kinase PKR is required for p38 MAPK activation and the innate immune response to bacterial endotoxin. EMBO J 19(16):4292-7.

Govorkova EA, Kaverin NV, Gubareva LV, Meignier B, Webster RG. 1995. Replication of influenza A viruses in a green monkey kidney continuous cell line (Vero). J Infect Dis 172(1):250-3.

Govorkova EA, Murti G, Meignier B, de Taisne C, Webster RG. 1996. African green monkey kidney (Vero) cells provide an alternative host cell system for influenza A and B viruses. J Virol 70(8):5519-24.

Greenspan D, Palese P, Krystal M. 1988. Two nuclear location signals in the influenza virus NS1 nonstructural protein. J Virol 62(8):3020-6.

Griffin TJ, Seth G, Xie H, Bandhakavi S, Hu WS. 2007. Advancing mammalian cell culture engineering using genome-scale technologies. Trends Biotechnol 25(9):401-8.

Griffiths JB. 1987. Serum and growth factors in cell culture media--an introductory review. Dev Biol Stand 66:155-60.

Grimm D, Staeheli P, Hufbauer M, Koerner I, Martinez-Sobrido L, Solorzano A, Garcia-Sastre A, Haller O, Kochs G. 2007. Replication fitness determines high virulence of influenza A virus in mice carrying functional Mx1 resistance gene. Proc Natl Acad Sci U S A 104(16):6806-11.

Guan Y, Peiris JS, Poon LL, Dyrting KC, Ellis TM, Sims L, Webster RG, Shortridge KF. 2003. Reassortants of H5N1 influenza viruses recently isolated from aquatic poultry in Hong Kong SAR. Avian Dis 47(3 Suppl):911-3.

Guan Y, Shortridge KF, Krauss S, Webster RG. 1999. Molecular characterization of H9N2 influenza viruses: were they the donors of the "internal" genes of H5N1 viruses in Hong Kong? Proc Natl Acad Sci U S A 96(16):9363-7.

Guillot L, Le Goffic R, Bloch S, Escriou N, Akira S, Chignard M, Si-Tahar M. 2005. Involvement of toll-like receptor 3 in the immune response of lung epithelial cells to double-stranded RNA and influenza A virus. J Biol Chem 280(7):5571-80.

Guo Z, Chen LM, Zeng H, Gomez JA, Plowden J, Fujita T, Katz JM, Donis RO, Sambhara S. 2007. NS1 protein of influenza A virus inhibits the function of intracytoplasmic pathogen sensor, RIG-I. Am J Respir Cell Mol Biol 36(3):263-9.

Hale BG, Jackson D, Chen YH, Lamb RA, Randall RE. 2006. Influenza A virus NS1 protein binds p85beta and activates phosphatidylinositol-3-kinase signaling. Proc Natl Acad Sci U S A 103(38):14194-9.

Hale BG, Randall RE, Ortin J, Jackson D. 2008. The multifunctional NS1 protein of influenza A viruses. J Gen Virol 89(Pt 10):2359-76.

Haller O, Kochs G, Weber F. 2006. The interferon response circuit: induction and suppression by pathogenic viruses. Virology 344(1):119-30.

Halperin SA, Nestruck AC, Eastwood BJ. 1998. Safety and immunogenicity of a new influenza vaccine grown in mammalian cell culture. Vaccine 16(13):1331-5.

Hamm J, Mattaj IW. 1990. Monomethylated cap structures facilitate RNA export from the nucleus. Cell 63(1):109-18.

Hampson AW, Mackenzie JS. 2006. The influenza viruses. Med J Aust 185(10 Suppl):S39-43.

Harding HP, Novoa I, Zhang Y, Zeng H, Wek R, Schapira M, Ron D. 2000. Regulated translation initiation controls stress-induced gene expression in mammalian cells. Mol Cell 6(5):1099-108.

Hatada E, Fukuda R. 1992. Binding of influenza A virus NS1 protein to dsRNA in vitro. J Gen Virol 73 (Pt 12):3325-9.

Hatada E, Saito S, Fukuda R. 1999. Mutant influenza viruses with a defective NS1 protein cannot block the activation of PKR in infected cells. J Virol 73(3):2425-33.

Hatada E, Takizawa T, Fukuda R. 1992. Specific binding of influenza A virus NS1 protein to the virus minus-sense RNA in vitro. J Gen Virol 73 (Pt 1):17-25.

Hausmann J, Kretzschmar E, Garten W, Klenk HD. 1997. Biosynthesis, intracellular transport and enzymatic activity of an avian influenza A virus neuraminidase: role of unpaired cysteines and individual oligosaccharides. J Gen Virol 78 (Pt 12):3233-45.

Hay AJ, Lomniczi B, Bellamy AR, Skehel JJ. 1977. Transcription of the influenza virus genome. Virology 83(2):337-55.

Hay AJ, Skehel JJ, McCauley J. 1982. Characterization of influenza virus RNA complete transcripts. Virology 116(2):517-22.

Hayman A, Comely S, Lackenby A, Murphy S, McCauley J, Goodbourn S, Barclay W. 2006. Variation in the ability of human influenza A viruses to induce and inhibit the IFN-beta pathway. Virology 347(1):52-64.

Hechtfischer A, Marschall M, Helten A, Boswald C, Meier-Ewert H. 1997. A highly cytopathogenic influenza C virus variant induces apoptosis in cell culture. J Gen Virol 78 (Pt 6):1327-30.

Heil F, Hemmi H, Hochrein H, Ampenberger F, Kirschning C, Akira S, Lipford G, Wagner H, Bauer S. 2004. Species-specific recognition of single-stranded RNA via toll-like receptor 7 and 8. Science 303(5663):1526-9.

Herfst S, Schrauwen EJ, Linster M, Chutinimitkul S, de Wit E, Munster VJ, Sorrell EM, Bestebroer TM, Burke DF, Smith DJ and others. 2012. Airborne transmission of influenza A/H5N1 virus between ferrets. Science 336(6088):1534-41.

Hershey JW. 1991. Translational control in mammalian cells. Annu Rev Biochem 60:717-55.

Herz C, Stavnezer E, Krug R, Gurney T, Jr. 1981. Influenza virus, an RNA virus, synthesizes its messenger RNA in the nucleus of infected cells. Cell 26(3 Pt 1):391-400.

Heylbroeck C, Balachandran S, Servant MJ, DeLuca C, Barber GN, Lin R, Hiscott J. 2000. The IRF-3 transcription factor mediates Sendai virus-induced apoptosis. J Virol 74(8):3781-92.

Heynisch B, Frensing T, Heinze K, Seitz C, Genzel Y, Reichl U. 2010. Differential activation of host cell signalling pathways through infection with two variants of influenza A/Puerto Rico/8/34 (H1N1) in MDCK cells. Vaccine 28(51):8210-8.

Hinnebusch AG. 1994. The eIF-2 alpha kinases: regulators of protein synthesis in starvation and stress. Semin Cell Biol 5(6):417-26.

Hinshaw VS, Olsen CW, Dybdahl-Sissoko N, Evans D. 1994. Apoptosis: a mechanism of cell killing by influenza A and B viruses. J Virol 68(6):3667-73.

Hirsch AJ. 2010. The use of RNAi-based screens to identify host proteins involved in viral replication. Future Microbiol 5(2):303-11.

Hiscott J. 2007. Triggering the innate antiviral response through IRF-3 activation. J Biol Chem 282(21):15325-9.

Hiscott J, Kwon H, Genin P. 2001. Hostile takeovers: viral appropriation of the NF-kappaB pathway. J Clin Invest 107(2):143-51.

Hiscott J, Pitha P, Genin P, Nguyen H, Heylbroeck C, Mamane Y, Algarte M, Lin R. 1999. Triggering the interferon response: the role of IRF-3 transcription factor. J Interferon Cytokine Res 19(1):1-13.

Holsinger LJ, Lamb RA. 1991. Influenza virus M2 integral membrane protein is a homotetramer stabilized by formation of disulfide bonds. Virology 183(1):32-43.

Honda K, Taniguchi T. 2006. Toll-like receptor signaling and IRF transcription factors. IUBMB Life 58(5-6):290-5.

Hornickova Z. 1997. Different progress of MDCK cell death after infection by two different influenza virus isolates. Cell Biochem Funct 15(2):87-93.

Hsu MT, Parvin JD, Gupta S, Krystal M, Palese P. 1987. Genomic RNAs of influenza viruses are held in a circular conformation in virions and in infected cells by a terminal panhandle. Proc Natl Acad Sci U S A 84(22):8140-4.

Hu Y, Conway TW. 1993. 2-Aminopurine inhibits the double-stranded RNA-dependent protein kinase both in vitro and in vivo. J Interferon Res 13(5):323-8.

Ichijo H, Nishida E, Irie K, ten Dijke P, Saitoh M, Moriguchi T, Takagi M, Matsumoto K, Miyazono K, Gotoh Y. 1997. Induction of apoptosis by ASK1, a mammalian MAPKKK that activates SAPK/JNK and p38 signaling pathways. Science 275(5296):90-4.

Isaacs A, Burke DC. 1959. Viral interference and interferon. Br Med Bull 15:185-8.

Isken B, Genzel Y, Reichl U. 2012. Productivity, apoptosis, and infection dynamics of influenza A/PR/8 strains and A/PR/8-based reassortants. Vaccine 30(35):5253-61.

Jackson D, Killip MJ, Galloway CS, Russell RJ, Randall RE. 2009. Loss of function of the influenza A virus NS1 protein promotes apoptosis but this is not due to a failure to activate phosphatidylinositol 3-kinase (PI3K). Virology.

Jackson DA, Caton AJ, McCready SJ, Cook PR. 1982. Influenza virus RNA is synthesized at fixed sites in the nucleus. Nature 296(5855):366-8.

Janeway CA, Jr. 1989. Approaching the asymptote? Evolution and revolution in immunology. Cold Spring Harb Symp Quant Biol 54 Pt 1:1-13.

Janke R, Genzel Y, Wahl A, Reichl U. 2010. Measurement of key metabolic enzyme activities in mammalian cells using rapid and sensitive microplate-based assays. Biotechnol Bioeng 107(3):566-81.

Jennings PA, Finch JT, Winter G, Robertson JS. 1983. Does the higher order structure of the influenza virus ribonucleoprotein guide sequence rearrangements in influenza viral RNA? Cell 34(2):619-27.

Ji WT, Liu HJ. 2008. PI3K-Akt signaling and viral infection. Recent Pat Biotechnol 2(3):218-26.

Jones IM, Reay PA, Philpott KL. 1986. Nuclear location of all three influenza polymerase proteins and a nuclear signal in polymerase PB2. EMBO J 5(9):2371-6.

Julkunen I, Sareneva T, Pirhonen J, Ronni T, Melen K, Matikainen S. 2001. Molecular pathogenesis of influenza A virus infection and virus-induced regulation of cytokine gene expression. Cytokine Growth Factor Rev 12(2-3):171-80.

Jung D, Cote S, Drouin M, Simard C, Lemieux R. 2002. Inducible expression of Bcl-XL restricts apoptosis resistance to the antibody secretion phase in hybridoma cultures. Biotechnol Bioeng 79(2):180-7.

Kalbfuss B, Knochlein A, Krober T, Reichl U. 2008. Monitoring influenza virus content in vaccine production: precise assays for the quantitation of hemagglutination and neuraminidase activity. Biologicals 36(3):145-61.

Kalbfuss B, Wolff M, Morenweiser R, Reichl U. 2007. Purification of cell culture-derived human influenza A virus by size-exclusion and anion-exchange chromatography. Biotechnol Bioeng 96(5):932-44.

Karin M, Liu Z, Zandi E. 1997. AP-1 function and regulation. Curr Opin Cell Biol 9(2):240-6.

Karlas A, Machuy N, Shin Y, Pleissner KP, Artarini A, Heuer D, Becker D, Khalil H, Ogilvie LA, Hess S and others. 2010. Genome-wide RNAi screen identifies human host factors crucial for influenza virus replication. Nature 463(7282):818-22.

Kates M, Allison AC, Tyrell DA, James AT. 1962. Origin of lipids in influenza virus. Cold Spring Harb Symp Quant Biol 27:293-301.

Kato H, Sato S, Yoneyama M, Yamamoto M, Uematsu S, Matsui K, Tsujimura T, Takeda K, Fujita T, Takeuchi O and others. 2005. Cell type-specific involvement of RIG-I in antiviral response. Immunity 23(1):19-28.

Kato H, Takeuchi O, Akira S. 2006a. [Cell type specific involvement of RIG-I in antiviral responses]. Nippon Rinsho 64(7):1244-7.

Kato H, Takeuchi O, Sato S, Yoneyama M, Yamamoto M, Matsui K, Uematsu S, Jung A, Kawai T, Ishii KJ and others. 2006b. Differential roles of MDA5 and RIG-I helicases in the recognition of RNA viruses. Nature 441(7089):101-5.

Katze MG. 1995. Regulation of the interferon-induced PKR: can viruses cope? Trends Microbiol 3(2):75-8.

Katze MG, He Y, Gale M, Jr. 2002. Viruses and interferon: a fight for supremacy. Nat Rev Immunol 2(9):675-87.

Katze MG, Krug RM. 1990. Translational control in influenza virus-infected cells. Enzyme 44(1-4):265-77.

Katze MG, Tomita J, Black T, Krug RM, Safer B, Hovanessian A. 1988. Influenza virus regulates protein synthesis during infection by repressing autophosphorylation and activity of the cellular 68,000-Mr protein kinase. J Virol 62(10):3710-7.

Kawai T, Takahashi K, Sato S, Coban C, Kumar H, Kato H, Ishii KJ, Takeuchi O, Akira S. 2005. IPS-1, an adaptor triggering RIG-I- and Mda5-mediated type I interferon induction. Nat Immunol 6(10):981-8.

Keay L. 1978. The cultivation of animal cells and production of viruses in serum-free system. Methods Cell Biol 20:169-209.

Kekarainen T, Martinez-Guino L, Segales J. 2009. Swine torque teno virus detection in pig commercial vaccines, enzymes for laboratory use and human drugs containing components of porcine origin. J Gen Virol 90(Pt 3):648-53.

Kerr JF, Wyllie AH, Currie AR. 1972. Apoptosis: a basic biological phenomenon with wide-ranging implications in tissue kinetics. Br J Cancer 26(4):239-57.

Kibler KV, Shors T, Perkins KB, Zeman CC, Banaszak MP, Biesterfeldt J, Langland JO, Jacobs BL. 1997. Double-stranded RNA is a trigger for apoptosis in vaccinia virus-infected cells. J Virol 71(3):1992-2003.

Kilbourne ED. 1969. Future influenza vaccines and the use of genetic recombinants. Bull World Health Organ 41(3):643-5.

Kilbourne ED, Schulman JL, Schild GC, Schloer G, Swanson J, Bucher D. 1971. Related studies of a recombinant influenza-virus vaccine. I. Derivation and characterization of virus and vaccine. J Infect Dis 124(5):449-62.

Kim KB, Choi YH, Kim IK, Chung CW, Kim BJ, Park YM, Jung YK. 2002. Potentiation of Fas- and TRAIL-mediated apoptosis by IFN-gamma in A549 lung epithelial cells: enhancement of caspase-8 expression through IFN-response element. Cytokine 20(6):283-8.

Kistner O, Barrett PN, Mundt W, Reiter M, Schober-Bendixen S, Dorner F. 1998. Development of a mammalian cell (Vero) derived candidate influenza virus vaccine. Vaccine 16(9-10):960-8.

Klamt S, Saez-Rodriguez J, Gilles ED. 2007. Structural and functional analysis of cellular networks with CellNetAnalyzer. BMC Syst Biol 1:2.

Klenk HD, Rott R, Orlich M, Blodorn J. 1975. Activation of influenza A viruses by trypsin treatment. Virology 68(2):426-39.

Kochs G, Garcia-Sastre A, Martinez-Sobrido L. 2007. Multiple anti-interferon actions of the influenza A virus NS1 protein. J Virol 81(13):7011-21.

Krebs DL, Hilton DJ. 2001. SOCS proteins: negative regulators of cytokine signaling. Stem Cells 19(5):378-87.

Krug RM, Broni BA, Bouloy M. 1979. Are the 5' ends of influenza viral mRNAs synthesized in vivo donated by host mRNAs? Cell 18(2):329-34.

Kujime K, Hashimoto S, Gon Y, Shimizu K, Horie T. 2000. p38 mitogen-activated protein kinase and c-jun-NH2-terminal kinase regulate RANTES production by influenza virus-infected human bronchial epithelial cells. J Immunol 164(6):3222-8.

Kumar A, Haque J, Lacoste J, Hiscott J, Williams BR. 1994. Double-stranded RNA-dependent protein kinase activates transcription factor NF-kappa B by phosphorylating I kappa B. Proc Natl Acad Sci U S A 91(14):6288-92.

Kumar KP, McBride KM, Weaver BK, Dingwall C, Reich NC. 2000. Regulated nuclear-cytoplasmic localization of interferon regulatory factor 3, a subunit of double-stranded RNA-activated factor 1. Mol Cell Biol 20(11):4159-68.

Laemmli UK. 1970. Cleavage of structural proteins during the assembly of the head of bacteriophage T4. Nature 227(5259):680-5.

Lam WY, Tang JW, Yeung AC, Chiu LC, Sung JJ, Chan PK. 2008. Avian influenza virus A/HK/483/97(H5N1) NS1 protein induces apoptosis in human airway epithelial cells. J Virol 82(6):2741-51.

Lamb RA, Choppin PW. 1983. The gene structure and replication of influenza virus. Annu Rev Biochem 52:467-506.

Lamb RA, Krug RM. 2001. Orthomyxoviridae: The viruses and their replication. Howley DMKaPM, editor. Fields Virology, Lippincott Williams and Wilkins, Philadelphia: pp. 1487-1532.

Lan YQ, Zhang C, Xiao JH, Zhuo YH, Guo H, Peng W, Ge J. 2009. Suppression of IkappaBalpha increases the expression of matrix metalloproteinase-2 in human ciliary muscle cells. Mol Vis 15:1977-87.

Laver WG, Colman PM, Webster RG, Hinshaw VS, Air GM. 1984. Influenza virus neuraminidase with hemagglutinin activity. Virology 137(2):314-23.

Lee DC, Cheung CY, Law AH, Mok CK, Peiris M, Lau AS. 2005. p38 mitogen-activated protein kinase-dependent hyperinduction of tumor necrosis factor alpha expression in response to avian influenza virus H5N1. J Virol 79(16):10147-54.

Lee SB, Esteban M. 1994. The interferon-induced double-stranded RNA-activated protein kinase induces apoptosis. Virology 199(2):491-6.

Lee TG, Tomita J, Hovanessian AG, Katze MG. 1990. Purification and partial characterization of a cellular inhibitor of the interferon-induced protein kinase of Mr 68,000 from influenza virus-infected cells. Proc Natl Acad Sci U S A 87(16):6208-12.

Leib DA, Machalek MA, Williams BR, Silverman RH, Virgin HW. 2000. Specific phenotypic restoration of an attenuated virus by knockout of a host resistance gene. Proc Natl Acad Sci U S A 97(11):6097-101.

Lengyel P. 1987. Double-stranded RNA and interferon action. J Interferon Res 7(5):511-9.

Leonard WJ. 2001. Role of Jak kinases and STATs in cytokine signal transduction. Int J Hematol 73(3):271-7.

Leroux A, London IM. 1982. Regulation of protein synthesis by phosphorylation of eukaryotic initiation factor 2 alpha in intact reticulocytes and reticulocyte lysates. Proc Natl Acad Sci U S A 79(7):2147-51.

Levy DE, Garcia-Sastre A. 2001. The virus battles: IFN induction of the antiviral state and mechanisms of viral evasion. Cytokine Growth Factor Rev 12(2-3):143-56.

Li P, Nijhawan D, Budihardjo I, Srinivasula SM, Ahmad M, Alnemri ES, Wang X. 1997. Cytochrome c and dATP-dependent formation of Apaf-1/caspase-9 complex initiates an apoptotic protease cascade. Cell 91(4):479-89.

Li S, Min JY, Krug RM, Sen GC. 2006. Binding of the influenza A virus NS1 protein to PKR mediates the inhibition of its activation by either PACT or double-stranded RNA. Virology 349(1):13-21.

Lin C, Holland RE, Jr., Donofrio JC, McCoy MH, Tudor LR, Chambers TM. 2002. Caspase activation in equine influenza virus induced apoptotic cell death. Vet Microbiol 84(4):357-65.

Lin R, Hiscott J. 1999. A role for casein kinase II phosphorylation in the regulation of IRF-1 transcriptional activity. Mol Cell Biochem 191(1-2):169-80.

Lin R, Mamane Y, Hiscott J. 2000. Multiple regulatory domains control IRF-7 activity in response to virus infection. J Biol Chem 275(44):34320-7.

Lipsitch M, Plotkin JB, Simonsen L, Bloom B. 2012. Evolution, safety, and highly pathogenic influenza viruses. Science 336(6088):1529-31.

Liu SY, Sanchez DJ, Aliyari R, Lu S, Cheng G. 2012. Systematic identification of type I and type II interferon-induced antiviral factors. Proc Natl Acad Sci U S A 109(11):4239-44.

Lohr V, Rath A, Genzel Y, Jordan I, Sandig V, Reichl U. 2009. New avian suspension cell lines provide production of influenza virus and MVA in serum-free media: studies on growth, metabolism and virus propagation. Vaccine 27(36):4975-82.

Lu Y, Qian XY, Krug RM. 1994. The influenza virus NS1 protein: a novel inhibitor of pre-mRNA splicing. Genes Dev 8(15):1817-28.

Lu Y, Wambach M, Katze MG, Krug RM. 1995. Binding of the influenza virus NS1 protein to double-stranded RNA inhibits the activation of the protein kinase that phosphorylates the elF-2 translation initiation factor. Virology 214(1):222-8.

Ludwig S. 2007. Exploited defense: how influenza viruses take advantage of antiviral signaling responses. Future Virology 2(1):91-100.

Ludwig S, Ehrhardt C, Neumeier ER, Kracht M, Rapp UR, Pleschka S. 2001. Influenza virus-induced AP-1-dependent gene expression requires activation of the JNK signaling pathway. J Biol Chem 276(24):10990-8.

Ludwig S, Planz O. 2008. Influenza viruses and the NF-kappaB signaling pathway - towards a novel concept of antiviral therapy. Biol Chem 389(10):1307-12.

Ludwig S, Planz O, Pleschka S, Wolff T. 2003. Influenza-virus-induced signaling cascades: targets for antiviral therapy? Trends Mol Med 9(2):46-52.

Ludwig S, Pleschka S, Planz O, Wolff T. 2006. Ringing the alarm bells: signalling and apoptosis in influenza virus infected cells. Cell Microbiol 8(3):375-86.

Ludwig S, Pleschka S, Wolff T. 1999. A fatal relationship--influenza virus interactions with the host cell. Viral Immunol 12(3):175-96.

Ludwig S, Wang X, Ehrhardt C, Zheng H, Donelan N, Planz O, Pleschka S, Garcia-Sastre A, Heins G, Wolff T. 2002. The influenza A virus NS1 protein inhibits activation of Jun N-terminal kinase and AP-1 transcription factors. J Virol 76(21):11166-71.

Ludwig S, Wolff T, Ehrhardt C, Wurzer WJ, Reinhardt J, Planz O, Pleschka S. 2004. MEK inhibition impairs influenza B virus propagation without emergence of resistant variants. FEBS Lett 561(1-3):37-43.

Mabrouk T, Ellis RW. 2002. Influenza vaccine technologies and the use of the cell-culture process (cell-culture influenza vaccine). Dev Biol (Basel) 110:125-34.

Magor BG, Magor KE. 2001. Evolution of effectors and receptors of innate immunity. Dev Comp Immunol 25(8-9):651-82.

Mahy BW, Kangro HO. 1996a. Virology Methods Manual. Academic Press, London.

Mahy BWJ, Kangro HO. 1996b. Virology Methods Manual: Academic Press Limited. 36-37 p.

Mammen M, Dahmann G, Whitesides GM. 1995. Effective inhibitors of hemagglutination by influenza virus synthesized from polymers having active ester groups. Insight into mechanism of inhibition. J Med Chem 38(21):4179-90.

Maniatis T, Falvo JV, Kim TH, Kim TK, Lin CH, Parekh BS, Wathelet MG. 1998. Structure and function of the interferon-beta enhanceosome. Cold Spring Harb Symp Quant Biol 63:609-20.

Marie I, Durbin JE, Levy DE. 1998. Differential viral induction of distinct interferon-alpha genes by positive feedback through interferon regulatory factor-7. EMBO J 17(22):6660-9.

Marjuki H, Alam MI, Ehrhardt C, Wagner R, Planz O, Klenk HD, Ludwig S, Pleschka S. 2006. Membrane accumulation of influenza A virus hemagglutinin triggers nuclear export of the viral genome via protein kinase Calpha-mediated activation of ERK signaling. J Biol Chem 281(24):16707-15.

Martin K, Helenius A. 1991. Nuclear transport of influenza virus ribonucleoproteins: the viral matrix protein (M1) promotes export and inhibits import. Cell 67(1):117-30.

Mather KA, White JF, Hudson PJ, McKimm-Breschkin JL. 1992. Expression of influenza neuraminidase in baculovirus-infected cells. Virus Res 26(2):127-39.

Matlin KS, Reggio H, Helenius A, Simons K. 1981. Infectious entry pathway of influenza virus in a canine kidney cell line. J Cell Biol 91(3 Pt 1):601-13.

Mazur I, Wurzer WJ, Ehrhardt C, Pleschka S, Puthavathana P, Silberzahn T, Wolff T, Planz O, Ludwig S. 2007. Acetylsalicylic acid (ASA) blocks influenza virus propagation via its NF-kappaB-inhibiting activity. Cell Microbiol 9(7):1683-94.

Meguro H, Bryant JD, Torrence AE, Wright PF. 1979. Canine kidney cell line for isolation of respiratory viruses. J Clin Microbiol 9(2):175-9.

Mercille S, Jolicoeur P, Gervais C, Paquette D, Mosser DD, Massie B. 1999. Dose-dependent reduction of apoptosis in nutrient-limited cultures of NS/0 myeloma cells transfected with the E1B-19K adenoviral gene. Biotechnol Bioeng 63(5):516-28.

Mersich SE, Baumeister EG, Riva D, Lewis AP, Cadario ME, Pontoriero AV, Savy VL. 2004. Influenza circulating strains in Argentina exhibit differential induction of cytotoxicity and caspase-3 in vitro. J Clin Virol 31(2):134-9.

Merten OW. 2000. Safety for vaccine(e)s. Cytotechnology 34(3):181-3.

Merten OW. 2002. Development of serum-free media for cell growth and production of viruses/viral vaccines--safety issues of animal products used in serum-free media. Dev Biol (Basel) 111:233-57.

Meurs EF, Galabru J, Barber GN, Katze MG, Hovanessian AG. 1993. Tumor suppressor function of the interferon-induced double-stranded RNA-activated protein kinase. Proc Natl Acad Sci U S A 90(1):232-6.

Meylan E, Curran J, Hofmann K, Moradpour D, Binder M, Bartenschlager R, Tschopp J. 2005. Cardif is an adaptor protein in the RIG-I antiviral pathway and is targeted by hepatitis C virus. Nature 437(7062):1167-72.

Meylan E, Tschopp J, Karin M. 2006. Intracellular pattern recognition receptors in the host response. Nature 442(7098):39-44.

Mibayashi M, Martinez-Sobrido L, Loo YM, Cardenas WB, Gale M, Jr., Garcia-Sastre A. 2007. Inhibition of retinoic acid-inducible gene I-mediated induction of beta interferon by the NS1 protein of influenza A virus. J Virol 81(2):514-24.

Min JY, Krug RM. 2006. The primary function of RNA binding by the influenza A virus NS1 protein in infected cells: Inhibiting the 2'-5' oligo (A) synthetase/RNase L pathway. Proc Natl Acad Sci U S A 103(18):7100-5.

Min JY, Li S, Sen GC, Krug RM. 2007. A site on the influenza A virus NS1 protein mediates both inhibition of PKR activation and temporal regulation of viral RNA synthesis. Virology 363(1):236-43.

Mirschel S, Steinmetz K, Rempel M, Ginkel M, Gilles ED. 2009. PROMOT: modular modeling for systems biology. Bioinformatics 25(5):687-9.

Mohler L, Flockerzi D, Sann H, Reichl U. 2005. Mathematical model of influenza A virus production in large-scale microcarrier culture. Biotechnol Bioeng 90(1):46-58.

Mohsin MA, Morris SJ, Smith H, Sweet C. 2002. Correlation between levels of apoptosis, levels of infection and haemagglutinin receptor binding interaction of various subtypes of influenza virus: does the viral neuraminidase have a role in these associations. Virus Res 85(2):123-31.

Montagnon BJ, Fanget B, Nicolas AJ. 1981. The large-scale cultivation of VERO cells in micro-carrier culture for virus vaccine production. Preliminary results for killed poliovirus vaccine. Dev Biol Stand 47:55-64.

Morris SJ, Smith H, Sweet C. 2002. Exploitation of the Herpes simplex virus translocating protein VP22 to carry influenza virus proteins into cells for studies of apoptosis: direct confirmation that neuraminidase induces apoptosis and indications that other proteins may have a role. Arch Virol 147(5):961-79.

Mukaigawa J, Nayak DP. 1991. Two signals mediate nuclear localization of influenza virus (A/WSN/33) polymerase basic protein 2. J Virol 65(1):245-53.

Murakami S, Horimoto T, Mai le Q, Nidom CA, Chen H, Muramoto Y, Yamada S, Iwasa A, Iwatsuki-Horimoto K, Shimojima M and others. 2008. Growth determinants for H5N1 influenza vaccine seed viruses in MDCK cells. J Virol 82(21):10502-9.

Nakagawa Y, Kimura N, Toyoda T, Mizumoto K, Ishihama A, Oda K, Nakada S. 1995. The RNA polymerase PB2 subunit is not required for replication of the influenza virus genome but is involved in capped mRNA synthesis. J Virol 69(2):728-33.

Nath ST, Nayak DP. 1990. Function of two discrete regions is required for nuclear localization of polymerase basic protein 1 of A/WSN/33 influenza virus (H1 N1). Mol Cell Biol 10(8):4139-45.

Nayak DP, Hui EK, Barman S. 2004. Assembly and budding of influenza virus. Virus Res 106(2):147-65.

Nayak DP, Lehmann S, Reichl U. 2005. Downstream processing of MDCK cell-derived equine influenza virus. J Chromatogr B Analyt Technol Biomed Life Sci 823(2):75-81.

Nemeroff ME, Barabino SM, Li Y, Keller W, Krug RM. 1998. Influenza virus NS1 protein interacts with the cellular 30 kDa subunit of CPSF and inhibits 3'end formation of cellular pre-mRNAs. Mol Cell 1(7):991-1000.

Nemeroff ME, Qian XY, Krug RM. 1995. The influenza virus NS1 protein forms multimers in vitro and in vivo. Virology 212(2):422-8.

Neri LM, Borgatti P, Capitani S, Martelli AM. 2002. The nuclear phosphoinositide 3-kinase/AKT pathway: a new second messenger system. Biochim Biophys Acta 1584(2-3):73-80.

Neumann G, Castrucci MR, Kawaoka Y. 1997. Nuclear import and export of influenza virus nucleoprotein. J Virol 71(12):9690-700.

Neumann G, Hughes MT, Kawaoka Y. 2000. Influenza A virus NS2 protein mediates vRNP nuclear export through NES-independent interaction with hCRM1. EMBO J 19(24):6751-8.

Newby CM, Sabin L, Pekosz A. 2007. The RNA binding domain of influenza A virus NS1 protein affects secretion of tumor necrosis factor alpha, interleukin-6, and interferon in primary murine tracheal epithelial cells. J Virol 81(17):9469-80.

Nicholson KG, Wood JM, Zambon M. 2003. Influenza. Lancet 362(9397):1733-45.

Nieto A, de la Luna S, Barcena J, Portela A, Ortin J. 1994. Complex structure of the nuclear translocation signal of influenza virus polymerase PA subunit. J Gen Virol 75 (Pt 1):29-36.

Nimmerjahn F, Dudziak D, Dirmeier U, Hobom G, Riedel A, Schlee M, Staudt LM, Rosenwald A, Behrends U, Bornkamm GW and others. 2004. Active NF-kappaB signalling is a prerequisite for influenza virus infection. J Gen Virol 85(Pt 8):2347-56.

O'Neill RE, Talon J, Palese P. 1998. The influenza virus NEP (NS2 protein) mediates the nuclear export of viral ribonucleoproteins. EMBO J 17(1):288-96.

Ohyama K, Nishina M, Yuan B, Bessho T, Yamakawa T. 2003. Apoptosis induced by influenza virus-hemagglutinin stimulation may be related to fluctuation of cellular oxidative condition. Biol Pharm Bull 26(2):141-7.

Olschlager V, Pleschka S, Fischer T, Rziha HJ, Wurzer W, Stitz L, Rapp UR, Ludwig S, Planz O. 2004. Lung-specific expression of active Raf kinase results in increased mortality of influenza A virus-infected mice. Oncogene 23(39):6639-46.

Olsen CW, Kehren JC, Dybdahl-Sissoko NR, Hinshaw VS. 1996. bcl-2 alters influenza virus yield, spread, and hemagglutinin glycosylation. J Virol 70(1):663-6.

Osterhaus A, Fouchier R, Rimmelzwaan G. 2011. Towards universal influenza vaccines? Philos Trans R Soc Lond B Biol Sci 366(1579):2766-73.

Pahl HL. 1999. Activators and target genes of Rel/NF-kappaB transcription factors. Oncogene 18(49):6853-66.

Palache AM, Brands R, van Scharrenburg GJ. 1997. Immunogenicity and reactogenicity of influenza subunit vaccines produced in MDCK cells or fertilized chicken eggs. J Infect Dis 176 Suppl 1:S20-3.

Palese P, Compans RW. 1976. Inhibition of influenza virus replication in tissue culture by 2-deoxy-2,3-dehydro-N-trifluoroacetylneuraminic acid (FANA): mechanism of action. J Gen Virol 33(1):159-63.

Palese P, Tobita K, Ueda M, Compans RW. 1974. Characterization of temperature sensitive influenza virus mutants defective in neuraminidase. Virology 61(2):397-410.

Palese P, Zavala F, Muster T, Nussenzweig RS, Garcia-Sastre A. 1997. Development of novel influenza virus vaccines and vectors. J Infect Dis 176 Suppl 1:S45-9.

Pau MG, Ophorst C, Koldijk MH, Schouten G, Mehtali M, Uytdehaag F. 2001. The human cell line PER.C6 provides a new manufacturing system for the production of influenza vaccines. Vaccine 19(17-19):2716-21.

Pauli EK, Schmolke M, Wolff T, Viemann D, Roth J, Bode JG, Ludwig S. 2008. Influenza A virus inhibits type I IFN signaling via NF-kappaB-dependent induction of SOCS-3 expression. PLoS Pathog 4(11):e1000196.

Pearson G, Robinson F, Beers Gibson T, Xu BE, Karandikar M, Berman K, Cobb MH. 2001. Mitogen-activated protein (MAP) kinase pathways: regulation and physiological functions. Endocr Rev 22(2):153-83.

Pichlmair A, Schulz O, Tan CP, Naslund TI, Liljestrom P, Weber F, Reis e Sousa C. 2006. RIG-I-mediated antiviral responses to single-stranded RNA bearing 5'-phosphates. Science 314(5801):997-1001.

Pinto LH, Holsinger LJ, Lamb RA. 1992. Influenza virus M2 protein has ion channel activity. Cell 69(3):517-28.

Place RF, Haspeslagh D, Hubbard AK, Giardina C. 2001. Cytokine-induced stabilization of newly synthesized I(kappa)B-alpha. Biochem Biophys Res Commun 283(4):813-20.

Planz O. 2006. [Influenza viruses and intracellular signalling pathways]. Berl Munch Tierarztl Wochenschr 119(3-4):101-11.

Platanias LC. 2005. Mechanisms of type-I- and type-II-interferon-mediated signalling. Nat Rev Immunol 5(5):375-86.

Pleschka S, Wolff T, Ehrhardt C, Hobom G, Planz O, Rapp UR, Ludwig S. 2001. Influenza virus propagation is impaired by inhibition of the Raf/MEK/ERK signalling cascade. Nat Cell Biol 3(3):301-5.

Plotch SJ, Bouloy M, Krug RM. 1979. Transfer of 5'-terminal cap of globin mRNA to influenza viral complementary RNA during transcription in vitro. Proc Natl Acad Sci U S A 76(4):1618-22.

Plotch SJ, Bouloy M, Ulmanen I, Krug RM. 1981. A unique cap(m7GpppXm)-dependent influenza virion endonuclease cleaves capped RNAs to generate the primers that initiate viral RNA transcription. Cell 23(3):847-58.

Polyak SJ, Tang N, Wambach M, Barber GN, Katze MG. 1996. The P58 cellular inhibitor complexes with the interferon-induced, double-stranded RNA-dependent protein kinase, PKR, to regulate its autophosphorylation and activity. J Biol Chem 271(3):1702-7.

Poon LL, Pritlove DC, Sharps J, Brownlee GG. 1998. The RNA polymerase of influenza virus, bound to the 5' end of virion RNA, acts in cis to polyadenylate mRNA. J Virol 72(10):8214-9.

Price GE, Smith H, Sweet C. 1997. Differential induction of cytotoxicity and apoptosis by influenza virus strains of differing virulence. J Gen Virol 78 (Pt 11):2821-9.

Price PM, Reichelderfer CF, Johansson BE, Kilbourne ED, Acs G. 1989. Complementation of recombinant baculoviruses by coinfection with wild-type virus facilitates production in insect larvae of antigenic proteins of hepatitis B virus and influenza virus. Proc Natl Acad Sci U S A 86(5):1453-6.

Prostko CR, Dholakia JN, Brostrom MA, Brostrom CO. 1995. Activation of the double-stranded RNA-regulated protein kinase by depletion of endoplasmic reticular calcium stores. J Biol Chem 270(11):6211-5.

Qian XY, Chien CY, Lu Y, Montelione GT, Krug RM. 1995. An amino-terminal polypeptide fragment of the influenza virus NS1 protein possesses specific RNA-binding activity and largely helical backbone structure. RNA 1(9):948-56.

Qiu Y, Krug RM. 1994. The influenza virus NS1 protein is a poly(A)-binding protein that inhibits nuclear export of mRNAs containing poly(A). J Virol 68(4):2425-32.

Randall RE, Goodbourn S. 2008. Interferons and viruses: an interplay between induction, signalling, antiviral responses and virus countermeasures. J Gen Virol 89(Pt 1):1-47.

Rehwinkel J, Tan CP, Goubau D, Schulz O, Pichlmair A, Bier K, Robb N, Vreede F, Barclay W, Fodor E and others. 2010. RIG-I detects viral genomic RNA during negative-strand RNA virus infection. Cell 140(3):397-408.

Ritter JB, Wahl AS, Freund S, Genzel Y, Reichl U. 2010. Metabolic effects of influenza virus infection in cultured animal cells: Intra- and extracellular metabolite profiling. BMC Syst Biol 4:61.

Roberts PC, Compans RW. 1998. Host cell dependence of viral morphology. Proc Natl Acad Sci U S A 95(10):5746-51.

Robertson JS, Schubert M, Lazzarini RA. 1981. Polyadenylation sites for influenza virus mRNA. J Virol 38(1):157-63.

Roedig JV, Rapp E, Genzel Y, Reichl U. 2011a. Impact of different influenza cultivation conditions on HA N-Glycosylation. BMC Proc 5 Suppl 8:P113.

Roedig JV, Rapp E, Hoper D, Genzel Y, Reichl U. 2011b. Impact of host cell line adaptation on quasispecies composition and glycosylation of influenza A virus hemagglutinin. PLoS One 6(12):e27989.

Romano PR, Zhang F, Tan SL, Garcia-Barrio MT, Katze MG, Dever TE, Hinnebusch AG. 1998. Inhibition of double-stranded RNA-dependent protein kinase PKR by vaccinia virus E3: role of complex formation and the E3 N-terminal domain. Mol Cell Biol 18(12):7304-16.

Rott R, Scholtissek C. 1970. Specific inhibition of influenza replication by alpha-amanitin. Nature 228(5266):56.

Ruigrok RW, Barge A, Durrer P, Brunner J, Ma K, Whittaker GR. 2000. Membrane interaction of influenza virus M1 protein. Virology 267(2):289-98.

Ruigrok RW, Calder LJ, Wharton SA. 1989. Electron microscopy of the influenza virus submembranal structure. Virology 173(1):311-6.

Saeed MF, Kolokoltsov AA, Freiberg AN, Holbrook MR, Davey RA. 2008. Phosphoinositide-3 kinase-Akt pathway controls cellular entry of Ebola virus. PLoS Pathog 4(8):e1000141.

Saito T, Nakaya Y, Suzuki T, Ito R, Saito T, Saito H, Takao S, Sahara K, Odagiri T, Murata T and others. 2004. Antigenic alteration of influenza B virus associated with loss of a glycosylation site due to host-cell adaptation. J Med Virol 74(2):336-43.

Salvesen GS. 1999. Programmed cell death and the caspases. APMIS 107(1):73-9.

Samuel CE. 2001a. Antiviral actions of interferons. Clin Microbiol Rev 14(4):778-809, table of contents.

Samuel CE. 2001b. Antiviral actions of interferons. Clinical Microbiology Reviews 14(4):778-809.

Sarkar SN, Peters KL, Elco CP, Sakamoto S, Pal S, Sen GC. 2004. Novel roles of TLR3 tyrosine phosphorylation and PI3 kinase in double-stranded RNA signaling. Nat Struct Mol Biol 11(11):1060-7.

Sato M, Hata N, Asagiri M, Nakaya T, Taniguchi T, Tanaka N. 1998. Positive feedback regulation of type I IFN genes by the IFN-inducible transcription factor IRF-7. FEBS Lett 441(1):106-10.

Schmitt AP, Lamb RA. 2005. Influenza virus assembly and budding at the viral budozone. Adv Virus Res 64:383-416.

Scholtissek C. 1995. Molecular evolution of influenza viruses. Virus Genes 11(2-3):209-15.

Schultz-Cherry S, Dybdahl-Sissoko N, Neumann G, Kawaoka Y, Hinshaw VS. 2001. Influenza virus ns1 protein induces apoptosis in cultured cells. J Virol 75(17):7875-81.

Schultz-Cherry S, Hinshaw VS. 1996. Influenza virus neuraminidase activates latent transforming growth factor beta. J Virol 70(12):8624-9.

Schulze-Horsel J, Genzel Y, Reichl U. 2008. Flow cytometric monitoring of influenza A virus infection in MDCK cells during vaccine production. BMC Biotechnol 8:45.

Schulze-Horsel J, Schulze M, Agalaridis G, Genzel Y, Reichl U. 2009. Infection dynamics and virus-induced apoptosis in cell culture-based influenza vaccine production-Flow cytometry and mathematical modeling. Vaccine 27(20):2712-22.

Schwarzer J, Rapp E, Hennig R, Genzel Y, Jordan I, Sandig V, Reichl U. 2009. Glycan analysis in cell culture-based influenza vaccine production: influence of host cell line and virus strain on the glycosylation pattern of viral hemagglutinin. Vaccine 27(32):4325-36.

Seitz C, Frensing T, Hoper D, Kochs G, Reichl U. High yields of influenza A virus in Madin-Darby canine kidney cells are promoted by an insufficient interferon-induced antiviral state. J Gen Virol 91(Pt 7):1754-63.

Seitz C, Isken B, Heynisch B, Rettkowski M, Frensing T, Reichl U. 2012. Trypsin promotes efficient influenza vaccine production in MDCK cells by interfering with the antiviral host response. Appl Microbiol Biotechnol 93(2):601-11.

Seki Y, Inoue H, Nagata N, Hayashi K, Fukuyama S, Matsumoto K, Komine O, Hamano S, Himeno K, Inagaki-Ohara K and others. 2003. SOCS-3 regulates onset and maintenance of T(H)2-mediated allergic responses. Nat Med 9(8):1047-54.

Seo SH, Hoffmann E, Webster RG. 2002. Lethal H5N1 influenza viruses escape host anti-viral cytokine responses. Nat Med 8(9):950-4.

Seth RB, Sun L, Chen ZJ. 2006. Antiviral innate immunity pathways. Cell Res 16(2):141-7.

Seth RB, Sun L, Ea CK, Chen ZJ. 2005. Identification and characterization of MAVS, a mitochondrial antiviral signaling protein that activates NF-kappaB and IRF 3. Cell 122(5):669-82.

Shapira SD, Gat-Viks I, Shum BO, Dricot A, de Grace MM, Wu L, Gupta PB, Hao T, Silver SJ, Root DE and others. 2009. A physical and regulatory map of host-influenza interactions reveals pathways in H1N1 infection. Cell 139(7):1255-67.

Shapiro GI, Gurney T, Jr., Krug RM. 1987. Influenza virus gene expression: control mechanisms at early and late times of infection and nuclear-cytoplasmic transport of virus-specific RNAs. J Virol 61(3):764-73.

Sharma K, Tripathi S, Ranjan P, Kumar P, Garten R, Deyde V, Katz JM, Cox NJ, Lal RB, Sambhara S and others. 2011. Influenza A virus nucleoprotein exploits Hsp40 to inhibit PKR activation. PLoS One 6(6):e20215.

Sharma S, tenOever BR, Grandvaux N, Zhou GP, Lin R, Hiscott J. 2003. Triggering the interferon antiviral response through an IKK-related pathway. Science 300(5622):1148-51.

Shi L, Summers DF, Peng Q, Galarz JM. 1995. Influenza A virus RNA polymerase subunit PB2 is the endonuclease which cleaves host cell mRNA and functions only as the trimeric enzyme. Virology 208(1):38-47.

Shin YK, Li Y, Liu Q, Anderson DH, Babiuk LA, Zhou Y. 2007a. SH3 binding motif 1 in influenza A virus NS1 protein is essential for PI3K/Akt signaling pathway activation. J Virol 81(23):12730-9.

Shin YK, Liu Q, Tikoo SK, Babiuk LA, Zhou Y. 2007b. Influenza A virus NS1 protein activates the phosphatidylinositol 3-kinase (PI3K)/Akt pathway by direct interaction with the p85 subunit of PI3K. J Gen Virol 88(Pt 1):13-8.

Shuai K. 2000. Modulation of STAT signaling by STAT-interacting proteins. Oncogene 19(21):2638-44.

Sidorenko Y, Reichl U. 2004. Structured model of influenza virus replication in MDCK cells. Biotechnol Bioeng 88(1):1-14.

Simmons NL. 1982. Cultured monolayers of MDCK cells: a novel model system for the study of epithelial development and function. Gen Pharmacol 13(4):287-91.

Siren J, Imaizumi T, Sarkar D, Pietila T, Noah DL, Lin R, Hiscott J, Krug RM, Fisher PB, Julkunen I and others. 2006. Retinoic acid inducible gene-I and mda-5 are involved in influenza A virus-induced expression of antiviral cytokines. Microbes Infect 8(8):2013-20.

Skehel JJ, Bizebard T, Bullough PA, Hughson FM, Knossow M, Steinhauer DA, Wharton SA, Wiley DC. 1995. Membrane fusion by influenza hemagglutinin. Cold Spring Harb Symp Quant Biol 60:573-80.

Smith GL, Hay AJ. 1982. Replication of the influenza virus genome. Virology 118(1):96-108.

Soebiyanto RP, Sreenath SN, Qu CK, Loparo KA, Bunting KD. 2007. Complex systems biology approach to understanding coordination of JAK-STAT signaling. Biosystems 90(3):830-42.

Stanley WM. 1945. The Preparation and Properties of Influenza Virus Vaccines Concentrated and Purified by Differential Centrifugation. J Exp Med 81(2):193-218.

Stasakova J, Ferko B, Kittel C, Sereinig S, Romanova J, Katinger H, Egorov A. 2005. Influenza A mutant viruses with altered NS1 protein function provoke caspase-1 activation in primary human macrophages, resulting in fast apoptosis and release of high levels of interleukins 1beta and 18. J Gen Virol 86(Pt 1):185-95.

Steinhauer DA. 1999. Role of hemagglutinin cleavage for the pathogenicity of influenza virus. Virology 258(1):1-20.

Steinhauer DA, Holland JJ. 1987. Rapid evolution of RNA viruses. Annu Rev Microbiol 41:409-33.

Subbarao K, Katz JM. 2004. Influenza vaccines generated by reverse genetics. Curr Top Microbiol Immunol 283:313-42.

Subbarao K, Klimov A, Katz J, Regnery H, Lim W, Hall H, Perdue M, Swayne D, Bender C, Huang J and others. 1998. Characterization of an avian influenza A (H5N1) virus isolated from a child with a fatal respiratory illness. Science 279(5349):393-6.

Sun SC, Ganchi PA, Ballard DW, Greene WC. 1993. NF-kappa B controls expression of inhibitor I kappa B alpha: evidence for an inducible autoregulatory pathway. Science 259(5103):1912-5.

Susin SA, Lorenzo HK, Zamzami N, Marzo I, Snow BE, Brothers GM, Mangion J, Jacotot E, Costantini P, Loeffler M and others. 1999. Molecular characterization of mitochondrial apoptosis-inducing factor. Nature 397(6718):441-6.

Takaoka A, Yanai H. 2006. Interferon signalling network in innate defence. Cell Microbiol 8(6):907-22.

Takizawa T, Fukuda R, Miyawaki T, Ohashi K, Nakanishi Y. 1995. Activation of the apoptotic Fas antigen-encoding gene upon influenza virus infection involving spontaneously produced beta-interferon. Virology 209(2):288-96.

Takizawa T, Matsukawa S, Higuchi Y, Nakamura S, Nakanishi Y, Fukuda R. 1993. Induction of programmed cell death (apoptosis) by influenza virus infection in tissue culture cells. J Gen Virol 74 (Pt 11):2347-55.

Takizawa T, Ohashi K, Nakanishi Y. 1996. Possible involvement of double-stranded RNA-activated protein kinase in cell death by influenza virus infection. J Virol 70(11):8128-32.

Takizawa T, Tatematsu C, Nakanishi Y. 2002. Double-stranded RNA-activated protein kinase interacts with apoptosis signal-regulating kinase 1. Implications for apoptosis signaling pathways. Eur J Biochem 269(24):6126-32.

Takizawa T, Tatematsu C, Ohashi K, Nakanishi Y. 1999. Recruitment of apoptotic cysteine proteases (caspases) in influenza virus-induced cell death. Microbiol Immunol 43(3):245-52.

Talon J, Horvath CM, Polley R, Basler CF, Muster T, Palese P, Garcia-Sastre A. 2000. Activation of interferon regulatory factor 3 is inhibited by the influenza A virus NS1 protein. J Virol 74(17):7989-96.

Tan SL, Ganji G, Paeper B, Proll S, Katze MG. 2007. Systems biology and the host response to viral infection. Nat Biotechnol 25(12):1383-9.

Taylor DR, Lee SB, Romano PR, Marshak DR, Hinnebusch AG, Esteban M, Mathews MB. 1996. Autophosphorylation sites participate in the activation of the double-stranded-RNA-activated protein kinase PKR. Mol Cell Biol 16(11):6295-302.

Taylor DR, Shi ST, Romano PR, Barber GN, Lai MM. 1999. Inhibition of the interferon-inducible protein kinase PKR by HCV E2 protein. Science 285(5424):107-10.

Thornberry NA. 1998. Caspases: key mediators of apoptosis. Chem Biol 5(5):R97-103.

Tobita K. 1975. Permanent canine kidney (MDCK) cells for isolation and plaque assay of influenza B viruses. Med Microbiol Immunol 162(1):23-7.

Tobita K, Sugiura A, Enomote C, Furuyama M. 1975. Plaque assay and primary isolation of influenza A viruses in an established line of canine kidney cells (MDCK) in the presence of trypsin. Med Microbiol Immunol 162(1):9-14.

Tong S, Li Y, Rivailler P, Conrardy C, Castillo DA, Chen LM, Recuenco S, Ellison JA, Davis CT, York IA and others. 2012. A distinct lineage of influenza A virus from bats. Proc Natl Acad Sci U S A 109(11):4269-74.

Tosh PK, Jacobson RM, Poland GA. 2010. Influenza vaccines: from surveillance through production to protection. Mayo Clin Proc 85(3):257-73.

Tree JA, Richardson C, Fooks AR, Clegg JC, Looby D. 2001. Comparison of large-scale mammalian cell culture systems with egg culture for the production of influenza virus A vaccine strains. Vaccine 19(25-26):3444-50.

Treiman M, Caspersen C, Christensen SB. 1998. A tool coming of age: thapsigargin as an inhibitor of sarco-endoplasmic reticulum Ca(2+)-ATPases. Trends Pharmacol Sci 19(4):131-5.

Turner D, Wailoo A, Nicholson K, Cooper N, Sutton A, Abrams K. 2003. Systematic review and economic decision modelling for the prevention and treatment of influenza A and B. Health Technol Assess 7(35):iii-iv, xi-xiii, 1-170.

Ueda M, Yamate M, Du A, Daidoji T, Okuno Y, Ikuta K, Nakaya T. 2008. Maturation efficiency of viral glycoproteins in the ER impacts the production of influenza A virus. Virus Res 136(1-2):91-7.

Ulmanen I, Broni BA, Krug RM. 1981. Role of two of the influenza virus core P proteins in recognizing cap 1 structures (m7GpppNm) on RNAs and in initiating viral RNA transcription. Proc Natl Acad Sci U S A 78(12):7355-9.

Uthaisangsook S, Day NK, Bahna SL, Good RA, Haraguchi S. 2002. Innate immunity and its role against infections. Ann Allergy Asthma Immunol 88(3):253-64; quiz 265-6, 318.

van der Vries E, Collins PJ, Vachieri SG, Xiong X, Liu J, Walker PA, Haire LF, Hay AJ, Schutten M, Osterhaus AD and others. 2012. H1N1 2009 Pandemic Influenza Virus: Resistance of the I223R Neuraminidase Mutant Explained by Kinetic and Structural Analysis. PLoS Pathog 8(9):e1002914.

van Wielink R, Harmsen MM, Martens DE, Peeters BP, Wijffels RH, Moormann RJ. 2011. MDCK cell line with inducible allele B NS1 expression propagates delNS1 influenza virus to high titres. Vaccine 29(40):6976-85.

Varghese JN, Colman PM. 1991. Three-dimensional structure of the neuraminidase of influenza virus A/Tokyo/3/67 at 2.2 A resolution. J Mol Biol 221(2):473-86.

Verhagen AM, Ekert PG, Pakusch M, Silke J, Connolly LM, Reid GE, Moritz RL, Simpson RJ, Vaux DL. 2000. Identification of DIABLO, a mammalian protein that promotes apoptosis by binding to and antagonizing IAP proteins. Cell 102(1):43-53.

Vester D, Kluge, S., Rapp, E., Genzel, Y., Reichl, U. 2009. Virus-host cell interactions in vaccine production cell lines infected with different human influenza A virus variants: a proteomic approach

to be submitted.

Vester D, Rapp E, Gade D, Genzel Y, Reichl U. 2009. Quantitative analysis of cellular proteome alterations in human influenza A virus-infected mammalian cell lines. Proteomics 9(12):3316-27.

Vester D, Rapp E, Kluge S, Genzel Y, Reichl U. 2010. Virus-host cell interactions in vaccine production cell lines infected with different human influenza A virus variants: a proteomic approach. J Proteomics 73(9):1656-69.

Vines A, Wells K, Matrosovich M, Castrucci MR, Ito T, Kawaoka Y. 1998. The role of influenza A virus hemagglutinin residues 226 and 228 in receptor specificity and host range restriction. J Virol 72(9):7626-31.

Vreede FT, Jung TE, Brownlee GG. 2004. Model suggesting that replication of influenza virus is regulated by stabilization of replicative intermediates. J Virol 78(17):9568-72.

Wada N, Matsumura M, Ohba Y, Kobayashi N, Takizawa T, Nakanishi Y. 1995. Transcription stimulation of the Fas-encoding gene by nuclear factor for interleukin-6 expression upon influenza virus infection. J Biol Chem 270(30):18007-12.

Wang C, Lamb RA, Pinto LH. 1994. Direct measurement of the influenza A virus M2 protein ion channel activity in mammalian cells. Virology 205(1):133-40.

Wang P, Palese P, O'Neill RE. 1997. The NPI-1/NPI-3 (karyopherin alpha) binding site on the influenza a virus nucleoprotein NP is a nonconventional nuclear localization signal. J Virol 71(3):1850-6.

Wang W, Riedel K, Lynch P, Chien CY, Montelione GT, Krug RM. 1999. RNA binding by the novel helical domain of the influenza virus NS1 protein requires its dimer structure and a small number of specific basic amino acids. RNA 5(2):195-205.

Wang X, Basler CF, Williams BR, Silverman RH, Palese P, Garcia-Sastre A. 2002. Functional replacement of the carboxy-terminal two-thirds of the influenza A virus NS1 protein with short heterologous dimerization domains. J Virol 76(24):12951-62.

Wang X, Hinson ER, Cresswell P. 2007. The interferon-inducible protein viperin inhibits influenza virus release by perturbing lipid rafts. Cell Host Microbe 2(2):96-105.

Wang X, Li M, Zheng H, Muster T, Palese P, Beg AA, Garcia-Sastre A. 2000. Influenza A virus NS1 protein prevents activation of NF-kappaB and induction of alpha/beta interferon. J Virol 74(24):11566-73.

Wareing MD, Tannock GA. 2001. Live attenuated vaccines against influenza; an historical review. Vaccine 19(25-26):3320-30.

Weber F, Kochs G, Gruber S, Haller O. 1998. A classical bipartite nuclear localization signal on Thogoto and influenza A virus nucleoproteins. Virology 250(1):9-18.

Wek RC, Jiang HY, Anthony TG. 2006. Coping with stress: eIF2 kinases and translational control. Biochem Soc Trans 34(Pt 1):7-11.

White E. 1996. Life, death, and the pursuit of apoptosis. Genes Dev 10(1):1-15.

Wiley SR, Schooley K, Smolak PJ, Din WS, Huang CP, Nicholl JK, Sutherland GR, Smith TD, Rauch C, Smith CA and others. 1995. Identification and characterization of a new member of the TNF family that induces apoptosis. Immunity 3(6):673-82.

Wolff T, Zielecki F, Abt M, Voss D, Semmler I, Matthaei M. 2008. Sabotage of antiviral signaling and effectors by influenza viruses. Biol Chem 389(10):1299-305.

World Health O. 2005. Recommended composition of influenza virus vaccines for use in the 2005-2006 influenza season. Wkly Epidemiol Rec 80(8):71-5.

Wright PF, Webster RG. 2001. Orthomyxoviruses. Hawley DMKaPM, editor. Fields Virology, Lippincott Williams & Wilkins, Philadelphia: pp. 1564.

Wurzer WJ, Ehrhardt C, Pleschka S, Berberich-Siebelt F, Wolff T, Walczak H, Planz O, Ludwig S. 2004. NF-kappaB-dependent induction of tumor necrosis factor-related apoptosis-inducing ligand (TRAIL) and Fas/FasL is crucial for efficient influenza virus propagation. J Biol Chem 279(30):30931-7.

Wurzer WJ, Planz O, Ehrhardt C, Giner M, Silberzahn T, Pleschka S, Ludwig S. 2003. Caspase 3 activation is essential for efficient influenza virus propagation. EMBO J 22(11):2717-28.

Xu LG, Wang YY, Han KJ, Li LY, Zhai Z, Shu HB. 2005. VISA is an adapter protein required for virus-triggered IFN-beta signaling. Mol Cell 19(6):727-40.

Yamamoto M, Sato S, Mori K, Hoshino K, Takeuchi O, Takeda K, Akira S. 2002. Cutting edge: a novel Toll/IL-1 receptor domain-containing adapter that preferentially activates the IFN-beta promoter in the Toll-like receptor signaling. J Immunol 169(12):6668-72.

Yasuda J, Nakada S, Kato A, Toyoda T, Ishihama A. 1993. Molecular assembly of influenza virus: association of the NS2 protein with virion matrix. Virology 196(1):249-55.

Ye Z, Liu T, Offringa DP, McInnis J, Levandowski RA. 1999. Association of influenza virus matrix protein with ribonucleoproteins. J Virol 73(9):7467-73.

Yin MJ, Yamamoto Y, Gaynor RB. 1998. The anti-inflammatory agents aspirin and salicylate inhibit the activity of I(kappa)B kinase-beta. Nature 396(6706):77-80.

Yoboua F, Martel A, Duval A, Mukawera E, Grandvaux N. 2010. Respiratory syncytial virus-mediated NF-kappa B p65 phosphorylation at serine 536 is dependent on RIG-I, TRAF6, and IKK beta. J Virol 84(14):7267-77.

Yoneyama M, Kikuchi M, Natsukawa T, Shinobu N, Imaizumi T, Miyagishi M, Taira K, Akira S, Fujita T. 2004. The RNA helicase RIG-I has an essential function in double-stranded RNA-induced innate antiviral responses. Nat Immunol 5(7):730-7.

Youil R, Su Q, Toner TJ, Szymkowiak C, Kwan WS, Rubin B, Petrukhin L, Kiseleva I, Shaw AR, DiStefano D. 2004. Comparative study of influenza virus replication in Vero and MDCK cell lines. J Virol Methods 120(1):23-31.

Young DF, Andrejeva L, Livingstone A, Goodbourn S, Lamb RA, Collins PL, Elliott RM, Randall RE. 2003. Virus replication in engineered human cells that do not respond to interferons. J Virol 77(3):2174-81.

Young LS, Dawson CW, Eliopoulos AG. 1997. Viruses and apoptosis. Br Med Bull 53(3):509-21.

Yuen KY, Chan PK, Peiris M, Tsang DN, Que TL, Shortridge KF, Cheung PT, To WK, Ho ET, Sung R and others. 1998. Clinical features and rapid viral diagnosis of human disease associated with avian influenza A H5N1 virus. Lancet 351(9101):467-71.

Zahn RC, Schelp I, Utermohlen O, von Laer D. 2007. A-to-G hypermutation in the genome of lymphocytic choriomeningitis virus. J Virol 81(2):457-64.

Zhang P, Samuel CE. 2008. Induction of protein kinase PKR-dependent activation of interferon regulatory factor 3 by vaccinia virus occurs through adapter IPS-1 signaling. J Biol Chem 283(50):34580-7.

Zhirnov OP, Klenk HD. 2007. Control of apoptosis in influenza virus-infected cells by up-regulation of Akt and p53 signaling. Apoptosis 12(8):1419-32.

Zhirnov OP, Konakova TE, Garten W, Klenk H. 1999. Caspase-dependent N-terminal cleavage of influenza virus nucleocapsid protein in infected cells. J Virol 73(12):10158-63.

Zhirnov OP, Konakova TE, Wolff T, Klenk HD. 2002. NS1 protein of influenza A virus down-regulates apoptosis. J Virol 76(4):1617-25.

Zilberstein A, Kimchi A, Schmidt A, Revel M. 1978. Isolation of two interferon-induced translational inhibitors: a protein kinase and an oligo-isoadenylate synthetase. Proc Natl Acad Sci U S A 75(10):4734-8.

Zurcher T, Marion RM, Ortin J. 2000. Protein synthesis shut-off induced by influenza virus infection is independent of PKR activity. J Virol 74(18):8781-4.

Zurcher T, Pavlovic J, Staeheli P. 1992a. Mechanism of human MxA protein action: variants with changed antiviral properties. EMBO J 11(4):1657-61.

Zurcher T, Pavlovic J, Staeheli P. 1992b. Nuclear localization of mouse Mx1 protein is necessary for inhibition of influenza virus. J Virol 66(8):5059-66.

10 Appendix

10.1 Tables of chemicals, cell culture reagents, molecular biology tools, consumables, and technical equipment

Table 10-1: List of chemicals.

Name	Supplier	Article N°
2-Aminopurine nitrate salt (198.1 g/mol)	Sigma-Aldrich Chemie GmbH, Steinheim	A2380
2-Phosphoglycerate (2-PG)	Sigma-Aldrich Chemie GmbH, Steinheim	G9891
Acrylic amide 30% (Mix 37,5 : 1)	Applichem GmbH, Darmstadt	A3626
Ammonium persulfate (APS)	Sigma-Aldrich Chemie GmbH, Steinheim	A3678
Beta-acetic acid	Carl Roth GmbH, Karlsruhe	KK62.1
Beta-Mercaptoethanol	AppliChem GmbH, Darmstadt	A4338
Bovine serum albumine (BSA)	AppliChem GmbH, Darmstadt	A1391
Bromophenolblue	AppliChem GmbH, Darmstadt	A2331
Disodium phosphate	Merck KGaA, Darmstadt	106566
EDTA (Triplex)	Merck KGaA, Darmstadt	324503
Ethanol 99%	Carl Roth GmbH, Karlsruhe	9065
Formaldehyde	AppliChem GmbH, Darmstadt	A0877
Glycerol	AppliChem GmbH, Darmstadt	A3739
Glycerole-2-phosphate	Sigma-Aldrich Chemie GmbH, Steinheim	G6376
Glycine	AppliChem GmbH, Darmstadt	A1067
Hydrochloric acid (HCL, 32%)	Carl Roth GmbH, Karlsruhe	9277
Isopropanol	Carl Roth GmbH, Karlsruhe	6752
Methanol	Carl Roth GmbH, Karlsruhe	KK44.1
Milk powder	Carl Roth GmbH, Karlsruhe	T1452
Phenylmethanesulfonyl fluoride (PMSF)	Sigma-Aldrich Chemie GmbH, Steinheim	P7626
Ponceau S red	Sigma-Aldrich Chemie GmbH, Steinheim	09276
Potassium chloride	Merck KGaA, Darmstadt	529552
Potassium dihydrogen phosphate	Merck KGaA, Darmstadt	105108
Protease inhibitor cocktail	Roche GmbH, Penzberg	11697498001
Sodium chloride	Merck KGaA, Darmstadt	567441
Sodium dodecyl sulfate (SDS)	AppliChem GmbH, Darmstadt	A1112
Sodium fluoride	Sigma-Aldrich Chemie GmbH, Steinheim	S7920
Sodium hydrogen carbonate	Carl Roth GmbH, Karlsruhe	8551
Sodium hydroxide	Carl Roth GmbH, Karlsruhe	6771
Sodium molybdate	Sigma-Aldrich Chemie GmbH, Steinheim	S6646
Sodium pyrophosphate tertrabasic	Sigma-Aldrich Chemie GmbH, Steinheim	P8010
Sodium orthovanadate	Sigma-Aldrich Chemie GmbH, Steinheim	S6508
TEMED (PlusOne™)	GE Healthcare, Munich	17-1312-01

Tris	AppliChem GmbH, Darmstadt	A1086.5000
Tris-Cl	AppliChem GmbH, Darmstadt	A3452
Triton X-100	Sigma-Aldrich Chemie GmbH, Steinheim	9002-93-1
Trypan blue	Merck KGaA, Darmstadt	1117320025
Tween 20	Merck KGaA, Darmstadt	655204

Table 10-2: List of cell culture reagents.

Name	Supplier	Article N°
F-12K Nutrient Mixture Kaighn's (1x) liquid	Life Technologies GmbH, Darmstadt	21127022
Glucose	Carl Roth GmbH, Karlsruhe	X997.3
Glutamine	Sigma-Aldrich Chemie GmbH, Steinheim	G-3126
TNF-alpha	Calbiochem/Merck KGaA, Darmstadt	654205
Trypsin (2.5%, porcine), 0.5 mg/mL	Life Technologies GmbH, Darmstadt	27250-018
GMEM without glutamine	Sigma-Aldrich Chemie GmbH, Steinheim	G5154
Fetal calf serum (FCS)	Pan Biotech GmbH, Aidenbach	3302-P250922
Peptone	Lab M, Lancs, UK	MC033
Peptone	BD	211677

Table 10-3: List of molecular biology kits and tools.

Name	Supplier	Article N°
CellTiter-Glo® luminescent cell viability assay	Promega GmbH, Mannheim	G7571
Agar for molecular biology	AppliChem GmbH, Darmstadt	A3477
Dual-Luciferase® reporter assay system	Promega GmbH, Mannheim	E1910
Lipofectamine™ 2000 transfection reagent	Life Technologies GmbH, Darmstadt	12566-014
MagicMark™ XP western protein standard	Life Technologies GmbH, Darmstadt	LC5602
M-MuLV reverse transcriptase reaction buffer	New England Biolabs Inc.	B0253S
Neon® transfection system	Life Technologies GmbH, Darmstadt	MPK10096
NucleoSpin® RNA II RNA preparation kit	Macherey-Nagel GmbH, Dueren	740955
PageRuler™ prestained protein ladder	Fermentas/Thermo Fisher Scientific Inc.	SM0671
PCR primers	Invitrogen/Life Technologies GmbH, Darmstadt	
pGL4.10 vectors (firefly, GFP-pMax, renilla)	Promega GmbH, Mannheim	E6651
Pierce® BCA protein assay kit	Thermo Fisher Scientific Inc.	23225
RevertAid™ reverse transcriptase	Thermo Fisher Scientific Inc.	EP0441

RiboLock™ RNAse inhibitor	Thermo Fisher Scientific Inc.	EO0381
Rotor-Gene SYBR green PCR kit	Qiagen GmbH, Hilden	204072
siLentFect lipid reagent for RNAi	BioRad Laboratories GmbH, Munich	170-3361
siRNAs (PKR, IκBα)	Eurogentec Deutschland GmbH, Cologne	
SuperSignal West Dura substrate	Perbio Science/Thermo Fisher Scientific Inc.	34075

Table 10-4: List of consumables.

Name	Supplier	Article N°
Cell culture flasks	Greiner Bio-One GmbH,	
Cell scraper	Greiner Bio-One GmbH,	540080
Cryo.s™ vials	Greiner Bio-One GmbH	121261
Eppendorf tubes (0.5, 1.5, 2 mL)	Eppendorf AG, Hamburg	0030 121.023/3810X/0030 120.094
Glassware	Schott AG, Mainz	
Injekt® 40 Duo injection needles	B. Braun Melsungen AG	9166432V
Microliter syringe #705	Hamilton Bonaduz AG	80539
Millipak 0.22 µM membrane filters	MilliPore/Merck KGaA	MPGL04GK2
Parafilm® M	Brand GmbH, Wertheim	701605
Polystyrene 96-well microtiter plates	Greiner Bio-One GmbH, Frickenhausen	650101-ORT/651101

Table 10-5: List of utilized technical gear and equipment.

Device	Manufacturer
Avanti J20 centrifuge	Beckman Coulter GmbH, Krefeld
Biofuge Primo R	Kendro Laboratory Products GmbH
Biometra T3000 thermal cycler	LABRepCo Inc., USA
Cellferm Pro Spinner BS1600	DasGip Technology GmbH, Jülich
Centro LB960 Microplate Luminometer	Berthold Technologies GmbH, Bad Wildbad
ChemoCam HR 16-3200	Intas, Goettingen
Heracell T6060 Incubator	Heraeus Holding, Hanau
HERAsafe® Clean bench	Thermo Electron Corporation, USA
Infinite M200 NanoQuant Microplate Reader	Tecan Group Ltd., Switzerland
InoLab® 7110 pH meter	WTW GmbH, Weilheim
Magnetic stirrer STrawBerRY IKA®	IKA®-Werke GmbH, Staufen
Microscope Axiovert 40C	Carl Zeiss AG, Jena
Milli-Q Advantage A10, Milli PAK®	MilliPore/Merck KGaA, Darmstadt
Mini Trans-Blot® Electrophoretic Transfer Cell	BioRad Laboratories GmbH, Munich
Multichannel pipettes and Multipette®	Eppendorf AG, Hamburg

Neon® Transfection system	Life Technologies GmbH, Darmstadt
OxyProbe® D140 SN50970	Broadley-James Corp., USA
pH probe, 405-DPAS-SC-K85/200	Mettler-Toledo GmbH, Giessen
Pipettor with charging point	Hirschmann GmbH, Ebestadt
Power Pac™ Basic	BioRad Laboratories GmbH, Munich
QIAgility benchtop PCR setup instrument	Qiagen GmbH, Hilden
Reax Top Vortex	Heidolph Instruments GmbH, Schwabach
Rotor-Gene Q real-time PCR thermocycler	Qiagen GmbH, Hilden
Shaker Polymax 1040	Heidolph Instruments GmbH, Schwabach
Special accuracy scale Kern 620-3	Kern & Sohn GmbH, Balingen
TE 1402S balance	Sartorius Stedim GmbH, Goettingen
Varioklav 65T autoclave	HP Medizintechnik GmbH, Oberschleissheim
Vi-Cell™ XR cell viability analyzer	Beckmann Coulter GmbH, Krefeld
Water bath HBA basic	Memmert GmbH, Schwabach

10.2 $TCID_{50}$ data PR8-NIBSC plaque isolation

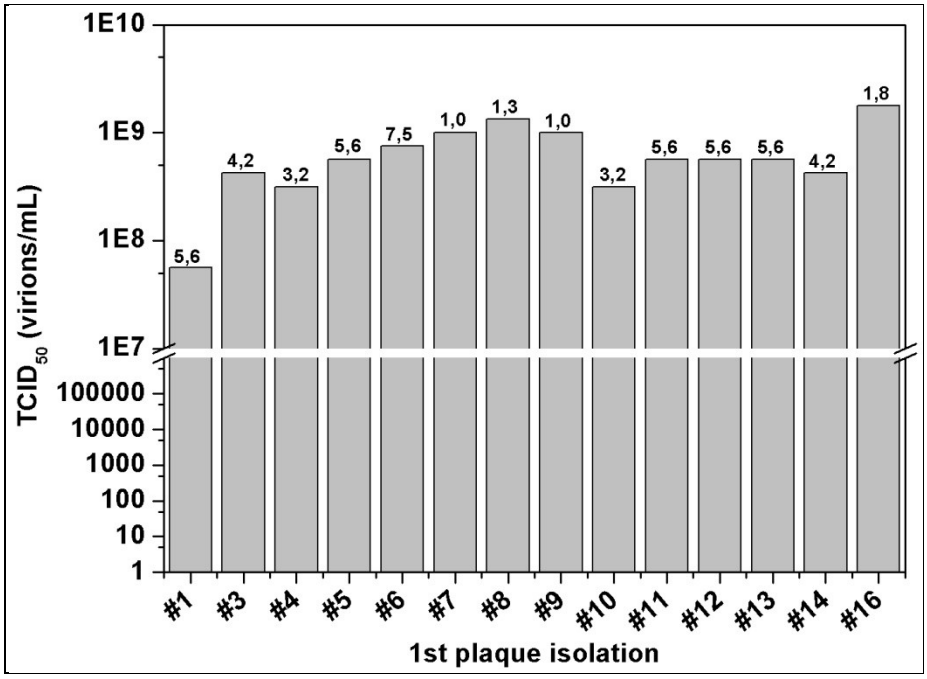

Figure 10.2-1. Plaque assay using MDCK cells to isolate and purify PR8-NIBSC variants in seed virus stocks.
After propagation in T-flasks for one passage, plaque isolates were harvested and the concentration of infectious virus particles determined in the TCID50 assay.

10.3 Amino acid sequence alignments of human vs. canine IRF-3, Stat2, and PKR

Source: http://blast.ncbi.nlm.nih.gov/Blast.cgi

Marked in red are the phosphorylated amino acids that are detected by respective phospho-specific antibodies.

>ref|XP_533616.3| PREDICTED: interferon regulatory factor 3 [Canis lupus familiaris]
Length=377

GENE ID: 476412 IRF3 | interferon regulatory factor 3 [Canis lupus familiaris] (10 or fewer PubMed links)

Score = 569 bits (1467), Expect = 0.0, Method: Compositional matrix adjust.
Identities = 279/372 (75%), Positives = 310/372 (83%), Gaps = 0/372 (0%)

```
Query  55   QAWAEATGAYVPGRDKPDLPTWKRNFRSALNRKEGLRLAEDRSKDPHDPHKIYEFVNSGV  114
            +AWAE +GAY PG+DKPDLPTWKRNFRSALNRKE LR+AEDRSKDPHDPHK+YEFV SG
Sbjct  5    RAWAEVSGAYTPGKDKPDLPTWKRNFRSALNRKEELRVAEDRSKDPHDPHKVYEFVISGA  64

Query  115  GDFSQPDTSPDTNGGGSTSDTQEDILDELLGNMVLAPLPDPGPPSLAVAPEPCPQPLRSP  174
            G+  + DT PDTNG  STSDTQED L+ELLG+MVL P PD GP SL V PE  P  L SP
Sbjct  65   GNLPELDTFPDTNGRYSTSDTQEDTLEELLGDMVLTPFPDEGPSSLVVVPEQTPPLLLSP  124

Query  175  SLDNPTPFPNLGPSENPLKRLLVPGEEWEFEVTAFYRGRQVFQQTISCPEGLRLVGSEVG  234
            ++D P P PN  P ENPLKRLLVP EEWEFEVTAFYRGRQVFQQT+SCP GLRLV +  G
Sbjct  125  TIDLPAPCPNSEPPENPLKRLLVPDEEWEFEVTAFYRGRQVFQQTVSCPRGLRLVAAAGG  184

Query  235  DRTLPGWPVTLPDPGMSLTDRGVMSYVRHVLSCLGGGLALWRAGQWLWAQRLGHCHTYWA  294
            D  LPG P+ LPDPG+ +TD+ VM YVR VLSCLGGGLALWRAGQ LWA+RLGHCHTYWA
Sbjct  185  DTMLPGQPIILPDPGVLVTDKTVMGYVRRVLSCLGGGLALWRAGQQLWARRLGHCHTYWA  244

Query  295  VSEELLPNSGHGPDGEVPKDKEGGVFDLGPFIVDLITFTEGSGRSPRYALWFCVGESWPQ  354
            + EELLP+S   P GEVPKD++G +FDL PF+ DLI F +GS  SPRY LWFCVGE WPQ
Sbjct  245  LGEELLPDSSPRPGGEVPKDEDGDLFDLRPFVSDLIAFIKGSRHSPRYTLWFCVGEPWPQ  304

Query  355  DQPWTKRLVMVKVVPTCLRALVEMARVGGASSLENTVDLHISNSHPLSLTSDQYKAYLQD  414
            DQPWTK+LVM+KVVPTCLRAL+EMAR+ GASSLENTVDLHISNS+PL+LTSDQYKAYLQD
Sbjct  305  DQPWTKKLVMLKVVPTCLRALLEMARLEGASSLENTVDLHISNSYPLTLTSDQYKAYLQD  364

Query  415  LVEGMDFQGPGE  426
            LVE MDF   GE
Sbjct  365  LVEDMDFWVTGE  376
```

> ref|XP_538232.2| PREDICTED: signal transducer and activator of transcription 2 isoform 1 [Canis lupus familiaris]
Length=854

GENE ID: 481111 STAT2 | signal transducer and activator of transcription 2, 113kDa [Canis lupus familiaris]

Score = 1462 bits (3785), Expect = 0.0, Method: Compositional matrix adjust.
Identities = 736/863 (85%), Positives = 775/863 (90%), Gaps = 21/863 (2%)

```
Query  1    MAQWEMLQNLDSPFQDQLHQLYSHSLLPVDIRQYLAVWIEDQNWQEAALGSDDSKATMLF  60
            MAQWEMLQNLD+PFQDQLHQLYS SLLPVDIRQ+LAVWIEDQNWQEAALG+DDSK  MLF
Sbjct  1    MAQWEMLQNLDNPFQDQLHQLYSDSLLPVDIRQHLAVWIEDQNWQEAALGNDDSKVNMLF  60

Query  61   FHFLDQLNYECGRCSQDPESLLLQHNLRKFCRDIQPFSQDPTQLAEMIFNLLLEEKRILI  120
            FHFLDQL YECGRC QDPE  LLQHNLRKF RDIQ   Q PTQLAEMIFNLLLEEKRIL
Sbjct  61   FHFLDQLKYECGRCGQDPECFLLQHNLRKFYRDIQALPQGPTQLAEMIFNLLLEEKRILT  120

Query  121  QAQRAQLEQGEPVLETPVESQQHEIESRILDLRAMMEKLVKSISQLKDQQDVFCFRYKIQ  180
            QAQRAQLEQG+P L+TPVESQQ EIESRIL+L+AMME+LVKSISQLKDQQDVFCFRYKIQ
Sbjct  121  QAQRAQLEQGDPALKTPVESQQDEIESRILELKAMMERLVKSISQLKDQQDVFCFRYKIQ  180

Query  181  AKGKTPSLDPHQTKEQKILQETLNELDKRRKEVLDASKALLGRLTTLIELLLPKLEEWKA  240
            A+ K  SLDPHQ ++ ++LQETLNELD+RRKEVLDA+KALLGRLTTLIELLLPKLEEWKA
Sbjct  181  AQVKKFSLDPHQMRQHQLLQETLNELDRRRKEVLDATKALLGRLTTLIELLLPKLEEWKA  240
```

```
Query  241  QQQKACIRAPIDHGLEQLETWFTAGAKLLFHLRQLLKELKGLSCLVSYQDDPLTKGVDLR  300
            QQQKACI AP + GLEQLE WFTAGAKLLFHLRQLL+ELKGLS LVSYQDDPLT GV+LR
Sbjct  241  QQQKACIGAPQEGGLEQLEKWFTAGAKLLFHLRQLLEELKGLSHLVSYQDDPLTAGVNLR  300

Query  301  NAQVTELLQRLLHRAFVVETQPCMPQTPHRPLILKTGSKFTVRTRLLVRLQEGNESLTVE  360
             AQV ELLQRLLHR FVVETQPCMPQTPHRPLILKTGSKFT+RTRLLVRLQEGNESLT E
Sbjct  301  KAQVLELLQRLLHRGFVVETQPCMPQTPHRPLILKTGSKFTIRTRLLVRLQEGNESLTAE  360

Query  361  VSIDRNPPQLQGFRKFNILTSNQKTLTPEKGQSQGLIWDFGYLTLVEQRSGGSGKGSNKG  420
            VSID+NP Q QGFRKFNILTSNQKTLTPEKGQSQGLIWDFGYLTLVEQRSGG GKG NKG
Sbjct  361  VSIDKNP-QSQGFRKFNILTSNQKTLTPEKGQSQGLIWDFGYLTLVEQRSGGPGKGCNKG  419

Query  421  PLGVTEELHIISFTVKYTYQGLKQELKTDTLPVVIISNMNQLSIAWASVLWFNLLSPNLQ  480
             LGVTEELHIIS TVKYTYQGLK+ELKTDTLPVVIISNMNQ+SIAWASVLWFNLLS N Q
Sbjct  420  MLGVTEELHIISITVKYTYQGLKEELKTDTLPVVIISNMNQVSIAWASVLWFNLLSSNPQ  479

Query  481  NQQFFSNPPKAPWSLLGPALSWQFSSYVGRGLNSDQLSMLRNKLFGQNCRTEDPLLSWAD  540
            NQQFFS+PP APWSLLGPALSWQFSSYVGRGL+ DQLSMLRNKLFGQN RTE  LLSWAD
Sbjct  480  NQQFFSSPPMAPWSLLGPALSWQFSSYVGRGLDPDQLSMLRNKLFGQNSRTEGALLSWAD  539

Query  541  FTKRESPPGKLPFWTWLDKILELVHDHLKDLWNDGRIMGFVSRSQERRLLKKTMSGTFLL  600
            FTKRESPPGKLPFWTWLDKILELVHDHLKDLWNDGRIMGFVSRS+ERRLLKKT+SGTFLL
Sbjct  540  FTKRESPPGKLPFWTWLDKILELVHDHLKDLWNDGRIMGFVSRSKERRLLKKTISGTFLL  599

Query  601  RFSESSEGGITCSWVEHQDDDKVLIYSVQPYTKEVLQSLPLTEIIRHYQLLTEENIPENP  660
            RFSE+SEGGITCSWVEHQDDDKVLI S+QP+TKEVLQSLPLT+IIRHYQLLTEENIPENP
Sbjct  600  RFSETSEGGITCSWVEHQDDDKVLINSLQPFTKEVLQSLPLTKIIRHYQLLTEENIPENP  659

Query  661  LRFLYPRIPRDEAFGCYYQEKVNLQERRKYLKHRLIVVSNRQVDELQQPLELKPEPELES  720
            L FLYPRIPRDEAFGCYYQEKVNL+ERRKYLKHRLIVVSNRQVDELQQPLELKPEPE ES
Sbjct  660  LCFLYPRIPRDEAFGCYYQEKVNLEERRKYLKHRLIVVSNRQVDELQQPLELKPEPEAES  719

Query  721  LELELGLVP--EPELSLDLEPLLKAGLDLGPELESVLESTLEPVIEPTLCMVSQTVPEPD  778
            LELE GL P  + E  L+LEPLL AGLDLGP         LEP++EPTL MV Q V EPD
Sbjct  720  LELETGLDPLLQQEPCLELEPLLAAGLDLGP--------PLEPMLEPTLDMVPQGVSEPD  771

Query  779  QG----------PVSQPVPEPDLPCDLRHLNTEPMEIFRNCVKIEEIMPNGDPLLAGQNT  828
             G          P SQ VPEPDLP DLRHLNTE MEIFRN +KIEEIMPNGDPLLAGQN
Sbjct  772  LGPELRLEPLPDPASQAVPEPDLPHDLRHLNTEEMEIFRNSMKIEEIMPNGDPLLAGQNI  831

Query  829  VDEVYVSRPSHFYTDGPLMPSDF  851
            +DE YV   SHFYTDGPL+PSD+
Sbjct  832  MDEAYVFHSSHFYTDGPLIPSDY  854
```

> ref|NP_001041600.1| UGM interferon-induced, double-stranded RNA-activated protein kinase [Canis lupus familiaris]
gb|AAX58777.1| GM eukaryotic translation initiation factor 2-alpha kinase 2 [Canis lupus familiaris]
Length=532

GENE ID: 611397 EIF2AK2 | eukaryotic translation initiation factor 2-alpha kinase 2 [Canis lupus familiaris] (10 or fewer PubMed links)

```
 Score =   638 bits (1646),  Expect = 0.0, Method: Compositional matrix adjust.
 Identities = 342/553 (62%), Positives = 409/553 (74%), Gaps = 28/553 (5%)

Query  1    MAGDLSAGFFMEELNTYRQKQGVVLKYQELPNSGPPHDRRFTFQVIIDGREFPEGEGRSK  60
            MA      FF+EELN + QK   VLKY EL   GP H+ RFTFQ IID RE+PE EG+SK
Sbjct  1    MANQRPPSFFIEELNIFCQKHRKVLKYNELSKEGPAHNLRFTFQAIIDEREYPEAEGKSK  60

Query  61   KEAKNAAAKLAVEILNKEKKAVSPLLLTTTNSSEGLSM---GNYIGLINRIAQKKRLTVN  117
            KEA+N AAKLA+EIL+KE KAVS L L TT++SEGL +   GNYIG +NR+AQK++L+VN
Sbjct  61   KEARNTAAKLALEILHKENKAVSSLSLPTTDTSEGLGLEGVGNYIGRMNRLAQKEQLSVN  120

Query  118  YEQCASGVHGPEGFHYKCKMGQKEYSIGTGSTKQEAKQLAAKLAYLQILSEETSVKSDYL  177
            YEQ      GPE FH +CK+GQKEY IG G+TKQEAK LAAK AY QI SE+T + +D
Sbjct  121  YEQWELKDCGPERFHCRCKIGQKEYDIGKGATKQEAKHLAAKFAYEQIQSEQTLMNAD--  178

Query  178  SSGSFATT-CESQSNSLVTSTLASESSSEGDFSADTSEINSNSDSLNSSSLLMNGLRNNQ  236
             SGS+ T+  +S++N+L+ S  AS+S  E +FS      N N D++++S   ++  R ++
Sbjct  179  -SGSWTTSPSDSRNNTLMRSLCASKSPLENNFSP-----NCNRDNVDNSPSSLSNARYSE  232

Query  237  RKAKRSLAPRFDLPDMKETKYTVDKRFGMDFKEIELIGSGGFGQVFKAKHRIDGKTYVIK  296
            +K KR+LAP F  P  KE KYTV+ RF  DF EIE IGSGG+GQVFKAKH+IDGK YVIK
Sbjct  233  KKVKRTLAPTFSSPMTKEHKYTVELRFASDFTEIEPIGSGGYGQVFKAKHKIDGKIYVIK  292

Query  297  RVKYNNEK-AEREVKALAKLDHVNIVHYNGCWDGFDYDPETSDDSLESSDYDPENSKNSS  355
            RVKY+++K  EREVKALA LDHVNIVHY  CW G               DY+PE+S N S
Sbjct  293  RVKYDSDKKVEREVKALAALDHVNIVHYRSCWAG--------------EDYNPEDSVNPS  338

Query  356  RSKTKCLFIQMEFCDKGTLEQWIEKRRGEKLDKVLALELFEQITKGVDYIHSKKLIHRDL  415
            R+ TKCLFIQMEFCDKGTLEQWI+ RRG++ DK LALELFEQI  GV+YIHSK+LIHRDL
Sbjct  339  RT-TKCLFIQMEFCDKGTLEQWIDNRRGKEQDKPLALELFEQIVAGVNYIHSKQLIHRDL  397

Query  416  KPSNIFLVDTKQVKIGDFGLVTSLKNDGKRTRSKGTLRYMSPEQISSQDYGKEVDLYALG  475
            KP NIFLVDTK +KIGDFGLVTSLK+   RT +KGTLRYMSPEQISSQ+YGKEVD++ALG
Sbjct  398  KPGNIFLVDTKHIKIGDFGLVTSLKDFANRTSNKGTLRYMSPEQISSQEYGKEVDIFALG  457

Query  476  LILAELLHVCDTAFETSKFFTDLRDGIISDIFDKKEKTLLQKLLSKKPEDRPNTSEILRT  535
            LILAELL++C T  ET K F +LR G  SD+FD +EK LLQKLLS +P  RPN SEIL T
Sbjct  458  LILAELLYICPTVSETLKIFKELRAGKFSDVFDAREKQLLQKLLSLEPMKRPNASEILET  517

Query  536  LTVWKKSPEKNER  548
            L  WK    K  R
Sbjct  518  LKDWKNVAGKKSR  530
```

10.4 Standard operating procedures (SOPs)

10.4.1 Work instruction Nr. M/ 04 (Medium preparation of GMEM)

date: 14.06.2001 **author: I. Behrendt** **checked:**
changed at: 20.06.2006 **author: S. Koenig** **checked:**
changed at: 30.05.2008 **author: S. Koenig** **checked:**
translated: 10.12.2008 **by:** **A. Neumann**

Production of Glasgow-MEM-full media (Z – media) from self produced partial solutions
(GMEM-media made of powder media + FCS + 20% lab-M-peptone) **and (V-media)**
from self produced partial solutions (GMEM-media made of powder media + 20% lab-M-peptone)

1.0 Aim

Production of full media to cultivate MDCK cells in culture bottles and bioreactors. All parts of the media are already prepared as sterile solutions (FCS) or are sterile produced and have only to be pipetted.

2.0 Material

- fetal calf serum (FCS, Co. Gibco, order.no. 10270-106): 500 mL-bottle
- Glasgow-MEM-media (BHK21 powder media based, see work instruction no. M/03)
- lab-M-peptone F.M.V. (Co. idg, Great Britain, order. no.: MC 33)
- Schott flask 1 L
- scale
- sterile bottle

3.0 Method
3.1 Preparation of the 20 percent peptone-solution:

- solve 200 g lab-M-peptone in 80°C warm water and fill up to 1 L.
- fill in a 1 L bottle.
- immediately autoclave 30 min in 105°C.

3.2 Composition of the full media:

- thaw the bottle with FCS in the refrigerator over night
- warm up all partial solutions up to room temperature and weigh them on the scale in to a sterile bottle under the bench instructions for 1L-media Z-media:
- weigh 890 mL of glasgow-MEM-media in to a sterile 1L-bottle
- add 100 mL FCS, and 10 mL 20-percent lab-M-peptone
- note the used charge in your worksheet
- complete declaration of the bottles (Z..., Date)
- put sterile test on

instruction for 1L-media V-media:

- weight 990 mL of glasgow-MEM-media in to a sterile 1L-bottle
- add 10 mL 20-percent lab-M-peptone
- note the used charge in your worksheet
- complete declaration of the bottles (Z..., Date)
- put sterile test on

4.0 Storage

- ready full media can be stored in a refrigerator for about 3 months
  but the stability of glutamine and other ingredients can start to decrease after 4 weeks
- defreezed FCS is savable for 6 months at 6°C
- 20-percent lab-m-peptone is savable for 6 months at 4°C.

10.4.2 Work instruction Nr. Z/ 04 (MDCK cell passaging)

date: 14.04.2000	**author: Dr. Annett Kiesel**	**checked:**
changed at: 09.07.2003	**author: Ilona Behrendt**	**checked:**
changed at: 20.06.2006	**author: Susanne Koenig**	**checked:**
changed at: 11.09.2006	**author: Nancy Schlawin**	**checked:**
translated at: 17.12.2008	**by: F. Weber**	**checked:**

Passaging of MDCK-cells in serum- free medium

1.0 Ziel

Langzeitkultivierung und Vermehrung von Zellen, zur Beimpfung mit verschiedenen Virusarten
und spaeteren Aufarbeitung.

2.0 Materialien

- Kultur mit konfluent gewachsenen Zellen (25-cm^2-, 75-cm^2-, 175-cm^2-Flasche oder 850-cm^2-Rollerflasche);
  MDCK-Zellen: 4- bis 6-Tage alte, konfluent gewachsene Kultur
  - Trypsin/ EDTA-Loesung (0,05% Trypsin/ 0,02% EDTA, 37°C), 1:10-Verduennung aus Stammloesung, siehe Arbeitsanweisung M/07
- Vollmedium (GlasgowMEM komplett gemischt mit 10% FCS und Tryptosephosphatboullion/Pepton), siehe Arbeitsanweisungen M/02 oder M/04
  - PBS (Raumtemperatur) siehe Arbeitsanweisung M/01
  - foetales Kaelberserum (FCS) (auf Raumtemperatur vorwaermen) Firma:Gibco/Best.Nr.:10270106
  -

3.0 Methode

- Kulturflaschen aus dem Brutschrank nehmen und desinfizieren, unter die Werkbank stellen
- Kulturflaschen aufschrauben, Deckel mit Oeffnungen nach oben legen (Deckel nach hinten legen, so dass man nicht darueber fasst beim Arbeiten)
- altes Medium in eine sterile Abfallflasche abgiessen (nicht den Rand beruehren!)
- die Zellen mit PBS-Loesung 2x waschen (s. Volumentab., I), gebrauchtes PBS in die sterile Abfallflasche abgiessen (dazwischen die T-Flaschen immer zuschrauben und schwenken)
- Trypsin/ EDTA-Loesung zupipettieren, ein duenner Fluessigkeitsfilm genuegt (s. Volumentab., II), und die Zellen bei 37 °C für ca. 20 min inkubieren
- in der Zwischenzeit neue Kulturflasche mit entsprechender Menge Medium befuellen (s. Volumentab., IV)

- nach 10 min Trypsininkubation die Flasche zum erstenmal leicht schuetteln, dann Zellen weiterinkubieren (insgesamt ca. 20 bis 30 min.) bis sich die Zellen nach erneutem kraeftigen Schuetteln vom Boden abloesen
  (optische Kontrolle und/oder unterm Mikroskop angucken)
- zum Abstoppen der enzymatischen Reaktion FCS (s. Volumentab., III) zu den abgeloesten Zellen geben
- durch mehrmaliges (ca. 2-3x) Aufziehen des Inhaltes der Flasche in eine Pipette erfolgt eine Zellvereinzelung
  (um Schaum zu vermeiden, Pipetteninhalt am Flaschenboden oder an der Innenseite der Flasche auslaufen lassen!)
  - von dieser Zellsuspension entnimmt man 1/3tel bis 1/6tel (bei Inkubation in Flaschen mit gleichem Volumen) und pipettiert dieses jeweils in eine der vorbereiten Flaschen (Berechnung der Einsaatdichte siehe unter Punkt 5 oder 6).
  - ***Beachte!*** Fuer Zellkultivierung Deckel mit Membran benutzen (CO_2-durchlaessig), bei Arbeiten mit Virus in den T-Flaschen, geschlossenen Deckel (ohne Membran) nehmen.
- Flaschen im Brutschrank bei 37 °C und 5 % CO_2 inkubieren

4.0 Volumentabelle

Kulturgefaess	**PBS zum Waschen** (I)	**Trypsin/EDTA** (II)	**FCS** (III)	**Vollmedium** (IV)
25-cm^2-Flasche	1.0 5 – 10 mL	1 mL	1 mL	15 - 20 mL
75-cm^2-Flasche	10 – 15 mL	3 mL	3 mL	50 mL
175-cm^2-Flasche	15 – 20 mL	5 mL	5 mL	100 - 125 mL
850-cm^2-Rollerflasche	40 – 50 mL	10 mL	10 mL	250 mL

5.0 „Faustregeln“ für die Anzucht von MDCK-Zellen

- Ausgangskultur: 4- bis 6-Tage alte, konfluent gewachsene Kultur (zu alte Kulturen vermeiden)
  - Weiterkultivierung der Zellen in einer Kulturflasche mit gleichem Volumen: 1/3tel bis 1/6tel der Zellen in die neue Flasche geben.
  - Vermehrung der Zellen für den Fermenter: Ampulle – T75 – T175 – Rollerflasche: jeweils die gesamten Zellen in das naechstgroessere Kulturgefaess ueberfuehren (Ampulle mit 2 - 5x10^6 Zellen/mL,; wenn weniger Zellen oder alte Zellen: Zwischenstufe über T25)

Zellen nicht untereinander austauschen (bei Kontaminationsgefahr nicht mehr genau nachvollziehbar, woher diese stammt
fuer eine Reaktorkultivierung Zellen aus einer Passagierung kleiner 20 verwenden
stets eine T 75 Flasche parallel zur Fermentation als back-up laufen lassen

6.0 Einsaat

6.1 Ermittlung des Einsaatvolumens

- ermittelte Zellzahl der trypsinierten Flasche Z (z. B. 1,2 x 10^6 Zellen / mL)
- Tage, in denen die Zellen bis zur Konfluenz wachsen sollen T (z. B. 4 d)
- empirisch ermittelte Einsaatdichte E, bei der die Zellen nach T Tagen in dem verwendeten Kulturgefaess konfluent sind (z. B. 0,8 x 10^7 Zellen pro 175 cm^2 werden benoetigt, um in 4 Tagen eine konfluente Kultur in einer 175-cm^2-Flasche zu erhalten)

- Rechnung: E : Z = Volumen [mL]

  Bsp:
  (0,8 x 10^7 Zellen) : (1,2 x 10^6 Zellen/mL) = 6,7 mL

  In eine 175-cm^2-Flasche muessen 6,7 mL einer Zellsuspension, die 1,2 x 10^6 Zellen/mL enthaelt, pipettiert werden, um nach 4 Tagen eine konfluente Kultur zu erhalten.

6.2 Bestimmung der Einsaat

Einsaat = Zellen pro cm^2
= (Einsaatvolumen x Zellzahl) : Oberflaeche
Bsp.:
= (6, 7 mL x 1,2 x 10^6 Zellen/mL) : 175 cm^2 = 4,6 x 10^4 Zellen/cm^2
6,7 mL der Zellsuspension (mit 1,2 x 10^6 Zellen/ml) ergeben in einer 175-cm^2-Flasche eine Einsaat von 4,6 x 10^4 Zellen/cm^2.

- Was ist ein guter Richtwert pro cm^2 ?
  z.B. : 3,3 x 10^4 cells/ cm2 fuer Bioreaktor (≈ 3,0 x 10^5 cells/ml)
  2,9 x 10^4 cells / cm^2 fuer Rollerflaschen in 4 Tagen oder
  1,5 x 10^4 cells / cm^2 fuer Rollerflaschen in 7 Tagen
  7,6 x 10^4 cells/ cm^2 fuer T 175 (1:6 gesplittet)
  4,3 x 10^4 cells/ cm^2 fuer T175 (5ml) in Rollerflasche (850 cm^2)

7.0 Lagerung

Zellen wachsen in:
T-Flaschen bei 37°C im CO_2-Brutschrank im N1.06
Rollerflaschen im 37°C Rollerflaschenschrank im N1.06 oder im 37°C Brutraum auf den Rollerflaschengestell
Spinner cei 37°C im Brutraum auf einen Ruehrer

Die eingefrorenen Zellen werden im Fluessigstickstoffbehaelter im N1.12 gelagert.
Die Dokumentation erfolgt ueber Tabellen mit den jeweiligen Farbcode und Kennnummern die in einem Ordner im Raum N 1.06 abgeheftet sind.

10.4.3 Arbeitsanweisung Nr. M/ 07 (Trypsin and EDTA preparation)

Datum: 8.12.2000 **Autor: Ilona Behrendt** **geprüft:**
überarbeitet: 17.12.03 **Autor: Susanne König** **geprüft:**
überarbeitet: 17.11.05 **Autor: Susanne König** **geprüft:**
überarbeitet: 20.05.10 **Autor: Claudia Best** **geprüft:**

Herstellung der Trypsin- EDTA- Stammlösung (10x) zum Ablösen von Zellkulturen

1.0 Ziel

Herstellung der Trypsin- EDTA- Stammlösung (10x) für das Ablösen von adherenten Zellen aus Zellkulturflaschen.

2.0 Material

- Trypsin, 1:250, Pulver (Gibco, Bestellnr.: 27250-018), befindet sich im Raum N. 1.06 bei 4°C
  (bei einer neuen Trypsincharge, von Gibco immer das Analysenzertifikat zu schicken lassen, da dort die Aktivitätsangabe (BAEE- Wert) vermerkt ist!!)
- unsteriles PBS, befindet sich im Raum N. 1.06 bei RT
- EDTA (Sigma, Bestellnr.: ED2SS), befindet sich im Raum N. 1.06 bei RT

- Präzisionswaage
- Spatel, Wägeschälchen
- 250 mL Becherglas
- 250 mL Messzylinder
- Magnetrührer + Rührstäbchen
- Vakuumpumpe, befindet sich im Raum N. 1.07 unter dem Abzug
- 250 mL Nalgene Sterilfilter (gelb, 0,22 µm)
- S2 Sterilbank
- 2 Caso-Bouillons
- Pipettierhilfe Pipettus akku
- sterile Einmalpipetten
- sterile 50 mL Falkonröhrchen

3.0 Methode

Es ist darauf zu achten das der BAEE- Wert (Aktivitätsangabe) zwischen 600 – 800 U/mg liegt. Falls dieser kleiner oder höher sein sollte, muss die Einwaagemenge neu berechnet werden.

- für 250 mL werden 1,25 g Trypsin und 0,5 g EDTA auf der Präzisionswaage eingewogen
- diese beiden Substanzen gibt man zusammen mit 250 mL unsterilem PBS in ein Becherglas
- die Lösung wird auf dem Magnetrührer solange gerührt bis sich die Substanzen vollständig aufgelöst haben
- danach wird die Lösung mit der Vakuumpumpe in ein 250 mL Nalgenes Filtersystem steril filtriert
- unter der S2 Sterilbank werden aus dem Nalgenen Filtersystem 5 mL Try zuerst die 2 Caso- Bouillons als Steriltests ab
- jeweils 50 mL der Trypsinstammlösung werden mit Einmalpipetten in die sterilen Falconröhrchen hinein pipettiert
- zum Schluß werden die Röhrchen gut verschlossen und einzeln beschriftet (Trypsin 10x, Herstellungs-datum, steril)
- das dazugehörige Datenblatt (V/02.1) wird ausgefüllt und im Ordner für Zellkulturlösungen abgeheftet

4.0 Lagerung

Die Lagerung erfolgt bei 4 °C. Die Haltbarkeit beträgt 1 Jahr.
Es ist darauf zu achten, daß trotz der Lagerung bei 4°C, die Aktivität des Trypsinpulvers abnimmt.
Um dies rechtzeitig zu erkennen, wird bei Auffälligkeiten des Ablösevorganges während der Zellpassagierung, wie z.B. längere Ablösedauer, die techn. Assistentin informiert.
Sollten sich die Auffälligkeiten bestätigen, erfolgt somit eine Neubestellung des Trypsinpulvers von der Firma Gibco.

5.0 Verwendung

- diese 10x konzentrierte Trypsinstammlösung wird zum Ablösen der Zellen von Carriern aus dem Bioreaktor, Wavereaktor u.v.m. verwendet
- zum Ablösen der Zellen von T-Flaschen bzw. Rollerflaschen muß diese Lösung noch 1:10 verdünnt werden, da sie sonst dafür zu stark konzentriert ist

6.0 Herstellung von verdünnter Trypsin- EDTA- Lösung (1x)

Material

- 1 Falcon Trypsinstammlösung (10x), befindet sich im Raum N. 1.06 bei 4°C
- steriles PBS, befindet sich im Raum N. 1.06 bei RT
- 10 sterile 50 mL Falconröhrchen
- Pipettierhilfe Pipettus akku

- sterile Einmalpipetten
- S2 Sterilbank

Herstellung

- unter der S2 Sterilbank pipettiert man 5 mL von der Trypsinstammlösung in jedes der 10 Falconröhrchen
- danach wird in jedes Falcon noch 45 mL des sterilem PBS dazugegeben
- zum Schluß werden die Falcons gut verschlossen, etwas geschüttelt, und beschriftet
  (Trypsin 1x, Herstellungsdatum, steril)

- die Lagerung erfolgt ebenfalls bei 4 °C

10.4.4 Working instruction Nr. Z / 02 (MDCK cell thawing)

Thawing of MDCK cells

1.0 Intention

Gently unfreezing on MDCK cells (stocking in liquid nitrogen).

2.0 Material

- cells in cryo- tube stocked in liquid nitrogen
- nitrogen storage container
- protective clothing: thermo- gloves and shield
- water quench 37°C
- culture bottle (T25, better T75)
- full medium (completely mixed with FCS and tryptosephosphatboullion or peptone) or serum- free medium (Episerf, Optipro, Ex- Cell) – preheat on room temperature
- cleaned work bench
- pipette, pipette Tipps (sterile)
- disinfection solution (Descosept AF / Cleanisept) inside a aerosol can
- Sterillium for hand disinfection

3.0 Method

- switch on the work bench 15 min before beginning work, disinfect it
- disinfect tips, pipettes and medium and place under the bench
- put on the gloves and disinfect them
- add the medium inside a cell culture bottle under the sterile bench (20mL in a T25- bottle; 50mL in a T75- bottle)
- take the cells out of the nitrogen container (wearing protective clothing!!!) und unfreeze them quickly

Freezant DMSO is toxic. Unfreeze the cells quickly to add them into the medium for dilution!!
Never shake cryo- tubes overhead – contamination hazard!

- disinfect the cryo- tubes after melting of the last ice clump and place them under the work bench
- fill the content inside a culture bottle by using adequate pipette (culture bottle should contain at least 20mL medium to dilute the DMSO enough)
- at problems during growing:
  1. accomplish a changing of the medium to eliminate DMSO completely
     after attaching of the cells (ca. 4- 12h) (see work instruction Z/03) or

2. add currently unfreezing cells in a 50mL Falcon- tube, filled up with 40mL medium (37°C);
   Centrifuge the cells at 500 x g for 5min at room temperature; pipette off the medium and add the cells into an adequate volume of medium (for example 50mL) and transfer it into a cell culture bottle (for example T75)

10.4.5 Arbeitsanweisung Nr. Z / 06 (Cryoconservation of cells)

Datum: 14.04.2000 **Autor: Dr. Annett Kiesel** **geprüft:**
überarbeitet: 21.11.2005 **Autor: Susanne König** **geprüft:**
überarbeitet: 05.01.2007 **Autor: Claudia Best** **geprüft:**
überarbeitet: 24.10.2007 **Autor: Claudia Best** **geprüft:**

Kryokonservierung von Zellen

1.0 Ziel

Schaffung einer **W**orking **C**ell **B**ank (**WCB**) zur langjährigen Nutzung von Zellen für Zellkulturarbeiten.
Das „Haltbarmachen“ von Zellen für eine längere Zeit, mit der Lagerung in flüssigen Stickstoff (-196°C).
Als Schutzsubstanz dient DMSO, welches die Kristallbildung innerhalb und außerhalb der Zellen sowie die partielle Dehydratation des Cytoplasmas verhindert.

2.0 Material

- konfluente Zellkulturflaschen (nicht älter als 4 Tage)
- S2 Sterilbank
- steriles PBS bei RT in N.1.06
- steriles Trypsin (1x Konzentration, 600 - 800 Units/mg) bei 4°C in N.1.06
- FCS bei 4°C im N. 1.06
- serumfreies Medium bei 4°C im Kühlraum N. 1.13
- sterile 50 mL Falcons
- sterile, - 196 °C beständige, 2 mL Kryoröhrchen mit Beschriftung (Zelllinie, Passagennummer, Einfrierdatum)
- Einfrierboxen mit Beschriftung (Zelllinie, Passagennummer, Einfriermedium, Einfrierdatum, Zellzahl pro Kryo)
- Primo R Kühlzentrifuge + Zentrifugeneinsatz
- Vi-Cell XR Zellzählgerät
- sterile Einmalpipetten + Pipettus Akku
- steriles DMSO (Ampulle) bei RT in N. 1.06
- - 20 °C Gefrierschrank in N. 1.06
- - 70 °C Tiefkühlschrank in N.1.11
- - 196 °C Behälter mit flüssigen Stickstoff in N. 1.12
- persönliche Schutzausrüstung: Kittel, Schutzbrille, lange Thermohandschuhe, Nitril- Einmalhandschuhe

Einfriermedium für Zellen in serumhaltigen Medien
- **F**oetales **K**älber**s**erum, **FCS** z.B. PAN Bestellnr.: 3302-P250922
- **10 – 15% DMSO** Sigma, Bestellnr.: D2650

Einfriermedium für Zellen in serumfreien Medien
- serumfreies Medium (Ex-Cell, Episerf,…)
- **< 10 % DMSO** Sigma, Bestellnr.: D2650
  (→ siehe Datenblätter der Zellkultur)

3.0 Methode

- unter der S2 Sterilbank die Zellkulturflaschen zweimal mit sterilen PBS waschen
- Zellen mit der entsprechenden Menge an Trypsin ablösen (z.B. für T175 = 6 mL), und mit der gleichen Menge an Medium die Ablösereaktion abstoppen
- bei serumfreien Zellkulturen mit dem serumfreien Medium oder PBS abstoppen (vergl. Arbeitsanweisung Z/ 04 und Z/ 05)
- die Zellsuspension in ein steriles 50 mL Falkon Röhrchen überführen
- Röhrchen mit FCS oder serumfreien Medium auf 45 mL auffüllen
- 1 mL Probe daraus entnehmen, und die Zellzahl mit dem Vi-Cell XR bestimmen
- das Falkon in der Primo R Kühlzentrifuge bei 500 x g 5 min zentrifugieren
- nach Berechnung des Volumens vom Einfriermedium, wird die klare Überstandslösung im Falkon bis zum Zellpellet entnommen
- das Zellpellet wird im Einfriermedium verdünnt, so dass eine **Endkonzentration von 2 – 4 x 10^6 Zellen/Kryo,** (Angabe von ECACC für MDCK Zellen) entsteht
- 1,6 mL der Einfrierlösung in die beschrifteten Kryoröhrchen pipettieren, und in die beschrifteten Boxen stellen
- die Boxen zuerst für 2 h in den -20°C Gefrierschrank stellen, dann über Nacht bei –80°C einfrieren, und zum Schluß den flüssigen Stickstoffbehälter überführen
- ein Datenblatt mit Informationen über Zelllinie, Passagennummer, Einfriermedium und Einfrierdatum und Zellzahl / Kryo wird im Zellkulturordner angelegt

4.0 Kontrolle

- nach 3 - 4 Wochen werden die frisch eingefrorenen Zellen getestet auf, a) sind sie steril, b) wachsen sie in der Zellkulturflasche mit serumhaltigen bzw. serumfreien Medium wieder an
- ist die Charge unsteril, so wird diese entsorgt → Dokumentation im Datenblatt des Zellkulturordners
- sollten die Zellen nicht anwachsen, dann ein zweites Kryo auftauen und nochmal testen
- ist wieder kein Anwachsen der Zellen zu beobachten, so erfolgt die entgültige Entsorgung der Charge

5.0 Berechnung der Einsaatmenge der Zellsuspension pro Kryo

Zellzahl: 9,5 x 10^5 Z/mL x 45mL (Volumen an FCS oder serumfreien Medium)
= **4,3 x 10^7 Z/mL** in 45mL

Soll: 2 - 4 x 10^6 Z/mL **Ist**: 9 Kryos mit ca. 1,6mL = 14,4 mL

$$\frac{\textbf{4,3 x } 10^7 \textbf{ Z/mL}}{14{,}4\text{mL}} = \textbf{3,07 x } 10^6 \textbf{ Z/Kryo}$$

Zusammensetzung des Einfriermedium

14,4 mL = 100%
x mL = 10% x =1,44 mL **DMSO**

14,4 mL – 1,44 mL = 12,96 mL **FCS / serumfreies Medium**

1,44 mL DMSO + 12,9 mL FCS / serumfreien Medium → auf das Zellpellet geben, mischen und in die Kryos verteilen

6.0 Lagerung

- die Zellen sind in der Gasphase des flüssigen Stickstoffs für mindestens 10 Jahre haltbar
- bei –80°C können die Zellen bis zu 3 Monate gehalten werden

7.0 Entsorgung des DMSO

- geöffnet nicht lange haltbar (zerfällt an der Luft)
- nach dem Öffnen den Rest entsorgen (Abfallbeauftragter Herr Schäfer Tel.: 185)
- DMSO ist sehr giftig und wird durch die Handschuhe von der Haut aufgenommen
- wenn DMSO auf die Handschuhe gelangt ist, diese sofort wechseln.
- DMSO nur kurz öffnen, nicht inhalieren.

10.4.6 Kurzanleitung Zellzählgerät ViCell XR (ViCell short operating instruction)

Version 1.5
Erstellt am: 29.03.2006
Aktualisiert am 08.08.2008
Autor: J. Schulze-Horsel

1. Im Vorfeld zu beachten

- Das Gerät darf nur nach Einweisung durch die dafür zuständige Person bzw. nach Absprache durch eine andere eingewiesene Person benutzt werden.
- Die zu messende Probe darf **auf keinen Fall Microcarrier** enthalten, da sonst das Gerät verstopft wird!
- Validierter Messbereich (für Zelltyp „MDCK 100“: $9.6*10^4$ bis $1,0*10^7$ Zellen/mL (Gesamtzellzahl)

2. Material

Originalprodukte von Beckman Coulter:

Nr. 383260	Single Pack	250 Messungen, Reagenzien plus Probengefäße (ca. 240 Euro)
Nr. 383194	Quad Pack	1000 Messungen (4x Single Pack = ca. 845 Euro)
Nr.		Probengefäße (ViCell Cups)

Die Probengefäße können gespült und mehrmals verwendet werden.
Die Komponenten des Reagenzienpacks sind entweder bereits vorhanden oder können selbst hergestellt werden:

- Trypanblaulösung: 0,4 % w/v Trypanblau und 0,15 mol/L Natriumchlorid in vollentsalztem Wasser (VE-Wasser)
  mit Papierfilter vorfiltriert, anschliessend 0,45 µm filtriert
- Desinfektionsmittel: Isopropanol (2-Propanol), 90 %
- Reinigungsmittel: Beckman Coulter Clenz (Nr. 8448222, 5 Liter)
- Pufferlösung dH_20, z.B. MilliQ-Wasser

Das benötigte Reagenzienvolumen pro 250 Messungen ist:.
- Trypanblaulösung ca. 110 mL
allen anderen Reagenzien ca. 220 mL benötigt

Auffüllen der Reagenzien:

Wenn das aktuelle Reagenzienpack leer ist, im Menü „Instrument“, „Replace reagent pack“ auswählen und den schrittweisen Anweisungen folgen.
Anstelle eines neuen Reagenzienpacks werden die Flaschen des vorhandenen Packs mit dem entsprechend benötigten Volumen (110 bzw. 220 mL) aufgefüllt.
Die Abfallflasche wird in eine Schottflasche umgegossen, autoklaviert und anschliessend in den Trypanblau-Abfall entsorgt.

3. Einschalten und Ausschalten der Geräte

Einschalten:

- ViCell einschalten (Schalter auf der Rückseite)
- Computer einschalten
- Software „ViCELL XR 2.03“ starten

Ausschalten:

- Software schließen
- Rechner herunterfahren
- ViCell ausschalten

4. Zellzählung

Anforderungen an die Zellsupension:

- Probenvolumen: minimal 0,5 mL, maximal 1,5 mL im Probengefäß
- Konzentrationsbereich (Herstellerangaben): $1{,}0 * 10^4$ bis $1{,}0 * 10^7$ Zellen/mL
- Proben mit einer Konzentration > $1{,}0 * 10^7$ Zellen/mL müssen vorverdünnt werden
- Proben, die Carrier enthalten können, müssen filtriert werden (< 100 µm), z.B. mit:
  - Partec Celltrics 100 µm, Nr. 04-0042-2318)
  - Becton Dickinson Bioscience Discovery Labware, Cell strainer, 70 µm, Nr. 352235

Messung:

5.1. Probe in Original-Probengefäß pipettieren und in das Probenkarussell stellen
5.2. „Log in sample“auswählen, dann im Untermenü eingeben:
- Pobenposition im Karussell angeben
- falls nötig: Probenbezeichnung eingeben

- Zelltyp auswählen (Standard: MDCK 50)
- „Dilution factor“ überprüfen: für unverdünnte Proben: 1.0
- für sehr wichtige Proben: „Save images“ auswählen (Speicher: 1 MB/Bild)
- Speichern der Ergebnisse als eigene Excel-Datei oder als Zeile in „Multi-run file“: „bpt_datensammlung.xls“ als Standarddatei auswählen
- zum Messen: „OK“ oder nächste Probe eingeben („Next sample“)

5.3. Start der Messung: „Start queue“, Dauer einer Messung: 3 Minuten

5.4. Gerät reinigt sich selbständig, Probengefäß wird ausgeworfen

5.5. das Karussell wird nach weiteren Proben durchsucht, die dann mit fortlaufender Nummerierung gemessen werden (sofern nicht anders eingelogt)

5.6. Speicherort für gezählte Proben (in Excel-Dateien): lokal und im Netzwerk
c:\daten\ViCell\Excell\
h:\bio\daten\vicellxr\Excell\
Wenn auf der lokalen Festplatte (c:\) kein Speicherplatz mehr vorhanden ist, müssen die lokalen Dateien in den gleichen Ordner auf dem Laufwerk (h:\) kopiert werden. Nach der Sicherung können die lokalen Dateien gelöscht werden. Die Ordner dürfen nicht gelöscht oder umbenannt werden.
Bei Problemen mit dem Speichern auf Spiegellaufwerk Software neu starten.

6. Aufzeichnung von Bioprozessen

Um Zellzählungen verschiedener Proben einer Zeitreihe zusammen zu speichern und auszuwerten, ist es sinnvoll diese als „Bioprocess“ zu sammeln und in einer Datei abzulegen.

- „File“ => „New Bioprocess“
- Bezeichnung für den Prozess vergeben, z.B. Fermentation100
- Zelltyp auswählen
- Speicherdatei auswählen, Daten werden im Unterordner \data\ abgelegt
- in der linken Menüleiste wird ein Icon hinzugefügt (Symbol: Erlenmeyerkolben)
- Messen der Proben des Prozesses: Icon anwählen und Probe eingeben („Log in sample“)

7. Messen von infizierten Zellproben

Mit dem ViCell können auch Zellzählungen von infizierten Kulturen gemacht werden. Dabei sind folgende Besonderheiten zu beachten:

- Vor dem Messen: die Schale mit gebrauchten Probengefäßen (innen) sowie die Abfallflasche entleeren
- Probengefäße unter der Virusbank befüllen
- Nach dem Messen: Schale in den Probengefäß-Virusabfall entleeren und desinfizieren, Inhalt der Abfallflasche in flüssigen Virusabfall geben

8. Enfernung von Microcarriern aus der Flusskammer

Die Flusskammer hat eine Höhe von ca. 100 µm. Daher können sich Microcarrier, die sich in den Proben befinden, in der Kammer festsetzen. Das kann zu veränderten Messwerten führen.
Um Microcarrier aus der Kammer zu entfernen folgende Prozedur durchführen:

- Probengefäß mit 2,5 mL verdünnter Natriumhypochlorid-Lösung (10 %ig, Sigma) füllen und in die erste Position des Probentellers stellen (1:10 verdünnen: 0,250 mL Natriumhypochlorid-Lösung + 2,25 mL Wasser)
- Befehl „Decontaminate“ im Menü „Instrument“ ausführen, dabei Anweisungen befolgen
- Die Reinigung dauert ca. 13 Minuten.
- Anschliessend kontrollieren, ob die Flusskammer frei ist („Instrument“ -> „Live-Image“)

Die Option „Live-Image“ wieder deaktivieren

10.4.7 Arbeitsanweisung Nr. V/ 03 (Virus propagation in culture vessels)

Datum: 08.05.2000	**Autor: Dr. Annett Kiesel**	**geprüft:**
überarbeitet: 08.11.2005	**Autor: Claudia Best**	**geprüft:**
überarbeitet: 18.04.2006	**Autor: Claudia Best**	**geprüft:**
überarbeitet: 26.09.2007	**Autor: Claudia Best**	**geprüft:**

Virenvermehrung in Kulturflaschen

1.0 Ziel

Viren gehören nicht zu den Lebewesen im engeren Sinne, da sie sich u. a. nicht selbständig vermehren können. Zur Vermehrung benötigen Viren einen Wirt, der die Replikation und Proteinbiosynthese der viruseigenen Erbinformation (RNA oder DNA) und der virusspezifischen Proteine übernimmt. Es ist dabei natürlich wichtig, daß der Wirt (z. B. die MDCK-Zelle), noch vital genug ist, um diese Stoffwechselleistungen zu erbringen.

2.0 Material

- Virusbeimpfungsstandard (Lagerung: - 70 °C, N. 1.11)
- MDCK Zellkultur mit konfluent gewachsenen Zellen **4 – 6 Tage alt** (T-Flasche, Rollerflasche, Bioreaktor)
- Trypsinlösung zur Virusinfektion (**500 U/mL oder 5000 U/mL**, Lagerung -20 °C, N. 1.06)
- V-Medium (Glasgow-MEM mit 1% Lab-M-Peptone, Lagerung: 4 °C N. 1.13)
- steriles PBS (20 °C, RT, N. 1.06)
- sterile Pipetten, Pipettierhilfe
- S2-Sterilbank
- Meliseptol, MBT oder anderes für behüllte Viren zugelassenes Desinfektionsmittel
- Autoklavierbeutel für den Abfall

3.0 Methode

- unter der S2-Sterilbank, das alte Medium der Zellkultur in eine sterile Abfallflasche abgießen
- die Zellen mit steriler PBS-Lösung 3x waschen, zwischendurch das PBS in die Abfallflasche abgießen
- V- Medium je nach Volumen der Zellkultur dazu geben

- danach die berechnete Menge an Trypsinlösung, als auch vom Virusbeimpfungsstd. dazugeben
- die Verschlußkappen der Zellkulturflaschen werden mit Parafilm abgedeckt, danach für 3 Tage bei 37 °C in den CO_2- Brutschrank stellen (N.1.07)
- alles, was mit den Viren in Kontakt kam, muß vor dem Entnehmen aus der S2- Sterilbank von außen mit **MBT** desinfiziert werden (Einwirkzeit des Desinfektionsmittels beachten, i. d. R. ca. 2 min)
- Abfallbeutel nach Gebrauch gründlich verschließen (z. B. zukleben) und sobald wie möglich autoklavieren (20 min bei 121 °C).
- wenn verbrauchte Medien mit Virusmaterial anfallen, diese mit 2%iger Essigsäure desinfizieren (10 – 20 mL/L; bei Medium mit Phenolrot bis Farbumschlag auf gelb)

Kulturgefäß zum Beimpfen	Menge an **V-Medium** (GMEM+ Lab-M-Pepton)	Menge an **Trypsin (500 U/ mL)**	„**Standard**"-Menge an **Viruslösung**
T25 (25 cm^2)	10 mL	0,1 mL	0,04 mL
T75 (75 cm^2)	50 mL	0,5 mL	0,20 mL
T175 (175 cm^2)	125 mL	1,0 mL	0,40 mL
RF (850 cm^2)	250 mL	2,5 mL	1,00 mL
Sixfors (Carrier, Cytodex 1)	500 mL	5,0 mL	2,00 mL
Wavereaktor (Carrier, Cytodex 1)	1,0 L	10,0 mL	variabel, je nach MOI
DasGip Anlage (Carrier, Cytodex 1)	1,0 L	10,0 mL	variabel, je nach MOI
Biostat B-Plus (Carrier, Cytodex 1)	1,0 L	10,0 mL	variabel, je nach MOI
		Trypsin 5000 U/mL	
Bioreaktor 5 L (Carrier, Cytodex 1)	4,50 L	5,0 mL	Std. 10,0 mL
Bioreaktor 15 L (Carrier, Cytodex 1)	15,0 L	15,0 mL	variabel, je nach MOI

4.0 Lagerung

Die Viren können vor der Ernte direkt in den Zellkulturgefäßen eingefroren werden. Sie halten sich bei –70°C mehrere Jahre, bei –20°C mehrere Monate. Kurzfristig (max. 8 Wochen) kann Virusmaterial in größeren Volumen bei 2°C bis 8°C gelagert werden, z. B. vor weiteren Aufarbeitungen.

5.0 Arbeitsblatt

V/ 03.1

6.0 Beispielberechnung des MOI´s

MOI = **M**ultiplicity **o**f **I**nfection Anzahl der

$TCID_{50}$ Wert des Virusbeimpfungsstd. : 4,30 x 10^7 Viren/ mL

Ermittelte Gesamtzellzahl z. B. von RF: 1,25 x 10^7 Z/mL * 30 mL (15 mL Trypsin + 15 mL FCS)

= 37,5 x 10^7 Zellen gesamt

7.0 Bespielberechnung der Trypsinmenge zur Virusinfektion

Trypsinkonzentration der Stammlösung : 5000 Units/ mL

Gewünschte Trypsinkonzentration pro Zelle: **2,0 * 10^{-6} Units/ Zelle** (MDCK)

Zellzahl nach 96 h z.B. im Bioreaktor: 1,0 x 10^6 Z/ mL * 4500 mL = **4,50 * 10^9 Zellen**

Zellzahl nach 96 h z.B. im Bioreaktor: 1,0 x 10^6 Z/ mL * 4500 mL = **4,50 * 10^9 Zellen**

$TCID_{50}$ Wert des Virusbeimpfungsstd. : 1,59 * 10^7 V/ mL

Gewünschter MOI – Wert: 0,025

Zellzahl nach 96 h z.B. im Sixfors: 1,0 x 10^6 Z/ mL * 500 mL = **5,0 * 10^8 Zellen**

5,0 * 10^8 Zellen	^	**MOI 1,00**
5,0 * 10^7 Zellen	^	**MOI 0,10**
5,0 * 10^6 Zellen	^	**MOI 0,01**
2,5 * 10^7 Zellen	^	**MOI 0,05**
1,25 * 10^7 Zellen	^	**MOI 0,025**

$$\frac{1{,}59 * 10^7 \text{ Viren}}{1 \text{ mL}} = \frac{1{,}25 * 10^7 \text{ Zellen}}{X \text{ mL}} = 0{,}786 \text{ mL} = 786 \mu\text{L Virusmenge zur Beimpfung}$$

10.4.8 SOP V/05 HA-Assay

Version: 2.2 (20.01.2011) Author: Verena Lohr Approved:

Hemagglutination assay (HA assay)

This SOP is based on the SOP written by Bernd Kalbfuß, Version 2.1 (04.12.2006)

1. Introduction

The HA assay is used to detect influenza virus particles (infectious and non-infectious). Influenza viruses carry the protein hemagglutinin (HA) on their surface which binds to specific glycosylation patterns on proteins which are located on the outer membrane of a cell. Thus, virus particles bin to cells and by using erythrocytes as cell system, influenza virus particles can cross-link erythrocytes with each other. This agglutination of erythrocytes can be observed in wells of a round bottom well plate as agglutinated erythrocytes sediment like a carpet at the bottom of the well instead of a point-like sedimentation.
By titrating the virus containing sample, one can determine a critical concentration of the sample at which this switch in sedimentation behaviour occurs. The negative logarithm of this dilution has been defined as the logarithmic HA titer (or simply log-titer) and is a measure for the concentration of influenza virus particles in the sample. The inverse of the dilution has been termed HA activity with units HAU/100 µL and is also supposed to be proportional to the number of virions in the sample.

There are two ways in which one can analyze the HA assay (procedure of pipetting is the same for both methods):

i) a classical analysis in which the experimenter visually evaluates the HA titer
ii) a photometric analysis which uses an automated procedure in order to minimize subjectivity and which includes an additional dilution step that increases sensitivity and reduces the error of the method

2. Materials

- Protective clothing: lab coat, protective gloves (Nitrile)
- Centrifuge (e.g. Primo R, Hera, N1.06)
- Sterile kryotubes
- Influenza virus samples (active or chemically inactivated)
- Internal HA standard (= control which is an chemically inactivated influenza virus sample with defined HA titer, stored at -80°C in N1.11, produced as described in SOP HA assay from Bernd Kalbfuß, Version 2.1 (04.12.2006))
- Erythrocyte suspension (conc. approximately 2.0×10^7 erythrocytes/mL, stored at 4 °C in N1.06, produced as described in SOP V/07 from Claudia Best (07.06.2007))
- Unsterile phosphate buffered saline, PBS (stored in N1.06, produced as described in SOP M/01 from Claudia Best (26.09.2007))

- Unsterile transparent 96well round bottom microtiter plates (stored in N1.06, e.g. Greiner Bio-One, Cat.No. 650101) + transparent disposable lids (stored in N1.06, e.g. Greiner Bio-One, Cat.No. 656101)
- 100 µL micropipette + disposable tips
- 8x100 µL or 8x300 µL multichannel micropipette + disposable tips
- Electronic 8x1200 µL multichannel pipette + 1250 µL disposable tips
- 2 reservoirs for multichannel micropipette (PBS, erythrocyte suspension)
- Plate photometer (e.g. Tecan spectra, Tecan Instruments, N1.07)

3. Sample preparation

Infected cell culture with cells and without microcarrier should be filled directly into sterile kryotubes or other sterile tubes and centrifuged at 300xg for 5 min at 4 °C. If cells can not be settled at this g force, choose an appropriate centrifugation setting. After the centrifugation step transfer the supernatant into a new sterile kryotube and freeze at -80 °C.

4. Assay procedure

It is absolutely necessary to pipet exactly in this assay!!
Active samples have to be handled under S2 work bench! For handling outside the safety hood (e.g. when scanning the microtiter plate with the spectrometer), keep disinfectant or citric acid ready in case of accidental spillage!

4.1 Classical method

The titration of influenza virus by the classical method is based on the method described by Mahy and Kangro (Mahy and Kangro 1996b).

1. Pre-dilute samples which are known to be highly concentrated in PBS (all samples which have a HA activity above 3.0 log HA units/100 µL should be diluted). Typically, a 1:10 pre-dilution is sufficient. Samples from cell culture normally do not require this pre-dilution. However, this has to be decided from the assay performer.

2. Fill the wells of column 2-12 with 100 µL PBS each. Wells B, D, F and H of column 1and 2 are filled with 29.3 µL PBS.

3. Perform the following steps with a 100 µL pipette under S2 work bench! Don't spray disinfectant onto reservoirs and microtiter plates.
   The wells 1 and 2 of row A are filled with 100 µL of internal HA standard. Beneath these, a pre-dilution of internal HA standard is prepared by adding 70.7 µL of HA standard to wells 1 and 2 of row B. These 4 wells are prepared accordingly for the samples in rows 3 to 8. This means that on each plate 3 samples can be prepared. If there are more samples, an additional plate is necessary. Standard is necessary on every second plate.

Pipetting scheme for pipetting internal HA standard and samples onto microtiter plate

	1	2	3
A	100 µL HA standard	100 µL HA standard	…
B	70.7 µL HA standard 29.3 µL PBS	70.7 µL HA standard 29.3 µL PBS	...
C	100 µL sample 1	100 µL sample 1	…
D	70.7 µL sample 1 29.3 µL PBS	70.7 µL sample 1 29.3 µL PBS	…
E	...	...	…

4. Mix column 2 three times with a multichannel pipette and transfer 100 µL of column 2 to column 3. Empty the pipette tips completely once before the transfer. Mix again three times and continue the serial dilution until the end of the plate (column 12). The remaining 100 µL should be disposed. Each well has to be filled with 100 µL after finishing these steps. Add 100 µL of erythrocyte suspension into each well by using an electronic multichannel pipette. Mix the suspension well before you start! Start pipetting at the column with the highest dilution (column 12. *For each plate new tips have to be used!*
5. Each well which has been pipetted faulty should be marked as the values from these wells need to be eliminated during assay evaluation!
6. Incubate the plates for at least 3 hours under the work bench. If the assay is not analyzable, incubation must be prolonged (over night if necessary).
7. Evaluate the results visually. Therefore, mark every well which shows a perfect erythrocyte dot with a (●) and each imperfect dot with a (○). Record your findings by taking the document “AB-HA_Testauswertung_3.pdf”. The last dilution with an imperfect dot is the end point of the titration and is expressed as log HA units per test volume (100 µL). The inverse of this dilution gives the HA activity [HAU/100 µL].
8. Compare the measured titer of the internal standard with its nominal titer. The difference (*nominal-measured*) has to be added to the titer of each sample. If two or more standards were analyzed (e.g. because 3 plates were assayed) use the mean difference. If the measured titer of internal standard is more than 0.3 log HAU/100 µL different from its nominal titer, re-do the whole assay!
9. After evaluation of the titer microtiter plates scan them (see section 4.1) or dispose them into S2 waste!!

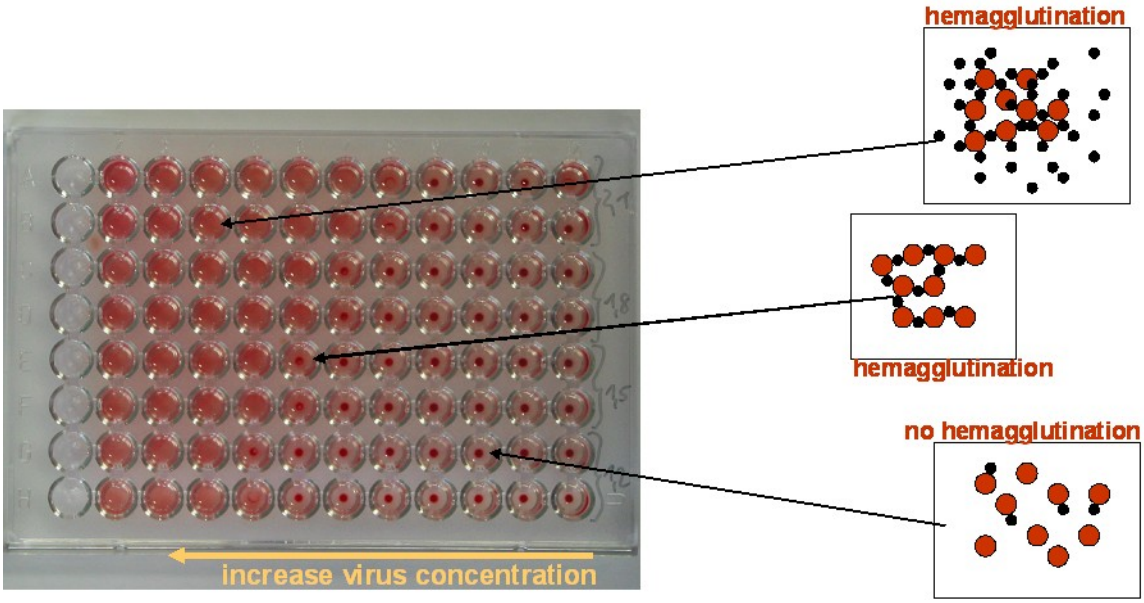

Scheme for determination of HA titers in micro titer plate (example shows HA titers from 1.2-2.1 log HA units/100 µL in double determination)

Overview on dilutions and resulting HA titers (log HA units/100 µL)

	1	2	3	4	5	6	7	8	9	10	11	12
Dilution	1:1	1:2	1:4	1:8	1:16	1:32	1:64	1:128	1:256	1:512	1:1024	1:2048
HA titer (100 µL sample)	0	0.3	0.6	0.9	1.2	1.5	1.8	2.1	2.4	2.7	3.0	3.3
HA titer (70.7 µL sample)	0.15	0.45	0.75	1.05	1.35	1.65	1.95	2.25	2.55	2.85	3.15	3.45

4.1.1 Points to consider

- The detection limit of this assay is 0.15 log HAU/100 µL. This corresponds to approximately $2.0x10^7$ virions/mL; assuming that the number of erythrocytes is proportional to the number of virus particles (each virus particle binds to one erythrocyte).
- The assay has been validated with a standard deviation of +- 0.03 log HAU/100 µL which is the dilution error.
- The confidence interval for HA activity was determined to be +15/-13 % (with a confidence level of 95 %).
- The validation has been made for the assay procedure which is described here. If you change singular steps in your procedure, be aware that validation is not valid then.
- Before you start with serious analyses, train yourself in pipetting accurately and precisely, e.g. by measuring standard samples several times.

- HA activity may suffer depending on sample treatment and storage conditions. Thus, do not freeze a measured sample and re-thaw it. Probably, HA titer has then been changed.

4.2 Photometric analysis

In order to minimize subjectivity (dependence on the experimenter), the titration result is evaluated photometrically using an automated procedure. However, this evaluation is restricted to samples with titer >1.0 log HAU/100 µL. Otherwise, sample titers have to be evaluated with the classical method.

4.2.1 Measurement of extinction

1. Perform all steps which are described for the classical method.
2. Cover microtiter plates containing active virus samples with an appropriate lid.
3. Make sure that Tecan photometer is switched on. Open the software “iControl” and choose “HA protocol” from the list of used protocols. The settings should be defined as follows: Messfilter 700 nm, Referenzfilter none, 10 Blitze, Temperatur 0.0 °C, Schüttelmodus none. (Changes can be made by clicking on button “Messparameter definieren”, but should not be done for standard HA protocol.)
4. After having inserted the plate into the reader, click the button “Messung starten”. You will be asked for a file name first and to put your plate onto the tray afterwards. The measurement will be carried out immediately afterwards.
   It is of utmost importance to remove either the lid before scanning and to remove any condensed water from the bottom of a microtiter plate before scanning!!
5. Save extinction data as Excel-file in the folder “/bpt/data/Tecan/HA_assay/2010/…” using the file name pattern “<Number>-<Date>_<Experimenter>.xls (e.g. 145_10-03-31_CB). If more than one plate will be measured, let the excel file from the first plate open. Then, the results from the following plate will be saved as a new sheet in this file. You have to rename the sheets after your measurement in order to document which sheet belongs to which plate.
6. Repeat step 4 and 5 for each plate of the assay run.

4.2.2 Evaluation of HA titers

A data evaluation template (Excel-file) has been prepared. The evaluation procedure is described in the following. You have to enable macros for the sheet to work properly!

7. Open the data evaluation template (“/bpt//Labor/HA_neu/Data_Evaluation_ Template.xls”) and save a **copy** in the appropriate folder (/bpt/usp/Labor/HA_neu/data/2010/...).
8. Import your extinction data. Therefore, copy all values and paste them into data-sheet. Delete extinction values of all wells that suffered from erroneous pipetting! As long as affected wells are not within the zone of transition, the assay result may be unaffected.

9. Adjust the sample names and dilutions in the “Report” sheet. Fill all empty header fields and transfer the remarks from the run protocol. Specify the internal standard used and the position of the internal standard (normally, position 1 and 9). If only one standard was measured, specify the same position twice.
10. Click “Evaluate” to start HA titer evaluation.
11. Check difference between nominal titer of the standard and the evaluated titer. Re-do the assay if both values differ more than 0.3 log HAU/100 µL.
12. Check all fitted curves in the “Evaluation” sheet. If fitting of extinction values has not been made by a sigmoidal curve, then re-analyze the sample. Be careful, if this maybe is due to a low titer of the sample. Then take titers evaluated by the classical method.

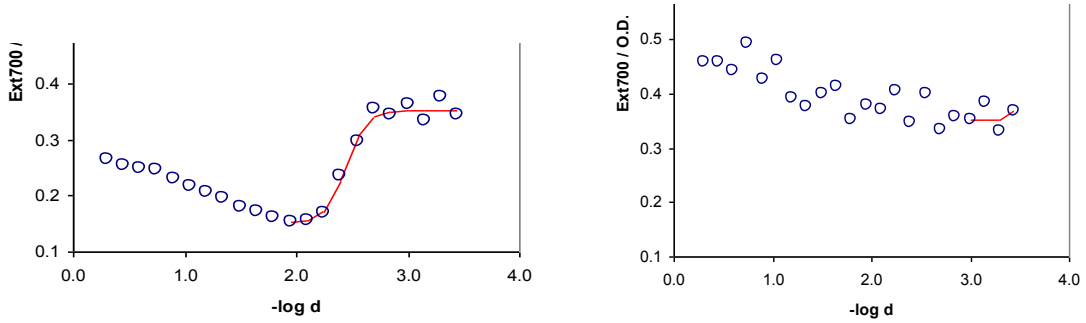

Evaluation of the transition point by a Boltzmann function. Left: correct fitting, right: erroneous fitting which would lead to high titer evaluation if curve is not checked and rejected

13. Compare the evaluated titers with the results obtained by the classical method. The discrepancy should be less than 0.3 log HAU/100 µL.
14. Save the document and make at least one hardcopy of the “Report” and “Evaluation” sheets. Documents are collected in a folder located in N1.07 and N0.13.

5. Sample storage

If samples are kept at below -70 °C, they can be stored up to five years without loss of HA activity. Anyway, this holds true for samples which have been prepared as described in this document (see sample preparation). After this period, it cannot be guaranteed that measured HA activities resemble the original values.

10.4.9 Arbeitsanweisung V/08_Version 2.1 ($TCID_{50}$ Assay)

Datum: 2.06.08 Autor: Ilona Behrendt geprüft:
geändert: 26.09.2011 Autor: Britta Isken geprüft:

Bestimmung des $TCID_{50}$

1.0 Ziel

Bestimmung der Virusverdünnung, bei der 50% der adhärenten Zellen infiziert werden.

2.0 Material

2.1. Zellanzucht und Virusvermehrung

- 4-8 Tage alte konfluente MDCK-Zellen aus Zellkulturflaschen (T175 oder RF)
- PBS steril (Arbeitsanweisung Nr. M/01)
- Trypsin 10000 BAEE / mL in Milli-Q-Wasser, sterilfiltriert (Trypsin, Sigma, Bestell-Nr. T-7409) Lagerung bei –70 °C für Virusinfektion
- Zellkulturmedium (GMEM + 1% Lab-M-Pepton + 10% FCS) siehe Arbeitsanweisung Nr. M/04
- Virusmedium (GMEM + 1% Lab-M-Pepton) siehe Arbeitsanweisung Nr. M/04
- Gentamicin 10 mg / mL (Invitrogen, Bestell-Nr. 11130-036) Lagerung: Raumtemperatur
- 96-Wellplatten 400 µL Inhalt steril mit flachem Boden mit Deckel (für Zellkultur) (Cellstar, Greiner bio-one, Bestell-Nr. 655180)
  (für jede Probe wird eine Wellplatte benötigt)
- Reaktionsgefäße 1,5 mL, sterilisiert für Verdünnungsreihen
- sterile Pipetten, Pipettierhilfe
- 100 µL Pipette
- Elektronische Einkanalpipette 1 mL (Eppendorf)
- Elektronische Mehrkanalpipette 1250 µL (Eppendorf)
- Pipettenspitzen 100 µL (Plastibrand, steril)
- Pipettenspitzen 1250µL (Eppendorf, steril)
- Multipette mit Combitips 10 ml (Eppendorf, Combitips plus biopure)
- 1 sterile Schottflaschen (250 oder 500 mL)
- 4 Pipettierbehälter, sterilisiert
- 2 kleine Laborschalen, sterilisiert
- Warnhinweisaufkleber: Biogefährdend

2.2. Fixierung und Färbung

- 80%ige Acetonlsg. in Wasser (Aceton, p.A.)
- Primärantikörper entspechend dem zu testenden Virus
  z.B. - (Equine Influenza A Ziegenserum , final bleed, goat 613, vom 2.08.01, nano

Tools)(1:100 mit PBS verdünnt)
- Influenza Anti A/Wisconsin/67/2005 H_3N_2 (HA Serum sheep) von NIBSC
- Influenza Anti B/Malaysia/2506/2004 (HA Serum sheep) von NIBSC

- Influenza Anti A/PR/8/34 H_1N_1 (HA Serum sheep) von NIBSC
- PBS steril (Arbeitsanweisung Nr. M/01)
- konfluent bewachsene Zellkulturflaschen (T75 oder RF)
- Sekundärantikörper (Invitrogen, Bestellnr.: A-11015)
- 100 µL 8-Kanal-Pipette mit Pipettenspitzen
- Laborschale
- 3 Pipettierbehälter
- Entsorgungsbehälter Aceton

3.0 Methode

Anmerkung zur Generierung der Proben: Standardmäßig wird der Infektionsüberstand vor dem Wegfrieren nicht zentrifugiert, in Ausnahmefällen (wie MDCK.SUS2 Zellen) kann eine Zentrifugation bis 5000 x g durchgeführt werden, da sie keinen Einfluss auf den $TCID_{50}$ Wert hat.

3.1 Zellanzucht und Virusvermehrung

A) Zellanzucht
- konfluente MDCK-Zellen aus Zellkulturflaschen 3-mal mit PBS waschen und mit der vorgeschriebenen Menge Trypsin (1 mg/mL) 20 min bei 37 °C abtrypsinieren, mit Z-Medium abstoppen (siehe Arbeitsanweisung Nr. Z/04)
- Zellkulturmedium mit Gentamicin vermischen (100 mL Zellkulturmedium mit 1 mL Gentamicin)
- abtrypsinierte Zellen mit angesetztem Zellkulturmedium auf eine Zellzahl von 4 - 5 * 10^5 Zellen / mL verdünnen (siehe Arbeitsanweisung Zellzahlbestimmung)
- 10 mL der Zellsuspension werden ca. für eine Zellkulturplatte benötigt
- je 100 µL der Zellsuspension werden mit der Elektronischen 8-Kanalpipette in jedes Well der Zellkulturplatte pipettiert
- die Zellen 1 - 2 Tage bei 37 °C mit 5 % CO_2 inkubieren (mikroskopische Beurteilung der Konfluenz der Zellen → müssen dicht bewachsen sein – wenn dies nicht der Fall sein sollte, ist der Versuch hier abzubrechen)

B) Herstellen der Virusverdünnung
- Virusmedium mit Trypsin und Gentamicin versetzen, 100 mL Medium + 20 µL Trypsin + 1,0 mL Gentamicin (100 mL VM reichen für ca. 10 Verdünnungsreihen) → VM
- Je 900 µL des Virusmediums in 8 – 10 Eppendorfcups (je nach benötigter Verdünnungsstufen) pipettieren. Virusverdünnung nach dem folgenden Schema in Eppendorfcups herstellen: mit einer Eppendorfpipette 100 µL aus der zu bestimmenden Probe oder dem Standard entnehmen und in das erste Eppendorfcup geben, 5 mal durch auf- und abpipettieren mischen, mit einer neuen Pipettenspitze 100 µL in das nächste Eppendorfcup geben, fortfahren bis zum Ende.

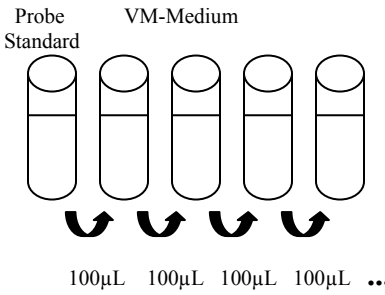

10^0	10^1	10^2	10^3	10^4	10^5	10^6	10^7	10^8

C) Virusvermehrung

- die Zellkulturplatten 2 mal mit je 100 µL PBS je Well mit der elektronischen 8-Kanal-pipette waschen (entleeren: in Laborschale ausschütten)
- mit einer Eppendorfpipette je 100 µL der Virusverdünnung auf je 8 Wells der Zellkulturplatte geben (mit der höchsten Verdünnungsstufe beginnen)
- in die Reihen 1, 2, 11 und 12 werden nur je 100 µL Virusmedium (mit Trypsin + Gentamicin) je Well gegeben (diese Wells dienen als Nullkontrolle, Randeffekte können dann ausgeschlossen werden)
- einzusetzende Verdünnungsstufen:
  bei einem HA über 2,7: $10^3 – 10^{10}$
  bei einem HA von 2,1 bis 2,7 (Standard, Saatvirus für Fermentationen) : $10^1 – 10^8$
  bei einem HA unter 2,1: $10^0 – 10^7$

	1	2	3	4	5	6	7	8	9	10	11	12
A	Virus-Medium	Virus-Medium	**10^1**	**10^2**	**10^3**	**10^4**	**10^5**	**10^6**	**10^7**	**10^8**	Virus-Medium	Virus-Medium
B	Virus-Medium	Virus-Medium	**10^1**	**10^2**	**10^3**	**10^4**	**10^5**	**10^6**	**10^7**	**10^8**	Virus-Medium	Virus-Medium
C	Virus-Medium	Virus-Medium	**10^1**	**10^2**	**10^3**	**10^4**	**10^5**	**10^6**	**10^7**	**10^8**	Virus-Medium	Virus-Medium
D	Virus-Medium	Virus-Medium	**10^1**	**10^2**	**10^3**	**10^4**	**10^5**	**10^6**	**10^7**	**10^8**	Virus-Medium	Virus-Medium
E	Virus-Medium	Virus-Medium	**10^1**	**10^2**	**10^3**	**10^4**	**10^5**	**10^6**	**10^7**	**10^8**	Virus-Medium	Virus-Medium
F	Virus-Medium	Virus-Medium	**10^1**	**10^2**	**10^3**	**10^4**	**10^5**	**10^6**	**10^7**	**10^8**	Virus-Medium	Virus-Medium
G	Virus-Medium	Virus-Medium	**10^1**	**10^2**	**10^3**	**10^4**	**10^5**	**10^6**	**10^7**	**10^8**	Virus-Medium	Virus-Medium
H	Virus-Medium	Virus-Medium	**10^1**	**10^2**	**10^3**	**10^4**	**10^5**	**10^6**	**10^7**	**10^8**	Virus-Medium	Virus-Medium

- die Platten mit Virus mit einem Warnhinweis versehen und 1 Tag bei 37 °C mit 5 % CO_2 inkubieren

D) Trypsinzugabe

- Virusmedium mit Trypsin und Gentamicin versetzen (100 mL Medium + 40 µL Trypsin + 1 mL Gentamicin)
- Je 100 µL dieses Mediums in jedes Well pipettieren – elektronische 8-Kanalpipette, darauf achten dass kein Virus verschleppt wird (von rechts nach links – von der höchsten Verdünnungsstufe zur niedrigsten pipettieren, Reihe für Reihe) nach jeder Platte die Pipettenspitzen verwerfen
- die Virusplatten nochmals 1 Tag bei 37 °C mit 5 % CO_2 inkubieren

3.2 Fixierung und Färbung

A) Vorbereitung des Primärantikörpers (nur bei dem Equine Influenza A Ziegenserum notwendig, wenn kein gereinigter Antikörper mehr vorhanden ist)

- der Primärantkörper für Equine Influenza A Ziegenserum ist ein polyklonaler Antikörper gegen den Pferdeinfluenza-Virus, aber auch gegen Zellbestandteile, deshalb müssen die Antikörper gegen die Zellen vorher absorbiert werden, sonst überdecken sie die Fluoreszenz der mit Viren infizierten Zellen
- 1 – 2 Tage alte konfluent bewachsene Zellkulturflasche dreimal mit PBS waschen
- auf eine T25 – Flasche 1 mL , auf eine T75 – Flasche 3 mL des verdünnten Primärantikörpers geben und 30 min bei 37 °C inkubieren (1 mL 1:100 verdünntes Serum reicht für eine Zellkulturplatte – dementsprechende Menge inkubieren)
- der gereinigte Primärantikörper kann bei –20 °C eingefroren werden

B) Fixierung

- Medium in Laborschale mit vorgelegter 2%iger Essigsäure in der Sterilbank abgießen und virusgerecht entsorgen
- auf jedes Well 100 µL eiskalte 80 %ige Acetonlösung pipettieren (Acetonlsg.in Eisbehälter stellen – nicht in den Kühlschrank → Kühlschränke sind nicht Ex geschützt)
- die Zellkulturplatten 30 min zum fixieren auf Eis oder in den Kühlraum stellen → Virus inaktiviert (die weiteren Schritte können außerhalb der Sterilbank durchgeführt werden)
- Zellkulturplatten 2 mal mit PBS spülen – (Aceton-PBS-Gemisch in Abfallbehälter sammeln- zur Entsorgung –Herrn Schäfer geben)

C) Färbung

- gereinigten Primärantikörper für Equine Influenza A Ziegenserum 1 : 100 mit PBS verdünnen, alle anderen Primärantikörper werden 1 : 200 verdünnt
- je 50 µL davon auf jedes Well mit elektronischer 8-Kanalpipetten geben und 60 min bei 37 °C inkubieren
- nach dieser Zeit 2-mal mit PBS waschen
- den Sekundärantikörper 1 :500 mit PBS verdünnen
- wieder je 50 µL davon auf jedes Well pipettieren und 60 min bei 37 °C inkubieren
- 2 mal mit PBS waschen, nach dem letzen Waschschritt 100 µL PBS auf jedes Well geben

4.0 Auswertung und Berechnung

- die Auswertung erfolgt an einem Fluoreszenzmikroskop
- jedes Well in dem Virus gefunden wird (fluoreszierende Zellen) wird als positiv gewertet (1), jedes Well ohne fluoreszierende Zellen als negativ (0) und in das Arbeitsblatt eingetragen
- die Berechnung erfolgt nach der Gleichung von Spearman und Kärber:

$$(\log \text{Virus } 100\%) + (0{,}5) - \frac{\text{kumulativ } 100\ \%}{\text{Anzahl Tests (pro Verdünnung)}} = \log \text{Virus} / 100\ \mu L$$

Beispiel:

	1	2	3	4	5	6	7	8	9	10	11	12
A	0	0	1	1	1	1	1	1	1	0	0	0
B	0	0	1	1	1	1	1	1	1	0	0	0
C	0	0	1	1	1	1	1	1	0	0	0	0
D	0	0	1	1	1	1	1	1	0	0	0	0
E	0	0	1	1	1	1	1	1	0	0	0	0
F	0	0	1	1	1	1	1	1	1	0	0	0
G	0	0	1	1	1	1	1	0	0	0	0	0
H	0	0	1	1	1	1	1	1	1	0	0	0
	0	**0**	**10^{-1}**	**10^{-2}**	**10^{-3}**	**10^{-4}**	**10^{-5}**	**10^{-6}**	**10^{-7}**	**10^{-8}**	**0**	**0**

0: kein Virus, negatives well; 1: Virus, positives well

Verdünnungsstufe	Anzahl positive wells / Gesamtzahl wells	Anzahl positiver wells kumulativ
10^{-5}	8 / 8	19
10^{-6}	7 / 8	11
10^{-7}	4 / 8	4
10^{-8}	0 / 8	0

Beispielrechnung:

(-5) + 0,5 - 19/8 = - 6,875 = y ; $10^{6,875}$ Viren/100µL = $10^{7,875}$ V/mL = 7,50 x 10^{7} Viren/mL

5.0 Festlegung des Referenzwertes

Für jeden neu hergestellten Standard wird von mindestens 2 Personen je zweimal eine Sechsfachbestimmung durchgeführt. Daraus wird der Mittelwert für den jeweiligen Standard berechnet, der als Referenzwert verwendet wird.

10.4.10 Arbeitsanweisung MoBi 1 (Western blot)

Datum:	**13.02.2009**	**Autor: Nancy Wynserski**	**geprueft:**
ueberarbeitet:	**07.07.2010**	**Autor: Björn Heynisch**	**geprueft:**

Western Blot mit anschließender Immundetektion

1.0 Ziel

Elektrotransfer von Proteinen auf eine Trägermembran nach zuvor erfolgter gelelektrophoretischer Auftrennung mittels SDS-PAGE.

2.0 Material

- Acrylamid 30 %
- Ammoniumperoxidisulfat (Applichem A3626,500)
- Aqua dest.
- β-Mercaptoethanol
- Bromphenolblau (Amersham Biosciences 17-1329-01)
- BSA (Applichem A3912.100)
- Farbstoff Ponceau Rot
- Glycin (Applichem A106.5000)
- Glycerol (Sigma. A1123)
- Methanol (Roth 4627.2)
- NaCl (Merck 1.06404.5000)
- PVDF-Membran (Millipore IPVH00010; Porengroesse 0,45 µm)
- SDS (Applichem A1112, 1000)
- SuperSignal® West Dura Extended Duration Substrate (Thermo Scientific-Pierce 34076)
- Temed (Amersham Biosciences 17-1312-01)
- Tris (Applichem A 1086.1000)
- Tris-Cl (Applichem A 3452.1000)
- Tween 20 (Merck 8.17072.1000)
- Protein Marker Magic Mark (Invitrogen)
- Milchpulver
- Geraetschaften:
  - Pipetten , Spitzen
  - Bechergläser , Rührfisch
  - Gelkammer, Gelkämme, Gelkassette, Glasplatten, Eis-Akku
  - Blotklemme, Pads und Filterpapiere

- Thermomixer , Zentrifuge
- Spannungsquelle
- Plastikwanne
- Rührer, Schüttler
- Whatman Papier

2.1. Puffer und Lösungen

→ APS (Ammoniumperoxidisulfat) 10 %ig
- 500 mg/5 ml in H_2O bidest.
- Aliquots à 500 µl bei -20 °C lagern

→ Bromphenolblau (gesättigt)
- 50 mg/100 ml in H_2O bidest.

→ BSA 3 %
- 3 g BSA/ 100 ml TTBS

→ Lämmlipuffer (4x)
- 250 mM Tris-Cl pH 6,8 2,0 ml (1.0 M) (12,114 g/100 ml)
- 40 % Glycerol 3,2 ml
- 8 % SDS 0,64 g
- 0,05 % Bromphenolblaulsg. 1.6 ml
- 10 % β-Mercaptoethanol 0,8ml
- H_2O bidest. 0,4 ml
- Aliquots à 500 µl bei -20 °C lagern
-

→ 10x Laufpuffer mit SDS (1 L)
- 1 % SDS 10 g
- 1,92 M Glycin 144 g
- 250 mM Tris 30,3 g
-

→ 10x Laufpuffer ohne SDS (1 L)
- 1,92 M Glycin 144 g
- 250 mM Tris 30,3 g
-

→ Sammelgelpuffer 0,5 M TricCl pH 6,8
- 12,114 g/ 200 ml in H2O bidest.
- Lagerung 4 °C
-

→ SDS 10 %ig
- 5 g / 50 ml in H_2O bidest.
-

→ Strip-Puffer pH 6,7 (1 L)
- 62,5 mM Tris 7,571 g
- 2 % SDS 20 g
- 100 mM β-Mercaptoethanol 350 µl/50 ml Puffer (Abzug!)
-

→ TBS 10x pH 7,6 (1 L)
- 200 mM Tris 24,2 g
- 1,37 M NaCl 80 g
- TTBS: TBS mit 0,1 % Tween 20
-

→ TTBS
- TBS + 0,1 % Tween 20
-

→ Transferpuffer

- 10 % MeOH
- 10 % Elektrophoresepuffer ohne SDS
- 80 % H_2O bidest.
-

→ Trenngelpuffer 1,5 M Tris-Cl pH 8,8

- 36,342 g/ 200 ml in H2O bidest
- Lagerung 4 °C

3.0 Methode

3.1. Herstellung SDS-Gel

- Kammer vorbereiten
- Glasplatten mit 1mm Spacern, vorher mit EtOH putzen, in den Glasplattenhalter einbauen und im Gießgestell einspannen
- zuerst ein Trenngel gießen und mit Isopropanol überschichten, ca. 45 min aushärten lassen
- danach Sammelgel gießen und die Kämme hineinsetzen

Trenngel 2x1mm

	7,5% Gel	8% Gel	10% Gel	12% Gel	15% Gel
H_2O	7,8	4,63	3,97	3,29	2,99
Acrylamid 30 %	2,5	2,66	3,33	4	5
Tris-Cl pH 8,8	2,5	2,5	2,5	2,5	2,5
SDS 10%	0,1	0,1	0,1	0,1	0,1
APS10%	0,1	0,1	0,1	0,1	0,1
TEMED	0,01	0,01	0,01	0,01	0,01

[ml]

Sammelgel 2x1ml

	3% Gel
H_2O	6,3
Acrylamid 30 %	1
Tris-Cl pH 6,8	2,5
SDS 10%	0,1
APS10%	0,1
TEMED	0,01

[ml]

3.2.Probenvorbereitung

- Proteinproben je nach gewünschter Konzentration einstellen
- mit 4x red. Lämmli Ladepuffer versetzen
- Proben 5min bei 95 °C im Thermomixer erhitzen, abkühlen lassen auf Eis
- zentrifugieren 10 sec

3.3. Gel beladen

Tipp: die Taschen vorher kennzeichnen, erleichtert das Auftragen der Proben

- Gelkammer mit Elektrophoresepuffer (SDS Laufpuffer) befüllen, Vorsicht: keine Luftblasen am Unterrand des Gels
- Kämme entfernen und die Taschen mit einer Spritze mit Laufpuffer ausspülen, da sich evtl. noch Gelreste in den Taschen befinden können
- 4 µl Marker (Magic Mark) und Proteinproben langsam in die Taschen pipettieren, max. 25 µl (extra lange Spitzen verwenden)
- Strom einstellen bei 15 mA pro Gel bis zum Erreichen des Trenngels, danach 25 mA pro Gel (Dauer bei 2 Gelen ca. 1,5 - 2h)

3.4.Blotten

- Pads und Filterpapiere in einer Schale mit Transferpuffer äquilibrieren
- Membran beschriften und äquilibrieren:
    - 15 sec Methanol
    - 2 min in H20 bidest.
    - mindestens 5 min in Transferpuffer
- Gel in Transferpuffer äquilibrieren
- Blotklemme mit schwarzer Seite nach unten in die Schale mit Transferpuffer legen
- Blotklemme zusammenbauen:
    - Pad
    - 2 Filterpapiere
    - Gel mit Lauffront nach innen
    - PVDF-Membran – Luftblasen wegstreichen
    - 2 Filterpapiere
    - Pad
- Klemmkasten in Vorrichtung einspannen (schwarz zu schwarz)
- Rührfisch in Plastikwanne
- Vorrichtung in Plastikwanne geben
- Eis-Akku einsetzen
- Kammer mit Transferpuffer auffüllen
- das ganze System in eine Schale auf Rührer setzen
- Strom: 100 V für 1 bis 1,5 h
- mit Farbstoff Ponceau Rot anfärben als Kontrolle für 1 min, mit fließendem Leitungswasser für einige Sekunden entfärben

3.5.Blockieren

- 1 h in TTBS (5 % Milchpulver oder 3 % BSA)
- 3 x 5 min waschen mit TTBS

3.6. Antikörper

- 1. AK über Nacht, 4 °C auf Schüttler
    - Verdünnung in TTBS (5 % Milchpulver oder 3 % BSA)
- 3 x 10 min inTTBS waschen
- 2. AK 1h bei RT
    - Verdünnung TTBS (5 % Milchpulver oder 3 % BSA)
- 3 x 10 min in TTBS waschen

3.6. Detektion

- 1,5 ml Pierce-Substratlösung für 2 Blots: 750 µl Lösung A + 750 µl Lösung B vermischen
- Mix auf Blot für 1 min inkubieren
- Blot in Folie auf ebener, lichtundurchlässiger Unterlage platzieren
- Blot scannen (siehe Anleitung Phospholumineszenzimager)

3.7 Strippen

- 350 µl β-Mercaptoethanol/50 ml Stripp-Puffer frisch dazugeben (Abzug !)
- Blot mit Stripp-Puffer im Wasserbad bei 50 °C für 10 min inkubieren
- 4 x 5min TBS
- mit dem Blockieren fortfahren

4.0 Verwendung

Der Western Blot dient zum immunologischen Nachweis bestimmter Proteine und ggf. ihrer posttranslationaler Modifikationen wie z.B. Phosphorylierungen.

5.0 Lagerung

Fertige Membranen können im getrockneten Zustand bei -80 °C gelagert und anschließend erneut gestrippt und mit Antikörpern analysiert werden.

5.1 Lagerung der durch RIPA Lyse gewonnenen Proben

Es erfolgte bisher keine systematische Überprüfung der Lagerbarkeit von Proben, die mittels RIPA Puffer gewonnen worden sind. Es gibt jedoch Anhaltspunkte für die Western Blot Analytik von Phosphoproteinen. Auf empirischen Erfahrungswerten basierend lässt sich sagen, dass nach mehr als 6 Monaten der Probenaufbewahrung bei -70°C es zu einer allmählichen Abnahme der Signalstärke im Western Blot kommen kann.

10.4.11 Arbeitsanweisung Nr. Mobi 2 (Real-time PCR)

Datum: 17.08.2010	**Autor: Nancy Wynserski**	**geprueft:**
ueberarbeitet:	**Autor:**	**geprueft:**

Real Time PCR

1.0 Ziel

Virusquantifizierung und Genexpressionsmessung in adhärenten Zellen

2.0 Material

2.1. Zellkultur Labor
- Zellkulturgefäß (für mind. 2E+05 bis max. 5E+06 Zellen/ml)
- Zellkulturmedium, Zellen, Virus entspechend Versuchsvorlagen
- PBS (Raumtemperatur) siehe Arbeitsanweisung M/01
- Trypsin/ EDTA-Loesung (0,05% Trypsin/ 0,02% EDTA, 37°C), 1:10-Verduennung aus Stammloesung, siehe Arbeitsanweisung M/07, (Lagerung +4°C, N.1.06)
- Trypsinlösung zur Virusinfektion (500 U/mL, Lagerung -20 °C, N. 1.06)
- Pipetten steril, Pipettierhilfe
- Spitzen steril,
- 2ml Tubes steril;
- S2-Sterilbank
- Meliseptol, MBT oder anderes für behüllte Viren zugelassenes Desinfektionsmittel
- Autoklavierbeutel für den Abfall

2.2. Molekularbiologisches Labor

- gestopfte Spitzen, (Gilson, Bestellnr. 1000µl DF1000ST; 200µl DF200ST; 30µl DF30ST; 10µl DFL10ST)
- Rotor-Gene SYBR Green PCR Kit (Qiagen, Bestellnr. 1054586)
- SP Rotor-Gene SYBR Green PCR Kit (Qiagen, Bestellnr. 1054605)
- RevertAid™ H Minus RT (Fermentas, Bestellnr. EP0452)
- Ribolook™ RNase Inhibitor (Fermentas, Bestellnr. EO0382)
- SafeSeal Tubes 1,5ml, 2,0ml (Sarstedt, Bestellnr. 72.706.400, 72.695.400)
- NucleoSpin RNA Virus (Macherey-Nagel Bestellnr. 740956.250
- NucleoSpin RNA II (Macherey-Nagel Bestellnr. 740955.250)
- Primer (siehe Methode RT, qRT-PCR; bzw. Primersequenzen)
- Rotor Disc (Qiagen, Bestellnr. 981311)
- Geräte: Heraeus Zentrifuge
  Thermocycler T3000
  Qiagility Roboter
  Rotor-Disc Heat Sealer
  Rotor-Gene Q

3.0 Methode

3.1.Zelleinsaat
- siehe Arbeitsanweisung Z/04
- das benötigte Zellkulturgefäß sollte nicht unter 2E+05 bzw. über 5E+06 Zellen/ml liegen (siehe Probenahme),
da sonst keine ausreichende Menge an RNA zur Verfügung steht oder es auch zu einer Überladung kommen kann
- Versuchsbedingungen beachten (Zelleinsaat, Zellanzuchtsdauer etc.)

3.2. Virusinfektion
- siehe Arbeitsanweisung V/03
- Versuchsbedingungen beachten (moi, Trypsinkonzentration etc.)

3.3. Probenahme

3.3.1 Überstandsproben
- Virusüberstand in 2ml Tube pipettieren
- bei 300g 5min abzentrifugieren (siehe Arbeitsanweisung Nr.V/05 HA Assay)
- Überstand in neues Tube pipettieren , Zellpellett für intrazelluläre RNA Probenahme aufbehalten
- Proben für Virus PCR und HA bei -80°C wegfrieren, sammeln

NucleoSpin RNA Virus Kit (Macherey-Nagel) :

-Aufbereitung: 600µl RAV1 (+ Carrier RNA) und 150µl Probe im 1,5ml Tube mischen und vortexen
- Inkubation 5min bei 70°C
- 600µl 96-100% igen Ethanol zugeben, 10-15 sec vortexen
- 700µl lysierte Probe auf NucleoSpin Säule geben, 1min 8000g zentrifugieren (2x), Durchfluss entfernen
- 500µl Puffer RAW zugeben, 1min 8000g zentrifugieren, Durchfluss entfernen
- 600µl Puffer RAV3 zugeben, 1min 8000g zentrifugieren, Durchfluss entfernen
- 200µl Puffer RAV3 zugeben, 5min 11000g zentrifugieren, Durchfluss entfernen
- NucleoSpin Säule in eine neues steriles Tube geben und mit 50µl 70°C warmen RNase freies H2O 1-2min inkubieren, zentrifugieren 1min 11000g
- Proben sofort auf Eis stellen, bzw wegfrieren bei -80°C

3.3.2 Zelluläre Proben
- Zellen mit 350µl RA1 Puffer + 1/100 β-Mercaptoethanol versetzen(siehe Protokoll RNA II Kit), durch mehrmaliges auf und ab pipettieren der Probe dann in 2ml Tube überführen, ggf. die restlichen Zellen von der Überstandsprobenahme mit dem selben Puffer aufnehmen

NucleoSpin RNA II Kit (Macherey-Nagel) :
- die Proben bei 11000g 1min durch Schreddersäule zentrifugieren

(ab diesem Schritt können die Proben gesammelt und bei -80°C weggefroren werden)
- 350µl 70% Ethanol zugeben, 2-5s vortexen
- RNA auf Säule geben, 30s 11000g zentrifugieren, Durchfluss entfernen
- 350µl 70% MDB Puffer zugeben, 1min 11000g zentrifugieren, Durchfluss entfernen
- 95µl rDNase reaction mixture (10µl rDNase + 90µl rDNase Puffer) zugeben, 15min bei RT inkubieren
- 200µl RA2 zu der rDNase mixture geben, 30s 11000g, Durchfluss entfernen
- 600µl RA3 Waschpuffer zugeben, 30s 11000g; Durchfluss entfernen
- 2500µl RA3 Waschpuffer zugeben, 30s 11000g; Durchfluss entfernen
- 60µl RNase freies Wasser zugeben, 1min inkubieren; 1min 11000g zentrifugieren
- Proben sofort auf Eis stellen, bzw wegfrieren bei -80°C
- Konzentrationsbestimmung am Tecan

3.4. Reverse Transkriptase PCR

3.4.1. RT von Überstandsproben

Ansatz: pro Reaktion ein 10µl Ansatz
5 µl probe
0,5 µl Uni12 Primer (1µg/µl)
65°C 5min (Thermocycler)
2µl Puffer
0,8 µl dNTP`s (12,5mMol)
0,25 µl Ribolook Inhibitor
0,5 µl HRT-
0,95µl RNase freies H2O
70°C 60min (Thermocycler)
4°C ∞

3.4.2. RT von Zellulären Proben

Ansatz: pro Reaktion in 10µl
zwischen 0,3 µg/µl bis max 1,2 µg/µl Probe einsetzen
Rest mit RNase freiem Wasser auf 5µl auffüllen
0,5µl OligodT Primer zugeben (0,5µg/µl)
65°C 5min (Thermocycler)
2 µl Puffer
0,8 µl dNTP`s (12,5mMol)
0,25 µl Ribolook Inhibitor
0,5 µl HRT-
0,95 µl RNase freies H2O
70°C 60min (Thermocycler)
4°C ∞

3.5. Real Time PCR

die Real Time PCR erfolgt mit Hilfe des Qiagility Roboter (siehe Bedienungsanweisung)

Standard: 10µl Ansatz

- 2,76 µl Wasser RNase freies H2O
- 5,0 ml 2xMastermix (SYBR Green PCR Kit)
- 0,24 ml PrimerMix (1µg/µl)

3.6. Rotorgene

M1 PCR	activation	95°C	5min
	denaturation	95°C	3sec
	annealing extention	60°C 95°C	25sec 60sec
	Melting curve	50°C- 95°C	delta T=1
qFast PCR	activation	95°C	5min
	denaturation	95°C	5sec
	annealing extention	60°C 95°C	15sec 60sec
	Melting curve	50°C- 95°C	delta T=1

4.0 Verwendung

5.0 Lagerung

die Lagerung der Proben erfolgt bei -80°C in N 1.12

10.5 List of supervised undergraduate research projects

Stefan Heldt, Otto-von-Guericke-Universität Magdeburg, Studienarbeit (2008):
„Analyse der virusinduzierten Interferon-Signalkaskade in adhärenten Säugetierzellkulturen“

Kristina Heinze, Hochschule Anhalt, Masterarbeit (2009):
„Charakterisierung der Induktion antiviraler Signalwege in Abhängigkeit verschiedener Infektionsbedingungen im Kontext eines Influenza Impfstoffproduktionsprozesses“

Bianca Kaps, Friedrich-Alexander-Universität Erlangen-Nürnberg, Masterarbeit (2010):
„Analysis of the antiviral signal transduction in mammalian cells infected with influenza A virus in the context of a vaccine production process“

10.6 **Publications, conference talks, and poster contributions**

Heynisch, B., Frensing, T., Heinze, K., Seitz, C., Genzel, Y., Reichl, U.,
Differential activation of host cell signaling pathways through infection with two variants of influenza A/PR/8/34 (H1N1) in MDCK cells, **Vaccine 2010; 28(51):8210-8**

Seitz, C., Isken, B., Heynisch, B., Rettkowski, M., Frensing, T., Reichl, U.,
Trypsin promotes efficient influenza vaccine production in MDCK cells by interfering with the antiviral host response, **Appl Microbiol Biotechnol. 2012; 93(2):601-11**

Frensing, T., Seitz, C., Heynisch, B., Patzina, C., Kochs, G., Reichl, U.,
Efficient influenza B virus propagation due to deficient interferon-induced antiviral activity in MDCK cells, **Vaccine 2011; 29(41):7125-9**

Heynisch, B., Frensing, T., Seitz, C., Genzel, Y., Reichl, U.,
Analysis of the impact of innate immunity of MDCK cells on virus replication in influenza vaccine production, **Vortrag**, 1st European Congress of Applied Biotechnology, Berlin, 2011

Heynisch, B., Frensing, T., Seitz, C., Reichl, U.,
Induction of innate immunity signaling pathways in MDCK cells and their relevance in a bioprocess for influenza vaccine production, **Vortrag**, 6th Workshop Molecular Interactions, Berlin, 2010

Heynisch, B., Frensing, T., Seitz, C., Genzel, Y., Reichl, U.,
Analysis of innate immunity signaling pathways in MDCK cells in an influenza virus vaccine production process, Poster, 22nd ESACT Meeting, Vienna, 2011

Heynisch, B., Frensing, T., Seitz, C., Genzel, Y., Reichl, U.,
Differential activation of host cell signaling pathways through infection with two variants of influenza A/PR/8/34 H1N1 in MDCK cells, Poster, 4th European Congress of Virology / Annual Spring Meeting of GfV, Cernobbio, Lake Como, 2010

Heynisch, B., Schulze-Horsel, J., Frensing, T., Genzel, Y., Reichl, U.,
Analysis of Signaling Cascades and Host Cell Defense in a Bioprocess for Influenza Vaccine Production, Poster, 19th Annual Meeting of the German Society for Virology, Leipzig, 2009

Heynisch, B., Seitz, C., Frensing, T., Genzel, Y., Reichl, U.,
Systems biology of influenza virus-host cell interaction in a bioprocess for vaccine production, Poster, German Symposium on Systems Biology, Heidelberg, 2009

Heynisch, B., Seitz, C., Frensing, T., Genzel, Y., Reichl, U.,
Analysis of antiviral signaling cascades in a bioprocess for influenza vaccine production, Poster, 21st ESACT Meeting, Dublin, 2009

Heynisch, B., Seitz, C., Frensing, T., Genzel, Y., Reichl, U.,
Virus-host cell interactions in a bioprocess for influenza vaccine production-characterization of antiviral signaling pathways, Poster, Dechema Jahrestagung der Biotechnologen, Mannheim, 2009

Heynisch, B., Seitz, C., Vester, D., Frensing, T., Genzel, Y., Reichl, U.,
Systems biology of virus-host cell interactions-signal transduction during influenza virus replication in MDCK cells, Poster, XIV. International Congress of Virology, Istanbul, 2008

10.7 **Curriculum vitae**

Persönliche Daten

Name:	Björn Heynisch
Geburtsdatum:	27. September 1978
Geburtsort:	Staaken
Nationalität:	deutsch

Schule und Studium

09/1985-06/1991	Polytechnische Oberschule (POS) „Freundschaft und Frieden“, Brieselang
08/1991-06/1996	Goethe-Gymnasium, Nauen
08/1996-06/1997	Valley-High-School, Albuquerque, USA
08/1997-06/1999	Goethe-Gymnasium, Nauen, Schulabschluss: Abitur
11/1999-08/2000	Henning-von-Tresckow-Kaserne, Golm, Wehrdienst
10/2000-02/2007	Technische Universität Berlin, Studium der Biotechnologie Abschluss: Dipl.-Ing. für Medizinische Biotechnologie
02/2004-04/2004	Max-Planck-Institut für Molekulare Genetik, Berlin-Dahlem Studienarbeit: „SNP-Genotypisierung mit Hilfe eines Massenspektrometrie basierten Assays“, Betreuer: Dr. rer. nat. S. Sauer
04/2006-02/2007	Institut für Experimentelle Endokrinologie, Charité Berlin Diplomarbeit: „Influence of aminoglycoside antibiotics on the biosynthesis of selenoproteins“, Betreuer: Prof. Dr. rer. nat. L. Schomburg

Berufliche Tätigkeiten

10/2002-12/2003	Max-Planck-Institut für Molekulare Genetik, Berlin-Dahlem Studentische Hilfskraft, AG Reinhardt (Genomanalyse mariner und terr. Methan oxidierender Mikroorganismen)
06/2004-09/2005	Max-Planck-Institut für Molekulare Pflanzenphysiologie, Potsdam-Golm Studentische Hilfskraft, AG Scheible, AG Hincha (Erforschung von Stressresistenz an Kartoffel, Kultivierung und Genotypisierung von *A. thaliana*)

04/2007-12/2011	Doktorand am Max-Planck-Institut für Dynamik komplexer technischer Systeme, Magdeburg, als wissenschaftlicher Mitarbeiter der Otto-von-Guericke-Universität, Abteilung: Bioprozesstechnik (Leiter: Prof. Dr.-Ing. U. Reichl) Thema: „Impact of innate immunity of MDCK cells on virus replication in an influenza vaccine production process“
seit 03/2013	Baxter International Inc., Orth an der Donau, Österreich Quality Specialist/QC